TESIS DOCTORAL

UNIVERSIDAD DE GRANADA

ESCUELA TECNICA SUPERIOR DE INGENIERÍA DE CAMINOS, CANALES Y PUERTOS

DEPARTAMENTO DE INGENIERÍA DE LA CONSTRUCCIÓN Y PROYECTOS DE INGENIERIA

SKY-DIFFUSE RADIATION MODELS FOR THE GLOBE

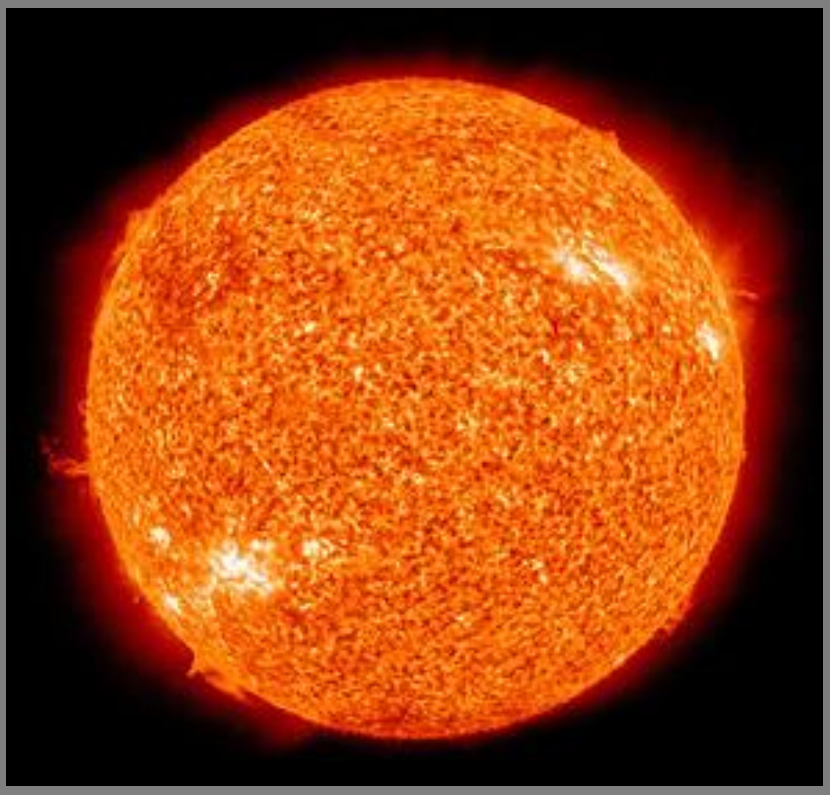

Saioa Etxebarria Berrizbeitia

PhD thesis 2017 Tesis doctoral

Editor: Universidad de Granada. Tesis Doctorales
Autora: Saioa Etxebarría Berrizbeitia
ISBN: 978-84-9163-474-4
URI: http://hdl.handle.net/10481/48219

UNIVERSIDAD DE GRANADA

ESCUELA TECNICA SUPERIOR DE INGENIERÍA DE CAMINOS, CANALES Y PUERTOS

DEPARTAMENTO DE INGENIERÍA DE LA CONSTRUCCIÓN Y PROYECTOS DE INGENIERIA

UNIVERSIDAD
DE GRANADA

SKY-DIFFUSE RADIATION MODELS FOR THE GLOBE

Saioa Etxebarria Berrizbeitia

TESIS DOCTORAL

PROGRAMA DE DOCTORADO EN INGENIERÍA CIVIL Y ARQUITECTURA

GRANADA, 2017

UNIVERSIDAD DE GRANADA

ESCUELA TECNICA SUPERIOR DE INGENIERÍA DE CAMINOS, CANALES Y PUERTOS

DEPARTAMENTO DE INGENIERÍA DE LA CONSTRUCCIÓN Y PROYECTOS DE INGENIERIA

UNIVERSIDAD
DE GRANADA

SKY-DIFFUSE RADIATION MODELS FOR THE GLOBE

Saioa Etxebarria Berrizbeitia

Doctoranda

Directores:

Dra. Eulalia Jadraque Gago

Dr. Tariq Muneer

GRANADA, 2017

El doctorando / The *doctoral candidate* **[SAIOA ETXEBARRIA BERRIZBEITIA]** y los directores de la tesis / and the thesis supervisor/s: **[PROFESSOR TARIQ MUNEER, DR. EULALIA JADRAQUE GAGO]**

Garantizamos, al firmar esta tesis doctoral, que el trabajo ha sido realizado por el doctorando bajo la dirección de los directores de la tesis y hasta donde nuestro conocimiento alcanza, en la realización del trabajo, se han respetado los derechos de otros autores a ser citados, cuando se han utilizado sus resultados o publicaciones.

/

Guarantee, by signing this doctoral thesis, that the work has been done by the doctoral candidate under the direction of the thesis supervisor/s and, as far as our knowledge reaches, in the performance of the work, the rights of other authors to be cited (when their results or publications have been used) have been respected.

Lugar y fecha / Place and date:

GRANADA, 19 DE MAYO DE 2017

Director/es de la Tesis / *Thesis supervisor/s;* Doctorando / *Doctoral candidate*:

For my parents

ACKNOWLEDGEMENTS

I would like, through these lines, to express my deepest gratitude to all those people who, with their help and support, have collaborated in carrying out this work.

My most sincere thanks to the directors of this thesis: Eulalia Jadraque Gago, for giving me the opportunity to do this doctoral thesis with her research group, for encouraging me to carry on as well as for always being available to answer my consults and doubts, for her essential help in every phase of this thesis and also for the good moments shared in both Edinburgh and Granada; Tariq Muneer, for believing in me from the beginning, for always finding the way to transmit his knowledge and his passion for rigorous and honest research, and for his advice, invaluable help and availability for any query.

Without their guidance and persistent help this doctoral thesis would not have been possible.

Special thanks also to the University of Granada, it is an honour to have had the opportunity to complete my thesis at this university. To the Edinburgh Napier University, for being part of my education as well as for providing me with everything I needed to work during my stays in Edinburgh.

I cannot forget the colleagues of the University of the Basque Country for their advice and encouragement.

All my family, especially my parents Sabin and Amaia and my brother Aitzol, because a part of this work is also theirs, and because they have helped me more than what they probably believe.

Ibai, for his help and confidence, and for being always there to remind me what really matters in life.

AGRADECIMIENTOS

A través de estas líneas, me gustaría expresar mi más profundo agradecimiento a todas aquellas personas que, con su ayuda y apoyo, han colaborado en la realización de este trabajo.

Siento una sincera gratitud hacia mis dos directores de tesis: Eulalia Jadraque Gago, por darme la oportunidad de realizar esta tesis doctoral en su grupo de investigación, por animarme a seguir adelante y estar siempre disponible para mis consultas y dudas, por su imprescindible ayuda en todas las fases de estas tesis y también por los buenos momentos compartidos tanto en Edimburgo como en Granada. Y Tariq Muneer, por haber creído en mí desde el primer momento, por saber transmitirme su conocimiento y su pasión por la investigación rigurosa y honesta, y por su inestimable ayuda y disponibilidad para cualquier consulta. Sin ellos, no estaría escribiendo estas líneas.

Gracias también a la Universidad de Granada, es para mí un honor haber tenido la oportunidad de realizar mi tesis doctoral en esta universidad. A la Edinburgh Napier University, por ayudar en mi formación, además de facilitarme todo lo necesario para trabajar durante mis estancias en Edimburgo.

A mis compañeros del Departamento de Ingeniería Mecánica de la Universidad del País Vasco por sus consejos y ánimos.

A toda mi familia, en especial a mis padres Sabin y Amaia así como a mi hermano Aitzol, porque una buena parte de este trabajo también es suya, y porque me han ayudado más de lo que probablemente ellos creen.

A Ibai, por sus consejos y confianza, y por estar siempre ahí para recordarme lo que realmente importa en la vida.

ABSTRACT

The increase of greenhouse gases concentration in the atmosphere causes the climate change and global warming. The excessive use of fossil fuels is the most relevant cause of this phenomenom. The emissions related to the burning of these fuels are concentrating in the atmosphere and leading to the warming of the Earth. Apart from the hazardous effects of the utilization of fossil fuels, it is important to note that their reserves are finite, and the enormous consumption of oil, gas and coal in the last 200 years has led to their depletion.

Renewable energy sources, also known as alternative or green energy sources, are naturally replenished, clean and environmental friendly with zero or almost zero emissions of greenhouse gases and pollutants. They have the potential to meet the worldwide current and future energy demand. The solar energy is the most promising green energy source.

For a proper design of solar energy application systems, it is essential to have solar radiation data. The starting point for the radiation data is almost always global and diffuse horizontal radiation in the form of hourly or sub-hourly data. It is not always possible to obtain a long-term series of hourly or sub-hourly data for the above-mentioned parameters. Global radiation at an hourly, daily or monthly frequency is the most commonly measured solar data and this is available for a limited number of stations. The measurement of the diffuse radiation is even scarcer due to higher operational costs associated to the measurements and meteorological offices tend to record the latter variable at much fewer locations.

On the contrary, through the work of NASA (http://eosweb.larc.nasa.gov/cgi-bin/sse/retscreen.cgi?email=rets@nrcan.gc.ca) it is now possible to obtain daily-averaged irradiation data for virtually any location in the world. These data include long-term estimates of meteorological quantities and surface solar energy fluxes obtained from satellite systems.

NASA data that now is available in public domain can be used to construct a computational chain to get all manner of solar energy calculations that require hourly horizontal and slope, global and diffuse radiation data.

Using established models, it is then possible to decompose the daily to averaged-hourly global irradiation. The missing link so far has been hourly averaged diffuse irradiation. In this study data was pooled from 19 world-wide locations to obtain a regression model to complete the above missing link. It was presently shown that the averaged–data regressions are distinctly different from previously available hour-by-hour regressions.

RESUMEN

El aumento de la concentración de gases de efecto invernadero en la atmósfera provoca el cambio climático y el calentamiento global. El uso excesivo de combustibles fósiles es la causa más relevante de este fenómeno. Las emisiones relacionadas con la combustión de estos combustibles se concentran en la atmósfera y conducen al calentamiento de la Tierra. Aparte de los efectos nocivos de la utilización de combustibles fósiles, es importante señalar que sus reservas son finitas y que el enorme consumo de petróleo, gas y carbón en los últimos 200 años ha llevado a su agotamiento.

Las fuentes de energía renovables, también conocidas como fuentes de energía alternativas o verdes, son naturalmente reabastecidas, limpias y respetuosas con el medio ambiente, con cero o casi cero emisiones de gases de efecto invernadero y contaminantes. Tienen el potencial para satisfacer la demanda mundial de energía actual y futura. La energía renovable más prometedora es la energía solar.

Para un diseño adecuado de sistemas de captación de energía solar, es esencial disponer de datos de radiación solar. El punto de partida para los datos de radiación es casi siempre la radiación global horizontal y la radiación difusa en forma de datos horarios o sub-horarios. No siempre es posible obtener una serie a largo plazo de datos por hora o por sub-hora para los parámetros antes mencionados. La radiación global a una frecuencia horaria, diaria o mensual es la más comúnmente medida de entre los datos solares y esto está disponible para un número limitado de estaciones. La medición de la radiación difusa es aún más escasa debido a los mayores costos operativos asociados a las mediciones y a que las oficinas meteorológicas tienden a registrar la última variable en número más escaso de lugares.

Por el contrario, a través de la página Web oficial de la NASA, es posible obtener datos de la radiación media diaria para prácticamente cualquier lugar en el mundo. Estos datos incluyen estimaciones a largo plazo de la meteorología y de los flujos de energía solar superficial obtenidos de los sistemas de satélite. Los datos de la NASA que en la actualidad están disponibles y que son de dominio público se pueden utilizar para desarrollar una serie computacional que permita obtener todos los cálculos de energía solar que requieran datos horarios horizontales y sobre un plano inclinado así como, globales y difusos.

Usando modelos establecidos, es posible descomponer la radiación global diaria a horaria promediada. El eslabón perdido hasta el momento ha sido obtener la radiación difusa horaria promediada. En este estudio se han agrupado datos de 19 ciudades del mundo para obtener un modelo de regresión que permita completar el eslabón perdido comentado anteriormente. Se ha demostrado que las regresiones de los datos promediados son distintas de las regresiones hora por hora previamente disponibles.

CONTENT

List of figures

List of tables

1. INTRODUCTION

Global warming and climate change issues are probably the greatest threats to this planet and most controversial topics of these present times.

In this consumer society, the presiding deity is money and the goal of all efforts is limitless growth and quick profit. Increase in consumption is closely linked to the economic growth and maintenance of economic activity and employment. However, when it crosses a certain threshold, consumption is transformed into consumerism, or excessive consumption.

The relationship between consumerism and climate change is undeniable. There is an insatiable desire for commodities and material possessions, and this dependence is essential for economic expansion. However, the production, processing and consumption of these commodities require the extraction and use of natural resources and have an impact in the environment.

After the industrial revolution in the end of the 19th century, population and income increase reached unprecedented levels of growth. The standard of living of the general population, although very unequally, also increased to levels never reached before, and therefore consumption of commodities began to increase too. More commodities lead to more people and this leads to more income, so more commodities need to be commercialized in order to keep people employed so they have income to consume more commodities. Consequently, pollution increased as consumption of commodities augmented, and therefore global warming and climate change began to be notorious (The relationship between consumerism and global warming.2016).

Climate change and global warming refer to an increase in average global temperatures, caused principally by increase in greenhouse gases such as carbon dioxide (CO_2) (Climate change and global warming introduction.2015). The Earth´s climate has not been constant through history. There have been at least seven cycles of glacial advance and retreat in the last 650.000 years, leading to the beginning of the modern climate era, and consequently of human civilization, with the end of the last ice age about 7,000 years ago (Climate change: How do we know.2017). Most of these climate alterations are attributed to the changes on the amount of solar energy that receives the planet caused by very small variations in Earth´s orbit.

The current warming trend is particularly significant because it is extremely likely to be the result of human activity, starting at the end of the 19th century (Rapacious consumerism and climate change.2016) and reinforcing in the mid-20th century. The average temperature on Earth has increased about 0.8° Celsius since pre-industrial times (Earth observatory.2014) and it is proceeding at a rate that is unprecedented over decades to millennia (Climate change: How do we know.2017).

Carbon dioxide and other gases have the nature to trap the heat, affecting the transfer of infrared energy through the atmosphere. Many of these greenhouse gases are essential to enable life on Earth, without them the heat would escape back into space and the average temperature in the world would be a lot colder (Climate change and global warming introduction.2015). However, if the presence of greenhouse gases becomes excessive, more heat than needed gets trapped, causing the Earth to warm in response (Climate change: How do we know.2017).

The dramatic increase of CO_2 presence in the atmosphere proves that human activity is responsible of causing the imbalance in the natural cycle of the greenhouse effect and related processes. When burning fossil fuels for heating, cooking, electricity, manufacturing or transportation, carbon is releasing to the atmosphere more rapidly than is being removed naturally through carbon sedimentation. Clearing forests for agricultural processes also transfer carbon from living biomass into the atmosphere.

These activities add extra amount of CO_2 in the atmosphere, and consequently the current atmospheric CO_2 concentrations are higher than they have been over the last half-million years (Climate change and global warming introduction.2015).

As mentioned before, the increase of greenhouse gases concentration in the atmosphere causes the climate change and global warming. There are several evidences for the rapid climate change: sea level rise, global temperature rise, warming oceans, shrinking ice sheets, declining artic ice level, glacial retreat, extreme events, ocean acidification, and decreased snow cover. Disappearance of cities that are below sea level, heat waves, droughts and intense storms, extinction of species, ecosystems destruction, diseases, disappearance of glaciers, economic instability and wars are some of the consequences of climate change (Climate change: How do we know.2017).

The excessive use of fossil fuels is the most relevant cause of the climate change. The emissions related to the burning of these fuels are concentrating in the atmosphere and

leading to the warming of the Earth. Apart from the hazardous effects of the utilization of fossil fuels, it is important to note that their reserves are finite, and the enormous consumption of oil, gas and coal in the last 200 years has led to their depletion.

Fossil fuels are old, they were formed millions of years ago when dead plants and animals were trapped under deposits and became buried underneath land. Compression over time fossilised the remains, creating carbon-rich fuel sources. The North Sea oil deposits for example are around 150 million years old. It is probable that humans used fossil fuel as far back as the Iron Age, but with the Industrial Revolution their extraction increased exponentially, consuming an enormous amount of them (The world factbook.2016). The reserves were fossil fuels have remained cannot be refilled when they are consumed, and with further use, they all are in danger of disappearance (When will fossil fuels run out.2017).

Some new reserves will be found and this will extend the deadline to some extent, but these will not last forever. New reserves of fossil fuels are becoming harder to find, and those that are being discovered are considerably smaller compared to the ones that have been found in the past (The world factbook.2016).

The quantity of fossil fuel reserves is uncertain, and there are many different opinions and calculations about this fact. According to the BP Statistical Review of World Energy (2016), the production to consumption ratio worldwide (R/P) is not higher than 120 year for the coal, in the case of natural gas it does not reach 60 years and it is around 50 years for the oil.

Consequently, it is evident that the current energy consumption is not sustainable anymore, and it is crucial to start being conscious of the threats the existing energy systems cause to the environment and therefore to the society and to reinforce the substitution of the present fuels to renewable fuel sources (When will fossil fuels run out.2017).

Renewable energy sources, also known as alternative or green energy sources, are naturally replenished, clean and environmental friendly with zero or almost zero emissions of greenhouse gases and pollutants. They have the potential to meet the worldwide current and future energy demand (Muneer, Asif, & Munawwar, 2005).

The sun is the most important source of renewable energy available; it drives the bases of the earth and causes most of the energy sources known today. Wind and hydro energy, biomass, and even fossil fuels are available because of the sun.

Solar energy can generate heat and electricity for domestic and industrial use, and research in the field has increased significantly the efficiency and capacity of solar energy technologies. However, the potential of solar applications is much higher than the present use of this energy source.

For a proper design of solar energy application systems, it is essential to have solar radiation data. Solar water heating, PV systems, daylighting, building air conditioning load and solar-driven ventilation systems are some of solar energy applications where solar radiation data are needed to get solar energy resource assessment, its transmission and to obtain the efficiency of energy delivery among others.

The starting point for the radiation data is almost always global and diffuse horizontal radiation in the form of hourly or sub-hourly data. It is not always possible to obtain a long-term series of hourly or sub-hourly data for the above-mentioned parameters. Global radiation at an hourly, daily or monthly frequency is the most commonly measured solar data and this is available only for a limited number of stations. For example, there are 71 and 31 stations that measure these parameters in the UK and Spain respectively. The measurement of the diffuse radiation is even scarcer due to higher operational costs associated to the measurements and meteorological offices tend to record the latter variable at much fewer locations. In the UK for example the diffuse radiation is recorded at only two locations.

On the contrary, through the work of NASA (http://eosweb.larc.nasa.gov/cgi-bin/sse/retscreen.cgi?email=rets@nrcan.gc.ca) it is now possible to obtain daily-averaged irradiation data for virtually any location in the world. These data include long-term estimates of meteorological quantities and surface solar energy fluxes obtained from satellite systems. These data meet the needs of renewable energy community and have been proven to be accurate enough to provide reliable solar and meteorological data for locations where measurements are scarce or non-existent.

NASA data that now is available in public domain can be used to construct a computational chain to get all manner of solar energy calculations that require hourly horizontal and slope, global and diffuse radiation data.

The aim of this study is to develop models to obtain **monthly-averaged hourly diffuse radiation** data, to improve solar energy systems to specific locations and applications using available data from NASA. For this purpose, the following steps were followed:

- ✓ Comparison between the irradiation data obtained from NASA with ground-based averaged measure data in order to verify their concordance.
- ✓ Review and analysis of the existing diffuse radiation models
- ✓ Analysis of hourly global and diffuse radiation values for the locations used in the study.
- ✓ Calculation of monthly-averaged hourly values for the global and diffuse radiation data considering the period for each variable.
- ✓ Regression of the monthly-average clearness index against the monthly-averaged diffuse ratio for each location.
- ✓ Analysis and study of the correlation between both variables.

2. INTRODUCCIÓN

El calentamiento global y las cuestiones relacionadas con el cambio climático son probablemente las mayores amenazas para este planeta y los temas más controvertidos en la actualidad.

Vivimos en una sociedad de consumo, donde únicamente impera el dinero y el objetivo primordial de las actividades desarrolladas es el crecimiento ilimitado y la ganancia rápida. El aumento del consumo está estrechamente relacionado con el crecimiento económico y con el mantenimiento de la actividad económica y el empleo. Sin embargo, cuando se atraviesa cierto umbral, el consumo se transforma en consumismo o consumo excesivo.

La relación entre consumismo y cambio climático es innegable. Existe un deseo insaciable de bienes y posesiones materiales, y esta dependencia es esencial para la expansión económica. Sin embargo, la producción, el procesamiento y el consumo de estos productos requieren la extracción y el uso de recursos naturales lo que genera un impacto en el medio ambiente.

Tras la revolución industrial a finales del siglo XIX, el crecimiento social y económico alcanzó niveles sin precedentes. El nivel de vida de la población en general, aunque muy desigual, aumentó a niveles nunca antes alcanzados, y por lo tanto el consumo de productos básicos también comenzó a aumentar. Más bienes de consumo conducen a un aumento de la población y este a más ingresos, así que más productos básicos necesitan ser comercializados para mantener a una población empleada para que de esta manera tengan ingresos para poder consumir más bienes básicos. En consecuencia, la contaminación aumentó a medida que aumentaba el consumo de productos básicos, por lo que el calentamiento global y el cambio climático comenzaron a ser notorios (The relationship between consumerism and global warming.2016).

El cambio climático y el calentamiento global provocan un aumento de la temperatura media mundial, causado principalmente por el aumento de los gases de efecto invernadero, tales como el dióxido de carbono (CO_2) (Climate change and global warming introduction.2015). El clima de la Tierra no ha sido constante a lo largo de la historia, ha habido al menos siete ciclos de avance y retroceso de los glaciares en los últimos 650.000 años, dando lugar al comienzo de la Era del Clima Moderno y, por consiguiente, de la

civilización humana, con el fin de la última Era de Hielo hace 7.000 años (Climate change: How do we know.2017). La mayoría de estas alteraciones climáticas se atribuyen a los cambios en la cantidad de energía solar que recibe el planeta causados por variaciones muy pequeñas en la órbita de la Tierra.

La tendencia actual en materia de calentamiento climático es particularmente significativa porque es muy probable que sea el resultado de la actividad humana. Comenzó a finales del siglo XIX (Rapacious consumerism and climate change.2016) y se refuerza a mediados del siglo XX. La temperatura media en la Tierra ha aumentado alrededor de 0.8° Celsius desde tiempos preindustriales (Earth observatory.2014) y está avanzando a un ritmo sin precedentes en miles de años (Climate change: How do we know.2017).

El dióxido de carbono y otros gases atrapan el calor de forma natural, afectando la transferencia de energía infrarroja a través de la atmósfera. Muchos de estos gases de efecto invernadero son esenciales para permitir la vida en la Tierra, sin ellos el calor volvería al espacio y la temperatura media en el mundo sería mucho más fría (Climate change and global warming introduction.2015). Sin embargo, si la presencia de gases de efecto invernadero es excesiva, queda atrapado más calor de lo necesario, causando el calentamiento de la tierra (Climate change: How do we know.2017).

El notable aumento de CO_2 presente en la atmósfera demuestra que la actividad humana es responsable de causar el desequilibrio en el ciclo natural del efecto invernadero y otros procesos relacionados. Al quemar combustibles fósiles para calefacción, cocinar, generar electricidad, fabricación o transporte, el carbono es liberado a la atmósfera más rápidamente que el eliminado de forma natural mediante su sedimentación. La deforestación de los bosques para los procesos agrícolas también transfiere el carbono de la biomasa viva a la atmósfera.

Estas actividades añaden una cantidad extra de CO_2 en la atmósfera y, en consecuencia, las actuales concentraciones atmosféricas de CO_2 son más altas de lo que han sido durante los últimos 50 millones de años (Climate change and global warming introduction.2015).

Como se mencionó anteriormente, el aumento de la concentración de gases de efecto invernadero en la atmósfera provoca el cambio climático y el calentamiento global. Existen varias evidencias que demuestran un rápido cambio climático: aumento del nivel del mar, aumento de la temperatura global, calentamiento de los océanos, reducción de las capas de hielo, descenso del nivel del hielo antártico, retroceso glaciar, acidificación del océano y

disminución de la cubierta de nieve. La desaparición de ciudades que están por debajo del nivel del mar, olas de calor, sequías e intensas tormentas, la extinción de especies, la destrucción de los ecosistemas, las enfermedades, la desaparición de los glaciares, la inestabilidad económica y las guerras son algunas de las consecuencias del cambio climático (Climate change: How do we know.2017).

El uso excesivo de combustibles fósiles es la causa más relevante del cambio climático. Las emisiones relacionadas con la combustión de estos combustibles se concentran en la atmósfera y conducen al calentamiento de la Tierra. Aparte de los efectos peligrosos de la utilización de combustibles fósiles, es importante señalar que sus reservas son finitas y el enorme consumo de petróleo, gas y carbón en los últimos 200 años ha llevado a su agotamiento.

Los combustibles fósiles son viejos, se formaron hace millones de años cuando las plantas y animales muertos quedaron atrapados bajo depósitos y fueron enterrados bajo la tierra. La compresión a través del tiempo fosilizó los restos, creando fuentes de combustible ricas en carbono. Los depósitos de petróleo del Mar del Norte, por ejemplo, tienen unos 150 millones de años. Es probable que los seres humanos usaran combustibles fósiles desde la Edad de Hierro, pero con la Revolución Industrial su extracción aumentó exponencialmente, consumiendo una enorme cantidad de ellos (The world factbook.2016). Las reservas donde los combustibles fósiles han permanecido no se pueden rellenar después de consumidos y están en peligro de desaparición (When will fossil fuels run out.2017).

Algunas nuevas reservas serán encontradas y esto ampliará el plazo hasta cierto punto, pero éstas no durarán para siempre. Las nuevas reservas de combustibles fósiles son cada vez más difíciles de encontrar, y las que se están descubriendo son considerablemente más pequeñas en comparación con las que se encontraron en el pasado (The world factbook.2016).

La cantidad de reservas de combustibles fósiles es incierta, y hay muchas opiniones y estimaciones diferentes sobre este hecho. Según el BP Statistical Review of World Energy (2016), la relación producción-consumo en todo el mundo (R/P) no es superior a 120 años para el carbón, en el caso del gas natural no alcanza los 60 años y los 50 años para el petróleo.

En consecuencia, es evidente que el actual consumo energético ya no es sostenible y es fundamental empezar a ser consciente de los daños que los sistemas energéticos actuales causan al medio ambiente y por lo tanto a la sociedad, y reforzar la sustitución de los actuales combustibles a fuentes de energía renovables (When will fossil fuels run out.2017).

Las fuentes de energía renovables, también conocidas como fuentes de energía alternativas o verdes, son naturalmente reabastecidas, limpias y respetuosas con el medio ambiente, con cero o casi cero emisiones de gases de efecto invernadero y contaminantes. Tienen el potencial de satisfacer la demanda mundial de energía actual y futura (Muneer, Asif, & Munawwar, 2005).

El sol es la fuente de energía renovable disponible más importante; impulsa las bases de la tierra y origina la mayoría de las fuentes de energía conocidas hoy en día. El viento y la energía hidráulica, la biomasa, e incluso los combustibles fósiles existen gracias al sol.

La energía solar genera calor y electricidad para uso doméstico e industrial además, la investigación en este campo ha mejorado significativamente la eficiencia y el desarrollo de tecnologías que tienen como fuente la energía solar. Sin embargo, el potencial de las aplicaciones solares es mucho mayor que el uso actual de esta fuente de energía.

Para un diseño adecuado de los sistemas de aplicación de energía solar, es esencial disponer de datos de radiación solar. El calentamiento solar de agua, los sistemas fotovoltaicos, la iluminación natural, el acondicionamiento de edificios y los sistemas de ventilación accionados por energía solar son algunas de las aplicaciones de la energía solar que necesitan datos de radiación solar para obtener la evaluación de recursos de energía solar y su transmisión.

El punto de partida para los datos de radiación es casi siempre la radiación horizontal global y difusa en forma de datos horarios o sub-horarios. No siempre es posible obtener una serie a largo plazo de datos horarios para los parámetros antes mencionados. La radiación global a una frecuencia horaria, diaria o mensual es la más comúnmente medida de entre los datos solares, pero aun así está disponible para un número limitado de estaciones. Por ejemplo, hay 71 y 31 estaciones que miden estos parámetros en el Reino Unido y España, respectivamente. La medición de la radiación difusa es aún más escasa debido a los mayores costos operativos asociados a las mediciones y las oficinas meteorológicas tienden a registrar la última variable en menos lugares. En el Reino Unido, por ejemplo, la radiación difusa se registra en dos lugares solamente.

Por otro lado, a través de la página Web oficial de la NASA (http://eosweb.larc.nasa.gov/cgi-bin/sse/retscreen.cgi?email=rets@nrcan.gc.ca) en la actualidad es posible obtener información media diaria para prácticamente cualquier lugar en el mundo. Estos datos incluyen estimaciones meteorológicas a largo plazo así como los flujos de energía solar superficial obtenidos de los sistemas satelitales. Estos datos han demostrado ser lo suficientemente precisos como para proporcionar datos solares y meteorológicos fiables para lugares donde las mediciones son escasas o inexistentes.

Los datos obtenidos de la NASA que actualmente están disponibles y son de dominio público pueden utilizarse para desarrollar una serie computacional que permita obtener todos los cálculos de energía solar que requieren datos horarios horizontales y sobre superficies inclinadas, globales y difusos.

El objetivo de este estudio es desarrollar modelos para obtener datos mensuales de la radiación difusa por hora, para mejorar los sistemas de captación de la energía solar en lugares y aplicaciones específicos, utilizando datos disponibles en la Web de la NASA. Para ello, se han seguido los siguientes pasos:

- ✓ Comparación entre los datos de irradiación obtenidos de la NASA con los datos medios medidos en la Tierra para verificar su concordancia.
- ✓ Revisión y análisis de los modelos de radiación difusa existentes
- ✓ Análisis de los valores horarios de radiación global y difusa para las localidades utilizadas en el estudio.
- ✓ Cálculo de los valores horarios medios mensuales de los datos de radiación global y difusa considerando el período de datos disponible para cada variable.
- ✓ Regresión del índice de claridad mensual medio frente a la relación difusa mensual para cada localidad.
- ✓ Análisis y estudio de la correlación entre ambas variables.

3. NOMENCLATURE

H: Annual, monthly and daily global horizontal solar radiation

H_0: Extraterrestrial radiation on a horizontal surface

H_d: Diffuse radiation

H_b: Beam or direct radiation

$k_t = \frac{H}{H_0}$: Clearness index

$k = \frac{H_d}{H}$: Diffuse ratio

$k_D = \frac{H_d}{H_0}$: Diffuse to extraterrestrial ratio

S: Sunshine duration

S_0: Length of the day

I_{SC}: Solar constant 1,367W/m^2

D: Number of days of the year starting from first January

φ: Latitude of the site

δ: Solar declination

ω: Hour angle

ω_s: Sunset hour angle

θ_S: Solar zenith angle

α: Solar elevation or altitude

θ: Incident algle with respect to the normal of the tilted surface

Rd: Conversion factor that accounts for the reduction of the sky view factor and anisotropic scattering

R: Ground reflected radiation that is intercepted by the tilted surface

r_D: Hourly to daily diffuse radiation ratio

r_G: Hourly to daily global/total radiation ratio

4. FUNDAMENTALS

4.1 SUN-EARTH GEOMETRY

The Earth revolves around the sun in an elliptical orbit, and the solar radiation that reaches the Earth is inversely proportional to the square of the distance between the Earth and the sun. There are several geometrical relationships between the horizontal and equatorial planes relative to the earth and sun and the incoming solar radiation. There are numerous angles to descrive these geometrical associations.

Azimuth angle

The azimuth γ (degrees) is the angle between sun´s beam projection on the horizontal plane and a reference direction, usually north, measured clockwise around the observer's horizon (Muneer, 2004).

Declination

The declination δ (degrees) is the angle between the sun-earth vector and the equatorial celestial plane. It is the angular position of the sun from the equatorial plane at solar noon (Badescu, 2008). It lies between -23.45° at the winter solstice and 23.45° at summer solstice and it is zero at vernal and autumnal equinoxes (Iqbal, 2012).

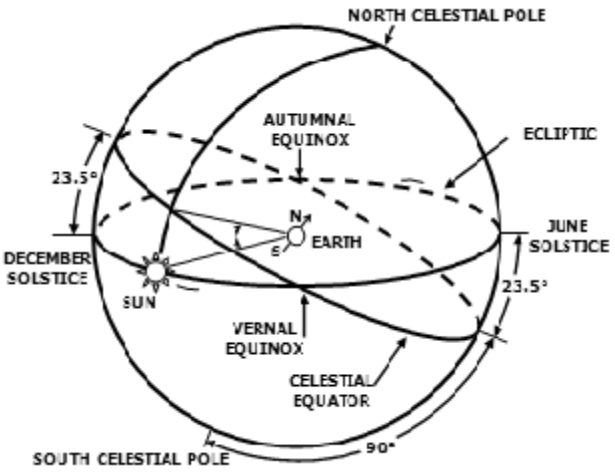

Figure 4.1: Declination angle (Iqbal, 2012)

Hour angle

The hour angle ω (degrees) is the sun´s angular position east or west of the local meridian (Muneer, 2004).

Incidence angle

The incidence angle σ (degrees) is the angle of the sun´s beam radiation and a surface at any given tilt. It can also be described as the angle that a solar ray makes with a line perpendicular to the surface. In this case, a surface that is perpendicular to the ray has an incident angle of 0° (Muneer, 2004).

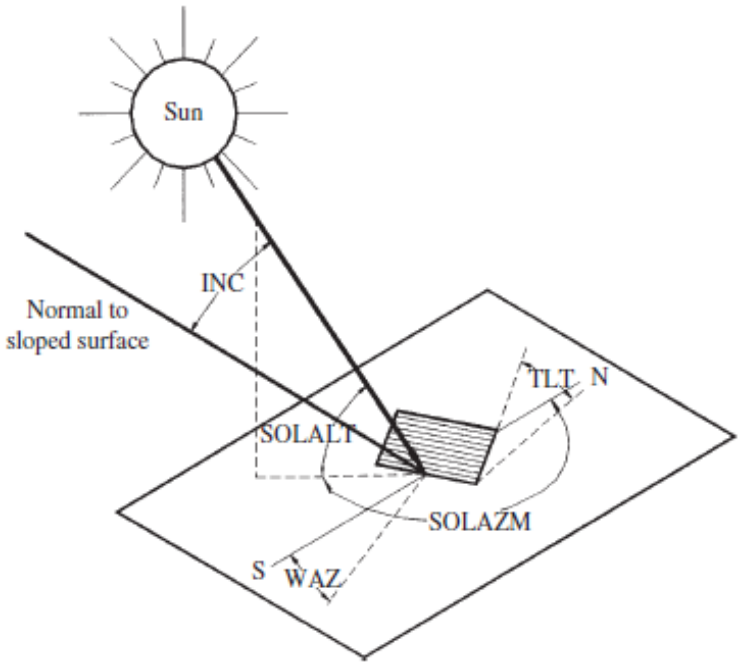

Figure 4.2: Sun-earth angles (Muneer, 2004)

Latitude (LAT)

The latitude Ø (degrees) describes the angular location north (positive) or south (negative) of the equator of a given location. It is the arc, measured in degrees, of a meridian between that place and the equator. It lies between -90° and 90°, being the North positive (Iqbal, 2012).

Length of the day

The length of the day S_o is the time duration between the sunrise and sunset (Muneer, 2004).

Longitude (LONG)

The longitude (degrees) of a place defines the the arc, measured in degrees, of a parallel between the place and the prime meridian (Greenwich meridian). It lies between 0° to 180°, either East or West (Iqbal, 2012).

Solar altitude

The solar altitude or elevation α (degrees) is the angular heigh of the middle of the solar disk above the observer´s celestial horizon. It is the complement of the zenith angle and it is an angle between 0° and 90° (Iqbal, 2012; Muneer, 2004).

Zenith angle

The zenith angle θ_s (degrees) is the angle between earth-sun vector and vertical (Iqbal, 2012).

4.2 SOLAR RADIATION

The solar radiation that gets the earth is compound by different constituents. It is therefore necessary to explain the meaning of these terms, as they will appear in this text.

Albedo (GROUND REFLECTED)

The albedo is the fraction of solar radiation that is reflected from the ground, it is the reflectance of the incident solar radiation. Knowledge of the foreground type and geometry is needed to have accurate knowledge of the albedo (Muneer, 2004).

Clearness index

The clearness index k_t is the ratio between the monthly average, daily or hourly global radiation on a horizontal surface and the monthly average, daily or hourly horizontal extraterrestrial radiation. This term is used in this work as a parameter to obtain further information of the diffuse radiation (Muneer, 2004).

Direct solar radiation (Beam)

Direct or beam radiation (Wh/m^2) is the part of the extraterrestrial solar radiation that reaches the earth as a collimated beam after weakening by the atmosphere. It is the part of

the solar radiation that reaches the earth without being scattered by the atmosphere (Badescu, 2008).

Diffuse radiation

When the solar radiation penetrates the atmosphere, part of it is depleted by absortion and scattering, and this part is the diffuse radiation (Wh/m^2). It can also be descrived as the amount of solar radiation that does not reach the earth as direct or beam radiation. Unclear atmosphere or reflections from clouds produce high diffuse values, whilst when there is clear sky conditions the diffuse fraction is minimal.

The term diffuse ratio refers to the diffuse radiation divided by the global radiation (Badescu, 2008).

Extraterrestrial radiation

The extraterrestrial radiation (Wh/m^2) is the radiation beyond the earth's atmosphere. It is also known as "top-of-atmosphere" (TOA) irradiance. It is the amount of radiation that a location in the earth would receive if there was not atmosphere or clouds. The extraterrestrial radiation is often used as the reference value against which actual solar energy measurements are compared. It depends on the solar constant, sun-earth distance ratio and declination angle (Badescu, 2008).

Global Horizontal Radiation

The global horizontal radiation (Wh/m^2) is the sum of the direct, diffuse and albedo radiation. However, as the groud reflected radiation is normally insignificant compared to the direct and diffuse components, global radiation is calculated as the sum of direct and diffuse radiation (Badescu, 2008).

Irradiation

Irradiation (Wh/m^2) is the cumulative energy incident on a surface in a given period of time (Muneer, 2004).

Solar constant

The solar constant (W/m^2) is the amount of solar power flux per unit area that would be incident on surface oriented perpendicularly to the rays at the top of the earth´s

atmosphere. The World Radiation Centre (WRC) has adopted the value of 1367 W/m^2 with an uncertainty of the order of 1% (Duffie & Beckman, 1991).

Solar radiation

Solar radiation (Wh/m^2) is defined as the energy emanating from the sun (Muneer, 2004).

Sunshine duration

The sunshine duration (hours) refers to the total hours of sunshine that occur when the solar disk is visible. This is a very useful indicator of the amount of solar radiation that reaches the earth surface (Muneer, 2004).

4.3 STATISTICAL TOOLS

The statistical tools are needed to check on the adequacy of the mathematical models that describe any physical process, such as the diffuse solar radiation (Muneer, 2004).

Coefficient of correlation R

Correlation is the degree of relationship between variables. It determines how well a linear or non-linear equation describes the relationship between variables.

The coefficient of correlation R is the square root of the coefficient of determination R^2. It measures the relationship of the variables based on a scale which ranges between -1 and 1. The negative or positive value of R will depend on the inter-relationship between x and y (if y increases when x increases R will be positive and vice versa).

Coefficient of determination R^2

The coefficient of determination R^2 is the ratio of the explained variation $\Sigma (Y_c - Y_m)^2$, to the total variation $\Sigma (Y_o - Y_m)^2$. Being Y_o the observed values and Y_c the calculated values of the dependent variable and Y_m the mean of the observed Y values.

The value of the ratio lies between 0 and 1, and a high value of the ratio is desirable since it shows a lower unexplained variation (Muneer, 2004).

Correlation

The correlation between variables is the degree of relationship between them. It determines how well a given equation describes the relationship between variables (Muneer, 2004).

Mean bias error, mean of absolute deviations and root mean square root

The mean bias errors (MBEs), mean of absolute deviations (MADs) and root square errors (RMSEs) will enable further information about the evaluation of a given model (Muneer, 2004).

The mean bias error (MBE) provides a measure of the overall trend of a given model. It indicates if the model tends to under predict or over predict the modelled values.

$$MBE = \frac{\Sigma(Y_C - Y_0)}{n} \quad (4.1)$$

The mean of absolute deviation (MAD) provides absolute measurements.

$$MAD = \frac{\Sigma abs(Y_C - Y_0)}{n} \quad (4.2)$$

The root mean square error (RMSE) highlights the repeatability of the model, since it gives a value to the level of scatter produced by the models.

$$RMSE = \sqrt{\frac{\Sigma(Y_C - Y_0)^2}{n}} \quad (4.3)$$

The physical unit of the above-mentioned formulas is the same as the dependent variable Y. In some cases, the non-dimensional NBE, MAD and RMSE (NDNBE, NDMAD and NDRMSE) are required. The following equations are used to calculate them.

$$MBE = \frac{\Sigma \frac{(Y_C - Y_0)}{Y_0}}{n} \quad (4.4)$$

$$MAD = \frac{\Sigma \frac{abs(Y_C - Y_0)}{Y_0}}{n} \quad (4.5)$$

$$RMSE = \sqrt{\frac{\sum \left(\frac{Y_C - Y_0}{Y_0}\right)^2}{n}} \quad (4.6)$$

Outliers

In solar radiation studies, there are often data that lie unusually far removed from the bulk of the data population. These data are called outliers and they suggest that the datum is not typical of the rest of the data, they indicate peculiarity. An outlier should be carefully examined to see if there is any logical explanation for its different behavior.

They should not be rejected automatically, since sometimes an outlier may provide information from unusual conditions. However, if the unusual behavior of these data is associated to erroneous observation, they could be rejected.

Statistically, quartile ranges are used to evaluate if an unusual data is or not an outlier. The mathematical definition of the **near outliers** is:

$$Lower\ near\ outlier\ limit = 1st\ quartile - 1.5 * (3rd\ quartile - 1st\ quartile) \quad (4.7)$$

$$Upper\ near\ outlier\ limit = 3rd\ quartile + 1.5 * (3rd\ quartile - 1st\ quartile) \quad (4.8)$$

The limits of **far outliers** are defined as follows:

$$Lower\ far\ outlier\ limit = 1st\ quartile - 3 * (3rd\ quartile - 1st\ quartile) \quad (4.9)$$

$$Upper\ far\ outlier\ limit = 3rd\ quartile + 3 * (3rd\ quartile - 1st\ quartile) \quad (4.10)$$

A high number of outliers in the data set mean that there is high degree of variability in the observations or a large set of suspicious data indicating poor station operation.

It is essential to the check the adequacy of a given mathematical model describing any physical process, such as solar radiation as it is the current case. There are several statistical examination methods to examine the appropriateness of the models. This analysis is important not only in the final stages of the work program, but more particularly in the initial phase (Muneer, 2004).

Regression

The regression is the mathematical technique of finding a line that best fit independent of individual judgement. The analysis involves the determination of the constants of the equation that can give a best fit. It is the procedure of fitting linear or non-linear models between a dependent and a set of independent variables. Adding the line of best fit can increase the value of a scatter graph (Muneer, 2004).

Scattergraph OR SCATTERPLOT

A scattergraph or scatterplot shows through a coordinate plane the relationship between two variables (Muneer, 2004).

Standard Deviation

The Standard Deviation (s) defines the degree to which numerical data tend to spread about an average value.

It is one of the most important of the measures of dispersion, i.e. the degree to which numerical data tend to spread about an average value (Muneer, 2004). It is calculated as follows:

$$s = \sqrt{\frac{\Sigma(calculated\ values - mean)^2}{number\ of\ observations}} \qquad (4.11)$$

Students´s t-distribution

The modeler will often have the question of what quantitative measure should be used to evaluate the R^2 value obtained for a given model. The R^2 value will clearly depend on the size of the data population. A lower value of R^2 fitted against a large database could be or not be more accurate than a model which used a smaller population. The student´s t-test can be used to answer that question since it is possible to compare two statistical models with this test (Muneer, 2004).

Table 4.1: Percentile values for Student´s distribution (Muneer, 2004)

Degree of freedom (d.f)	Percentile (P)				
	0.95	0.98	0.99	0.998	0.999
1	12.706	31.821	63.657	318.310	636.620
2	4.303	6.965	9.925	22.327	31.598
3	3.182	4.541	5.841	10.214	12.924
4	2.776	3.747	4.604	7.173	8.610
5	2.571	3.365	4.032	5.893	6.869
6	2.447	3.143	3.707	5.208	5.959
7	2.365	2.998	3.499	4.785	5.408
8	2.306	2.896	3.355	4.501	5.041
9	2.262	2.821	3.250	4.297	4.781
10	2.228	2.764	3.159	4.144	4.587
15	2.131	2.602	2.947	3.733	4.073
20	2.086	2.528	2.845	3.552	3.850
25	2.060	2.485	2.787	3.450	3.725
30	2.042	2.457	2.750	3.385	3.646
40	2.021	2.423	2.704	3.307	3.551
60	2.000	2.390	2.660	3.232	3.460
120	1.980	2.358	2.617	3.160	3.373
200	1.972	2.345	2.601	3.131	3.340
500	1.965	2.334	2.586	3.107	3.310
1000	1.962	2.330	2.581	3.098	3.300
∞	1.960	2.326	2.576	3.090	3.291

5. CURRENT ENERGY SITUATION

Energy is fundamental in the evolution of human condition. People´s survival is closely linked to their need for energy, and therefore energy production and consumption are two of the most important activities of humanity. Energy plays a fundamental role in the development of the civilization and currently society is dependent on the conversion of energy. It is rarely disputed the long-held assumption that the quality and standard of living of people is proportional to the quantity of energy used by a society (Basalla, 1980).

The development of energy is directly related to the evolution of civilization. Throughout history, the control of energy sources and flows has been the obsession of humanity. For tens of thousands of years, human only knew the caloric energy obtained from food converted into mechanical energy of working muscles. However, the human intellect developed the use of energy sources outside their own body and overtook their limits by using tools (Smil, 1994).

An adequate, secure, accessible and affordable supply of energy is crucial for the development of modern societies, eradication of poverty and improvement of human welfare. 24 hours cut in electricity in a city shows how much a society depends on the energy supply. The society, as we know it nowadays, would collapse without energy. Energy directly influences in the economic development and wealth generation. It could be defined as the convertible currency of the technology (Dincer, 2000).

5.1 ENERGY CONSUMPTION DEVELOPMENT

With the evolution of civilization, the global demand for energy has rapidly risen with the growth of human population, urbanization and modernization. The world population in 1800 was estimated to be around 1 billion (the first population census was introduced around that time in Sweden and England, so the estimation is quite uncertain). The global population in 2005 was 6.5 billion, whilst the population in the year 2015 was 7.35 billion. It has increased a 1.2% averaged yearly between the 2005 and 2015, therefore the population is 12.73% higher in 2015 than it was in 2005.

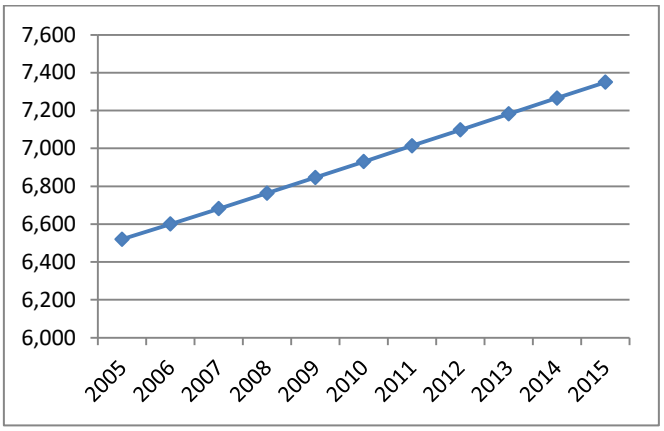

Figure 5.1: Evolution of global population (billion people) (World population prospect.2015)

The population of the world continues to increase at an alarming rate. Developing countries usually have higher growth rates despite lower accessibility to financial resources. This population growth is the result of a greater number of births than death, and it is called the "natural" growth. This can be affected by significant contributors such as contraceptive measures and abortion, wars and immigration and emigration (Population growth by country.2016).

The following table (see Table 5.1) shows how the population has progressed in the last years in different continents and regions of the world. The increase of population in Africa, which contributes the 16.14% of the global population, has been the greatest, being 28.90% higher in 2015 than 10 years ago (year 2005).

The population in Asia constitutes the 59.78% of the global population, and it has grown 11.37% in the last 10 years. The inhabitant quantity in Latin America and the Caribbean and Oceania has also risen 12.51% and 17.87% respectively between 2005 and 2015.

Potential causes of this growth in population are mentioned to be the decline in mortality rates for total and infant population, high fertility rates and immigration.

On the contrary, it is worth mentioning that in Europe and Northern America, where almost every nation´s financial situation is mature, the population has increased only 1.29% and 8.92% respectively.

The reasons of the slower growth in population in developed nations are thought to be the abundant availability of contraceptive options, changes in migratory trends in the countries

and increased education opportunities for women, which causes reduction in birth rates (Population growth by country.2016).

Table 5.1: Evolution of the global population (World population prospect.2015)

	2005	2010	2015	Increase (%)
WORLD	**6,519,636**	**6,929,725**	**7,349,472**	**12.73%**
AFRICA	**920,239**	**1,044,107**	**1,186,178**	**28.90%**
Egypt	74,942	82,041	91,508	22.11%
Morocco	30,385	32,108	34,378	13.14%
Zambia	12,044	13,917	16,212	34.61%
ASIA	**3,944,670**	**4,169,860**	**4,393,296**	**11.37%**
Bahrain	867	1,261	1,377	58.82%
India	1,144,326	1,230,985	1,311,051	14.57%
Kuwait	2,264	3,059	3,892	71.91%
EUROPE	**729,007**	**735,395**	**738,442**	**1.29%**
Portugal	60,210	62,717	64,716	7.48%
Spain	43,855	46,601	46,122	5.17%
UK	60,210	62,717	64,716	7.48%
LATIN AMERICA AND THE CARIBBEAN	**563,826**	**599,823**	**634,387**	**12.51%**
Argentina	39,145	41,223	43,417	10.91%
Brazil	188,479	198,614	207,848	10.28%
Venezuela	26,769	28,996	31,108	16.21%
NORTHERN AMERICA	**328,524**	**344,129**	**357.838**	**8.92%**
Canada	32,256	34,126	35,940	11.42%
EEUU	296,140	309,876	321,774	8.66%
OCEANIA	**33,369**	**36,411**	**39,331**	**17.87%**
Australia	20,274	22,163	23,969	18.23%
New Zealand	4,135	4,369	4,529	9.53%

It is also worth mentioning the increase of Barhain and Kuwait, which it has been 58.82% and 71.91% respectively. Even though they represent only the 0.03% and 0.09% of the total population in Asia, the fast-economic growth of the zone has accelerated considerably the population increase.

On the contrary, in the European countries such as Spain and United Kingdom (UK), the population growth is not that significant. In Portugal, there are fewer inhabitants nowadays than in the year 2005.

The trend in the coming years will be similar, and it is expected that economic development will continue to grow, which will directly affect in the population progress. The rapid population increase will take place above everything in developing countries (see Table 5.2). The estimations of the United Nations (UN) Population Division project that the population in Africa will double in 35 years. On the contrary, the population in Europe will be 4.29% lower than nowadays in the 2050.

Table 5.2: Population estimation by continents (World population prospect.2015)

	2015	2020	2030	2040	2050	2015-2050
Africa	1,186,178	1,340,103	1,679,301	2,063,030	2,477,536	**108.87%**
Asia	4,393,296	4,598,426	4,922,830	5,143,850	5,266,848	**19.88%**
Europe	738,442	739,725	733,929	721,355	706,793	**-4.29%**
Latin America and the Caribean	634,387	666,502	721,067	760,484	784,247	**23.62%**
Northern America	357,838	371,269	396,278	416,364	433,114	**21.04%**
Oceania	39,331	42,131	47,361	52,150	56,609	**43.93%**

Population increase necessarily implies higher energy consumption. But the increase in energy consumption is not linearly related to the rise in global population, the energy demand grows more quickly than the population (Dincer & Zamfirescu, 2014). In the last 200 years, the population has risen by a factor of 7, while the energy consumption is 20 times higher nowadays. Current energy use in rural areas of developing countries and estimations of the energy consumption in the past based on historic statistics, suggest that global average energy use in the 1800 was not higher than 20 GJ per capita (Asif & Muneer, 2007).

The demand for energy has risen together with the evolution of civilizations; it establishes the transition from penury to abundance (Muneer, 2010). While in the last century, the largest use of residential electricity was for lighting and appliances, nowadays, communication devices, computer, entertainment and the internet compound an important part of the electricity consumption (Dincer & Zamfirescu, 2014). Modernization trends across the world directly affect on the increase of the energy use, and it will

continue to rise while developing countries reach developed status and developed countries maintain their modernization tendency (Muneer et al., 2005).

Looking over the past records of industrialized countries profligate use of energy, developing countries are following the same energy consumption pattern. Migration to the already crowded cities of impoverished people looking for opportunity, as a result to people´s aspiration for improved life, accelerates the urbanization (Asif & Muneer, 2007).

Access to energy sources is a basic requirement for the economic and social development of any country (Muneer et al., 2005). Therefore, due to these facts, the per capita energy demand will continue to increase as the economy grows. The energy consumption has risen 9% in the 2010-2015-time period; while the population has increased 6% in the same period (see Figure 5.2).

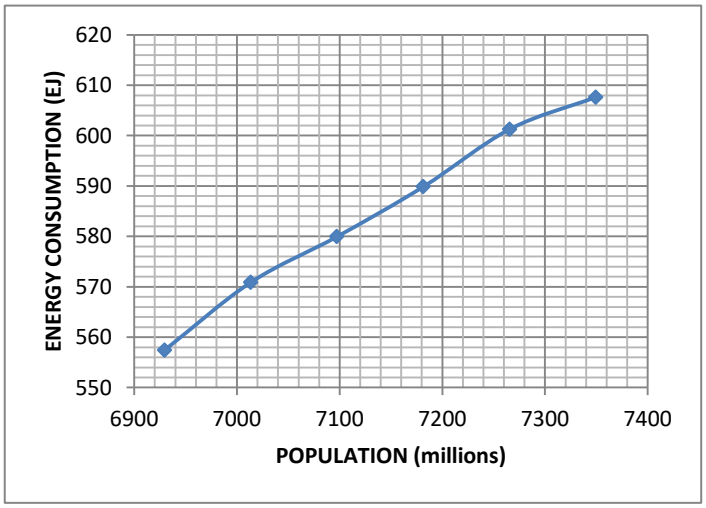

Figure 5.2: Energy consumption (exajoules) vs population (millions) (International energy outlook 2016.2016)

The UN estimations of the world population suggest that by 2030 there will be 8.5 billion inhabitants in the world, and the year 2040 the population will be 9.16 billion, 24.6% more than in 2015 (World population prospect.2015).

According to the worldwide energy demand, the International Energy Outlook (IEO) forecasts strong increase up to 2040. The global consumption is expected to rise 41.62% over the 2015-2040-time period.

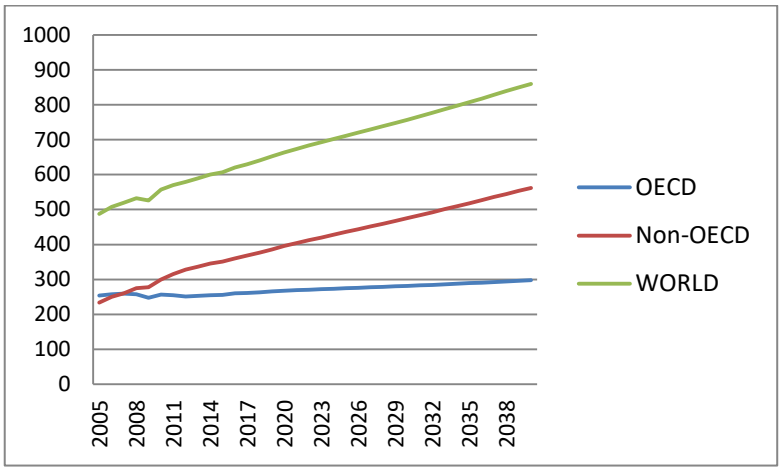

Figure 5.3: Evolution of energy consumption (International energy outlook 2016.2016)

* *OECD = Organization for Economic Cooperation and Development: Australia, Austria, Belgium, Canada, Chile, the Czech Republic, Denmark, Estonia, Finland, France, Germany, Greece, Hungary, Iceland, Ireland, Israel, Italy, Japan, Latvia, Luxembourg, Mexico, the Netherlands, New Zealand, Norway, Poland, Portugal, Slovakia, Slovenia, South Korea, Spain, Sweden, Switzerland, Turkey, the United Kingdom, the United States.*

The graph above (see Figure 5.3) shows the evolution of the energy use for OECD * and non-OECD countries according to the IEO2011 historical data and IEO2016 estimations. As reported by the IEO, the energy consumption of the emerging countries (non-OECD countries) exceeded the developed countries (OECD countries) consumption in 2007. In the 2010, the energy demand in the developing countries was already 16.62% higher than in the industrialized nations, while in the 2015 the difference was of 36.89%.

The records from the Statistical Review of World Energy by British Petroleum (BP) show similar result about the OECD and non-OECD countries energy consumption data in the years 2010 and 2015, confirming the International Energy Outlook predictions. In this case, the energy demand is 17.47% and 38.91% higher in the non-OECD nations respectively (International energy outlook 2016.2016; BP statistical review of world energy.2016).

It is also worth mentioning that the estimates of IEO2016 suggest that the use of energy in the non-OECD regions by the 2040 will be 88.87% higher than in the OECD regions.

Table 5.3: Energy consumption by region (BP statistical review of world energy.2016)

Energy consumption (EJ)				
	2005	**2010**	**2015**	**2005-2015**
WORLD	**458.04**	**510.01**	**550.45**	**20.18%**
AFRICA	**13.75**	**16.34**	**18.21**	**32.42%**
Algeria	1.37	1.63	2.29	66.97%
Egypt	2.60	3.38	3.61	38.81%
TOTAL ASIA PACIFIC	**155.15**	**196.23**	**230.21**	**48.38%**
India	16.48	22.65	29.33	77.97%
Australia	5.06	5.43	5.50	8.68%
MIDDLE EAST	**23.77**	**31.07**	**37.04**	**55.81%**
Kuwait	1.28	1.45	1.72	34.43%
EUROPE	**124.15**	**123.45**	**118.67**	**-4.41%**
Portugal	1.06	1.07	1.01	-5.12%
Spain	6.38	6.12	5.63	-11.75%
UK	9.58	8.81	8.01	-16.47%
LATIN AMERICA	**22.24**	**26.54**	**29.28**	**31.67%**
Argentina	2.89	3.33	3.66	26.81%
Brazil	8.69	10.92	12.26	41.11%
Venezuela	2.95	3.38	3.37	14.35%
NORTHERN AMERICA	**118.98**	**116.38**	**117.04**	**-1.63%**
Canada	13.56	13.25	13.81	1.85%
EEUU	98.40	95.68	95.48	-2.96%

The table above (Table 5.3) show how energy demand has evolved in the 2005-2015 period in different regions of the world.

The growth of the consumption of energy resources for Africa, Pacific zone of Asia, Latin America and Middle East have been 32.42%, 48.38%, 31.67% and 55.81% respectively. In the developed countries of Europe on the other hand, the energy consumption has decreased 4.41% in 10 years. In the Northern America nations, the energy demand has also decreased 1.63% in the same period.

According to the energy consumption evolution, the IEO estimates that the energy demand will increase up to 60.24% in the non-OECD nations between the years 2015 and 2040; while the energy demand rise in the OECD nations will be 16.14% for the same period (IEO2016). This is a direct consequence of the progress of the developing countries to developed status (International energy outlook 2016.2016).

Most estimations regarding the energy demand predict a growth of around 0.8% a year until 2020 for the developed countries while in the developing countries, while the same period, the energy demand is expected to rise 2.25% a year. The global consumption growth is estimated to be of an average of 1.8% a year. During the 2020-2040 period, the energy demand rise will slow down. The increase for developed and developing countries will be 0.5% and 2% a year. The estimates predict that the global energy demand will grow 1.3% a year (International energy outlook 2016.2016; Muneer et al., 2005). Therefore, the global energy consumption will grow as nations across the world keep on searching for increased prosperity.

There are several indicators which measure the standard of living. The gross domestic product and life expectancy are two important index of well-being. The table below (see Table 5.4) shows the gross domestic product, life expectancy and energy consumption per capita values for different nations.

Table 5.4: GDP, life expectancy (The world factbook.2016), energy consumption (The world bank.2016) and CO_2 emission per capita (CO2 emissions from fuel combustion highlights 2016.2016) in different regions

		GDP (thousands of $/capita)	**Life expectancy** (years)	**Energy consumption** (J/capita)	**Tonnes CO2/capita**
AFRICA	Algeria	14,500	76.8	5.22E+10	3.1574
	Egypt	11,800	72.7	3.71E+10	1.9342
TOTAL ASIA PACIFIC	India	6,200	68.5	2.54E+10	1.5592
	Australia	65,400	82.2	2.34E+11	15.8122
MIDDLE EAST	Bahrein	50,100	78.9	4.26E+11	21.7967
	Kuwait	70,200	78	4.09E+11	22.936
EUROPE	Portugal	27,800	79.3	8.72E+10	4.116
	Spain	34,800	81.7	1.05E+11	4.9929
	UK	41,200	80.7	1.25E+11	6.3136
LATIN AMERICA &THE CARIBBEAN	Argentina	22,600	77.1	7.93E+10	4.4768
	Brazil	15,600	73.8	6.02E+10	2.3099
	Venezuela	16,700	75.8	9.51E+10	5.0495
NORTHERN AMERICA	Canada	45,600	81.9	3.02E+11	15.6089
	EEUU	55,800	79.8	2.9E+11	16.2176

These data show that it is possible to achieve well-being at much lower levels of energy use index. Further energy consumption should be considered as either energy wastage or luxury. Portugal, Spain and UK are good examples of the previously mentioned fact. Bahrein and Kuwait, on the contrary, are clear examples of excesive energy wastage.

The Table 5.5 shows the evolution of the energy consumption in different sectors during the period 2010 and 2015 according to the sources of the United States Energy Information Administration (EIA) (International energy outlook 2016.2016). It also shows the estimated consumption for the following years.

Table 5.5: Energy consumption evolution by end-use sector (International energy outlook 2016.2016)

	2010	2011	2012	2013	2015	2020	2025
Residential sector	55.43	55.32	55.96	58.39	61.76	64.51	69.05
Commercial sector	30.41	30.62	30.93	32.10	34.00	36.43	39.28
Industrial sector	220.98	229.11	234.70	236.29	241.57	259.52	277.25
Transportation sector	105.90	108.54	110.01	112.23	115.08	122.26	129.76
Electric power sector	213.59	220.03	222.46	227.52	236.39	264.58	287.81

There are a couple of facts in the records that are worth mentioning.

First, the energy consumption in the industrial sector and electricity generation are the most relevant of all sectors. The Figure 6.4 show the contribution of each sector in the total energy consumption, being 35% and 34% the share of the industrial sector and electricity eneration respectively.

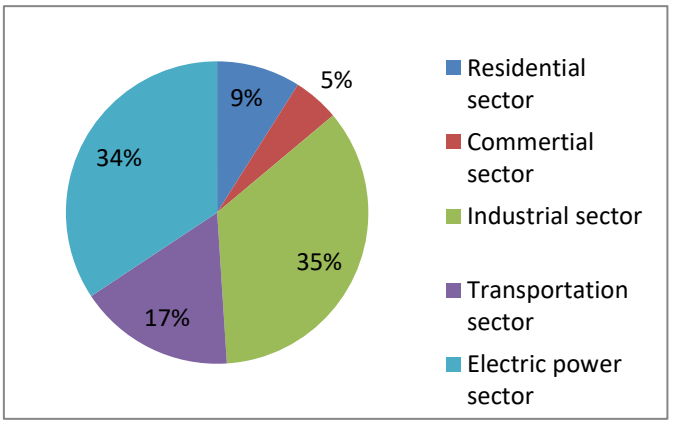

Figure 5.4: Energy consumption by end-use sector in 2015 (International energy outlook 2016.2016)

Secondly, the increase of the energy consumption in the residential sector, commercial sector and electric power sector was 11.4%, 11.8% and 10.6% respectively between 2010 and 2015 (see Table 5.5). It is expected that the electric power sector will suffer the strongest growth in the next decade. The IEO has estimated that it will increase 22% between 2015 and 2025 (International energy outlook 2016.2016).

5.2 FOSSIL FUELS AND NUCLEAR ENERGY SCENARIO

Any form of energy available on Earth, which can be converted into a useful form such as heat, electricity or mechanical power, is known as an *energy resource*. These energy resources are classified in three groups: fossil fuels, nuclear fuels and renewable energies. Energy resources are substances stored in the earth´s crust (fossil and nuclear fuels), flows (wind or water currents), lakes (potential energy of the water), thermal energy from inside the earth, sun´s electromagnetic energy (sunlight), and gravitational forces from the earth´s, moon´s and sun´s interaction (Dincer & Zamfirescu, 2014).

5.2.1 Fossil fuels

Historically fossil fuels, in their various forms, have served the human energy needs for thousands of years. These fuels, known as conventional or traditional fuels, are classified in three classes of materials: coal, oil (petroleum) and natural gas (Muneer et al., 2005).

Coal is a black or brownish-black sedimentary rock, mainly formed from organic substances obtained from fossilized plants with inserted mineral inclusions, which contains the energy stored by plats that lived hundreds of millions of years ago.

It is composed with a high amount of carbon, which is its primary chemical element, and hydrocarbons. Coal has an over 70% content of carbon by weight. It takes millions of years to form, and therefore it is classified as a nonrenewable energy source.

There are four main types of coal depending on the amount of carbon they contain and on the amount of heat energy, typically between 25-35 MJ, the coal can generate. Anthracite contains 86-97% of carbon and its heating value is usually the highest. Bituminous coal contains 45-86% carbon. It is followed by subbituminous coal, which typically is compounded by 35-45% of carbon. Its heating value is lower than the bituminous coal. The lignite coal has the lowest heating value, and it contains 25-35% carbon. These compositions

and heat values are determined by the pressure and heat that dirt and rocks covering the plants caused on them for millions of years (International energy outlook 2016.2016).

Major power plants and industrial processes in the metallurgical and cement industries mainly use coal as their energy source (Dincer & Zamfirescu, 2014).

Petroleum or crude oil is a mixture of hydrocarbon-based materials formed from plants and animals that lived millions of years ago. It is mainly found in liquid in very small spaces between sedimentary rocks in underground pools, or near the surface in tar sands (International energy outlook 2016.2016).

Alkanes, cycloalkanes, aromatics, paraffin, and naphthalene are the main components of petroleum. When the crude oil is taken from the reserves, it is sent to a refinery to separate the oil in different useable petroleum products. Gasoline, distillates such as diesel fuel and heating oil, jet fuel, waxes and lubricant oils are among others some of those products. Petroleum is mainly used in the transportation sector (Dincer & Zamfirescu, 2014).

Natural gas mainly contains methane, but iT also contains lesser amounts of hydrocarbon gas liquids and nonhydrocarbon gases. The same as coal and petroleum natural gas is found deep beneath the earth´s surface, where it was formed millions of years ago, when the remains of plants and animals decayed and accumulated in thick layers; and over time, sand, silt and rocks buried these layers (International energy outlook 2016.2016).

Although natural gas can be found all over the world, the Russian Federation has the largest reserves. This gas is mainly used in industries, fertilizer production and as domestic fuel for heating, cooking and sometimes for power generation (Dincer & Zamfirescu, 2014).

Wood and coal were the very first form of fossil fuels which served the society´s energy demand for a long time. It used to be a sustainable and stable energy source, since resources and forest were enough to fulfill the demand. Especially with the industrialization of the 19th century, civilization search for a higher efficiency in the energy technology, and the refined liquid phase fossil fuel, oil was created. Some time afterwards, natural gas, the gaseous phase of fossil fuels, was discovered. This fuel is even more efficient than oil (Asif & Muneer, 2007).

Fossil fuels are by far the most used energy source nowadays. However, these conventional energy resources face two major problems: depletion of resources and environmental impacts. These threats will be analyzed in depth in the 4.3 section.

5.2.2 Nuclear fuel

Nuclear energy is a largely carbon-free energy source which in theory could solve the problems associated to fossil fuels. This energy fuel is based in the energy concentrated in the core of the atoms.

Atoms are tiny particles made up of protons, neutrons and electrons. The core or nucleus of the atom contains protons and neutrons and it is surrounded by electrons. The energy present in the bonds that hold the nucleus together is enormous, and this energy can be released when those bonds are broken. In the nuclear fission, the atoms are split apart, and the energy released can be used to produce electricity.

This reaction takes places in nuclear power plant reactors, and most of them use uranium atoms to perform nuclear fission. Although uranium is a common metal found in rocks, nuclear energy source is considered to be nonrenewable (International energy outlook 2016.2016).

5.3 PROBLEMS ASSOCIATED WITH FOSSIL FUELS

As mentioned in the section 4.2 and according to data from the BP Statistical Review of World Energy June 2016 (BP statistical review of world energy.2016) fossil fuels are by far the leading energy source around the world. In the 2015, the 32.94% of the world energy demand was generated from petroleum, the 23.85% from natural gas and the 29.21% from coal. The remaining 9.57% was generated using renewable energy sources, while the 4.44% of the global consumption was provided from nuclear fuel.

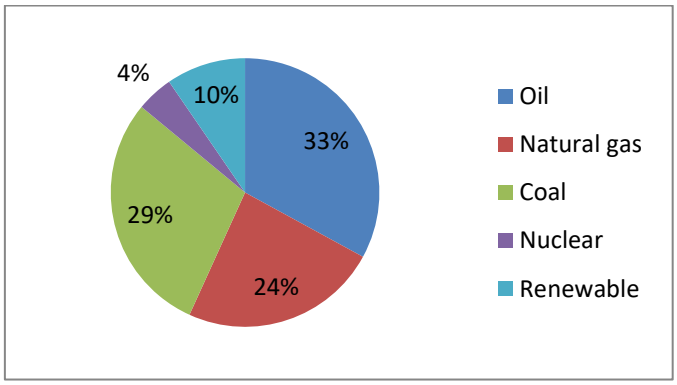

Figure 5.5: Energy consumption from different energy sources, 2015 (BP statistical review of world energy.2016)

This means that the 86% of the energy demand was provided from conventional fuels (see Figure 5.5).

Fossil fuels have a crucial importance in the world energy market (Shafiee & Topal, 2009). The Figure 5.6 shows the evolution of the energy consumption from different energy sources (in exajoules) in the 2004-2015 period.

The world heavily depends on fossil fuels (oil, natural gas and coal) to meet its energy demands (BP statistical review of world energy.2016). The enormous amount of energy generated from conventional fuels is negatively affecting the ecosystem of the planet (Asif & Muneer, 2007).

According to the estimated energy consumption values of the International Energy Outlook 2016, the energy sources in the upcoming years will not suffer substantial changes.

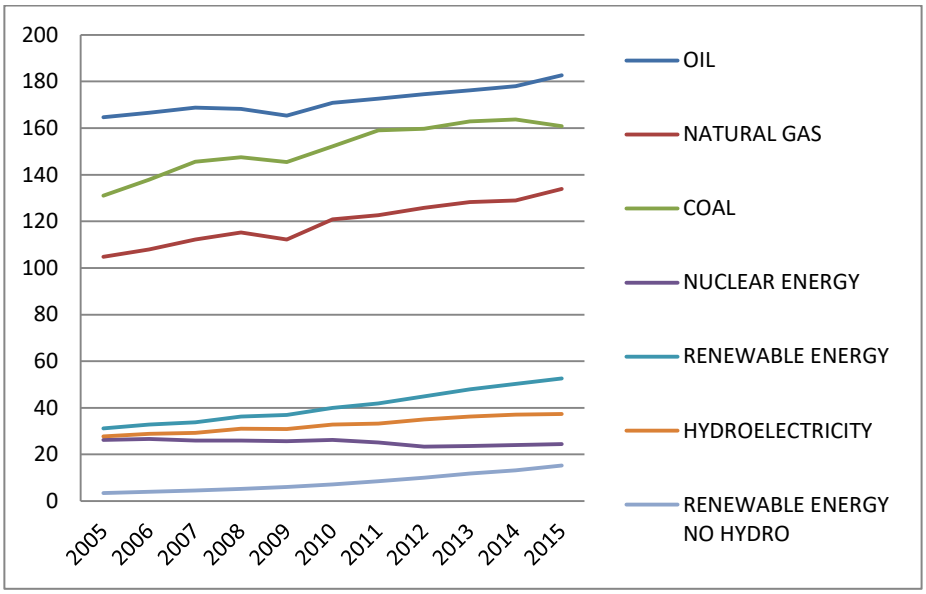

Figure 5.6: Evolution of energy consumption (EJ) by energy source (BP statistical review of world energy.2016)

Although the tendency will be lowering the dependence on fossil fuels, the data show that in the 2040 conventional fuels will still hold the major share of global energy supply (see Figure 5.7). The 78.24% of the total energy consumption is expected to be generated from fossil fuels (BP statistical review of world energy.2016).

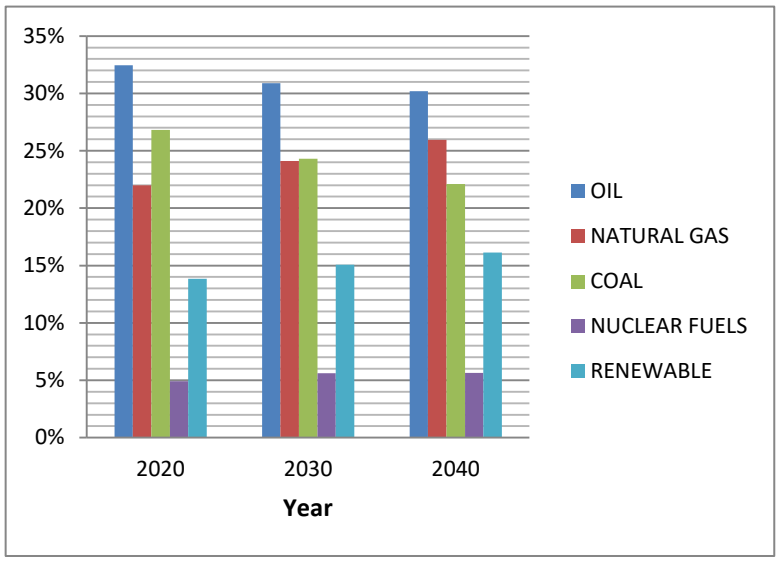

Figure 5.7: Energy consumption projections by energy source (International Energy Outlook 2016.2016)

The rapid diminishing of coal, petroleum and natural gas reserves across the world and the enormous environmental impact are the two major problems surrounding the disproportionate consumption of fossil fuels (Muneer et al., 2005). However, this

unsustainable situation also generates geopolitical and military conflicts and continuously rising energy cost (Asif & Muneer, 2007).

5.3.1 Fossil fuel depletion

Fossil fuels reserves are rapidly declining around the world. Nowadays, the world consumes in six weeks as much oil as it was burned in 1950 (Muneer et al., 2005), since, as mentioned in the previous chapter, energy consumption is increasing as the global population and development of countries are growing. This upcoming demand increases the stress on existing fuel reserves. There are various projections of global ultimate conventional oil reserves and when they will diminish. A high number of opinions among energy experts claimed that oil production would peak between 2004 and 2010. The University of Uppsala in Sweden also suggested that oil supplies would peak soon after 2010, and natural gas supplies immediately after that (Asif & Muneer, 2007). It was also reported by BP in the year 2003 that reserve to production ratio of fossil fuels in North America, Europe and Eurasia, and Asia Pacific was 10, 57 and 40 year respectively.

Views about world fossil fuel reserves differ and it is not possible to predict exactly when supplies will be exhausted. According to Salameh global oil supplies will stop meeting demand when between 2013 and 2020 oil production has peaked (Salameh, 2003). Turkey was shown as a typical example for emerging energy market in the developing country (Ediger, Akar, & Uğurlu, 2006). In the 2007 Asif and Muneer showed the energy reserves and years to depletion of non-renewable energies for India, China, Russia and Ethiopia based on a compound growth rate. The estimated years to exhaustion are about 315, 83, 1034 and 305 respectively for each country (Asif & Muneer, 2007). Thielemann et al. believe, from a geoscientific perspective that in the year 2100 there will be no bottleneck in coal supplies in the world (Thielemann, Schmidt, & Gerling, 2007).

Shafee and Topal claim that reserves of oil and gas did not diminish in the last decades, and they predict, using the three econometric models they have developed, that the depletion time for oil, coal and gas will be 35, 107 and 37 years respectively (Shafiee & Topal, 2009).

In the last years, many countries such as the USA, India and Ethiopia are trying to discover coal reserves. In fact, there have been new coal reserves discoveries in USA, Venezuela, Iran and Iraq among others. There are also attempts to find new clean coal utilization techniques (Khadse, Qayyumi, Mahajani, & Aghalayam, 2007), for example, the Department

of Energy (DOE) in the USA claimed to have discovered the way to generate power increasing the 25% efficiency of the traditional coal-fired power plants to over 50% through fuel cells and coal gasifiers based on Solid State Energy Conversion Alliance (SECA), including CO2 capture processes (Shafiee & Topal, 2009).

Due to the discovery of new reserves the fossil fuels will last longer than expected. Global proven oil reserves have increased by 24% over the last century but the reserves are enough to only meet 50.7 more years of oil consumption. The reserves of South and Central America will last the most, according to the current consumption they will diminish in 117 year, while the reserves in Asia Pacific will only last 14 years. As shown in the Figure 5.8, almost the half of the oil reserves is placed in the Middle East.

Natural gas has increased its reserves by 29.6 trillion cubic metres (tcm) over the last decade. Once again, the Middle East region holds the 42.8% of the global total reserves, and in this case, it has the highest reserve to production ratio, which is 129.5 year. The total reserves around the world are sufficient to meet 52.8 years of current production (BP Statistical Review of World Energy. 2016).

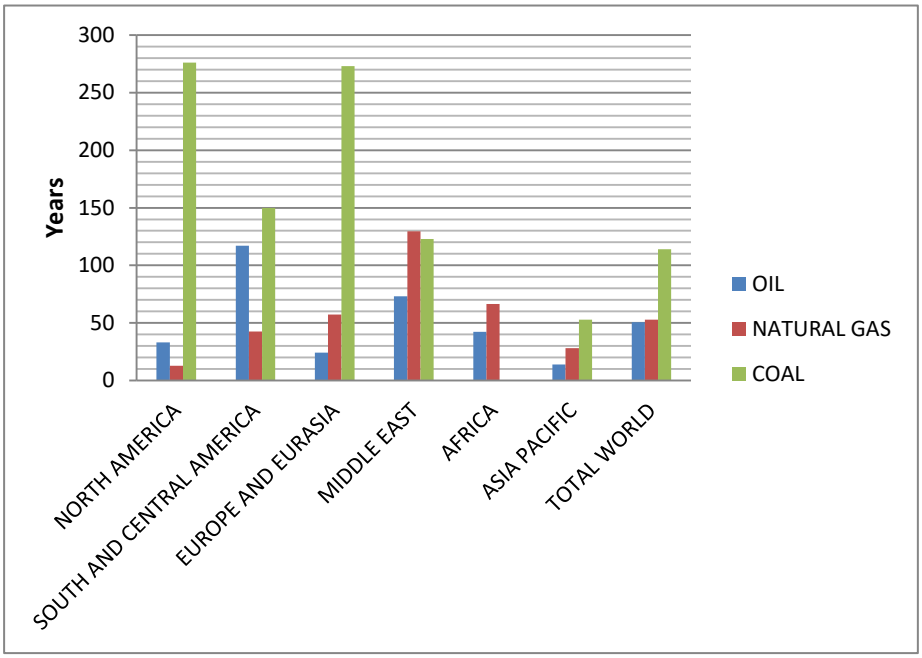

Figure 5.8: Reserve to production (R/P) ratio of fossil fuels y regions (BP Statistical Review of World Energy. 2016)

World coal reserves have by far the highest reserve to production (R/P) ratio for any fossil fuels. The reserves in 2015 were estimated to be enough to meet 114 more years of global production. By region, North America has the highest R/P ratio, 276 years. Europe and

Eurasia holds the largest proved reserves, and Asia Pacific holds the second largest reserves. However, the latter has a much higher production rate and this leaves the region with reserves for 53 more years, the lowest regional R/P ratio (BP Statistical Review of World Energy. 2016).

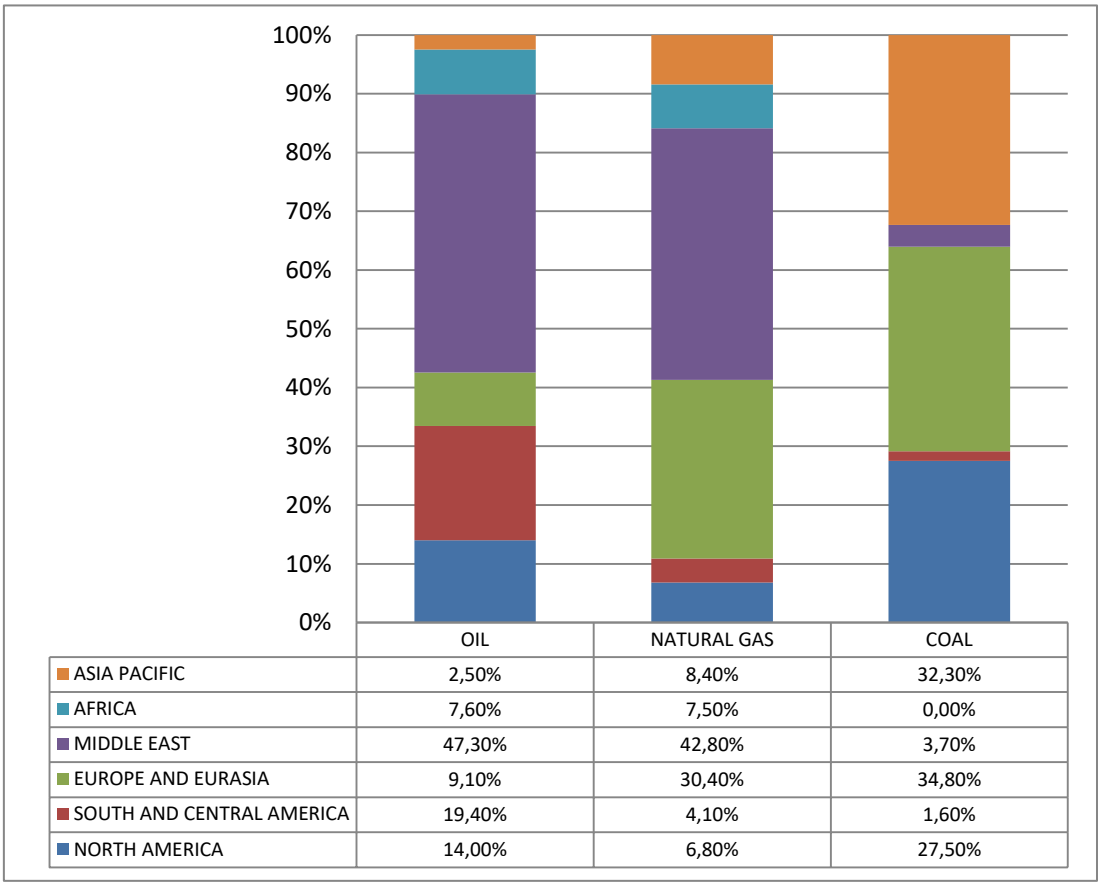

	OIL	NATURAL GAS	COAL
ASIA PACIFIC	2,50%	8,40%	32,30%
AFRICA	7,60%	7,50%	0,00%
MIDDLE EAST	47,30%	42,80%	3,70%
EUROPE AND EURASIA	9,10%	30,40%	34,80%
SOUTH AND CENTRAL AMERICA	19,40%	4,10%	1,60%
NORTH AMERICA	14,00%	6,80%	27,50%

Figure 5.9: Consumption oil, natural gas and coal by region (BP Statistical Review of World Energy. 2016)

According to Shafiee and Topal, coal constitutes approximately 65% of the fossil fuel reserves in the world. Besides, the location of the reserves of coal is not limited to one region, as it happens with oil and natural gas in the Middle East (see Figure 5.9).

These two geological facts support the fact that coal has the potential to be the most important fuel soon.

However, fossil fuel reserves trend mainly depends on two parameters, which are consumption and price. The annual energy consumption will increase at an average rate of 1.1%, according to the predictions of the Energy Information Administration (EIA). On the other side, economic conditions will affect the fluctuation of proven fossil fuel reserves. Therefore, fossil fuels reserves are dependent on their price (Shafiee & Topal, 2009).

5.3.2 Environmental impact

Energy and environment are intimately related. The present energy situation, led by fossil fuels, has an enormous and negative impact in the environment. Energy sector has a high responsibility in this regard since the substances that are generated during the production, distribution and consumption of the energy, result in undesirable environmental effects causing global impacts (Dincer & Zamfirescu, 2014).

During the last three decades, the risk and reality of environmental degradation have become more apparent. The environmental impact of human activities has grown dramatically due to the increase of world population, consumption, and industrial capacity among others (Dincer, 2000). Due to the coal exploration lands are degrading and the impact of mining on forest areas is worrying. Besides, the fluid and solid wastes generated when drilling for the onshore oil and gas production produce volatile organics with the potential to contaminate the surrounding water bodies.

Climatic impacts driven by human activities have dramatically changed the global environment. The Figure 5.10 shows a generic power production plant which consumes fuels to generate useful power, and in the process, it expels pollutants in the environment.

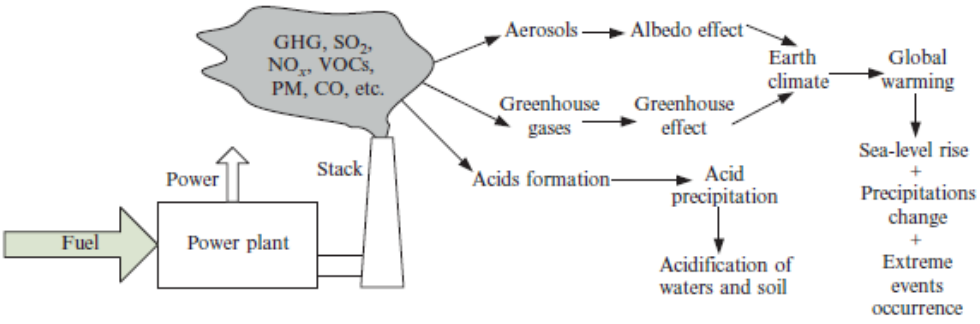

Figure 5.10: Environmental pollution from energy systems (Dincer & Zamfirescu, 2014)

This energy generation system causes pollutant and greenhouse gas (GHG) emissions, accidents, hazards, ecosystem degradation through air and water pollution, animal poisoning, carbon monoxide leakages, stratospheric ozone depletion and the emission of aerosols among others (Dincer & Zamfirescu, 2014). Throughout the 1970s legal environmental controls and analysis focused on conventional pollutants such as SO_2, NO_x or CO. Currently the environment concern and analysis is much more demanding and the control has extended to the globally significant pollutants such as CO_2, as well as to that of

micro air pollutants, which are usually toxic chemical substances and harmful in small doses (Dincer, 2000).

The spelled pollutants generated by the energy generation of the plant can be divided in two categories: GHG and aerosols. Greenhouse gases are the chemicals that produce the greenhouse effect. When released from natural and anthropogenic activities, they travel through the atmosphere and reach its upper layer, the troposphere. There, these gases absorb an important part of the infrared radiation emitted by the earth surface, causing the increase of the earth´s surface temperature (see Figure 5.10). This process is called the greenhouse effect (Dincer & Zamfirescu, 2014).

CO_2 is one of the most important greenhouse gases, and it is produced when energy is generated with conventional fuels and when forests are cut down and burned. It is estimated that CO_2 contributes about the 50% of the GHG (Dincer, 2000). During the last 150 years, CO_2 has been released at a rate of millions of times greater than the rate at which it was originally accumulated underground. Only through deforestation has released 20 Gt of carbon dioxide since 1800. However, there are many other gases contributing to the greenhouse effect. Agricultural activities and changes in land use emit methane (CH_4) and nitrous oxide (N_2O). Industrial processes generate halocarbons (CFCs, HFCs, PFCs) and other long-living gases such as Sulphur hexafluoride (SF6).

On the other hand, aerosols are continuously released to the atmosphere and concentrated in its upper layers. Aerosols reflect a portion of the incident solar radiation back into space, contributing to the earth´s albedo. This process is called the albedo effect.

The balance between the greenhouse and albedo effect establishes the earth´s temperature and regulates the earth´s climate. This climate control mechanism is a natural process. However, since the industrial revolution, the impact of the GHG has become more accentuated due to the increase of the emissions by energy, transportation and industrial sectors, inducing drastic changes in the environment and natural systems (Dincer & Zamfirescu, 2014).

Global warming leads the drastic changes in natural systems. Whether the cause is human activity or natural variability (and the evidences show it is humans), the world is getting warmer since the beginning of the Industrial Revolution. Global warming is the most important environmental problem related to energy consumption caused by the atmospheric concentration of GHG.

The ongoing temperature analysis performed by scientists at NASA´s Goddard Institute fof Space Studies (GISS) shows that the average global temperature on Earth has increased by about 0.8°C since 1880. Two thirds of the warming have occurred since 1975 at an estimated 0.15-0.20°C rate per decade.

Predictable cyclical events like night and day, summer and winter, and hard to predict wind and precipitation patterns cause significant variations in the temperatures that are experienced locally and in short periods. But the global temperature mainly depends on the amount of energy the planet receives from the sun and the amount it radiates back into space. The latter has high dependence on the chemical composition of the atmosphere, and the heat-trapping greenhouse gases affect significantly.

In order to know if a one-degree global temperature change is significant, it is enough to look in past records. A one to two-degree drop plunged the Earth into the Little Ice Age, and 20,000 years ago, a five degree drop buried a large part of North America under a towering mass (Earth Observatory.2014).

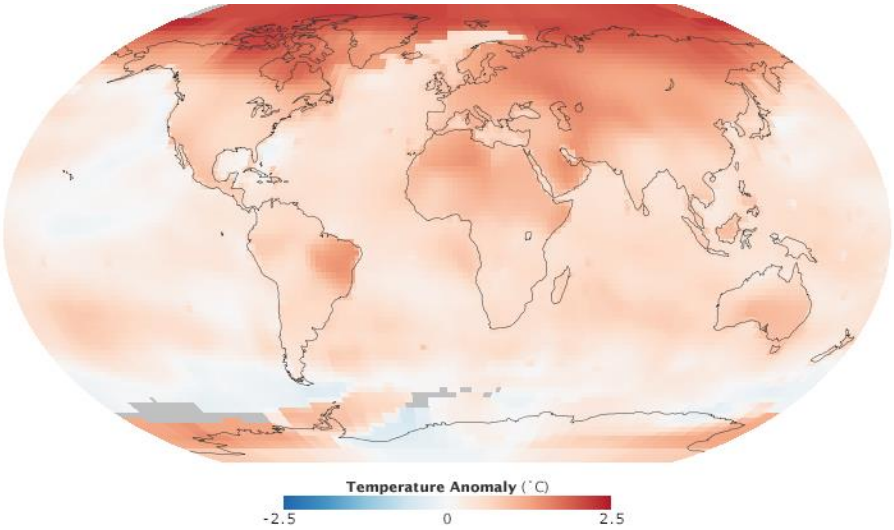

Figure 5.11: Temperature anomaly (Earth Observatory. 2014)

The map above (see Figure 5.11) compares how much warmer or colder a region nowadays than to the norm of that region in the 1951-1980-time period. The reason why this period was chosen as a base to compare temperatures is because the US National Weather Service uses a three-decade period to define average temperatures. The GISS began to analyze temperatures around 1980, so the most recent 30 years was the 1951-1980-time period (Earth Observatory.2014).

The figure below (Figure 5.12) shows the temperature values recorded by NASA (National Aeronautics and Space Administration), NOAA (National Oceanic and Atmospheric Administration), the Japan Meteorological Agency, and the Met Office Hadley Centre. Although there are variations, all of them show peaks and valleys in the same period, and more important, all of them show rapid warming in the past decades, being the last decade the warmest (Earth Observatory.2014).

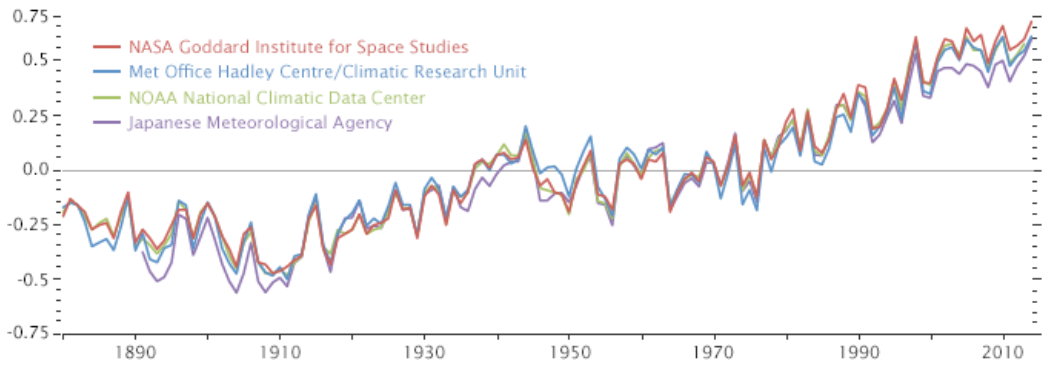

Figure 5.12: Annual temperature anomaly (°C) (Earth Observatory. 2014)

The increase in temperature causes dramatic impacts in the environment. The ice sheets and glaciers are melting at the highest rate since the record keeping began. Changes in the area and volume of the two polar ice sheets in Antarctica and Greenland are directly linked to the global climate changes, and could result in sea level increase. This fact would severally affect the densely populated coastal regions on Earth. Australian scientists' research suggested that the sea around Antarctica had shrunk 20% in the last 50 years, revealing new evidences of global warming (Muneer et al., 2005). The sea level is estimated to have risen 20 cm because of the permafrost ice melting (Dincer, 2000).

Many scientists predict that if fossil fuel consumption trend keeps the same as it is nowadays and the concentration of greenhouse gases continue to increase, the Earth´s temperature may increase another 2°C or even 4°C. It this happens, by the end of the 21st century the sea level could rise between 30 and 60 cm. This fact would have a dramatic impact, flooding coastal settlements, moving fertile zones for agricultural and food production to higher altitudes, and a decreasing availability of fresh water for irrigation and other basic uses. This phenomenon would put into risk the life of entire populations.

There has been observed changes in global precipitation patterns as well, and consequently there are more dry areas and more regional floating. Moreover, there is a higher frequency

of extreme events such as tsunamis, extreme winds, cyclones, earthquakes and tornadoes (Dincer & Zamfirescu, 2014).

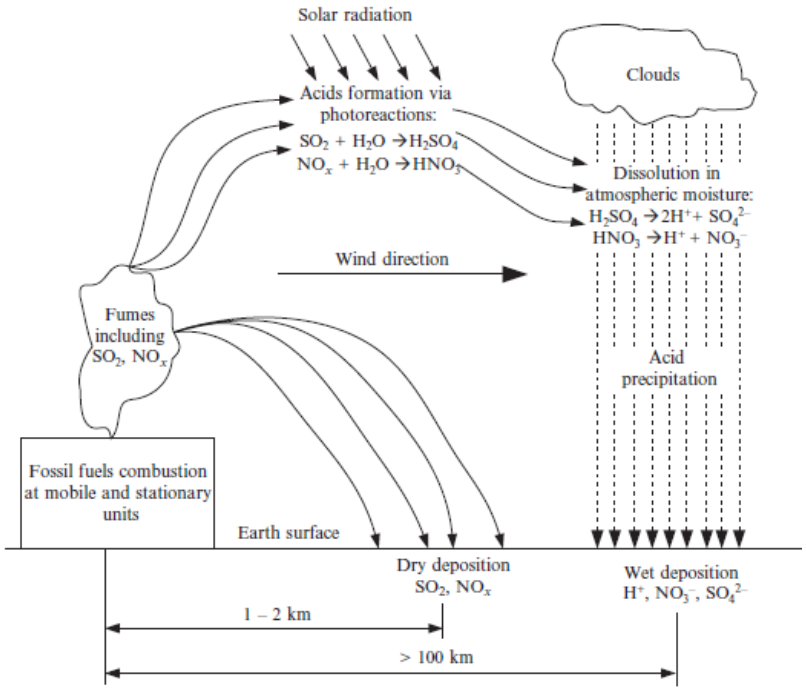

Figure 5.13: Acidic precipitation mechanism reference (Dincer & Zamfirescu, 2014)

Acidic precipitation is also a major environmental impact from energy systems (see Figure 5.13). Gaseous effluents expelled in the atmosphere particularly from both stationary and mobile sources such as smelters for nonferrous ores, industrial boilers, and transportation vehicle, can form acids that return to earth via precipitation on ecosystems that are exceedingly vulnerable to damage from excessive acidity. This acidification negatively affects all life systems as ecology of water systems and forests but it also affects to the historical and cultural ancient objects. The main sources of this acid rain deposition are the emissions of SO_2 and NO_x, mainly generated from electric power generation, residential heating and industrial energy use which account for 80% of SO_2 emissions, road transport is also an important source of NO_x emissions, and another source is sour gas treatment which produces H_2S that reacts to form SO_2 when exposed to air. These gases react with water and oxygen in the atmosphere and result in acids such as sulfuric and nitric acids. The acid rain produced by some countries often fall on other countries. The solution of this problem requires an appropriate control of these pollutants (Dincer, 2000).

The following evidences show the damages of acid precipitation (Dincer, 2000):

- Acidification of lakes, streams and ground waters.
- Toxicity to plants from excessive acid concentration.
- Damage to fish and aquatic life.
- Damage to forest and agricultural crops.
- Deterioration of materials.
- Influence of sulfate aerosols on physical and optical properties of clouds.

Another global environmental problem is the distortion and regional depletion of the stratospheric ozone layer. It is proven to be caused by the emission of CFCs, halons (chlorinated and brominated organic compounds) and NO_x. The ozone is located between altitudes of 12 and 25 km in the stratosphere and it naturally maintains equilibrium in the earth climate through the absorption of ultraviolet (UV) and infrared radiations. The depletion of the ozone can increase rates of skin cancer, eye damage and other harm to many biological species (Dincer, 2000).

The environmental impacts associated to the fossil fuel consumption are causing disastrous impacts not only on the environment but also on human health and economics. The World Health Organization 2004 year records show that as many as 160.000 people die each year from the side effects of climate change and the organization predicts that this number could double by 2020 (Muneer et al., 2005).

Climate change is also responsible for huge economic consequences. The economic loses associated to natural catastrophes such as floods and storms increased nine times between the 1960 and 1990-time period. According to Dincer economic loses between 1954 and 1959 were 35 billion United State Dollar (USD) while during the 1995 and 1999 period loses were around 340 billion USD. In the year 2004 as many as 190.000 people were killed in global warming associated natural catastrophes, doubling the people killed in 2003 (Dincer, 2000).

The current CO_2 emissions of industrialized countries are typically exceeding their sustainable limits. Records of CO_2 emissions show how the waste deluge has grown. Global CO_2 production increased from 27 to 30.45 billion tones between 2005 and 2010. In the 2011, 31 billion tonnes of CO_2 were emitted, and the 42% of the total was generated by the power sector, followed by transport with the 22% and industry generating the 21% of the global

emissions (Youinou, 2016). During the year 2014, the quantity of CO_2 emissions was 6.34% higher than in the year 2010, as much as 32.4 billion tons of CO_2 were emitted in just one year. The CO_2 level is projected to rise to 37.1 billion tones by the year 2025 if the current energy trend continues (see Figure 5.14, Figure 5.15 and Figure 5.16).

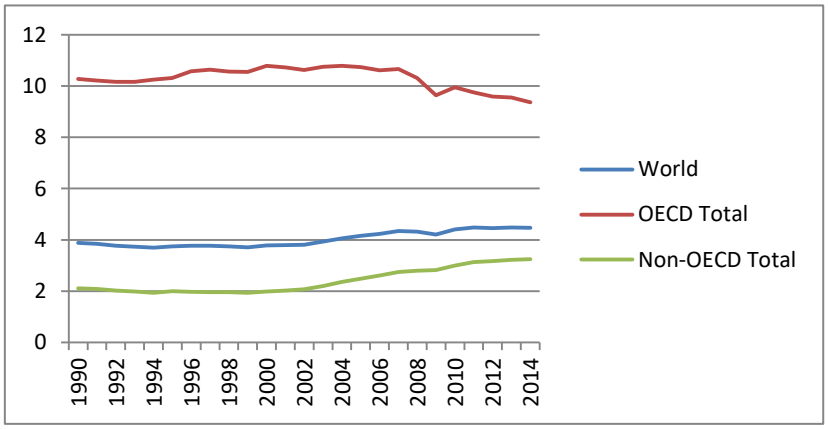

Figure 5.14: CO_2 emissions / population (tonnes CO_2/capita) (CO2 Emissions from Fuel Combustion Highlights 2016.2016)

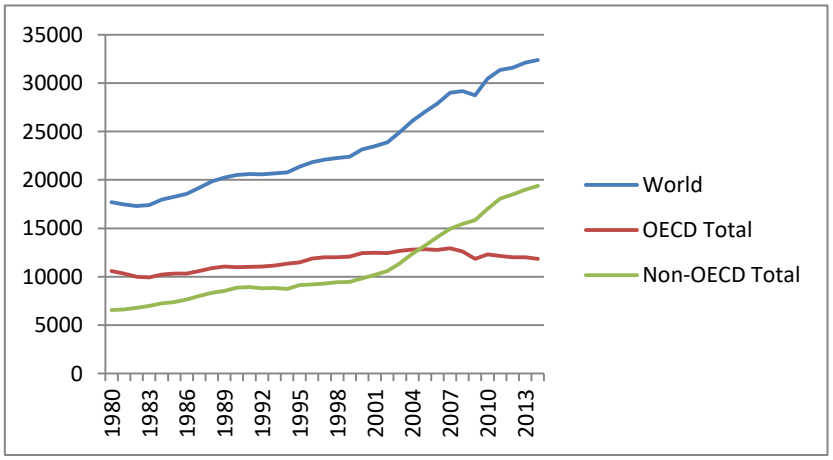

Figure 5.15: Million tonnes of CO_2 (CO2 Emissions from Fuel Combustion Highlights 2016.2016)

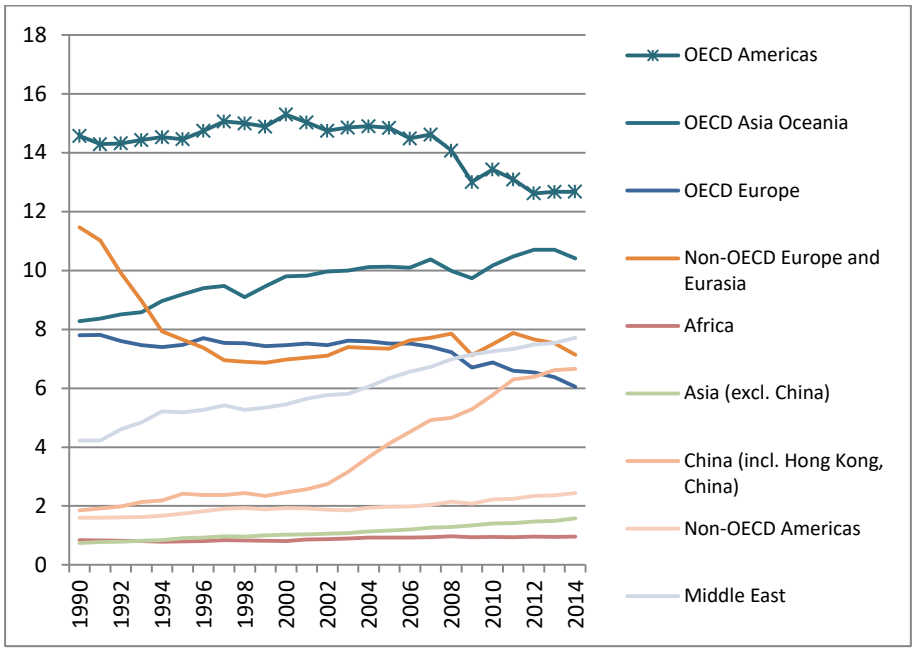

Figure 5.16: Tonnes CO2/capita (CO2 Emissions from Fuel Combustion Highlights 2016.2016)

Predictions of GHG emissions in the next 100 years are crucial in adapting the energy policy today and promoting the sustainable energy pathways (Dincer & Zamfirescu, 2014).

There are too many evidences showing that if the current energy consumption trend continuous unchanged, the degradation of the environment will have more and more negative impacts in the future. The humanity is not only facing global warming, but the hazard of air pollution, acid precipitation, ozone depletion, forest destruction, and emission of radioactive substances are real threats as well (Dincer, 2000).

5.3.3 **Security**

Energy security means a continuous availability of sufficient energy, at affordable prices and various forms. The economies all over the world and especially the ones of developed countries strongly depend on securing supplies of energy.

The conventional fuels reserves are unevenly distributed around the world, and this fact makes the energy security critical. Currently around the 50% of the oil is in the Middle East and due to the number of conflicts in the area, the region is considered as politically unstable.

The transportation from the well to the refineries and the storage in the service stations are complex, and they have always been a possible weakness of oil industry. However, the

threats of global terrorism and the present volatile geopolitical situation make this energy source even more unsecure.

Consequently, the present energy situation is not sustainable and secure supply of energy cannot be guaranteed. The effects of this unstable situation are already felt with price fluctuations when a minor event in the Middle East happens. An accident in the transportation of oil such as the sinking of a tanker or disruption of a major pipeline would have much more catastrophic economic and ecological effect (Asif & Muneer, 2007).

5.3.4 Oil price rise

The already mentioned increase of global demand for oil and the loss of production capacity of various oil rich countries in the world such as Iraq and Venezuela, led to the reduction of the excess oil production capacity. The current excess oil production is estimated to be less than one million barrels per day, which is not sufficient to cover an interruption of supply from almost any Organization of the Petroleum Exporting Countries (OPEC) producer (Boland, Huang, & Ridley, 2013).

Besides, the crude oil prices are enormously affected by the increase in demand of developing countries, extreme weather events and geopolitical features particularly in the Middle East (Asif & Muneer, 2007).

5.4 SUSTAINABILITY

It is increasingly accepted that energy consumers share responsibility for pollution and its cost. It has become an urgent issue to quickly change the energy systems from conventional to renewables that are sustainable, with the potential to meet the present and projected global energy demand. To limit the temperature increase caused by the GHG pollutants, the latest Inter-Governmental Panel on Climate Change (IPCC) report claims that the CO_2 emissions from the power sector need to be reduced at least by 90% below 2010 levels between 2040 and 2070.

If the energy consumption trend maintains unchanged, natural catastrophes frequency intensity will increase causing further damage to ecology of the world and in consequence to its inhabitants. Extreme weather events and sea level rise will damage physical

infrastructure. Water resources will also be affected with the variations on precipitation and vaporization patterns.

An immediate and radical change in the overall energy sector is needed to repair the already caused damaged of global warming and to avoid further threats (Dincer, 2000).

According to Youinou, nuclear energy is the second largest source of low-carbon electricity after hydropower (Youinou, 2016). It is true that nuclear power is a largely carbon-free energy source, and it could in theory replace fossil fuels. However, there are a range of problems associated to the use of nuclear power that have stopped its development for more than 20 years in most of Europe and North America (Muneer, 2010). Sackett ighlighted the following four critical challenged (Sackett, 2001):

- Cost: design variations, changes in safety requirements, large staffing requirements… are some of the facts that make the nuclear power twice as expensive as generating electricity from gas or wind.

- Radioactive waste: the radioactive gases that are produced in the nuclear power plants need to be contained in the operation of the plant. If these gases are released to the atmosphere, enormous health risks can occur. The mining and manipulation of the uranium used to produce nuclear energy are very risky and radiation leaks can occur. Furthermore, the spent radioactive nuclear fuel needs to be stored permanently. This fuel is toxic and its handling and disposal is an environmental threat for centuries. It is worth mentioning that the nuclear waste remains dangerous for 240,000 years.

- Safety: nuclear plants in developed countries are considered to be safe due to the high-level safety requirements. However, it is needed to monitor carefully many nuclear reactors operating in countries of the former Soviet Union to avoid another accident on the scale of Chernobyl.

- Proliferation of weapons materials: the material used to generate nuclear power could be proliferated to use in nuclear weapons.

In consequence of these four problems nuclear power is not only in a state of stagnancy but it is facing downward trend (Asif & Muneer, 2007). Furthermore, nuclear power is not cleaner than wind power. According to Hondo nuclear power has global warming potential

(GWP) of 22-30 gCO2/kWh while wind power´s GWP is 29 gCO2/kWh. In addition, nuclear power costs are estimated to double the fossil fuels costs (Hondo, 2005). In conclusion, nuclear energy is not an acceptable alternative to the fossil fuels.

As mentioned before, sustainable development is the solution to the current ecological, economic and development problems (Midilli, Dincer, & Ay, 2006).

6. SUSTAINABLE DEVELOPMENT

The extensive use of fossil based technologies and strategies have reached a level that is not tolerable anymore. The environmental degradation and social unstability are currently real threats and the long-term sustainability of the planet´s ecosystem is in a serious risk (Dincer, 2000). With the current energy system, it is imposible to find a balance between the production and consumption of energy and sustainability.

As mentioned in section 4, the massive consumption of conventional energy sources are facing 4 critical major problems: (a) environmental impact causing serious welfare and health problems, (b) depletion of the fuels, (c) safety problems associated to the unstable social and political situation of major fuel producer nations (d) and fluctuation of prices.

Apart from that, approximately the 17% of the global population (1.2 billion people) live without electricity, most of them in the sub-Saharian Africa and in the Asia-Pacific region (Renewables 2016 global status report.2016).

Economic and social developments require a cost effective and stable supply of energy. The current energy system is not bearable anymore.

There is an urgent need to develop permanent and effective sustainable energy strategies to avoid negative environmental and social impacts and to assure an estable energy supply and the correct interaction between nature and society at a reasonable cost (Midilli et al., 2006). Dincer (Dincer, 2000) defines the sustainable development as the "development that would meet the needs without compromising the ability of future generations to meet their own needs".

Midilli et al. claim that there are four main factors (see Figure 6.1) which need to be considered in this sustainable development (Midilli et al., 2006).

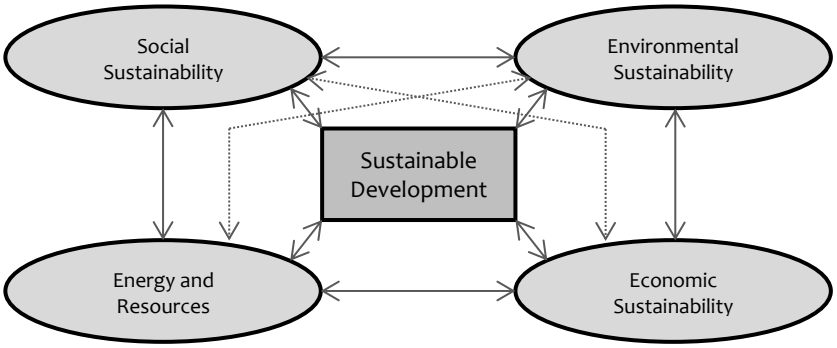

Figure 6.1: Factors affecting sustainable development and their interdependences (Midilli et al., 2006)

A fully sustainable and secure supply of energy is one of the most relevant factors to achieve in the process of a sustainable development. However, it also requires a long term availability and security of energy ressources at a reasonable cost and without negative social impacts, as well as an effective and efficient utilization of energy resources (Dincer, 2000).

During this period of transition from fossil fuel based economy system to an economy based on sustainable energy, environmental impact criteria and indicators for power generation technologies need to be established, since they directly affect on the pollution, economy and wealth of societies.

The diminishing of the current fuels has accelerated and increased efforts not only to the energy utilization efficiency improvement, but also to the recycling and reusing processes. The refuse and other solid wastes are used as supplementary fuel supplies, and recycling extends the lifetime of many natural resources in a profitable way being beneficial to the environment.

Enormous effort is being done to reduce the global energy consumption, and in consequence the negative effects on the environment, by improving energy efficiency and conservation. The potential of the energy efficiency is crucial in both energy production and consumption (Dincer & Zamfirescu, 2014). Thus, the following measures need to be considered when deciding sustainable energy development strategies in order to reduce the environmental impacts of energy systems (Lund, 2007):

- Energy savings on the demand side and energy conservation measures.
- Efficiency improvements in the energy generation systems.

- Replacement of fossil fuels by more environmentally bening energy sources.

The energy resources with zero or minimum negative environmental impact are commonly named renewable energy sources (Dincer & Zamfirescu, 2014). Developing and sustaining renewable energy supplies are a key factor in the sustainable development process. There is an undeniable connection between sustainability and renewable energies. They are claimed to be the most efficient and effective solutions to current environmental and social problems (Dincer, 2000), and the following factors confirm this theory:

- The environmental impact of renewable energy sources is much lower than other energy sources. The air, water and soil pollution and the loss of forest would reduce notoriously, and there would be fewer energy related illnesses and deaths (Midilli et al., 2006).

- The security of the energy supply would increase, reducing conflicts between countries regarding energy reserves and consequently gaining political stability and reducing accidents and importation dependance on the energy supply (Midilli et al., 2006).

- Green energy resources can provide a reliable and sustainable supply of energy indefinitely, since, if used carefully and consiouly, they cannot be depleted. This fact would de-couple the economic growth from the fossil fuels depletion and would ensure long-term availability of energy sources (Midilli et al., 2006).

- They can provide flexibility of the system and economic benefits to small isolated populations with the system decentralization. They favour local solutions which are somehow independent of the national network. They would improve the diversity of energy markets enhancing the decentralization, favoring local solutions that are somehow independent from the national network (Midilli et al., 2006).

- It would also contribute to create new employment opportunities especially in developing countries and local areas providing not only commercially attractive options to meet specific energy service needs (Asif & Muneer, 2007) but also economic benefits to small isolated areas (Midilli et al., 2006).

It is worth mentioning that the relation between renewable energy systems and sustainability is not only of great significance to the developed countries, developing or less

developed nations would also maximize the benefits from the green energy sources and technologies, since these energy systems would increase the energy use in these countries (Dincer, 2000). Moreover, if these strategies are effectively used, the global unrest associated to the current energy system would minimize.

The figure below (see Figure 6.2) presented by Midilli et al. summarizes the benefits that the application of sustainable green energy strategies would contribute in the social, environmental, technical and economic issues (Midilli et al., 2006).

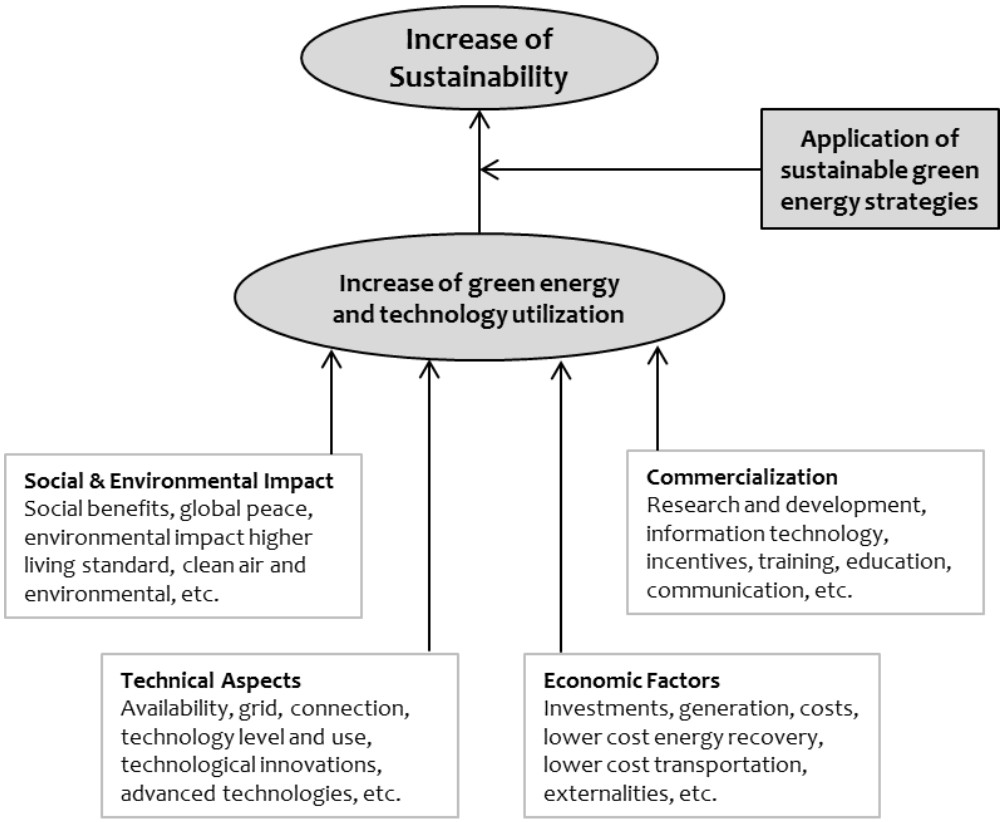

Figure 6.2: Major considerations involved in the development of green energy technologies for sustainable development (Midilli et al., 2006)

Consequently, due to all these reasons, renewable energy sources and technologies need to be considered as the alternative energy systems (Muneer et al., 2005). The key aspect of the global energy transition is an icrease in energy quality and decarboniztion (Asif & Muneer, 2007).

6.1 RENEWABLE ENERGY SYSTEMS

Renewable energy systems are able to convert natural phenomena into useful energy forms with a massive energetic potential (Dincer, 2000).

These energy resources are clean and environment friendly, with zero or almost zero emissions of both air pollutants and greenhouse gases, and have the potential to meet the current and future entire world´s energy demand. Energy sources such as solar, wind, biomass, wave and tidal energy, are abundant, inexhaustive and widely available and are easily accessible to mankind around the world (Muneer et al., 2005). Asif and Muneer show in the figure below (see Figure 6.3) the potential of various renewable energy sources (Asif & Muneer, 2007).

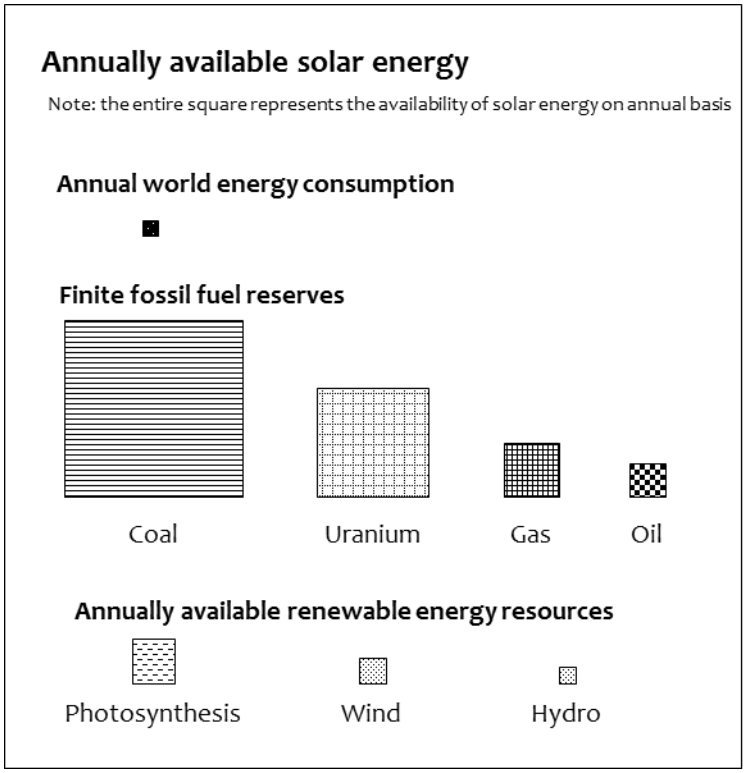

Figure 6.3: Potential of various renewable energy sources as compared to global energy needs (Asif & Muneer, 2007)

These natural sources have been used by human from the beginning of civilization: biomass was used for heating and cooking, wind power for moving ships and wind and hydropower for powering mills among other uses (Asif & Muneer, 2007).

Solar energy is the most important energy resource on earth. This energy is generated by termonuclear reactions in the sun, after traveling around 150 x 10^9 m to impact the earth. The sun´s surface reaches a temperature close to 6000 K and emits electromagnetic radiation in a wide spectrum. The earth receives this radiation from the Arctic to Artarctica. Solar radiation reaches these polar regions only about 6 months a year, whereas it reaches the maximum intensity in the Sunbelt region. Two heat exchangers connect the earth to the surrounding universe: the Sunbelt on the "hot side" and the polar regions on the "cold side".

The Figure 6.4 shows a thermodynamic model which explains the conversion of solar energy on earth. The reversible heat engine represents the earth, which absorves the incident solar radiation and drive the subsystems (precipitation, wind, ocean currents,…) which consume the useful work and generate irreversibility. This thermodynamic systems involves solar radiation crossing the system boundary at about 6000 K and the background radiation of the universe with a temperature of around 3 K.

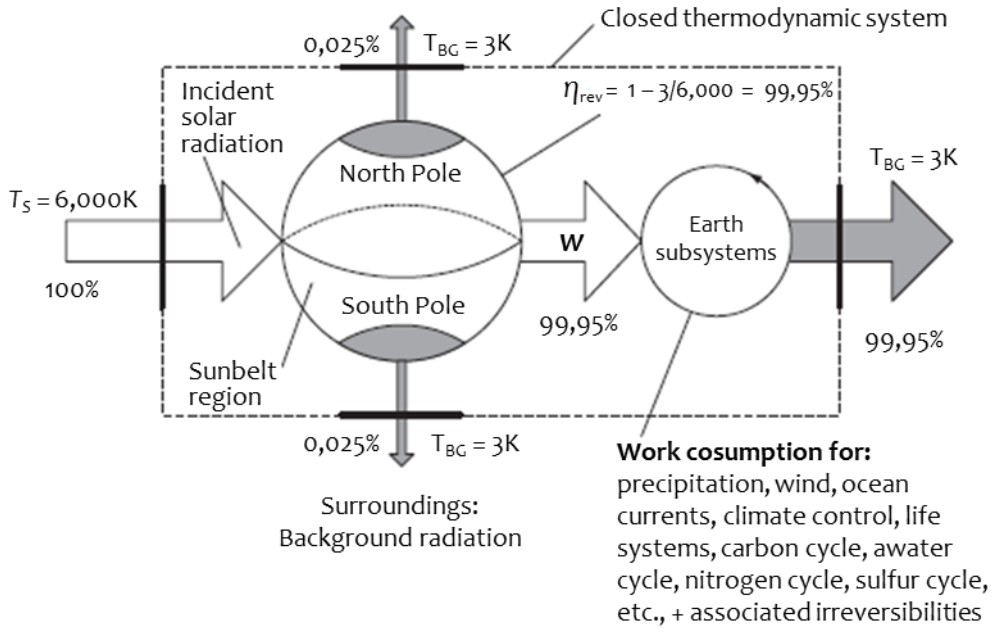

Figure 6.4: Thermodynamic model of the earth as a reversible heat engine coupled to various work-consuming earth subsystems (Dincer & Zamfirescu, 2014)

If the efficiency of the reversible heat engine is 99.95%, as claimed by Carnot, the 99.95% of the energy input received in the earth in the form of incident radiation can be converted into work. There is not energy accumulation on the earth, its climate is steady. This means that the totality of the work produced must be dissipated and rejected into the

surroundings. In the model, the subsystems dissipate the work converting it into heat. This heat is then rejected to the background radiation of the universe (Dincer & Zamfirescu, 2014).

The subsystem block of the thermodynamic model considers all the processes in the atmosphere, hydrosphere, biosphere, and lithosphere and the associated irreversibilities. Solar energy drives the bases of the earth. The following list includes them (Dincer & Zamfirescu, 2014):

- It regulates and maintains the climate and temperature.
- It powers the earth´s main cycles: water cycle, nitrogen cycle, carbon dioxide cycle,…
- It propels the precipitation and hydrological system.
- It generate winds by producing thermal and pressure gracients in the atmosphere.
- It produces ocean currents by induced temperature and density differences.
- It supplies energy to all life systems in the lithosphere and hydrosphere.

Therefore, all the energy forms on Earth derive from the sun.

34.77% of the incident solar radiation at the outer shell of the terrestrial atmosphere is scattered or reflected back into extraterrestial space. The earth aborves the remaining radiation (Dincer & Zamfirescu, 2014).

A 43% of the incoming extraterrestial solar radiation that is not scattered or absorved, represents beam radiation impacting land and oceans (Dincer & Zamfirescu, 2014). This focalized light reaches the earth and sea and provides a continuous stream of energy which warms living beings, grow crops via photosysthesis (Dincer, 2000), and heats the earth contributing to climate control (Dincer & Zamfirescu, 2014).

The theoretical potential of **solar energy** is immense. The solar radiation quantity that reach the earth is a lot higher than the annual global energy consumption. The large scale explotation of this energy source depends on the geographic position of the region, land availability and weather conditions.

Solar energy can be used to generate electricity, heat, cold, steam, light, ventilation and even hydrogen. Although its high versatility, efficiency and low cost, effective energy storage and high efficient end-use technologies need to be available.

Photovoltaic systems are one of these technologies. They convert solar light directly into electricity using a number of commonly crystaline silicon cells connected in series. The efficiency of these solar modules is 12 to 15%.

Solar thermal systems can generate electricity from the high temperature they produce. Parabolic trough systems, parabolic dish systems and solar power towers are the most common technologies used to generate electricity by solar heat. They use tracking mirrors reflecting solar radiation onto a power convertor unit.

Solar collectors can also partially meet the global consumption of low and medium temperature heat. One of the most important applications of this system is the solar domestic hot water system (SDHW). However, a central collector area can also be applied for districty heating.

Passive solar principles in building designs can reduce the energy consumption for heating, cooling, lighting and ventilation. Solar building applications include are based in the following principles: good insulation and south facing. Among the technologies used the most important are low-emission double-glazed windows, low-cost opaque insulation materials and high insulating buildings elements, transparent insulation material… (Johansson, McCormick, Nei, & Turkenburg, 2004).

The 22% of incoming radiation heats the earth and sea differentially, causing the evaporation of the ocean water and consequently precipitation at higher altitudes forming lakes and rivers. **Hydro-power** is caused by the elevation of the water level, thus it is a form of potential energy (Dincer & Zamfirescu, 2014).

These potential energy is mechanically converted to hydroelectricity. Rainfall changes from one region to another and it also varies in time, thus hydro-power is not evenly accessible. Detailed information on the local and geographical factors of the water are needed to know the energy potential.

Hydro-power is considered to be a mature technology, but even though it is unlikely to progress further, small scale hydropower could be further developed (Johansson et al., 2004).

Wind energy represents only the 0.21% of the incoming solar radiation. Wind is a form of solar energy dissipation, since it is the mechanical movement of air masses caused by pressure differences. This pressure gradients in two nearby locations are caused by the differential heating of solar radiation (Dincer & Zamfirescu, 2014).

The kinetic energy of wind currents is harvested by wind turbines, converting this energy to useful energy for human activities. Mean wind speed and its frecuency need to be considered to calculate the amount of energy that can be generated. Modern electronic components integrated in the wind turbines provide information to control output and generated excellent power quality. Developments in this field are making the integration of the wind energy in the current infraestructure more suitable (Johansson et al., 2004).

The photosyntesis process of green plants on the surface of the earth represents only the 0.02% of the beam radiation. Photosyntesis is the major source of energy and food worldwide, although its efficiency rate is very low due to its massive production of sucrose, glucose, cellulose and other chemical compounds. **Biomass** is derived from photosyntesis (Dincer & Zamfirescu, 2014).

Energy from biomass can be generated using plants, animal manure or municipal solid waste. These resources can be found abundantly in most places of the world. Currently most biomass is used in traditional manners, as fuel for households or small industries, and not in a sustainable way in the most cases.

The biomass challenge is to become sustainable and affordable on the management, conversion, and delivery to the market of the energy service (Johansson et al., 2004).

The figure below (see Figure 6.5) shows the breakdown of energy forms derived from incident solar radiation on earth (Dincer & Zamfirescu, 2014).

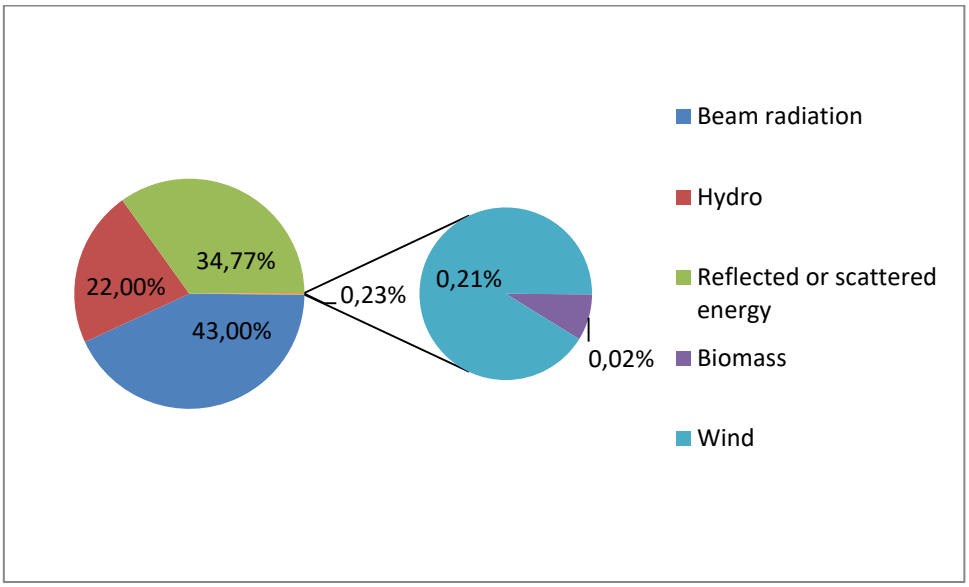

Figure 6.5: Breakdown of energy forms derived from incident solar radiation on earth (Dincer & Zamfirescu, 2014)

Tidal energy is a result of gravitational interaction of the moon-earth and sun-earth over the ocean water causing the lift of massive quantities of water (Dincer, 2000). Apart from the mentioned gravitational force, the inertia force caused by the planet´s rotation also takes part in the generation of the tidal energy (see Figure 6.6). Since the average radious of the Equator is 6000km, the centrifugal acceleration of the earth is 0.032 m/s^2. Thus, this centrifugal force together with the gravitational force of the cause an acceleration of 9.775 m/s^2 in the ocean waters at the equatorial plane. Therefore, the gravitational forces from the moon and sun, compounded with the effect of the earth´s gravity creates a net effect of rising waters (Dincer & Zamfirescu, 2014).

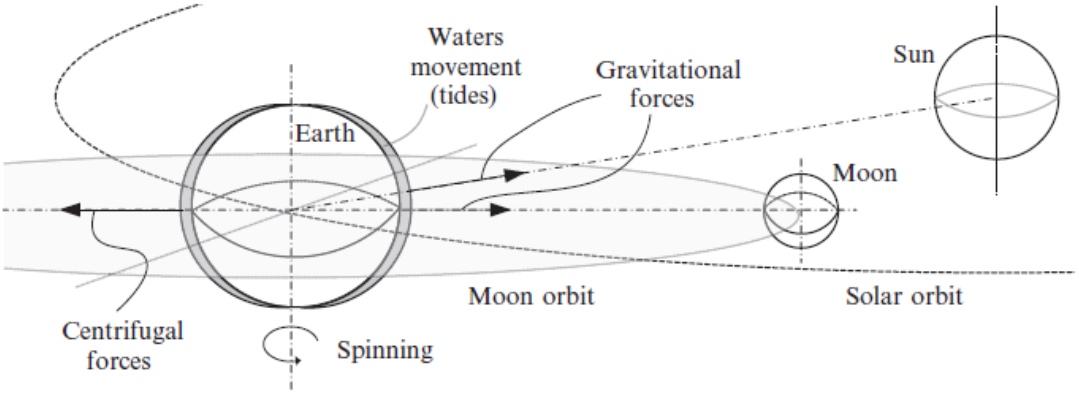

Figure 6.6: Tidal energy (Dincer & Zamfirescu, 2014)

Tidal energy is harvested with hydraulic turbine systems which generate power either at ebb tide or flood tide, or at both. Tiwari and Ghosal (Dincer & Zamfirescu, 2014) claimed that the estimated global energy that can be generated by tidal energy is 3 TW.

Another renewable energy form is **geothermal energy**, which is the thermal energy source of the earth´s core (Dincer & Zamfirescu, 2014), derived from the radioactive decay deep in the earth (Dincer, 2000). Heat from the earth´s core, which is estimated to be around 7,000°C, propagates to the surface mainly by heat conduction. Geothermal energy in the surface of the earth is about 2000 times less intense than the solar energy, and the temperature at 4,000 m below the surface is more or less uniform reaching around 363 K (Dincer & Zamfirescu, 2014).

The total amount of energy stored in the earth´s core is estimated to be 10^{16} PW (1 PW = 10^{15} W), whereas the intensity at the surface is about 0.1 W/m^2. This creates a global amount of 44 TW (1 TW = 10^{12} W) of geothermal energy. The conversion factor of geothermal energy systems currently is 0.1.

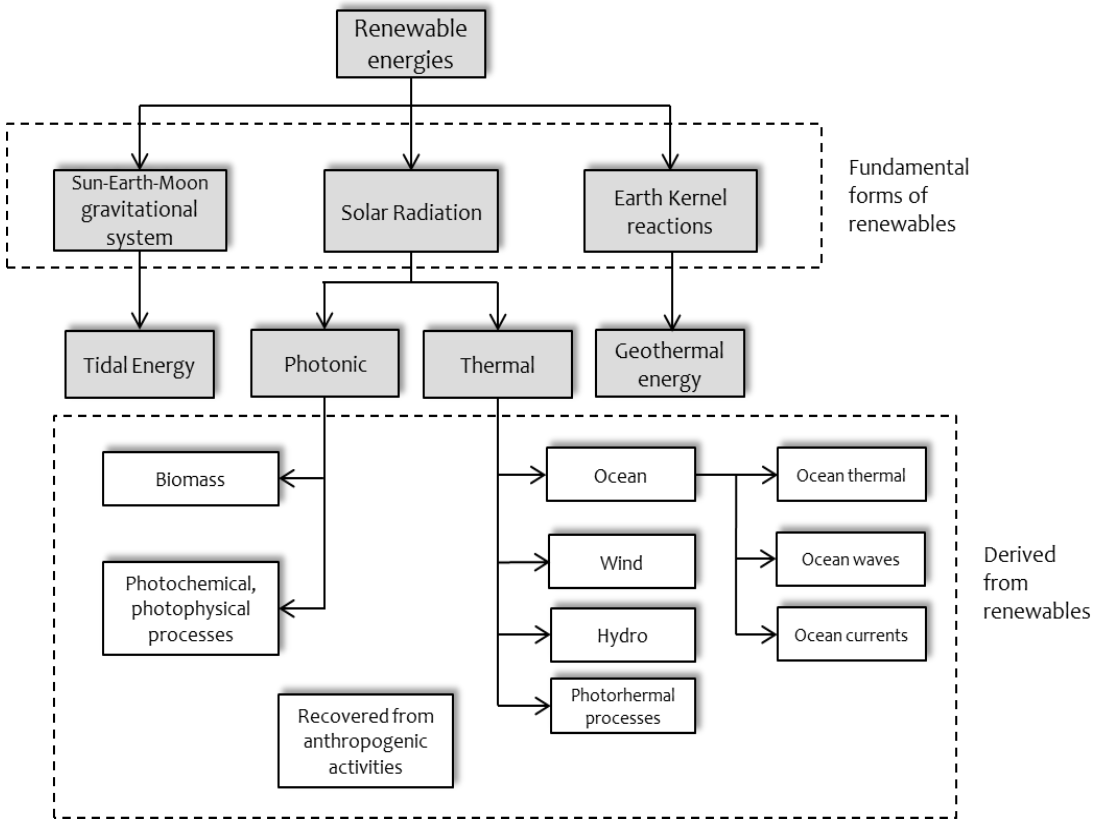

Figure 6.7: Classification of Renewable Energies (Dincer & Zamfirescu, 2014)

The Figure 6.7 shows the classification of natural and non-exhaustive energy sources in three main groups which are solar radiation, sun-earth-moon gravitational system and earth kernel reactions. These are the fundamental renewable energy resources.

The incoming solar radiation that enters the atmosphere is estimated to be 176 PW. Thus, the table below (see Table 6.1) summarizes the estimated global power generation potential from solar, wind, hydro and biomass energy.

There are several ways to harvest the beam radiation such as photovoltaic arrays, solar thermal panels and concentrated solar radiation systems. There are many conversion factors to estimate the amount of power that can be generated from solar radiation. The concentrated solar receivers' efficiency for example is about 25%. Hydro-power conversion factor is estimate to be around 0.8, while in the case of wind energy this factor is about 0.6. Biomass has a conservatively estimated conversion factor of 0.5, tidal energy has an estimated of 0.8, and in the case of geothermal energy it is suppose to be 0.1.

The comparizon between the renewable energy sources and the global daily energy demand is important to understand the real magnitude of enery supply and demand. The average global energy demand is 15 TW, and the table below (Table 6.1) summarizes the energy potentially available from the renewable sources mentioned above.

Table 6.1: Estimated global power generation potential from solar radiation (Dincer & Zamfirescu, 2014)

	% RADIATION	POWER (PW)	CONVERSION FACTOR	POWER (PW)
Solar energy	43.00%	74.82	0.25	18.705
Hydro-power	22.00%	38.28	0.80	30.624
Wind energy	0.21%	0.3654	0.60	0.21924
Biomass	0.02%	0.0348	0.50	0.0174

The figure below (see Figure 6.8) compares the current global energy consumption rate with the three fundamental renewable energy sources on earth. It is worth mentioning that the energy derived from solar radiation (beam radiation, hydro-energy, wind energy and biomass) is much more higher (more than 3000 times) than the rate of global energy demand. On the contrary, tidal energy can supply at a rate around six times smaller than the demand and the geothermal energy is available at a rate of around three times less than the global consumption.

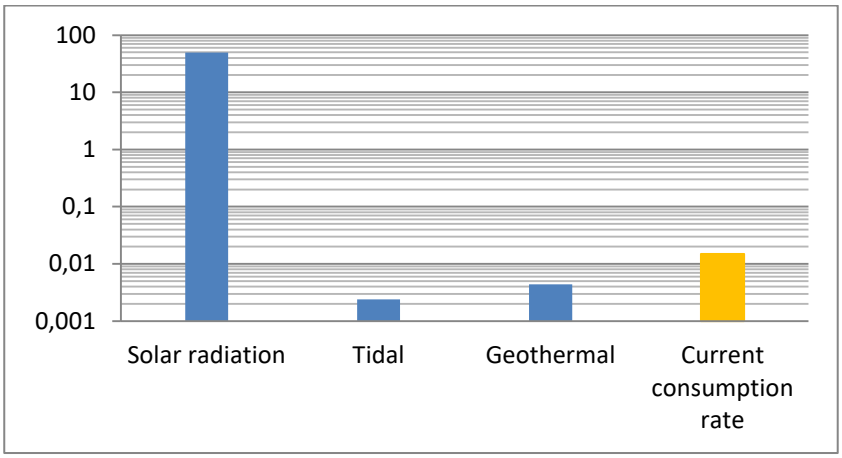

Figure 6.8: Current global energy consumption (PW) vs fundamental renewable energy sources power (PW) (Dincer & Zamfirescu, 2014)

The geographical and technical potential of the natural energy flows in the earth ecosystem exceeds by far the current energy use. The table below (Table 6.2) shows the long-term availability of renewable energy sources in order to undestand their potential.

Table 6.2: Global Renewable Resource Base (Exajoules a year) (Johansson et al., 2004)

Resource	Current use*	Technical potential	Theoretical potential
Hydropower	10,00	50,00	150,00
Biomass energy	50,00	>250	2.900,00
Solar energy	0,20	>1600	3.900.000,00
Wind energy	0,20	600,00	6.000,00
Geothermal energy	2,00	5.000,00	140.000.000,00
Ocean energy			7.400,00
TOTAL	62,40	>7500	>143000000

* The current use of secondary energy carriers (electricity, heat and fuels) is converted to primary energy using conversion factors involved.

The natural energy flows through the earth's ecosystem, and the geographical and technical potential of what they can produce for human needs, exceeds current energy use by many times (approximately 425 EJ in 2002). But to place renewable energy resources in perspective it is important to examine the longterm energy resource availability from the viewpoint of theoretical maximums, or ultimately recoverable resources. This is known as the theoretical potential.

6.2 IMPLEMENTATION OF RENEWABLE ENERGIES

Green energy sources are abundant, secure and safe, but the transition from a fossil fuel based society to a sustainable development is not simple. The first major challenge is to expand the amount of renewable energy in the supply system (Lund, 2007). The implementation of the renewable energy systems faces obstacles of a structural nature. The first main constrain is the centralization of the current economic and social energy and distribution system. The second barrier is the initial investmet the renewables require to start the implementation process. Coal, oil and nuclear energy also needed this initial finantial support (Jäger-Waldau, 2007).

Although there are strong business dynamics pushing for the accelerated transition to renewable energies, powerful businesses in the current power sector fear they may loose influence, and their strategies to slow down the transition and to push a centralized system for the green energy system may affect in the sustainable development (Schleicher-Tappeser, 2012). Furthermore, the renewable energy market will not have a regular development without the support policy of the public authorities such as direct subsidies favouring green sources or the obligation to the electricity producers to purchase a minimum percentage form renewable energy sources (Jäger-Waldau, 2007).

Therefore, new policies are needed to meet the needs of vulnerable people, reduce environmental pollution, and to ensure the energy security, in other words, to change course toward a sustainable path. First of all strategies need to be established, representing a plan to achieve a goal. Once the strategy is established, the policy must be elaborated. The policy represents the course of actions needed to implement the strategy (Dincer & Zamfirescu, 2014).

Oponents to the implementation of these sources claim that renewable energies are generally diffuse, sometimes intermitent and not fully accesible, and all have regional variabilities. It is true that these facts involve technical, insititutional and economical challenges and difficulties, but they are solvable with research and development.

Renewable energy systems are often considered to be not as cost effective as conventional energy technologies, since the benefits of green sources are not well understood. It is important to comprehend the operating and finantial attributes of renewable energies, which include modularity, flexibility and low operating costs, and are considerably different

from fossil fuel based systems (Dincer, 2000). When shaping sustainable energy policies and strategies, it is essential to be aware of the environmental and social benefits of the clean energy technologies and the negative effects of the current energy system which are conditioning the future of civilizations, economic and products (Schleicher-Tappeser, 2012).

The scale and pace of effective policy development need to be higher in order to achieve a sustainable path.

First of all, the global population needs to have enough information and a adecuate definition of sustainable development in order to support this transition. The following parameters could help in achieving a succesful implementation of the sustainability in the society (Dincer, 2000):

- Public awareness of the current reality and future threats.
- Information about energy utilization, environmental impacts and energy resources among others.
- Environmental education and training as a complement to the information.
- Innovative energy strategies in order to achieve an effective sustainable energy program.
- Promoting renewable energy resources and creating a strong basis for short and long term policies.
- Financing is also an essential tool to accelerate the implementation of renewable energy systems and technologies.
- Monitoring and evaluationg tools to see how succesful the implemented program is.

Secondly, together with the increasing public acceptance of the fact that energy consumers share responsibility for pollution, research and technological investments need to be done in order to strengthen the sustainable development.

Although a lot of work is still needed to be done and challenges remain, it is worth mentioning that significant progress has been made in the last years in the implementation

of the renewable energy resources in the energy systems, as Dincer claimed in 2000 (Dincer, 2000):

- Improvements in the collection and convertion efficiencies.
- Lowering the initial and maintenance costs.
- Increase on the reliability and applicability.
- Understanding the phenomena of renewable energy systems.

The year 2015 is a good example of the progress, since it was an extraordinary year for green energies. There were several developments in the fields of renewables, including the largest global capacity additions seen to date, enormous decline in global fossil fuel prices, increase in interest in energy storage systems, announcements of low prices in long-term renewable power contracts, and above all, an historic climate agreement in the United Nations Climate Conference in Paris, where 195 nations reached an agreement to limit the global warming to below 2° C (Renewables 2016 global status report.2016).

Even though this is not enough to avoid the threats of the climate change, most of the countries showed a clear commitment to adress the challenge and to get away from fossil fuels increasing renewable energy utilization and improving energy efficiency through their Intended Nationally Determined COntributions (INDCs) (Renewables 2016 global status report.2016).

The were noticiable steps forward in the four critical challenges of renewable energy systems development.

Distributed renewable energy (DRE) generation

Renewable energy sources offer energy, economic and environmental benefits, and in order to make the most of them the following activities need to be done accordingly: Research and development, technology assessment, standards development and technology transfer .

These activities will help potential users to see the benefits of adopting green technologies. Technology trasfer area is a key factor to accelerate the use of renewable energy sources in remote areas in a country (Dincer, 2000).

As mentioned before, over 1 billion people in the world struggles to get energy for their basic needs. Connections to the central electric grid is too expensive and difficult in many rural and peri-urban areas. Distributed renewable energy (DRE) systems are an alternative to the centralized energy system, and enables unaccesible areas to have power for basic needs.

Year 2015 noticed positive market trends and innovative business models in the distributed energy generation. Advances in technology and goverment support help in the expansion of the distributed renewable energy especially in the heating and cooking sector.

The Figure 6.9 shows the different distributed renewable energy systems that are installed in different countries.

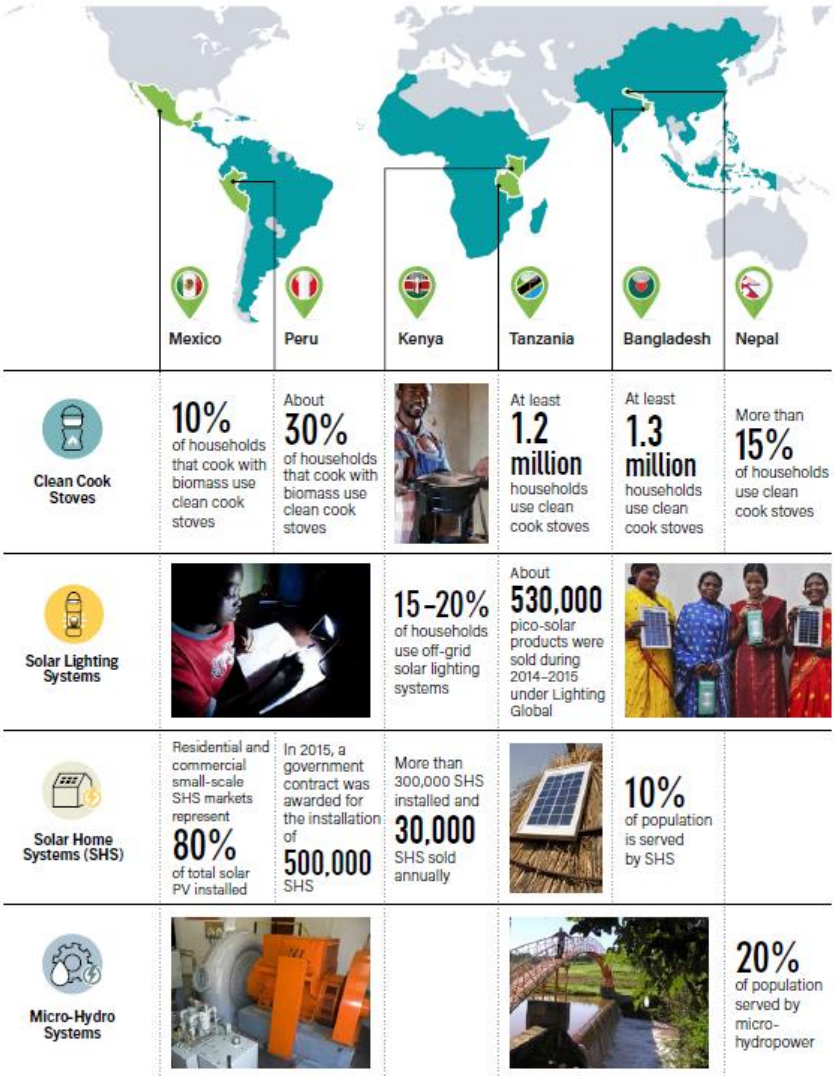

Figure 6.9: Market Penetration of DRE Systems in Selected Countries (Renewables 2016 global status report.2016)

The installed capacity of off-grid solar PV products also increased notoriously, with at least 70 countries with installed or programmed off-grid applications, representing an annual market of 300 million USD. Furthermore, there are thousands of renewable based mini-grids installed in Cambodia, China, Bangladesh, Marocco and Mali to enable energy access to remote regions, were people lived without electricity. It is estimated that DRE systems serve at least 100 million people worldwide, most of them through solar home systems (80%), but also through mini-grids and small-scale wind turbines (Renewables 2016 global status report.2016).

Some of the advantages of the distributed energy generation include the accecibility of remote communities, lower losses in the distribution and transmission process, the possibility of local and direct investments, local employment, a higher security and reliability in the supply and reductions in the environmental hazards.

Policy landscape

According to Dincer many govenments energy institutions and agencies are aware of the possibilities and opportunities of the renewbale energy systems and are supporting the these industry in the following ways (Dincer, 2000):

- Analyzing renewable energy opportunities to identify R&D and market strategies to meet technological goals.
- Cooperation between R&D and industry to develop and commercialize technologies.
- Encourage potential users to apply renewable energies.
- Provide technical support and advice to programs that are encouraging the increased use of renewable energies.

Goverment policies are also very important in the renewable energy integration process. Most of the worldwide nations adopted renewable energy support policies during the year 2015, and many juridisdictions made their existing polices more ambitious. The number of nations with renewable energy targets increased to 173 and there are at least 146 countries with renewable energy support policies at the national or provincial level (Renewables 2016 global status report.2016).

This fact supported the extension of the distributed renewable energy. Auctions, dedicated electrification targets and researches related to the clean renewable cooking are some of these policies. Incentives for certain renewable energy applications and import duties also helped in the DRE deployment.

The Figure 6.10 shows the evolution of policies in the three mentioned sectors.

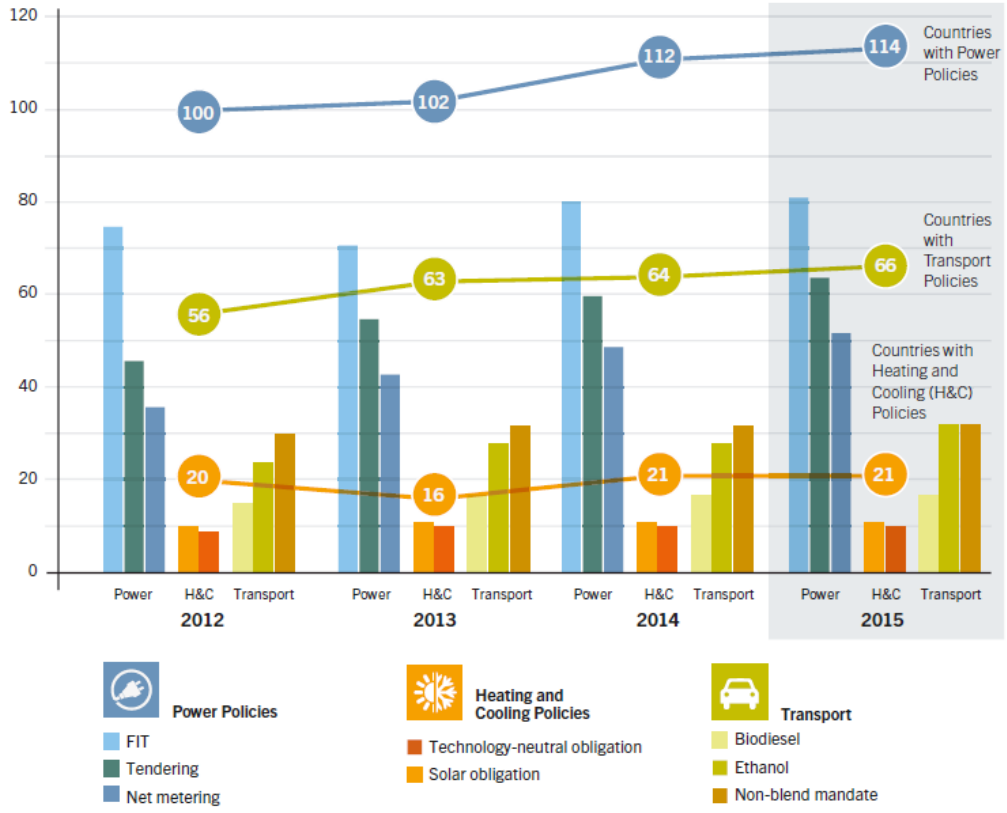

Figure 6.10: Number of Renewable Energy Policies and Number of Countries with Policies, by Type, 2012–2015

(Renewables 2016 global status report.2016)

The main focus of the policy makers is the renewable power generation, particulary in the solar photovoltaic (PV) and wind power technologies. Feed-in policies are the most effective regulatory mechanism in the promotion of renewable energy applications.

Renewable heating and cooling technologies in the other hand, have a much slower policy progress, and it has focused particularly in small-scale solar thermal heating mechanisms for commercial and residential buildings (Dincer, 2000).

The transport sector is also slowly progressing with the support of green strategies. However, most of the policies are mainly focused to the road transport through support for biofuel production and use. The integration of renewable energies in road, aviation, rail or

shipping and development and use electric vehicles is much slower and there is not enough interest to adopt new policies in this field (Renewables 2016 global status report.2016).

However, it is worth mentioning the influence of cities and municipalities in the global energy transition. Municipal governments and local-level climate based agreements have a great impact in teh promotion of renewable energy technologies on a large scale.

Amsterdam, Graz, Cape Town and Banff are good examples of the energy transition progress. The first two cities agreed to develop their renewable heat sectors, while the latters took regulatory measures to increase renewable power (Renewables 2016 global status report.2016).

In Denmark, wind and solar PV contributed more than the 50% of the total energy generation in the 2015. In Germany the contribution of renewable energies in the electricity generation reached the 19%, in Spain and Portugal 21% and in Ireland 23% (Energy, climate change & environment.2016).

In the transport sector, a biofuel blend mandate was introduced as a pilot initiative by goverments from Kenya, Mexico and Vietnam among others.

The global movement for 100% renewables is growing rapidly due to the undeniable presence of climate change and the community owned energy and local economic improvements.

The number of worldwide cities that have decided to achieve a 100% renewable energy in all sectors and to reduce the greenhouse gas emissions 80% by the year 2050 is growing quickly. They are important change makers, acting independently or collectively in order to share renewable energy knowledge and improve their goals through their participation in several high-profile global and regional partnerships (Renewables 2016 global status report.2016).

Investments

The global investment in renewable power and fuels increased 5% in 2015 compared to 2014 and exceed the previous record achieved in 2011. The investments in renewable power capacity, without considering hydropower, more than doubled the investments related to coal and natural gas based power generation capacity. If hydropower is considered the

difference between renewable and fossil fuel power generation is even greater (see Figure 6.11).

The investment in renewable energies in developiong countries in 2015 was for the first time greater than in developed countries. According to the Renewable Energy Policy Network (REN21), developiong countries invested 156 USD, 19% more than in the previous year. China played a crucial role, increasing the investments 17%, reaching 102.9 USD, and accounting the 36% of the global investement. Other countries such as India, Brazil, South Africa, Mexico, Chile, Morocco, Uruguay, the Philippines, Pakistan and Honduras also increased their investments notoriously (Renewables 2016 global status report.2016).

Among the industrialized countries, the United States increased their investment 11%, dominated by solar and wind power. On the contrary, Europe invested 21% less in 2015 than in the previous year. As a global, developed countries decreased 8% during the same period their investments in the renewable area (Renewables 2016 global status report.2016). This could be due to policy changes and uncertainties such as unexpected changes, new taxes on renewable generators and so on.

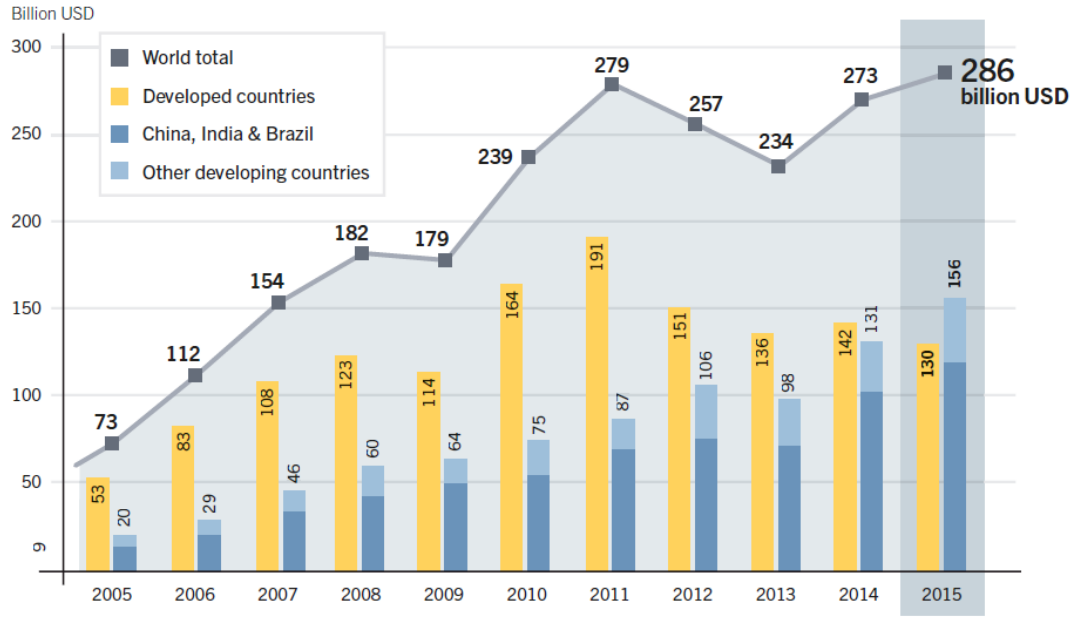

Figure 6.11: Global New Investment in Renewable Power and Fuels, Developed, Emerging and Developing Countries,2005–2015 (Renewables 2016 global status report.2016)

The clear majority of the investments in renewable capacity have been focused in the solar and wind power. While investments in other renewable energy sources decreased during 2015, they increased 9% in wind power and again solar power was the leading sector with an

increment of 12% in the investments. The figure below (Figure 6.12) shows the development of investments in each renewable energy technology.

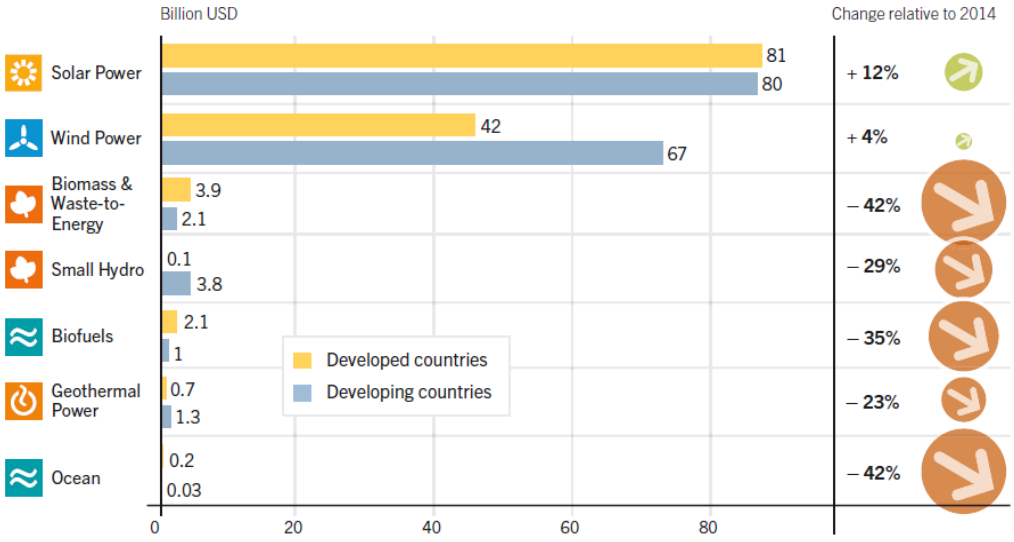

Figure 6.12: Global New Investment in Renewable Energy by Technology, Developed and Developing Countries, 2015 (Renewables 2016 global status report.2016)

Efficiency

According to the Renewable 2016 global status report "energy efficiency is the opportunity to deliver more services for the same energy input, or the same amount of services for less energy input". The energy efficiency is related to the losses at the stages of energy conversion, transport, transmission and use. The higher the efficiency is the lower the losses are. These losses can occur at any stage from the primary fuel extraction to the final use. Therefore, energy efficiency improvements and investments can take place at any phase of the chain from the energy production to use.

The efficiency has a key role not only in the reduction of greenhouse gas emissions and fuel poverty and improvements in public health. For this reason the interest on energy efficiency activities has increased at the international, regional, national and also sub-national levels.

The figure below (see Figure 6.13) shows the Energy Efficiency Policies and Targets that countries worldwide have implemented Renewable 2016 global status report (2016).

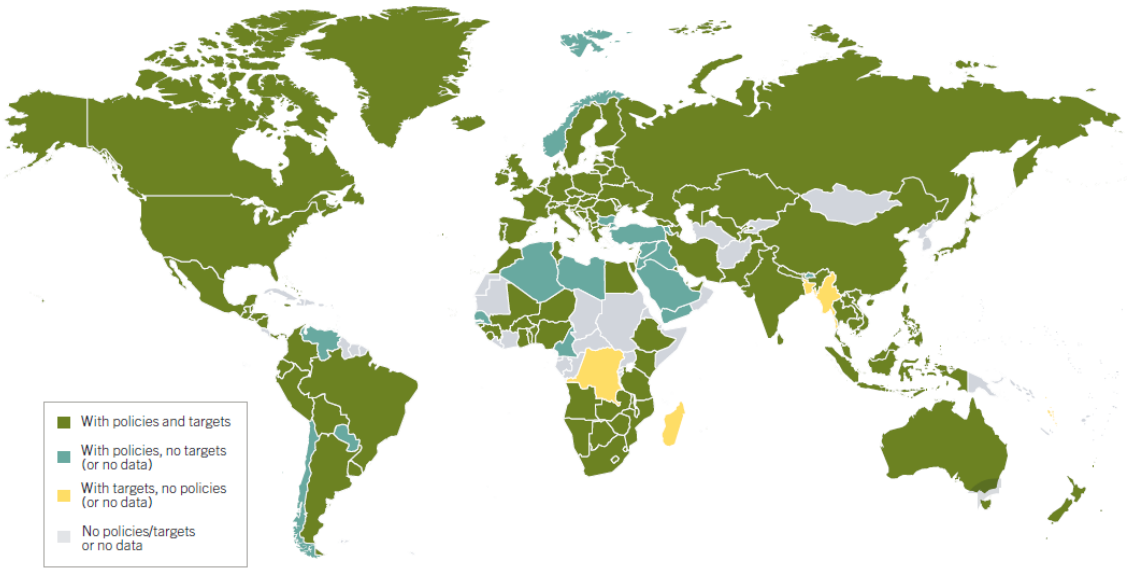

Figure 6.13: Countries with Energy Efficiency Policies and Targets, 2015 (Renewables 2016 global status report.2016)

6.3 PRESENT AND FUTURE OF RENEWABLE ENERGY CONSUMPTION

Currently, despite the substantial potential the renewable resources have, and the progress that several countries have made in the area, renewable energy systems still constitude a very small share of the total energy supply. Even though the use of these energies is growing fast, the aportation of renewable in the energy consumption is not increasing as rapidly.

The Table 6.3 shows the amount of renewable energies supply to the global energy consumption in the year 2015. The Figure 5.3 and Figure 5.7 in the previous section show the projections of the energy consumption according to the IEO (International energy outlook 2016.2016).

Table 6.3: Global energy consumption by source (Exajoules) (BP statistical review of world energy.2016)

	Fossil fuels	Nuclear	Renewable	TOTAL
WORLD	473.38	24.41	52.66	550.45
AFRICA	16.82	0.10	1.29	18.21
Algeria	2.29	0.00	0.00	2.29
Egypt	3.47	0.00	0.14	3.61
Total Asia Pacific	206.45	24.41	52.66	230.21
India	27.14	0.36	1.83	29.33
Australia	5.18	0.00	0.32	5.50
Middle East	36.73	0.03	0.27	37.04
Kuwait	1.72	0.00	0.00	1.72
Europe	93.50	11.05	14.12	118.67
Portugal	0.78	0.00	0.23	1.01
Spain	4.17	0.54	0.91	5.63
UK	6.55	0.67	0.79	8.01
Latin America and the Caribbean	21.65	0.21	7.41	29.28
Argentina	3.17	0.07	0.44	3.66
Brazil	8.02	0.14	4.10	12.26
Venezuela	2.65	0.00	0.72	3.37
Northern America	98.22	9.05	9.78	117.04
Canada	8.89	0.99	3.94	13.81
EEUU	82.12	7.95	5.41	95.48

According to the to the BP statistical review of world energy, the total share of renewable energies in the globlal energy consumption was 9.6%, while the fossil fuels constituded the 86% (BP statistical review of world energy.2016). The renewables 2016 global status report differs regarding to the amount of energy provided by renewable sources. As shown in Figure 6.14, aproximately the 19.2% of the global final energy consumption was provided by renewable energy systems.

Although there are differences between the two sources, the contribution of renewable energy technologies in the total energy generation is very low considering the potential of these energy sources.

The existing infraestructure for fossil fuels is deeply rooted in and it is not simple to displace it. Besides, energy demand in developed countries is growing very slowly. In developing countries, on the other hand, the energy demand is increasing very rapidly, and fossil fuels help in meeting this growing demand.

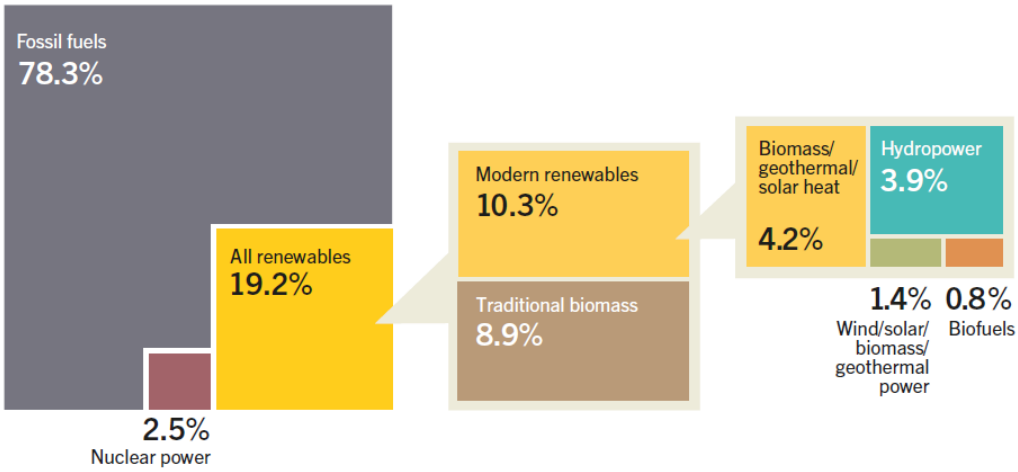

Figure 6.14: Estimated Renewable Energy Share of Global Final Energy Consumption, 2014 (Renewables 2016 global status report.2016)

The following section summarizes the evolution and current aportation of each renewable energy source.

Biomass Energy

Among the renewable energy technologies, bionergy is the source that contributes the most to the energy supply.

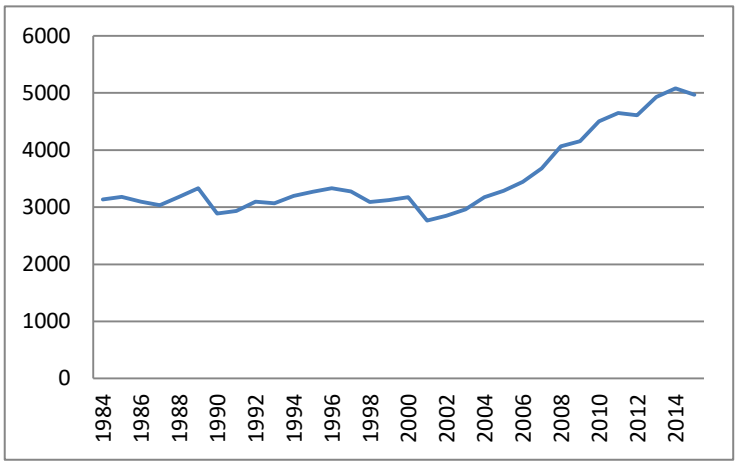

Figure 6.15: Biomass Energy Consumption (TJ) (Total energy.2016)

This kind of energy includes not only forestry and agricultural residuals and different type of wastes, but also material grown especifically for this purpose. The generation of biomass power has grown an average of 2% per year since 2010, however, as shown in the Figure 6.15 (Total energy.2016) the global consumption of biomass energy decreased during the year 2015.

The Figure 6.16, shows the evolution of bio-power global generation by country in the last years.

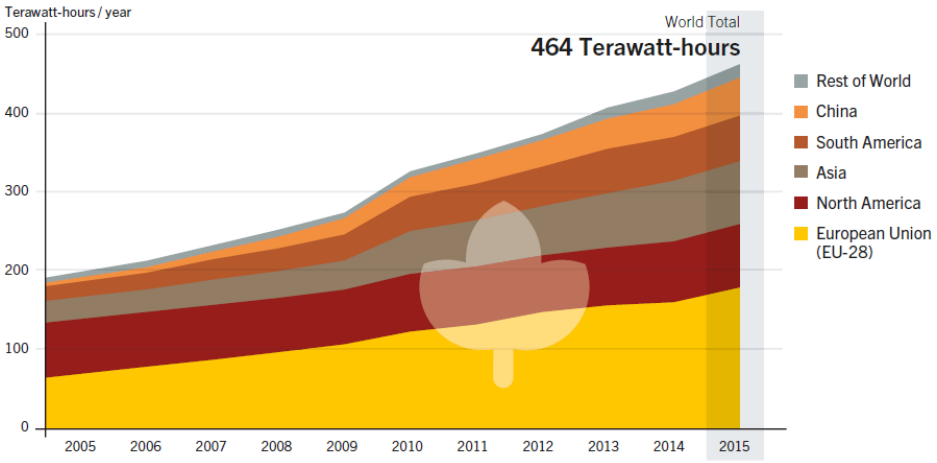

Figure 6.16: Bio-power Global Generation, by Country/Region, 2005–2015 (Renewables 2016 global status report.2016)

Biomass can be used as solid, liquid or gaes, and fuel can be converted directly into heat for cooking and heating in the residential sector and also at a larger scale in the industry. Biomass can also be converted to electricity or transformed into gas or liquid to generate fuel for transport. The most used fuel for transport is ethanol.

The use of biomass to generate heat is much larger than its use for electricity and transport. It is estimated that the 8.9% of the total biomass is used as traditional heating method, 2.2% for industry heating and 1.5% modern heating, while only the 0.8% and 0.4% of the biomass consumption are used in the transport and electricity sectors respectively. Solid biomass is mainly used for heating and to generate electricity, while liquid biofuel is the largest source in the transport sector.

Geothermal Energy

Geothermal energy sources are used for both heating and cooling and electricity generation. In the end of 2015 the countries that used geothermal energy to generate

energy the most were the United States (3.6 GW), the Philippines (1.9 GW), Indonesia (1.4 GW), Mexico (1.1 GW), Kenya (0.6 W) and Japan (0.5 GW) (Renewables 2016 global status report.2016). However, its increase in capacity in the last years has not been notorious. Geothermal energy has some disadvantages compared with other renewable energy systems. The high cost of drilling explorator holes and the risk of drilling a non-productive well are some of them. Appropiate financing guarantees could help in the research and progress in the technology and reduce investor risks and development costs (Energy, climate change & environment.2016).

The Figure 6.17 presents the geothermal energy consumption worldwide, and it can be appreciated that the increase of the consumption has not been notorious either.

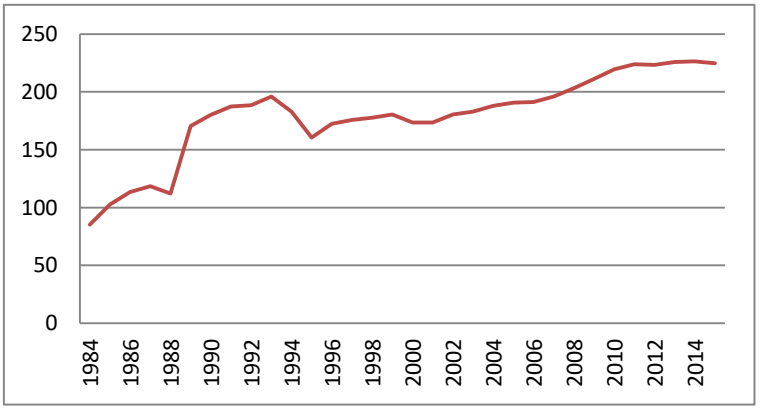

Figure 6.17: Geothermal Energy Consumption (TJ) (Total energy.2016)

The figure below (Figure 6.18) show the geothermal power capacity and additions in 2015 in different countries (Renewables 2016 global status report.2016).

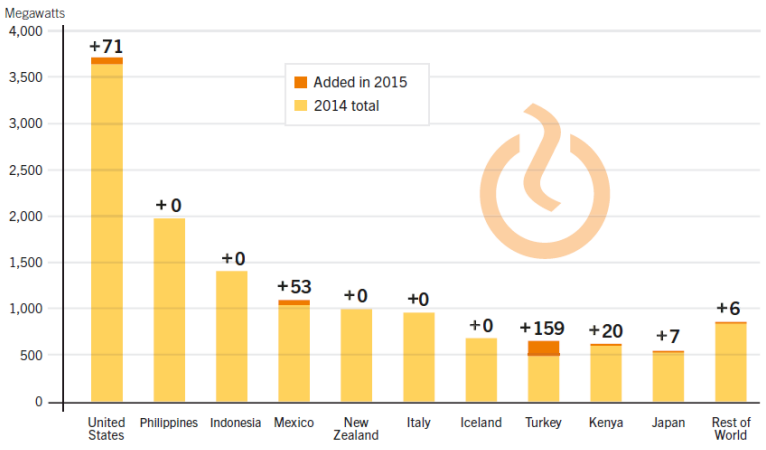

Figure 6.18: Geothermal Power Capacity and Additions, Top 10 Countries and Rest of World, 2015 (Renewables 2016 global status report.2016)

Hydropower

Hydropower is one of the oldest energy sources, since it has been used for thousends of year. It is the largest electricity source for electricity in the United States. Figure 6.19 shows the evolution of the global hydroelectricity power consumption and it is worth mentioning the decline it has suffered in the last years.

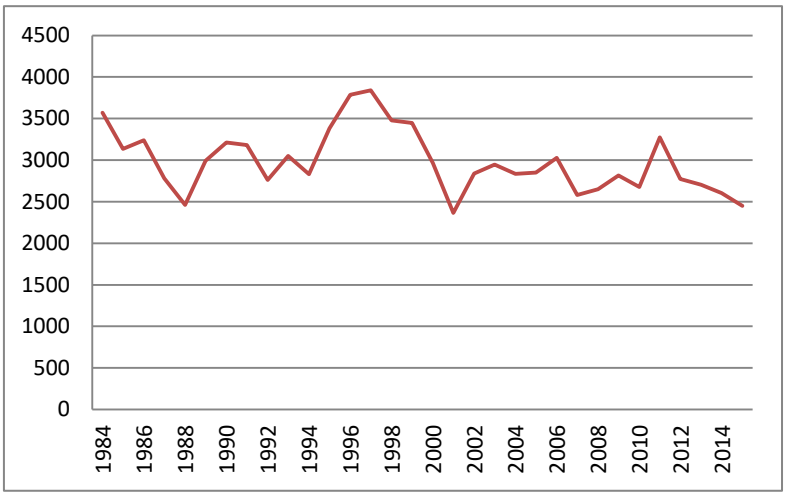

Figure 6.19: Hydroelectric Power Consumption (TJ) (Total energy.2016)

However, as shown in Figure 6.20, the capacity of hydroelectricity has increased in countries where this energy source contributes the most.

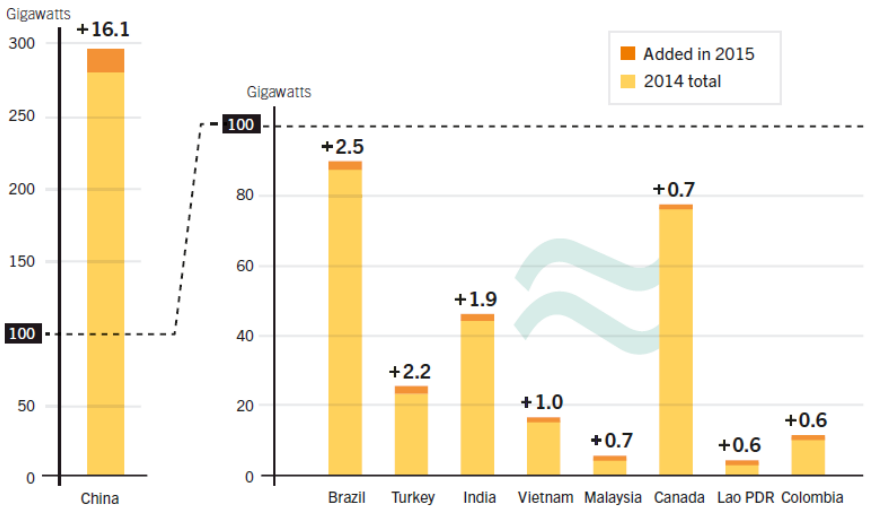

Figure 6.20: Hydropower Capacity and Additions, Top Nine Countries for Capacity Added, 2015 (Renewables 2016 global status report.2016)

Ocean Energy

Ocean energy includes tidal energy (range and streams), ocean waves, ocean currents, temperature gradients and salinity gradients. During the 2015 its contribution to the global energy generation remained constant in 530 MW.

Wind power

Wind power, together with solar energy, is the energy source that has suffered the most notorious increase among all energy sources (see Figure 6.21).

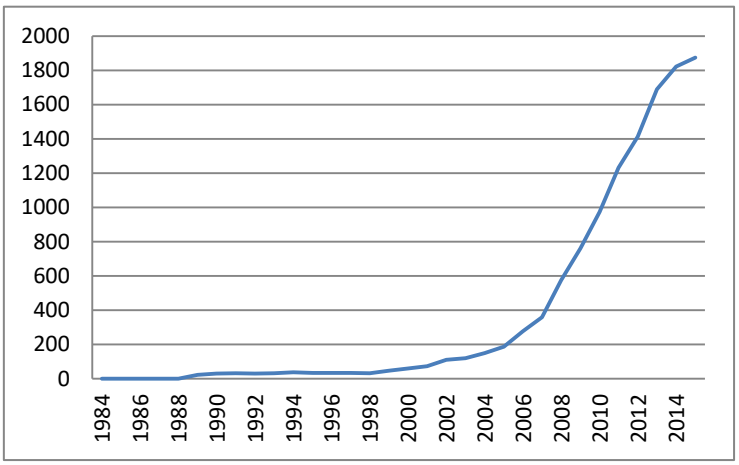

Figure 6.21: Wind Energy Consumption (TJ) (Total energy.2016)

During the last 5 years (see Figure 6.22), wind power has experienced more than the half of the wind power capacity increase (Renewables 2016 global status report.2016).

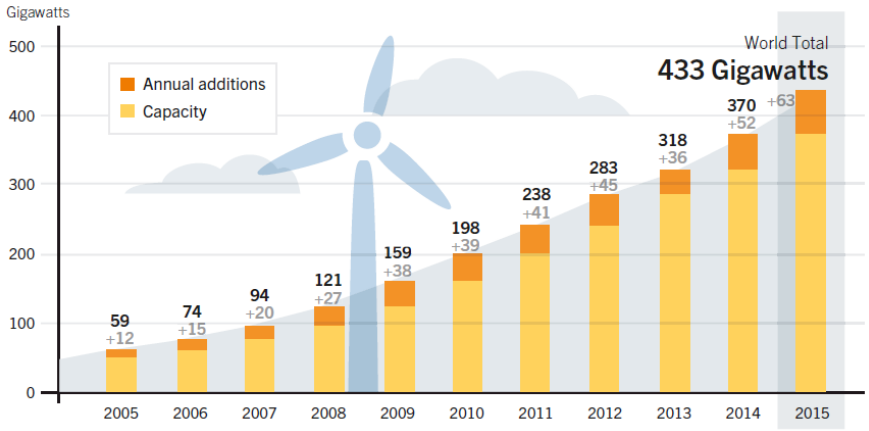

Figure 6.22: Wind Power Global Capacity and Annual Additions, 2005–2015 (Renewables 2016 global status report.2016)

This was due to significant technological innovation and improvements in supply chain efficiency. However, because of insufficient economic investment and uncertainities in the regulatory frame, offshore wind deployment is still below potential in many key markets (Energy, climate change & environment.2016).

Solar energy

Solar energy is the cleanest and most abundant renewable energy source available and developments in modern technology have contributed to each harness for a variety of uses. As mentioned before, solar energy can be used to generate electricity, heat for domestic or industrial use and to provide light.

Research in this field has enhanced considerably the capacity and efficiency of solar energy application systems, and the increase in solar energy consumption (see Figure 6.23) in the last years is proof of this fact.

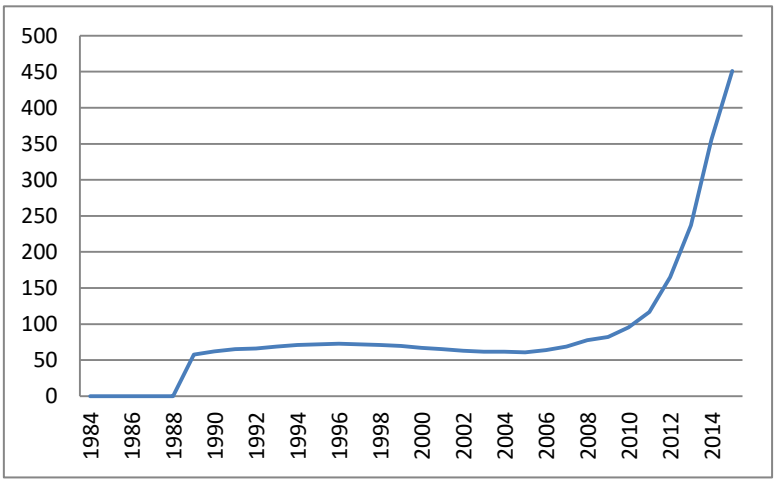

Figure 6.23: Solar Energy Consumption (TJ) (Total energy.2016)

- Solar PV

The global PV market increased form 280 MWp in 2000 to 16629 MWp in 2010, this means an average annual growth rate of 50%. Stable markets supported by feed-in tariffs helped in this development. This mechanism enabled thousands of small solar power producers to enter the electricity market (Schleicher-Tappeser, 2012).

Figure 6.24 shows the development of PV cell and modules productions between 1990 and 2004. Almost half of this increase was due to the German market (Jäger-Waldau, 2007).

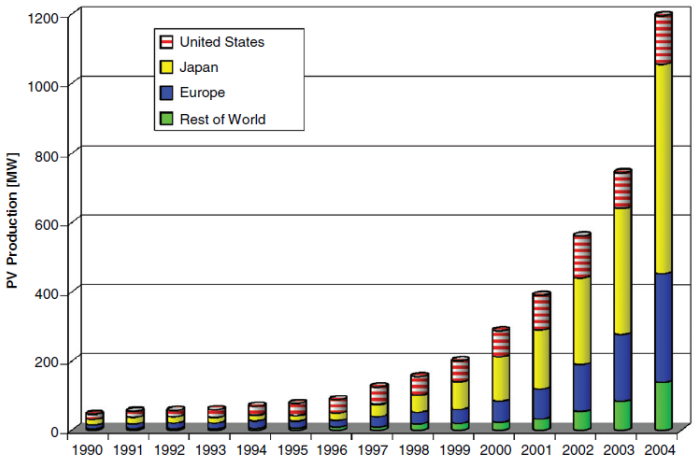

Figure 6.24: World PV Cell/Module Production from 1990 to 2004 (data source: PV News) (Jäger-Waldau, 2007)

The capacity of solar photovoltaics increased 25% during 2015 compared to the previous year. Demand for solar PV energy technology was concetrated in first world countries. However, emerging markets on all continents have started to contribute in the global increase of the electricity generation using PV panels (Renewables 2016 global status report.2016).

The figure below (see Figure 6.25) shows the evolution of solar PV global capacity by country.

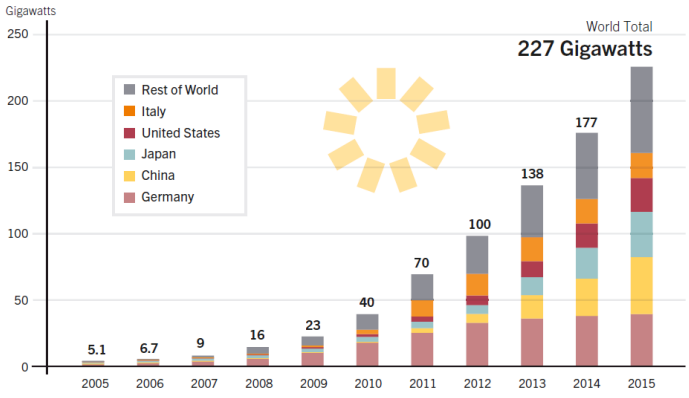

Figure 6.25: Solar PV Global Capacity, by Country/Region, 2005–2015 (Renewables 2016 global status report.2016)

- Solar thermal heating and cooling

Solar thermal technology is used for provide hot water and heating and cooling space. The capacity of this technology is continuously rising, although during 2015 the newly installed

capacity was 14% lower than in 2014. The Figure 6.26 summarizes the evolution of the global capacity in solar thermal capacity (Renewables 2016 global status report.2016).

Concentrating solar thermal plants (CSP) with thermal storage systems are able generate peak, intermediate or base-load electriciy. Therefore, with proper investments in the technology, CSP would be highly complementary to solar PV generation (Energy, climate change & environment.2016).

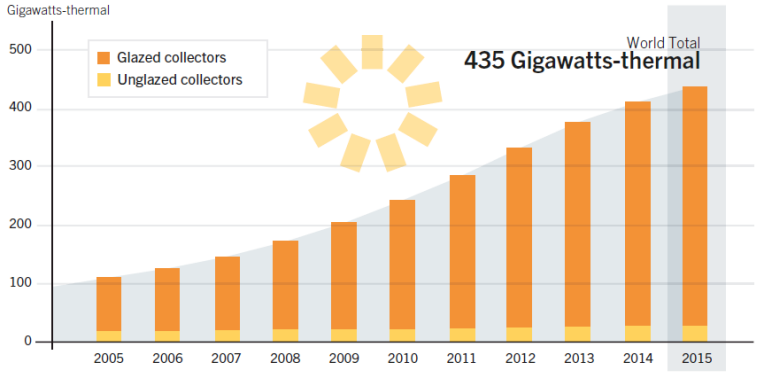

Figure 6.26: Solar Water Heating Collectors Global Capacity, 2005–2015 (Renewables 2016 global status report.2016)

In conclussion, there is enough potential in the technical and market aspects to significantly increase the current contribution of green energy sources to the energy demand, but a constant support for innovation and research is essential for all renewable technologies (Energy, climate change & environment.2016). Figure 6.27 presents the evolution of the renewable energy consumption worldwide. Although the trend is to increase the share of green energy sources, the total contribution is still far from the amount of fossil fuels used to generate energy.

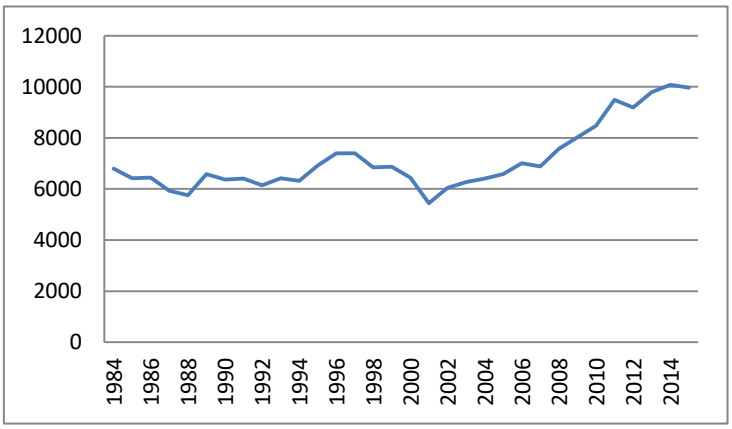

Figure 6.27: Total Renewable Energy Consumption (TJ) (Total energy.2016)

Figure 6.28 summarizes the net additions to power capacity that energy source (fossil, nuclear and renewable) and technology has suffered in 2015. It is worth mentioning that the interest in renewable energy systems is growing rapidly.

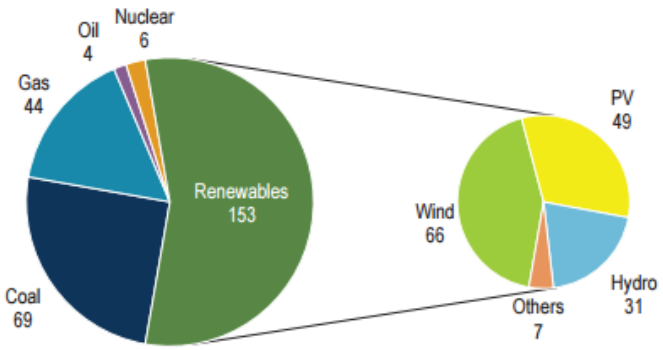

Figure 6.28: Net additions to power capacity (GW), 2015 (Energy, climate change & environment.2016)

Advanced renewable energy techonologies would be environmentally responsible and cost effective alternatives to the current energy generation. This would result in benefits in employment and economocic aspects with the R&D investment (Dincer, 2000).

Although their contribution in the global energy consumption is still low, renewable energy systems continue growing in both capacity and energy generation. This increase has been much more notorious in the power sector than in the heating and cooling and tranport areas. Bioenergy is still leading in the heat and transport areas, and hydropower generates the majority of renewable power generation. It is worth mentioning that solar photovoltaics and wind power are the most dynamic technologies (Renewables 2016 global status report.2016). The decrease in the cost of renewable energy power generation has helped in this fact. The Figure 6.29 show the evolution of the costs of solar and wind energy technologies (Energy, climate change & environment.2016).

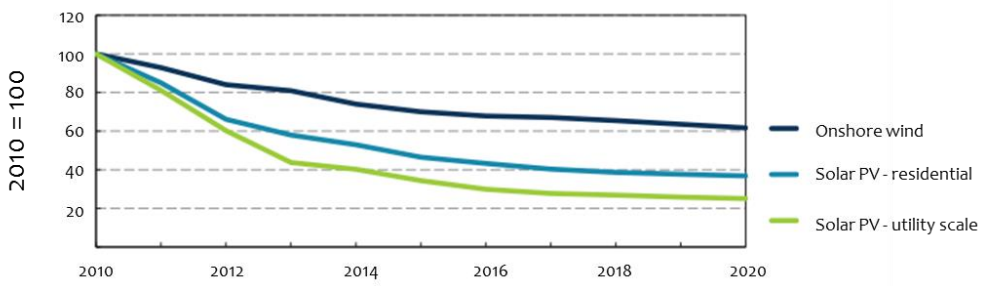

Figure 6.29: Falling indexed generation costs for renewables (Energy, climate change & environment.2016)

According to many publications such as the Renewables 2016 global status report, the annual global carbon dioxide (CO_2) emissions remained steady during 2014 and 2015. Improvements in energy efficiency, industrial restructuring and increase in renewable energy use led to possitive results. Nevertheless, the atmospheric emissions are expected to continue rising for some years in the developing countries, and the concentration of greenhouse gases in the atmosphere is continuously increasiang (Renewables 2016 global status report.2016).

The GHG emissions from power generator systems are also a very important indicator when implementing renewable energy technologies in the energy system. The figure below (Figure 6.30) show the grams of CO2 equivalent per kWh electricity produced. It is important to note that the life-cycle GHG emission of photovoltaic technologies are similar to nuclear power plants. Although the GHG emissions of both PV technologies and nuclear plants during the power generation phase are negligible, there are emission during the construccion and decommissioning phase. PV arrays are produced by high-tech procedures of silicone doping under vacuum. This process emits large quantities of GHG. Building a nuclear plant involves the construction of massive reinforced concrete structures, where large quantities of GHG are emitted (Dincer & Zamfirescu, 2014).

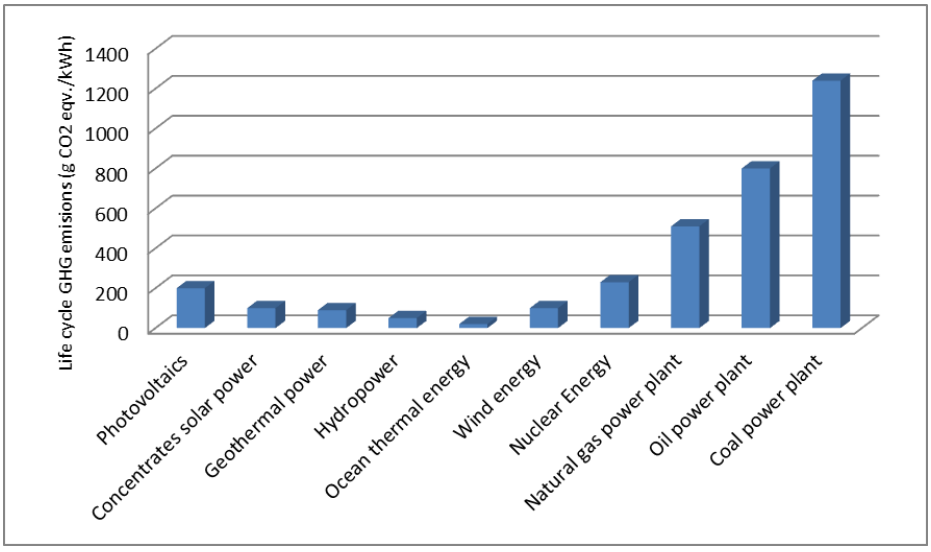

Figure 6.30: Lifecycle GHG emissions from various power generation technologies. Adapted from (Dincer & Zamfirescu, 2014)

7. SOLAR RADIATION

Solar radiation is the energy emitted by the sun, and it is the most abundant of all renewable and sustainable energy resources in the world. It is essential to all life on Earth and plays an essential role in the energy balance of physical, chemical and biological processes. The amount of solar radiation that reaches the earth directly influences the fluxes of sensible and latent heat, the hydrological cycle, terrestrial ecosystem and the climate (Wang et al., 2016). The autotrophs are organisms that through the photosyntesis process use solar energy, together with carbon dioxide and water to produce simple sugars. Therefore, they produce their own food from the sun. Heterotrophs, organisms that eat other organisms, could not exist without autotrophs since they need them to form the bottom level of the food chain. Thus, life depends on the solar radiation (Solar radiation: Sunlight and more.2016).

As mentioned in section 5 all the energy supplies available on Earth derive directly or indirectly from the sun. Conventional fuels, it is coal, oil and natural gas, come from ancient biological material, which millions of years ago took its energy from plant photosysthesis from the sun.

Wind energy and the evaporation of water to generate rainfall which acumulates in lakes and rivers, producing potential hydro energy, are also indirectly powered by the sun.

Direct solar energy is what it is usually undestood as solar power; it is the use of solar radiation to generate electriciy or heating.

The Earth´s weather processes, which determine the natural environment, are also dependant on the solar radiation (Muneer, 2004).

The sun is an inmense and inhexaustible energy source. Its diameter is $1.39x10^{9}$ m and the distance from the Earth is $1.5x10^{11}$ m. Its average temperature is 5,500° C.

Solar energy results from the nuclear fussion of hidrogen atoms that takes place in the sun, causing a mass loss which is transformed in energy and reaches the earth as solar radiation. Solar radiation value in the sun is 63,450,720 W/m^2, and the solar constant value, which is the average electromagnetic radiation per unit area that gets a plane perpendicular to the rays, is 1,367 W/m^2.

The transmission of the solar radiation from the sun to the Earth is made by electromagnetic waves. The frecuency and wave lenght of these electromagnetic waves define their energy, visibility and power of penetration. The speed of all of them in their way from the sun to the Earth through the space is 299,792 km/s. The combination of all the wave lenghts is the electromagnetic spectrum, and the electromagnetic radiation emitted by the sun defines the solar spectrum and includes the spectral regions from X-rays to radio waves (see Figure 7.1). This radiation is known as the extraterrestrial solar spectrum (ETS) (Badescu, 2008).

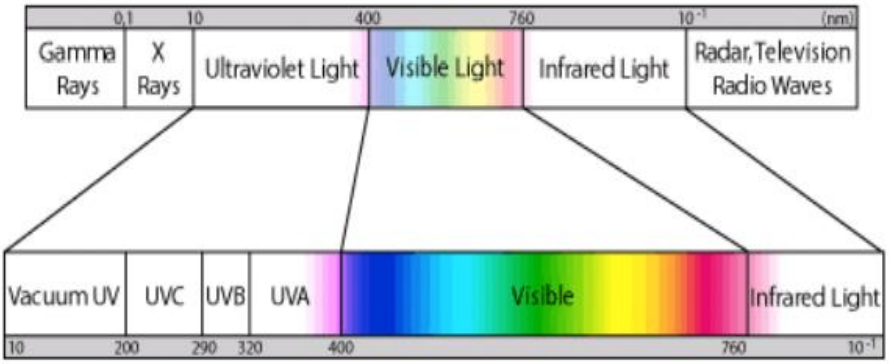

Figure 7.1: Extraterrestrial Solar Spectrum (Agencia estatal de meteorologia.2017)

The proportion of solar radiation in the different ranges of the spectrum is approximately 7% ultraviolet light, 43% visible light, 49% infrared light and 1% the rest of the wave lenghts (Agencia estatal de meteorologia.2017).

The distance between the Sun and the Earth varies by +/-1.7% a year because of the eccentricity of the Earth´s elliptical orbit. Thus, the intensity of the solar radiation varies +/-3.4% at the top of the atmosphere (Badescu, 2008).

7.1 SOLAR RADIATION COMPONENTS

The sun illuminates the earth with almost parallel rays of radiation. When this radiation gets to the Earth, there is an interaction between the photons in the beam and the atmosphere, and a part of the energy is removed by scattering and absortion of the photons out of the beam into random ways in the atmosphere (Badescu, 2008). Both fenomenums, scattering and absortion, influence the **extraterrestrial radiation** modifying the spectral energy that passes through the atmosphere (Aras, Balli, & Hepbasli, 2006). These scattered photons are known as the **diffuse radiation**. The photons that have not been scattered or absorved

remain almost parallel and constitute the **direct beam radiation.** The direct solar beam falls on a unit area perpendicular to the beam at the Earth´s surface. The sum of the diffuse and beam radiation flux that reaches a horizontal surface is called the global radiation. The difference between the global radiation at ground level and the radiation amount on the top of the atmosphere is the quantity of photons that the atmosphere has absorved or reflected away. Around 29% of the incoming solar radiation is reflected to space (Badescu, 2008).

The global solar radiation that reaches a non-horizontal surface is constituded by the diffuse and beam radiation that have been mentioned for a horizontal surface, and an additional radiation reflected from the ground, which is known as the global **ground-reflected radiation** or albedo. A proper estimate of the reflected radiation of a given terrain is essential for calculations related to the energy balance of vegetation, amount of potential transpiration, energy interception of windows, walls and roofs, and solar energy collectors. The small and large scale variations of albedo are due to spacial and temporal landscape changings and seasonal presence of snow and some extent moisture deposition in the earth (Muneer & Tham, 2013). Therefore, it needs to be considered especially in the northern latitudes, since the highly reflecting snow cover and low elevations of the sun may affect significantly. In order to estimate accurately the ground-reflected radiation value, information about the foreground type and geometry, its reflectivity, degree of isotropy, details of the surrounding skyline and the conditions of the sky are required (Badescu, 2008). The Figure 7.2 represents the solar radiation components.

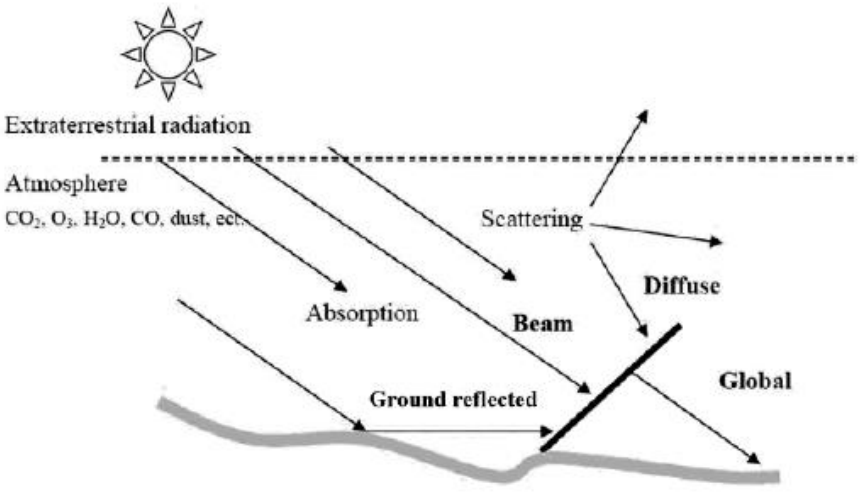

Figure 7.2: Solar Radiation components (Badescu, 2008)

The altitude and azimuth of the Sun are constantly changing during the day. Due to this fact, the angle of incident of the beam radiation, whith almost paralell rays, is constanly changing.

As Gueymard and DR. Myers claim "Lambert´s cosine law states that the flux on a plane surface produced by a collimated beam is proportional to the cosine of the incidence angel of the beam with the surface" (Gueymard & Myers, 2008).

These equations relate the global, beam and diffuse radiation with the solar elevation and zenith angle (which is equal to the incidence angle).

Horizontal sufaces:

$$H = H_b cos(\theta_s) + H_d = H_b sin(\alpha) + H_d \quad (7.1)$$

Tilted surfaces:

$$H = H_b cos(\theta) + R_d H_d + R \quad (7.2)$$

In conclussion, the terrestrial solar radiation not only depends on the solar and site altitude but also in the albedo, the atmospheric transparency, which is a function of aerosols and water vapor among others, and cloudiness. Aerosols in the atmosphere weakens the beam component, and therefore increases the diffuse radiation, thus it does not affect much in the global solar radiation value. Water vapor, weakens both diffuse and beam components of solar radiation, thus it decreases the global solar radiation.

The total extraterrestial and measured terrestrial global solar irradiation values for the same time and unit area can differ depending on the atmospheric conditions. Solar energy calculations are directly affected by the meteorological events (Badescu, 2008).

As mentioned before, solar radiation is essential to all lifes on earth. It is also closely related to daylight, which sustains the food chain through photosysnthesis. Visible light is one of the most relevant parts of the solar spectrum, and the best known by human beings together with the infrared radiation which is perceived as heat.

Solar radiation is therefore directly associated to the agricultural sector. The heating coefficient of a field, which is needed for the soil germination temperature and the energy

absorved in the photosyntheis process, commonly known as the process of green plants converting light into chemical energy, among others, depend on the wave length of the incident radiation, thus models are required for the aplication of the photobiology spectral irradiation.

It is also an essential factor in the breeding of cattle, sheep and other animals. Although the low absorptivity of animal´s coat and the insulating barrier in form of fleece, the limited availability of animals to vaporize moisture makes solar radiaton a must consider issue (Muneer, 2004).

Solar energy conservation devices depend on solar radiation too. Solar photovoltaic plants convert photons into electricity and solar thermal systems can also generate electricity from the elevated temperature they produce. This heat can also be used to meet the global heat consumption. An effective use of daylight can produce significant savings in energy consumption too, and innovative design and daylight applications such as passive solar design, are also dependant on the visible light part of the solar spectrum.

However, despite the potential of the energy emitted from the sun, which is free and abundant with a minimum impact on the environemnt, the efficiency of the technologies and applications, proper design and performance predictions of solar energy systems (de Miguel, Bilbao, Aguiar, Kambezidis, & Negro, 2001) depend on the accuracy of the knowledge about the solar radiation field at the surface.

Thus, it is fundamental to have a knowledge of the solar radiation that the Earth´s surface receives to understand the physical processes that happen in the Earth-atmosphere system and in the succesful development of solar energy utilization projects, especially in countries where the conventional sources of power are not easily available and in arid and semi-arid regions where sunshine is abundant (Mani & Chacko, 1973).

Accurate solar radiation data are not only essential for solar power generation and assessment of energy consumption in buildings, they are also important for agriculture, urban planning and atmospheric pollution analysis (Furlan, de Oliveira, Soares, Codato, & Escobedo, 2012).

7.2 IN SITU SOLAR MEASUREMENTS

The most precise way to estimate global, direct and diffuse solar radiation at the surface is the *in-situ* measurement.

However, the study of radiation is comparatively new. Until 1960 only three stations in the north-west Europe had recorded irradiation values for more than 25 years.

The measurement of the properties of the radiant energy is called radiometry. Solar radiation stations have radiometric instrumentation to collect information about the solar energy. These instruments can be divided into two main groups, broadband instruments which measure all wavelengths radiations and spectral instruments, which just measure a certain wavelenght radiation (Muneer, 2004). These are the most popular devices for solar radiation measurements.

Pyranometer

This instrument (see Figure 7.3) measures global solar radiation. Its measurent spectrum is usually 285-2,800 nm, although it is possible to add glass filters to reduce the spectral ranges to 525-2800 nm, 630-2800 nm, 700-2,800 nm, 780-2,800 nm and their combinations using instruments with differente colour domes. The total power absorved from the solar radiation activates a thermal detector which is in the sensing element. This proces generates heat, which flows to the heat sink through a thermal resistance. The temperature difference is converted into a small voltage, and this can be detected by the computer. Double glass envelope avoids temperature fluctuation and reduces thermal radiation losses (Muneer & Tham, 2013). The uncertainity of the nominal measurement is less than +/-2%, increasing with zenith angle, and the time constant is about 30 seconds. The calibration needs to be done against reference instruments or secondary standards.

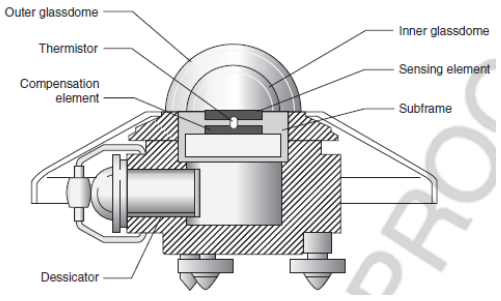

Figure 7.3: Pyranometer (Muneer & Tham, 2013)

Pyranometer with shading device

This kind of pyranometer (see Figure 7.4) measures the diffuse solar radiation. The shadow ring shades the direct radiation from the sun, and need to be adjusted according to the sun´s declination angle.

Figure 7.4: Pynanometer with shading device (Omni instruments.2015)

Pyrheliometer

This device is used to measure the direct solar radiation at normal incidence. The measure spectrum is 285 – 4,000 nm for field instruments with quartz window (Muneer, 2004). The pyrheliometer can measure the beam radiation as the sun moves, since it is equiped with a sun tracking system.

The collimator inside the device can include the complete sun´s disk, with an optimum aperture of 6°. A thermopile converts the thermal radiatian to an electrical voltage so it can be recorded in data loggers (Muneer & Tham, 2013). The uncertainity of the pyrheliometer is of less than +/-1% under laboratory conditions and +/-3% under field conditions and the time constant is about 1 minute (Muneer, 2004).

Pyrgeometer

The pyrgeometer (see Figure 7.5) measures long wave radiation, nominally 4-50 µm, which falls in the infrared radiation spectrum. It is compound with a dome mirror with solar blind filter coating, which eliminates short wave radiation, a thermopile, a temperature sensor and a sun shield which reduce the heat (Muneer & Tham, 2013).

Its accuracy is better than 2%, and the calibration is usually done against a blackbody emission source (Muneer, 2004).

Figure 7.5: Pyrgeometer (Muneer & Tham, 2013)

Albedometer

The albedometer is constructed with two pyranometers (see Figure 7.6). One of them is facing upwards and measures the global radiation, while the other one is facing downwards measuring the ground-reflected radiation.

$$Albedo = \frac{Reflected\ radiation}{Global\ radiation} \qquad (7.3)$$

Both provide output individually, and the albedo is the ratio between the two values.

Figure 7.6: Albedometer (Muneer & Tham, 2013)

Sunchine recorder

According to the World Meteorological Organizatio (WMO) (Muneer & Tham, 2013) the sunshine duration is defined as "sunshine duration during a given period is defined as the sum of that sub-period for which the direct solar irradiance exceeds 120 W/m^2".

The sunshine recorder is constructed with a solid glass spherical lens, which produces a trace on a treated paper when the beam irradation is above 120 W/m^2 (see Figure 7.7). This level can vary loosely depending on ambient conditions, however, the sunshine recorder is an economic and robust device and it is used extensively (Muneer & Tham, 2013).

Figure 7.7: Sunshine Recorder (Muneer & Tham, 2013)

Rotating shadow band radiometer (RSR)

This device can measure quasi-simultaneously the global and diffuse radiation components with a rotating shade. The measured spectrum is usually between 300-1,100 nm, and the instrument is silicon based. Direct radiation value can be estimated from the difference between the global and diffuse radiation values. Cosine and spectral corrections are necessary. The latter is needed to compensate for the insensitivity to IR radiation. The RSR´s response is very fast, and the overall accuracy under favorable conditions is better than 6%. The calibration is usually done against a reference pyranometer (Muneer, 2004).

However, there are many errors associated to the measurement of the solar radiation that require exceptional care and need to be taken into consideration. The most common cause of errors is due to the measuring equipment and their respective sensitivities, associated to the equipment arise from the sensors and their construction. These errors include:

- Cosine effect:

  This is the most apparent error and it is related to the angle at which radiation gets the sensing area. The lower the altitude of the sun is (sunrise and sunset) the greater error is. Cosine error is solved by excluding these values.

- Azimuth response:

  This innacuracy is associated to manufacturing errors. It can be caused by imperfections in the glass domes or the angular reflection properties of the black paint.

- Temperature response:

This is also an individual error for each device. Fluctuations in the sensor´s temperature cause percentage errors.

Spectral sensitivity, stability, nonlinearity, thermal inestability and zero offset due to nocturnal radiative cooling are also well known errors which are related to equiments (Muneer & Tham, 2013).

Site operation problems are another major cause of error. Instrument proximity to shading elements, electrical and magnetic fields, bird and insect activity or weather activities among others affects considerably in the results (Muneer, Younes, & Munawwar, 2007).

The most common errors associated to operational errors are: a) complete or partial shade-ring misaligned, b) dust, snow, dew, water droplets, bird droppings, c) incorrect sensor leveling, d) shading caused buildings, e) electric fields near cables, f) mechanical loadings on cables, g) improper screening or orientation of the vertical sensors from ground-reflected radiation, h) station shutdowns (Muneer & Tham, 2013).

The calibration of the instruments and the effect of temperature and ventilation need to be considered as well (Furlan et al., 2012). When measuring diffuse solar radiation, it is important to consider the blocking effect that is caused by the shadowing devices (Furlan et al., 2012). It is, therefore, essential to identify erroneous data and exclude or correct them. A quality control procedure was developed, based on physical and statistical tests, to remove suspeted outliers in the datasets (Muneer et al., 2007).

Despite the errors associated to the *in-situ* radiation measurements, they are still the most accurate radiation data. This information is indispensable for the design and assessment of solar energy utilization technologies (Zhang, Zhao, Deng, Xu, & Zhang, 2017). Ideally, solar radiation measured data should be available from a dense network of stations around the world where global, direct and diffuse radiations are routinely measured.

7.3 SOLAR RADIATION ESTIMATION MODELS

Unfortunately, solar radiation measurements are not easily available for many countries, especially for developing ones (Despotovic, Nedic, Despotovic, & Cvetanovic, 2016). The measurement of the energy received from the sun is expensive, thus few locations in the world have long-term and reliable measured radiation data sets (Muneer, 2004) mainly due

to the high initial investment and maintenance cost and technical requirements (Wang et al., 2016). Daylight measurement data are even more limited (Muneer, 2004).

In America for example, the ratio between stations measuring solar radiation to those measuring temperature is lower than 1:100 (Wang et al., 2016). In China, there are 756 meteorological stations in total, and only 122 of them have records of global solar radiation (Zhang et al., 2017). Within the UK and Spain, historical records of hourly global data are available for 71 and 31 stations, respectively.

Therefore, developing and applying proper methods to estimate solar radiation data, when measured records are not available, has been the focus of numerous solar studies. More readily available meteorological parameters have been used for this purpose (Wang et al., 2016; Zhang et al., 2017).

Prediction models to estimate radiation and daylight values would provide a notorious reduction in energy consumption, since they help to estimate real radiation values and reduce the uncertainty (Muneer, 2004).

Solar radiation and daylight have similar physical characteristics, thus modelling the quantity of one of them gives information to undestand the other. Both solar energy and daylight utilization for any location depends on the quantity of the available flux. The amount of solar radiation that gets to a surface depends on the geometry and microclimatic interaction between it and the surroundings (Muneer, 2004). The solar flux in any arbitrary surface suffers monthly as well as diurnal variations.

Artificial intelligence is a promising method to model solar radiation and a few models based on Artificail Neural Network (ANN) have been developed to estimate radiation in different regions of the world. An adaptative neuro-fuzzy approach was defined by Olatomiwa et al. using air temperature and sunshine duration to predict solar radiation in Nigeria (Olatomiwa, Mekhilef, Shamshirband, & Petković, 2015). The same researchers also developed a suppor vector machines firefly algorithm, ANN and Genetic Programming models to estimate solar radiation in the Iranian city (Olatomiwa et al., 2015). Park et al. used a topographic factor and sunshine duration to estimate the spatial distribution of solar radiation in South Korea (Park, Das, & Park, 2015). A Markov transitions matrix method was proposed by Aguiar et al. to estimate daily radiation values from clearness index (Aguiar, Collares-Pereira, & Conde, 1988). A Gaussian model for generating synthetic hourly radiation was also presented by Aguiar and Collares-Pereira (Aguiar & Collares-Pereira,

1992). Amrouche and Pivert used combine spatial modeling and ANN techniques to predict global radiation in two French locations (Amrouche & Le Pivert, 2014). Linares-Rodriguez et al. used ANN methods to estimate solar radiation based on latitude, longitude, day of the year and other climatic parameters in Spain (Linares-Rodríguez, Ruiz-Arias, Pozo-Vázquez, & Tovar-Pescador, 2011).

Furthermore, satellite images are also used to study the solar radiation spatial-temporal variations around the world. Hay was pioner in introducing the modeling methods for satellite based estimates of solar radiation at the Earth surface (Hay, 1993). Cano et al developed a method to estimate the global radiation form meteorological satellite data (Cano et al., 1986). Antonanzas-Torres et al. compared the globar solar radiation values from a satellite estimate model and on-ground measurement in Spain (Antonanzas-Torres, Cañizares, & Perpiñán, 2013).

However, most of the presented models to estimate solar radiation are based on parameters that are more readily available. Some of these parameters are extraterrestrial radiation, mean temperature, maximum temperature, soil temperature, relative humidity, number or rainy days, altitude, latitude, total presipitation, cloudiness and evaporation among others (Bakirci, 2009).

7.3.1 Models of solar global radiation vs sunshine duration - Review

Solar radiation depends on many astronomical and meteorological factors and in practical studies it is not possible to consider all of them (Badescu, 2008). The most commonly used parameter in the estimations is sunshine duration. The measurement of sunshine duration is easy and reliable and data are widely available (Bakirci, 2009). The first equation relating monthly average daily global radiation to average clear-sky daily global radiation and the sunshine duration fraction using an empirical correlation in form of a liner expression was developed by Angstrom (1924) (Angstrom, 1924; Zhang et al., 2017). Page and others replaced the clear-sky radiation with average daily extraterrestrial radiation on horizontal surface (Page, 1967). This modified correlation, also known as the Angstrom-Page model is the most typical empirical model in solar engineering (Zhang et al., 2017).

$$\frac{H}{H_0} = a + b\frac{S}{S_0} \quad (7.4)$$

This formula has been used for many years to estimate in practical applications annual, monthly and daily global solar irradiation (H) values. The values of H_o and S_o are fixed by deterministic expressions (Badescu, 2008).

For monthly values for example, the monthly average daily extraterrestrial radiation on a horizontal surface (H_o) can be determined with the following equation (Bakirci, 2009).

$$H_0 = \frac{24}{\pi} I_{SC} \left(1 + 0.033cos\frac{360D}{365}\right) x(cos\varphi cos\delta sin\omega_s + \frac{2\pi\omega_{ms}}{360} sin\varphi sin\delta) \quad (7.5)$$

Where the solar declination (δ) and the sunset hour angle (ω_s) can be calculated as:

$$\delta = 23.45sin\left[\frac{360(D+284)}{365}\right] \quad (7.6)$$

$$\omega_s = cos^{-1}[-tan\delta tan\varphi] \quad (7.7)$$

In the case of the monthly average day length S_o it can be estimated with the following equation (Bakirci, 2009).

$$S_0 = \frac{2}{15}\omega_{ms} \quad (7.8)$$

The model parameters 'a' and 'b' vary temporary and randonmly at a given station. In the models that have been elaborated so far, the parameters 'a' and 'b' have been considered as constant for the period of time used in the application (Badescu, 2008). The sunshine duration ratio is essential in estimating solar radiation. Many researchers have developed correlation models using different expression of the Angstrom-Page model, with quadratic, cubic, square root, exponential,… expressions and adapted to different locations (Zhang et al., 2017). Page´s model is thought to be applicable anywhere in the world; Khogali et al. used data measured in three different stations in Yemen (Khogali, Ramadan, Ali, & Fattah, 1983). Benson et al. presented two correlation equations for different period of a year depending on the climatic conditions (Benson, Paris, Sherry, & Justus, 1984). Alsaad

modified Angstrom´s equation for Amman (Alsaad, 1990). Tasdemiroglu and Sever developed a second-degree equation for six Turkish locations (Taşdemiroğlu & Sever, 1991). Bahel´s equation is a worldwide correlation based on data from 48 stations around the world (Bahel, Srinivasan, & Bakhsh, 1986).

Some of those regression models are given below (see Table 7.1).

Table 7.1: Global Radiation vs Sunshine duration models

Page (Page, 1961)	$\frac{H}{H_0} = 0.23 + 0.48\left(\frac{S}{S_0}\right)$	**(7.9)**
Khogali et al (Khogali et al., 1983)	$\frac{H}{H_0} = 0.191 + 0.571\left(\frac{S}{S_0}\right)$	**(7.10)**
	$\frac{H}{H_0} = 0.297 + 0.432\left(\frac{S}{S_0}\right)$	**(7.11)**
	$\frac{H}{H_0} = 0.262 + 0.454\left(\frac{S}{S_0}\right)$	**(7.12)**
Benson et al (Benson et al., 1984)	$\frac{H}{H_0} = 0.18 + 0.6\left(\frac{S}{S_0}\right)\ (January - March\ and\ October - December$	**(7.13)**
	$\frac{H}{H_0} = 0.24 + 0.53\left(\frac{S}{S_0}\right)$ (April – September)	**(7.14)**
Bahel eta al (Bahel et al., 1986)	$\frac{H}{H_0} = 0.175 + 0.552\left(\frac{S}{S_0}\right)$	**(7.15)**
Jain (P. Jain, 1986)	$\frac{H}{H_0} = 0.177 + 0.692\left(\frac{S}{S_0}\right)$	**(7.16)**
Alsaad (Alsaad, 1990)	$\frac{H}{H_0} = 0.174 + 0.615\left(\frac{S}{S_0}\right)$	**(7.17)**
Jain and Jain (S. Jain & Jain, 1988)	$\frac{H}{H_0} = 0.240 + 0.513\left(\frac{S}{S_0}\right)$	**(7.18)**
Soler (Soler, 1990)	$\frac{H}{H_0} = 0.18 + 0.66\left(\frac{S}{S_0}\right)\ January$	**(7.19)**
	$\frac{H}{H_0} = 0.20 + 0.60\left(\frac{S}{S_0}\right)\ February$	**(7.20)**
	$\frac{H}{H_0} = 0.22 + 0.58\left(\frac{S}{S_0}\right)\ March$	**(7.21)**
	$\frac{H}{H_0} = 0.20 + 0.62\left(\frac{S}{S_0}\right)\ April$	**(7.22)**
	$\frac{H}{H_0} = 0.24 + 0.52\left(\frac{S}{S_0}\right)\ May$	**(7.23)**

	$\frac{H}{H_0} = 0.24 + 0.53\left(\frac{S}{S_0}\right)\ June$	**(7.24)**
	$\frac{H}{H_0} = 0.23 + 0.53\left(\frac{S}{S_0}\right)\ July$	**(7.25)**
	$\frac{H}{H_0} = 0.22 + 0.55\left(\frac{S}{S_0}\right)\ August$	**(7.26)**
	$\frac{H}{H_0} = 0.20 + 0.59\left(\frac{S}{S_0}\right)\ September$	**(7.27)**
	$\frac{H}{H_0} = 0.19 + 0.60\left(\frac{S}{S_0}\right)\ October$	**(7.28)**
	$\frac{H}{H_0} = 0.17 + 0.66\left(\frac{S}{S_0}\right)\ November$	**(7.29)**
	$\frac{H}{H_0} = 0.18 + 0.65\left(\frac{S}{S_0}\right)\ December$	**(7.30)**
Luhanga and Andringa (Luhanga & Andringa, 1990)	$\frac{H}{H_0} = 0.241 + 0.488\left(\frac{S}{S_0}\right)$	**(7.31)**
Jain (P. Jain, 1990)	$\frac{H}{H_0} = 0.313 + 0.474\left(\frac{S}{S_0}\right)$	**(7.32)**
	$\frac{H}{H_0} = 0.307 + 0.488\left(\frac{S}{S_0}\right)$	**(7.33)**
	$\frac{H}{H_0} = 0.309 + 0.599\left(\frac{S}{S_0}\right)$	**(7.34)**
Louche et al (Louche, Notton, Poggi, & Simonnot, 1991)	$\frac{H}{H_0} = 0.206 + 0.546\left(\frac{S}{S_0}\right)$	**(7.35)**
Gopinathan and Soler (Gopinathan & Soler, 1992)	$\frac{H}{H_0} = 0.1538 + 0.7874\left(\frac{S}{S_0}\right)$	**(7.36)**
	$\frac{H}{H_0} = 0.1961 + 0.7212\left(\frac{S}{S_0}\right)$	**(7.37)**
Veeran and Kumar (Veeran & Kumar, 1993)	$\frac{H}{H_0} = 0.34 + 0.32\left(\frac{S}{S_0}\right)$	**(7.38)**
	$\frac{H}{H_0} = 0.27 + 0.65\left(\frac{S}{S_0}\right)$	**(7.39)**
Chegaar and Chibani (Chegaar & Chibani, 2001)	$\frac{H}{H_0} = 0.309 + 0.368\left(\frac{S}{S_0}\right)\ for\ Algiers\ and\ Oran$	**(7.40)**
	$\frac{H}{H_0} = 0.367 + 0.367\left(\frac{S}{S_0}\right)\ for\ Beni\ Abbas$	**(7.41)**
	$\frac{H}{H_0} = 0.233 + 0.591\left(\frac{S}{S_0}\right)\ for\ Tamanrasset$	**(7.42)**
Akpabio and Etuk (Akpabio & Etuk, 2003)	$\frac{H}{H_0} = 0.23 + 0.38\left(\frac{S}{S_0}\right)$	**(7.43)**

Ulgen and Hepbasli (Ulgen & Hepbasli, 2004)	$\frac{H}{H_0} = 0.2671 + 0.4754\left(\frac{S}{S_0}\right)$	**(7.44)**
Ulgen and Ozbalta (Ulgen & Ozbalta, 2000)	$\frac{H}{H_0} = 0.2424 + 0.5014\left(\frac{S}{S_0}\right)$	**(7.45)**
	$\frac{H}{H_0} = 0.0959 + 0.9958\left(\frac{S}{S_0}\right) - 0.3922\left(\frac{S}{S_0}\right)^2$	**(7.46)**
Akinoglu and Ecevit (Akinoğlu & Ecevit, 1990)	$\frac{H}{H_0} = 0.225 + 0.845\left(\frac{S}{S_0}\right) - 0.280\left(\frac{S}{S_0}\right)^2$	**(7.47)**
Tasdemiroglu and Sever (Taşdemiroğlu & Sever, 1991)	$\frac{H}{H_0} = 0.225 + 0.014\left(\frac{S}{S_0}\right) + 0.001\left(\frac{S}{S_0}\right)^2$	**(7.48)**
Yildiz and Oz (Yildiz & Oz, 1994)	$\frac{H}{H_0} = 0.2038 + 0.9236\left(\frac{S}{S_0}\right) - 0.3911\left(\frac{S}{S_0}\right)^2$	**(7.49)**
Aksoy (Aksoy, 1997)	$\frac{H}{H_0} = 0.148 + 0.668\left(\frac{S}{S_0}\right) - 0.079\left(\frac{S}{S_0}\right)^2$	**(7.50)**
Tahran and Sari (Tarhan & Sarı, 2005)	$\frac{H}{H_0} = 0.1874 + 0.8592\left(\frac{S}{S_0}\right) - 0.4764\left(\frac{S}{S_0}\right)^2$	**(7.51)**
	$\frac{H}{H_0} = 0.1520 + 1.1334\left(\frac{S}{S_0}\right) - 1.1126\left(\frac{S}{S_0}\right)^2 + 0.4516\left(\frac{S}{S_0}\right)^3$	**(7.52)**
Bahel (Bahel, Bakhsh, & Srinivasan, 1987)	$\frac{H}{H_0} = 0.16 + 0.87\left(\frac{S}{S_0}\right) - 0.61\left(\frac{S}{S_0}\right)^2 + 0.34\left(\frac{S}{S_0}\right)^3$	**(7.53)**
Samuel (Samuel, 1991)	$\frac{H}{H_0} = -0.14 + 2.52\left(\frac{S}{S_0}\right) - 3.71\left(\frac{S}{S_0}\right)^2 + 2.24\left(\frac{S}{S_0}\right)^3$	**(7.54)**
Newland (Newland, 1989)	$\frac{H}{H_0} = 0.34 + 0.40\left(\frac{S}{S_0}\right) + 0.17log\left(\frac{S}{S_0}\right)$	**(7.55)**
Almorox and Hontoria (Almorox & Hontoria, 2004)	$\frac{H}{H_0} = -0.0271 + 0.3096exp\left(\frac{S}{S_0}\right)$	**(7.56)**

7.3.2 Diffuse ratiation

Depending on the application, the frecuency at which solar radiation data are needed will be different. For the agricultural meteorology for example monthly-averaged or even annual-averaged data would be sufficient, whereas for solar energy technologies, which depend on solar radiation to convert it into electrical and thermal energy and to light and heat buildings, hour or even minute´s frecuency data are required by the researches (Muneer, 2004). The amount of energy generated from solar energy is a direct function of the amount of solar radiation received and the efficiency of the devices used in the conversion process (National renewable energy laboratory.2016).

However, most of the meteorological stations only have records of global radiation data measured on the horizontal plane. Weather stations rarely register direct and diffuse solar fractions (Bortolini, Gamberi, Graziani, Manzini, & Mora, 2013).

There are more meteorological stations that measure daily rather than hourly radiation values, and it is more common to have daily global values rather than global and diffuse values. According to Muneer a common measurement strategy would be the following (Muneer, 2004):

1. Daily global horizontal irradiation.
2. Daily diffuse and global horizontal irradiation.
3. Hourly global irradiation.
4. Hourly global and diffuse irradiation.
5. Beam radiation values for several orientation and tilts in addition to normal incidence using a pyrheliometer.

As Muneer claims, in the year 1985 there were 56, 23, 26, 19 and 2 stations in the first, second, third, fourth and fifth category respectively (Muneer, 2004).

Most of the radiometric stations are equiped with pyranometers to measure global solar radiation, but only few stations have equipent to measure the diffuse componente of the solar radiation (Paulescu & Blaga, 2016).

The measurement of diffuse and direct data is more expensive and relatively more complicated, and in consequence, these radiation records are even scarcer than the global radiation measurements (Despotovic et al., 2016). In the UK for example, since the year 2002, the diffuse radiation is recorded at only two locations, at North latitudes of Camborne (55.21°) and Lerwick (60.80°).

However, the contribution of the diffuse sky component in the radiation received in the earth´s surface is high enough to consider the diffuse radiation an essential parameter in solar energy projects.

In South Africa, where much of the country lies in the relatively cloud-free anticyclonic belt of Southern Hemisphere, the diffuse radiation contributes about the 30% of the annual

short-wave energy received. In most areas of South Africa, between 45 and 50 kcal/cm^2 are received indirectly over a year. This value is similar to 47 and 43 kcal/cm^2 that Brussels and Berlin receive respectively during a year, where the ratio between diffuse and total radiation is 0.55. In Antananarivo (Madagascar) the diffuse radiation contributes the 40% (70 kcal/cm^2) of the annual total radiation (Drummond, 1956).

The latitude and elevation of the location in question, the solar altitude, the value of the sun´s declination, the degree of atmospheric turbidity, the amount of water vapour present and the cloudiness will affect in the proportion of diffuse in the total solar radiation (Drummond, 1956).

The diffuse radiation is significant in many fields. One of those fields is the heat transfer application in buildings, where this radiation is particularly important in tropical and sub-tropical climates where the energy contribution can reach very high levels. It is also essential in interior illumination requirements, where in a south facing window for example, when certain types of clouds are present, the diffuse skylight entering the window can be ten times the value expected for cloudless-sky conditions. In the utilization of the solar energy, for example in the domestic supply of hot water, the diffuse radiation level can determine the continued efficiency of the process (Drummond, 1956). For flat plate collectors and house energy analysis, diffuse radiation data are also required (Boland et al., 2013).

The direct radiation, on the other hand, is essential to predict the performance and to design concentrating solar plants (Bortolini et al., 2013). And to size, adjust, simulate and monitore the PV panels in one location, both direct and diffuse solar radiation values are needed (Khorasanizadeh, Mohammadi, & Goudarzi, 2016).

Thus, for most applications sky-diffuse radiation values are needed, but there are other applications where the direct or beam solar radiation is more interesting.

In those situations, it is essential to develop correlation models to estimate both diffuse and direct radiation data from the global radiation records. However, according to Boland et al., the use of any model especifically developed to estimate diffuse radiation from knowledge of the global to calculate the direct radiation data, performs as fine as any model especifically designed to estimate the direct radiation data (Boland et al., 2013).

Therefore, many researchers have established empirical correlations to predict sky-diffuse radiation based on available input variables (Despotovic et al., 2016).

As mentioned before, the available radiation measurements are commondly for global radiation on a horizontal surface. However, very few applications use the horizontal configuration; solar collectors for example are mounted tilted at some angle to it. Solar iradiation data on sloped surfaces are essential prerequisites in many sciences. Agricultural metheorology, photobiology, animal husbandry, daylighting and solar energy utilization among others, require information about the availability of solar iradiation on slopes. The solar irradiation on a horizontal surface differs from the irradiation on a tilted surface (Muneer, 2004).

The limited availability of solar radiation data records makes it essential to estimate radiation values for sloped surfaces given values for horizontal surface. Thus, this is an added reason for estimating diffuse radiation values using correlation models (Boland et al., 2013), since both beam and diffuse radiation components are used to estimate slope radiation. It is not possible to merely estimate the radiation using trigonometric relationships, since the diffuse radiation is not isotropic over the sky dome (Badescu, 2008). The radiation that gets to the inclined collector does not only depend on its orientation but it is also sensitive to the assumed distribution that the diffuse radiation has accross the sky (Boland et al., 2013). Once direct and diffuse radiation values are estimated using correlation models, they can then be transported over tilted surfaces. This way, it is possible to estimate the performance of tilted flat plate collectors and other solar devises (El-Sebaii & Trabea, 2003).

Modeling the components of the equations 7.1 and 7.2 is the basis of the estimation methods (Badescu, 2008). The estimation models' accuracy and credibility will directly depend on the accuracy of the available radiation data of any location. The more detailed the records are, the more accurate the predictions will be (Muneer, 2004).

8. REVIEW OF SOLAR SKY-DIFFUSE RADIATION MODELS

As mentioned in section 7, in addition to their use in other disciplines such as agriculture, there are a large number of engineering applications where, beam and diffuse irradiation hourly or sub-hourly are required. The two components are used to estimate, among other things, slope radiation. A brief list of those applications may be drawn thus:

- Solar transmission through building fenestration.
- Daylight transmission through building fenestration.
- Sol-air temperature estimation for opaque building fabric.
- Solar water heating design and product assessment.
- Solar PV design and product assessment.

Following the original work of Liu and Jordan (Liu & Jordan, 1960) a great many number of research teams from around the world have produced regressions relating diffuse ratio (k) and clearness index (k_t) at an hourly, daily, monthly and annual frequency. Each of the above four category of regression is unique and statistically different as shown in the work of Muneer (Muneer, 2004) and Saluja et al. (Saluja, Muneer, & Smith, 1988).

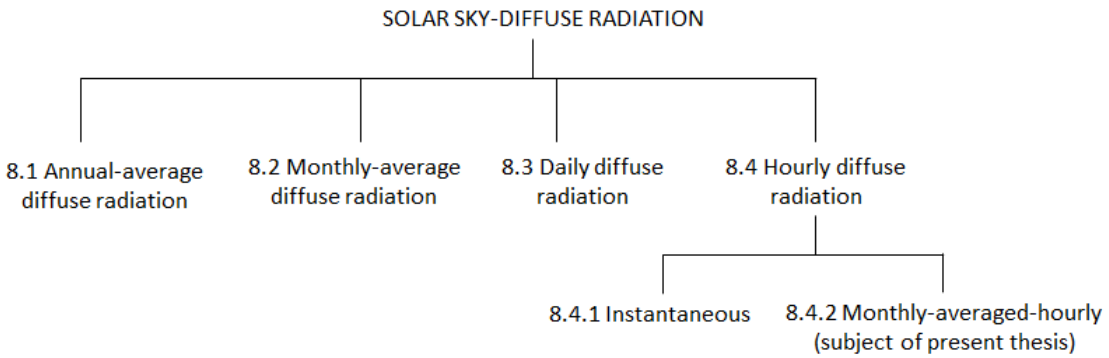

Figure 8.1: Solar sky-diffuse radiation model categories (own elaboration)

8.1 ANNUAL AVERAGE DIFFUSE RADIATION

Agricultural use of solar energy require monthly or even annual radiation data. As mentioned in section 7, the diffuse radiation records are very scarce, and correlation models need to be established in order to estimate the diffuse component from the available parameters.

It is proven that there is a strong correlation between the annual diffuse ratio and the annual clearness index. The equation 8.1 gives the regression between the two annual rations.

$$\frac{H_{d\ annual}}{H_{annual}} = 1 - 1.04k_{t\ annual} \qquad (8.1)$$

Many investigators have developed regression equations for different worldwide locations to prove this fact.

Hawas and Muneer (Muneer & Hawas, 1984) analyzed data from 13 stations in India and the annual global to extraterrestrial radiation fraction ($k_{t\ annual}$) varies between 0.53 and 0.61 in the tropics. Regading to the relationship between the diffuse and extraterrestrial radiation values, the ratio obtained from these data is 0.233.

Stanhill (Stanhill, 1966) used three years measurements of diffuse and global radiation in southern Israel to develop a correlation between the two values, and compared these relationships with those obtained in other locations to verify their applicability in the region. The ratio between the annual diffuse and extraterrestrial radiation reported by Stanhill for Gilat is 0.237.

Both values are very similar and show a high correlation between the diffuse ratio and clearness index. This ratio is also comparable to the values obtained for eight UK locations, as can be seen in the Table 8.1.

Table 8.1: Annual irradiation data for worldwide locations (Muneer, 2004)

Station	Country	$k_{t,annual}$	H_d/H	$k_{d,annual}$
Ahmedabad	India	0.58	0.38	0.22
Bhaunagar	India	0.61	0.36	0.22
Bombay	India	0.56	0.40	0.22
Calcutta	India	0.53	0.47	0.25
Goa	India	0.59	0.38	0.23
Jodhpur	India	0.65	0.34	0.22
Madras	India	0.57	0.41	0.24
Nagpur	India	0.58	0.38	0.22
New Delhi	India	0.61	0.39	0.24
Poona	India	0.58	0.40	0.23
Shillong	India	0.49	0.47	0.23
Trivandrum	India	0.56	0.45	0.25
Visakhaptnam	India	0.58	0.38	0.22
Gilat	Israel	0.66	0.36	0.24
Jersey	UK	0.47	0.51	0.24
Easthampstead	UK	0.40	0.59	0.24
London	UK	0.38	0.58	0.22
Aberporth	UK	0.44	0.56	0.25
Cambridge	UK	0.41	0.60	0.24
Aldergrove	UK	0.41	0.61	0.25
Eskdalemuir	UK	0.37	0.61	0.23
Lerwick	UK	0.39	0.63	0.24
Average				**0.233**

According to Muneer it is easily possible to compute the annual – average extraterrestrial irradiation. Therefore, using a universal value of 0.233 for the ration between the annual diffuse to extraterrestrial radiation, it would be possible to obtain annual diffuse radiation data for any location (Muneer, 2004).

8.2 MONTHLY AVERAGE DIFFUSE RADIATION

As mentioned in section 7, accurate knowledge of the solar radiation at any place is required especially by solar engineers and architects. The annual diffuse radiation data are not enough for various solar energy applications such as solar furnaces, concentrating collectors,… At least monthly diffuse radiation data are needed for these applications.

Therefore, for the locations where only the horizontal global radiation is recorded, models to estimate diffuse radiation are needed (Ulgen & Hepbasli, 2009).

While the most common models estimate monthly average daily global radiation as a function of the monthly average daily measure of sunshine duration (equation 8.2), the monthly average daily diffuse radiation has been estimated typically as a function of either the monthly average daily clearness index as an independent variable (equation 8.3) (Tarhan & Sarı, 2005), the fraction of possible number of bright sunshine hours or a combination of both (El-Sebaii, Al-Hazmi, Al-Ghamdi, & Yaghmour, 2010).

$$\frac{H}{H_0} = f\left(\frac{S}{S_0}\right) \quad (8.2)$$

$$k = \frac{H_d}{H} = g\left(\frac{H}{H_0}\right) = k_t \quad (8.3)$$

$$k = \frac{H_d}{H} = g\left(\frac{S}{S_0}\right) \quad (8.4)$$

Many empirical correlations to estimate the monthly-averaged daily diffuse radiation have been presented during the last decades (El-Sebaii & Trabea, 2003). The first correlation model between the monthly-averaged values of diffuse and global radiation was defined by Liu and Jordan (Liu & Jordan, 1960; Muneer, 2004). This model together with the one brought by Page are two of the most widely used correlations (Page, 1967). From this pioneer research, many empirical correlations have been developed by fitting datasets from different locations and time periods (Despotovic et al., 2016). Iqbal presented a correlation model between the diffuse fraction $\left(\frac{H_d}{H}\right)$ and the fraction of the possible number of sunshine hours $\left(\frac{S}{S_0}\right)$ (Iqbal, 1979). Gopinathan on the other hand, presented empirical models relating the diffuse ratio with the clearness index, fraction of sunshine hours and a combination of both (Gopinathan, 1988).

All the models include empirical constants that are dependent on the season and the geographical location, therefore, most models are only valid for an especific place. According to El-Sebaii and Trabea for example, a correlation between the diffuse ratio and clearness index is adequate to calculate the monthly average daily diffuse radiation in South Africa (El-Sebaii & Trabea, 2003).

Despotovic et al. reviewed and classified the most used correlation models to estimate the monthly average diffuse ratio in three groups: diffuse ratio vs clearness index, diffuse ratio vs. sunshine duration and diffuse ratio vs. combination of clearness index and sunshine duration. They also evaluated the models using ten statistical tools, presenting the most appropiate model for different climate zones.

The table below (see Table 8.2) shows some examples of the correlation models between diffuse ratio and clearness index (Despotovic et al., 2016).

Table 8.2: Monthly Average Diffuse radiation models

Liu and Jordan (Liu & Jordan, 1960)	$k = 1.39 - 4.027k_t + 5.531{k_t}^2 - 3.108{k_t}^3$	(8.5)
Page (Page, 1967)	$k = 1 - 1.13k_t$	(8.6)
Erbs (Erbs, Klein, & Duffie, 1982)	$k = 1.317 - 3.023k_t + 3.372{k_t}^2 - 1.769{k_t}^3$	(8.7)
Barbaro (Barbaro, Cannata, Coppolino, Leone, & Sinagra, 1981)	$k = 1.0492 - 1.3246k_t$	(8.8)
	$k = 1.0896 - 1.4797k_t + 0.1471{k_t}^2$	(8.9)
	$k = 13.9375 - 76.276k_t + 144.3846{k_t}^2 - 92.148{k_t}^3$	(8.10)
Elhadidy (Elhadidy & Abdel-Nabi, 1991)	$k = 1.039 - 1.741{k_t}^2$	(8.11)
	$k = -5.759 + 35.093k_t - 61.052{k_t}^2 + 33.115{k_t}^3$	(8.12)
Jain (P. Jain, 1990)	$k = -0.193 + 0.343k_t$	(8.13)
Tasdemiroglu (Taşdemiroğlu & Sever, 1991)	$k = 1.6932 - 8.2262k_t + 25.5532{k_t}^2 - 37.807{k_t}^3 + 19.8178{k_t}^4$	(8.14)
Tiris (Tiris, Tiris, & Türe, 1996)	$k = 0.583 + 0.9985k_t - 5.24{k_t}^2 + 5.322{k_t}^3$	(8.15)
Kaygurus (Kaygusuz & Ayhan, 1999)	$k = 0.789 - 0.869k_t$	(8.16)
Tarhan (Tarhan & Sarı, 2005)	$k = 0.9885 - 1.4276k_t + 0.5679{k_t}^2$	(8.17)
	$k = 1.027 - 1.6582k_t + 1.1018{k_t}^2 - 0.4019{k_t}^3$	(8.18)
Ibrahim (Ibrahim, 1985)	$k = 0.86 - 0.86k_t$	(8.19)
	$k = 0.636 - 0.279k_t - 0.194{k_t}^2 - 0.383{k_t}^3$	(8.20)
Klein (Klein, 1977)	$k = 1.390 - 4.027k_t + 5.531{k_t}^2 - 3.108{k_t}^3$	(8.21)
Iqbal (Iqbal, 1979)	$k = 0.958 - 0.982k_t$	(8.22)
	$k = 0.914 - 0.847k_t$	(8.23)
Bortolini (Bortolini et al., 2013)	$k = 0.9888 + 0.3950k_t - 3.7003{k_t}^2 + 2.2905{k_t}^3$	(8.24)
Trabea (Trabea, 1999)	$k = 0.534 + 0.384k_t - 1.036{k_t}^2$	(8.25)
Aras et al (Aras et al., 2006)	$k = 1.0212 - 1.1672k_t$	(8.26)
	$k = 1.1244 - 1.5582k_t + 0.3635{k_t}^2$	(8.27)
Ulgen and Hepbasli (Ulgen & Hepbasli, 2009)	$k = 0.6772 - 0.4841k_t$	(8.28)
	$k = 0.981 - 1.9028k_t + 1.9319{k_t}^2 - 0.6809{k_t}^3$	(8.29)
Haydar (Aras et al., 2006)	$k = 1.7111 - 4.9062k_t + 6.6711{k_t}^2 - 3.9235{k_t}^3$	(8.30)

8.3 DAILY DIFFUSE RADIATION

In many solar applications monthly average diffuse radiation data ara not enough. Daily or even hourly solar radiation data represent an important requirement. The first regression equation which relates the daily diffuse ratio and the daily clearness index was also developed by Liu and Jordan (Liu & Jordan, 1960). This correlation did not consider the shade ring for the computation of the clearness index, and they used just one value of the extraterrestrial irradiation for the middle of the month.

Many researches re-investigated the correlation of Liu and Jordan for different locations in the world and defined new models using daily-integrated values of diffuse and global solar radiation values. All the investigators calculated the extraterrestrial radiation for each day. In order to estimate the daily extraterrestrial radiation it is possible to use the following equation (Muneer, 2004).

$$H_0 = \left(\frac{0.024}{\pi}\right) I_{SC} \left[1 + 0.033cos\left(\frac{360DS_0}{365}\right)\right] \cdot \left[cos\varphi cos\delta sin\omega_s + \left(\frac{2\pi\omega_s}{360}\right) sin\varphi sin\delta\right] \quad (8.31)$$

Collares - Pereira and Rabl used 1-4 years data for five stations in the USA measured with a pyrheliometer. They confirmed Liu and Jordan´s model´s validity and concluded that the numerical inacuracies of the original work were due to the use of uncorrected values of diffuse radiation in the regression, use of a single value of extraterrestrial insolation during each month, and not taking into account seasonal variations in the diffuse to hemispherical ratio (Collares-Pereira & Rabl, 1979). However, they found a seasonal trend in the data, although they used all data as a group (Muneer, 2004).

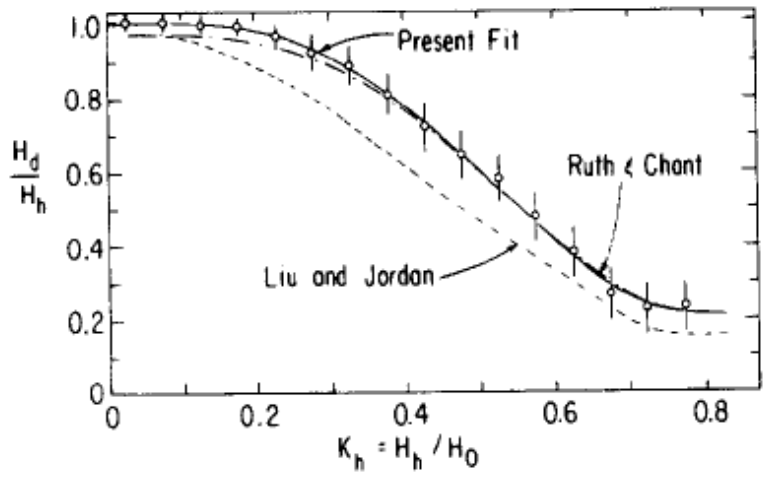

Figure 8.2: Comparison between models of daily diffuse ration vs clearness index (Collares-Pereira & Rabl, 1979)

Erbs et al. (Erbs et al., 1982) presented two seasonal regression equations, one for winter and another one for the rest of the year. The research was made using averaged values of the diffuse ratio over finite intervals of the clearness index (Muneer, 2004), and obtained an equation for each of the seasonal correlations. The equations from the summer data and spring and autum data were almost equal. The following equations represent the seasonal correlations (Erbs et al., 1982).

For ω_s<1.4208

$$k = 1 - 0.2727K_t + 2.4495k_t^2 - 11.9514k_t^3 + 9.3879k_t^4 \; for \; k_t < 0.715 S_0 = \frac{2}{15}\omega_s \qquad (8.32)$$

$$k = 0.143 \; for \; k_t \geq 0.715 \qquad (8.33)$$

For ω_s ≥1.4208

$$k = 1 + 0.28332k_t - 2.5557k_t^2 + 0.8448k_t^3 \; for \; k_t < 0.722 \qquad (8.34)$$

$$k = 0.175 \; for \; k_t \geq 0.722 \qquad (8.35)$$

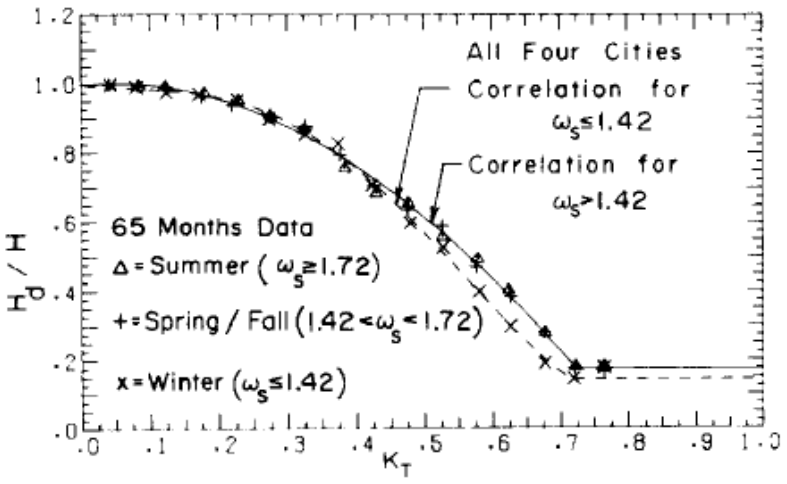

Figure 8.3: Comparison of the seasonal US data with the seasonal correlation between the daily diffuse fraction and k_t (Erbs et al., 1982)

Rao et al. used individual values of diffuse ratio against clearness index to develop a seasonal as well as an annual regression equation. They developed simple linear regression models and more than 85% in the variability of the ratio between diffuse and global radiation was explained by the models (Rao, Bradley, & Lee, 1984).

$$k = 1 \; for \; k_t \leq 0.2 \qquad (8.36)$$

$$k = 1.130 - 0.667k_t \; for \; 0.2 < k_t \leq 0.26 \qquad (8.37)$$

$$k = 1.403 - 1.725k_t \; for \; 0.26 < k_t \leq 0.75 \qquad (8.38)$$

In order to enable the comparison of their research with other models, they presented a fourth order polynomial regression model:

$$k = 0.9493 + 1.1314k_t - 5.7688k_t^2 + 4.5503k_t^3 - 1.2457k_t^4 \qquad (8.39)$$

Choudhary developed a model for New Delhi using only 3 months data, and obtained higher diffuse ratio values than the Liu and Jordan model (Choudhury, 1963). At first, he associated this to the high dust content in New Delhi and his small sample of data. However, as it was proven later, these higher diffuse ration values are due to the lack of compensation of the shade ring of shadow band in the Liu and Jordan study (Muneer, 2004).

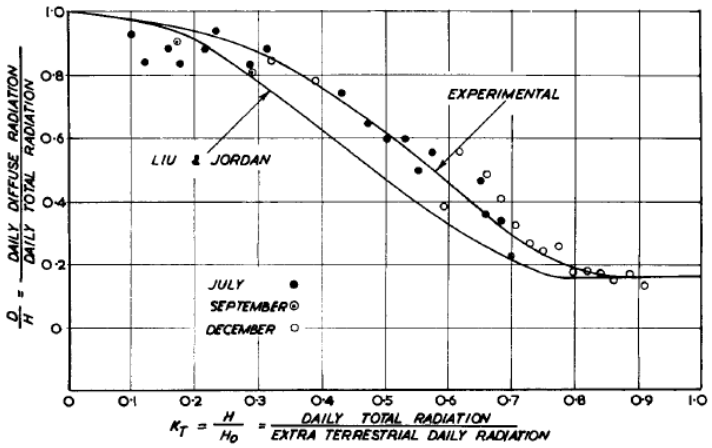

Figure 8.4: Statistical relationship between daily diffused and daily total radiation (Choudhury, 1963)

Muneer and Hawas (Muneer & Hawas, 1984) used 3 years data from 13 stations in India, all of them between 8.5° N and 28.5° N latitude, to develop correlations for each individual station as well as for the whole country of India. The Figure 8.5 shows the regression curves for the Indian locations, concluding a good correlation between the diffuse ratio and clearness index for individual locations (R^2=0.893-0.95) and for the whole country of India (R^2=0.89) (Muneer, 2004).

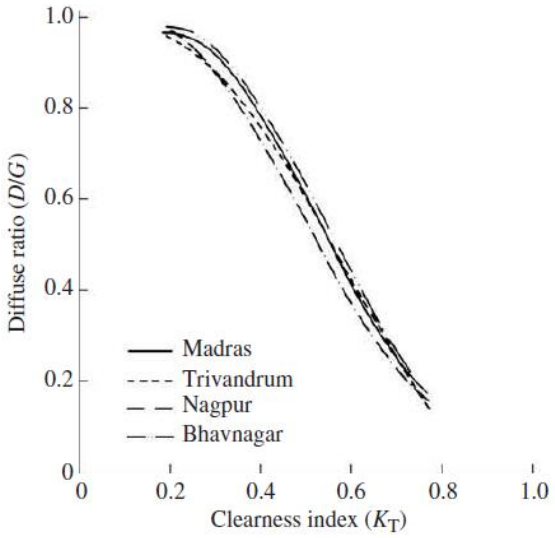

Figure 8.5: Regression curves for daily diffuse ratio – Indian locations (Muneer, 2004)

Ruth and Chant (Ruth & Chant, 1976) studied 7 years data for four Canadian stations (Toronto, Montreal, Goose Bay and Resolute Bay). The diffuse ratios obtained from their research were higher than the ones obtained from the Liu and Jordan model (Muneer, 2004), concluding that the correlation is latitude dependant and are not universaly applicable (Ruth & Chant, 1976).

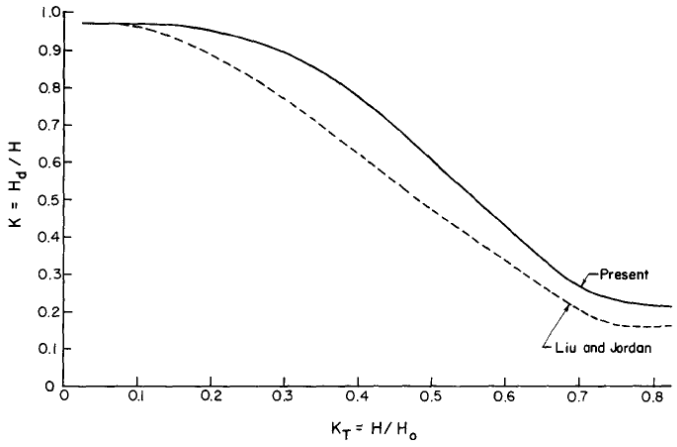

Figure 8.6: Comparison between the models of Ruth and Chant and Liu and Jordan (Ruth & Chant, 1976)

Tuller (Tuller, 1976) presented a model using 1 year daily data from four Canadian sations. He not only found a latitude effect in the results, but also investigated the effect of surface reflectivity on the diffuse radiation, concluding that it was responsible for only 27% of the variance of the diffuse transmission coefficient (diffuse radiation / extraterrestrial radiation) (Muneer, 2004).

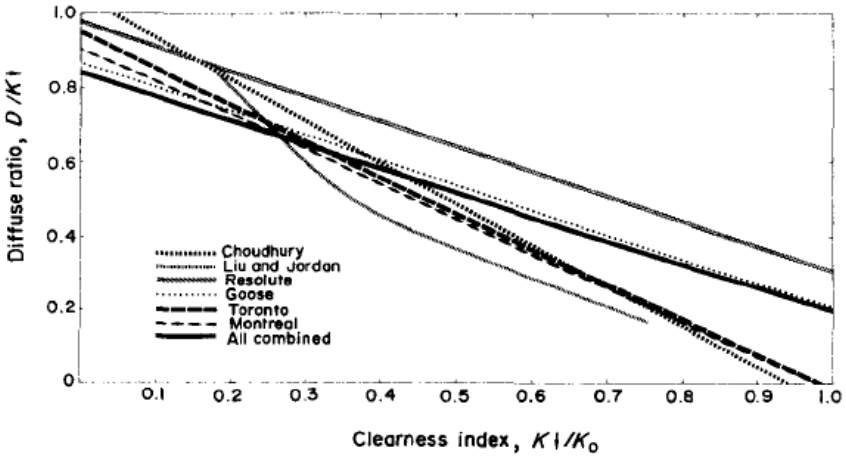

Figure 8.7: Relationship between monthly mean daily diffuse ratio and clearness index (Tuller, 1976)

Bartoli et al. developed a correlation model using 6 and 8 years data for two Italian locations, Macerata and Genova respectively. They defined individual regressions for each station (Bartoli, Cuomo, Amato, Barone, & Mattarelli, 1982).

Saluja and Muneer (Muneer & Saluja, 1985) studied 3 years data from five locations in the UK (Easthhampstead, Aberporth, Aldergrove, Eskdalemuir and Lerwick) and presented an individual regression equation for each station and a single correlation model for the five locations. The regressed curves are shown in Figure 8.8 (Muneer, 2004).

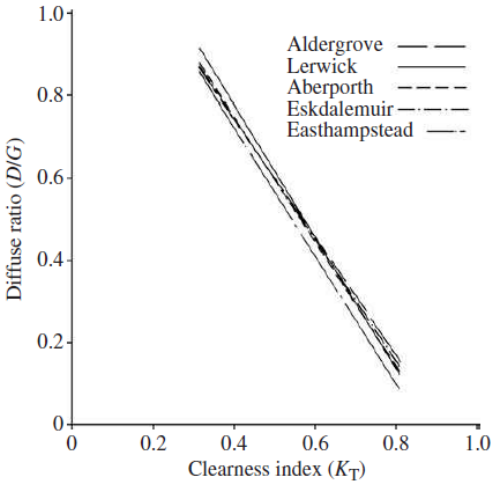

Figure 8.8: Regression curves for daily diffuse ratio – UK locations (Muneer, 2004)

8.4 HOURLY DIFFUSE RADIATION

As previously mentioned in section 8.3, monthly radiation data is not enough for many solar applications models. For those applications at least hourly radiation data are needed.

A typical scatter plot for hourly diffuse ratio (ratio of hourly diffuse to global irradiation) – clearness index (ratio of global to extraterrestrial irradiation) relationship is shown in Figure 8.9. The diffuse ratio is represented by k and the clearness index k_t.

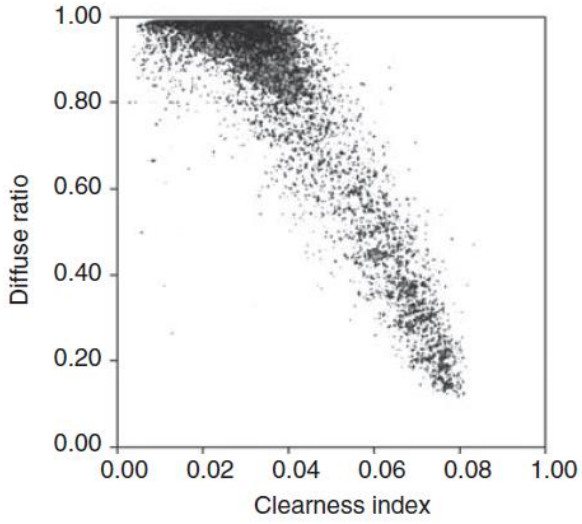

Figure 8.9: Hourly diffuse ratio versus clearness index for the UK (Muneer & Saluja, 1986)

This plot, obtained from hour-by-hour data provided by the UK Meteorological Office for the period 1981-1983 displays a convex shape. The regressed curve reported by Muneer and Saluja (Muneer & Saluja, 1986) is:

$$k = k = a_0 + a_1 k_t + a_2 k_t^2 + a_3 k_t^3; k_t > 0.2 \quad \textbf{(8.40)}$$

Values of "a" coefficients are different for each location (Easthampstead, Aberporth, Aldergrove, Eskdalemuir, Lerwick, United Kingdom).

Figure 8.10 shows the regressed curves for locations in UK and other countries. Three points are worth mentioning:

(i) For all the locations the k-k_t relationship displays a convex profile, and

(ii) For the UK as a whole, it is possible to build a single curvilinear relationship between k and k_t; however,

(iii) A single curve cannot be constructed to include world-wide locations.

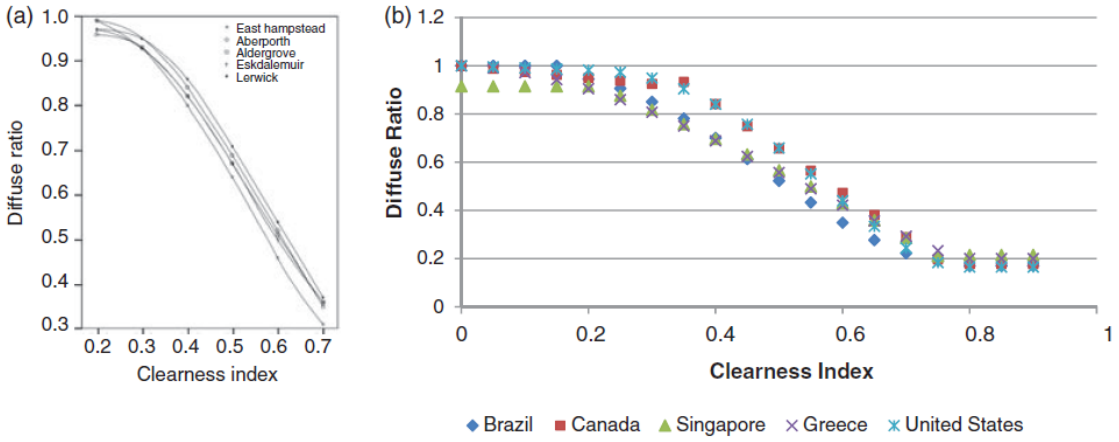

Figure 8.10: (a) Average hourly diffuse ratio versus clearness index for five locations in the UK; (b) average hourly diffuse ratio (y-axis) versus clearness index (x-axis) for five world locations.

8.4.1 Instantaneous hourly radiation

As mentioned in section 1, this work attempts to present a new model that relates averaged-diffuse irradiation to its global counterpart. All previous work has been related to regressions that involve hour-by-hour energy quantities. In the following paragraphs a brief

review of the older work is carried out as the basic mathematical formulation is unchanged, i.e. diffuse ratio is regressed against clearness index.

Liu and Jordan (Liu & Jordan, 1960) were pioneers in correlating the relationship between diffuse and global radiation on a horizontal surface; however, the original correlation of Liu and Jordan was developed for daily-not hourly values.

Many research teams have since determined hourly regressions that primarily relate k, the diffuse ratio (diffuse to global irradiation) to k_t, the clearness index (global to extra-terrestrial irradiation ratio) (see Table 8.3).

Orgill and Hollands, from information gathered in Toronto, Canada, proposed the linear model for the diffuse ratio (k) according to the hourly clearness index (k_t). This study was based upon 4 years of data for Toronto in Canada. The diffuse radiation was measured with a shadow-band pyranometer (Orgill & Hollands, 1977).

Erbs et al. followed the procedure of Orgill and Hollands to develop a correlation for the US locations (Fort Hood, TX; Maynard, MA; Raleigh, NC; Livermore, CA) with a latitude range of 31–42°N. Pyroheliometric data was used by them in which diffuse radiation was obtained via subtraction of direct radiation from global, measured with a pyranometer (Erbs et al., 1982).

Reindl et al. using data respectively from five European and North American locations analysed the influence of commonly measured climatic variables on the diffuse fraction by correlating the significant variables to reduce the standard error of Liu and Jordan type models. The new correlation reduced the composite residual sum of squares by 14.4% when compared to kt, correlation derived from the same data set. The reduced form of the correlation reduced the composite residual sum squares by 9.2%. When an independent data set is used, the new correlation reduced the residual sum of squares by 26% compared to the Erbs' correlation (Reindl, Beckman, & Duffie, 1990).

Hawlader using data from a tropical site in Singapore derived the second-order polynomial correlation. Equations were developed to estimate diffuse fraction of the hourly, daily and monthly global insolation on a horizontal surface (Hawlader, 1984). The hourly correlation equations showed a fairly similar trend to that of Orgill and Hollands (Orgill & Hollands, 1977) and Spenser (Spencer, 1982) supporting their views on latitude dependence.

Chandrasekaran and Kumar using data from a tropical environment in Madras, India, derived a fourth-order polynomial correlation (Chandrasekaran & Kumar, 1994). These correlations were compared to those defined by Orgill and Hollands, Erbs et al. and Reindl et al., which were obtained from data of temperate locations (Orgill & Hollands, 1977; Erbs et al., 1982; Reindl et al., 1990). The comparison was performed in terms of standard deviation and relative standard deviation. The results indicated that the proposed correlations are better. The best fits were obtained when the seasonal effects were taken into account. It is also showed that the hourly diffuse fraction is higher in the tropics than in temperate regions, with a substantially significant diffuse fraction during the rainy season when the hourly clearness index is high.

Boland et al. determined a model with data from a station in Victoria, Australia. Another model was also developed for 15-minute data values in order to ascertain if the smoothing generated by using hourly data makes a significant difference to overall results. A relevant finding was that the same model can be used for both 15-minute and hourly data (Boland, Scott, & Luther, 2001).

Miguel et al. used an assembled data set from several countries in the North Mediterranean Belt area, and yielded a thirdorder polynomial for hourly diffuse fraction correlations (de Miguel et al., 2001).

The performed data analysis showed that under overcast-sky conditions (low values of k) a large portion of the incoming radiation is scattered by the clouds in the atmosphere resulting in a large diffuse fraction. The significance of low solar altitudes in the diffuse solar fraction increases under clear sky (high values of k). Liu and Jordan´s model was recommended to calculate hourly diffuse from daily diffuse values since it reproduces the observed data series extremely well (Liu & Jordan, 1960).

Oliveira et al. (Oliveira, Escobedo, Machado, & Soares, 2002) using data from a tropical Sao Paolo site, Brazil, proposed a fourth-order polynomial correlation. It was deduced that the overall characteristics of the diffuse fraction correlation curves and their seasonal variations are similar to other places with equivalent latitude for hourly, daily and monthly values. Karatasou et al. (Karatasou, Santamouris, & Geros, 2003) based on data from Athens, Greece, proposed a third-order polynomial correlation. The goal of this study was to reduce the standard error of the current Liu and Jordan type correlations, when used for Athens location.

Soares et al. using the same data set as Oliveira et al. established a synthetic fourth order polynomial correlation by means of a neural network technique. It was found that the inclusion of the atmospheric long-wave radiation as an input improves the neural-network performance (Soares et al., 2004).

For the estimation of the hourly clearness index values it is necessary to estimate the hourly extraterrestrial radiation values. The following equation can be used for that purpose.

$$H_0 = I_{sc}[1 + 0.0172024 DS_0] \sin\alpha \qquad (8.41)$$

On the other hand traditional meteorological parameters, like air temperature and atmospheric pressure, are not as important as long-wave radiation which acts as a surrogate for cloud-cover information on the regional scale.

Table 8.3: Instantaneous Hourly radiation models

Orgill and Hollands (Orgill & Hollands, 1977)	$k = 1 - 0.249k_t \ \ for \ \ k_t < 0.35$	(8.42)
	$k = 1.157 - 1.84k_t \ \ for \ \ 0.35 \leq k_t \leq 0.35$	(8.43)
	$k = 0.177 \ \ for \ \ k_t < 0.75$	(8.44)
Erbs et al. (Erbs et al., 1982)	$k = 1 - 0.099k_t \ \ for \ \ k_t < 0.22$	(8.45)
	$k = 0.9511 - 0.160k_t + 4.388k_t^2 - 16.638k_t^3 + 12.336k_t^4 \ \ for \ \ 0.22 \leq k_t \leq 0.80$	(8.46)
	$k = 0.165 \ \ for \ \ k_t < 0.80$	(8.47)
Reindl et al. (Reindl et al., 1990)	$k = 1.02 - 0.249k_t \ \ for \ \ k_t < 0.3$	(8.48)
	$k = 1.45 - 1.67k_t \ \ for \ \ 0.3 < k_t < 0.78$	(8.49)
	$k = 0.147k_t \ \ for \ \ k_t \geq 0.78$	(8.50)
Hawlader (Hawlader, 1984)	$k = 0.915k_t \ \ for \ \ k_t \leq 0.225$	(8.51)
	$k = 1.135 - 0.9422k_t - 0.3878k_t^2 \ \ for \ \ 0.225 < k_t < 0.775$	(8.52)
	$k = 0.215k_t \ \ for \ \ k_t \geq 0.775$	(8.53)
Spencer (Spencer, 1982)	$k = a_3 - b_3k_t - 0{,}3878k_t^2 \ \ for \ \ 0{,}35 < k_t < 0{,}75$	(8.54)
Chandrasekaran and Kumar (Chandrasekaran & Kumar, 1994)	$k = 1.0086 - 0.178k_t \ \ for \ \ k_t \leq 0.24$	(8.55)
	$k = 0.9686 - 0.13250k_t - 1.4183k_t^2 + 10.1862k_t^3 + 8.3733k_t^4 \ \ for \ \ 0.4 < k_t < 0.80$	(8.56)
	$k = 0.197 \ \ for \ \ k_t > 0.80$	(8.57)
Boland et al. (Boland et al., 2001)	$k = 1/[1 + \exp(-5.0033 + 8.6025k_t)]$	(8.58)
Miguel et al. (de Miguel et al., 2001)	$k = 0.995 - 0.081k_t \ \ for \ \ k_t \leq 0.21$	(8.59)
	$k = 0.724 + 2.738k_t - 8.32k_t^2 + 4.967k_t^3 \ \ for \ \ 0.21 < k_t < 0.76$	(8.60)
	$k = 0.18 \ \ for \ \ k_t > 0.76$	(8.61)
Oliveira et al. (Oliveira et al.,	$k = 1 \ \ for \ \ k_t \leq 0.17$	(8.62)

2002)		
	$k = 0.97 + 0.8k_t - 3k_t^2 - 3.1k_t^3 + 5.2k_t^4 \ \ for \ \ 0.17 < k_t < 0.75$	(8.63)
	$k = 0.17 \ \ for \ \ k_t > 0.75$	(8.64)
Karatasou et al. (Karatasou et al., 2003)	$k = 0.9995 - 0.05k_t - 2.4156k_t^2 + 1.4926k_t^3 \ \ for \ \ 0 < k_t \leq 0.78$	(8.65)
	$k = 0.20 \ for \ \ k_t > 0.78$	(8.66)
Soares et al. (Soares et al., 2004)	$k = 1.0 \ for \ \ k_t \leq 0.17$	(8.67)
	$k = 0.90 + 1.1k_t - 4.5k_t^2 + 0.01k_t^3 + 3.14k_t^4 \ \ for \ \ 0.17 < k_t < 0.75$	(8.68)
	$k = 0.17 \ for \ \ k_t > 0.75$	(8.69)

9. MONTHLY-AVERAGED $\bar{k}$ - $\bar{k}_t$ RELATIONSHIP

The section 8 reviewed the k-k_t relationship that was based on annual, monthly, daily and hour-by-hour data. It was also shown that during the past 40 years such regressions, especially the ones for hour-by-hour radiation data, have been presented for very many regions of the world. It is, however, interesting to note that there is a dearth of such knowledge for diffuse ratio – clearness index regressions that are based on averaged data. There are no regressions available in literature for averaged-hourly data. The need to produce averaged $\bar{k} - \bar{k}_t$ relationship presently stemmed from two factors:

- As mentioned earlier, as of year 2002, all Meteorological Office stations, except for Camborne and Lerwick, have ceased to record diffuse component.

- Through the work of NASA (NASA. 2017) it is now posible to obtain daily-averaged irradiation data for virtually any location in the world. A sample of climatic data for Easthampsted (Bracknell, UK) is provided in Table 9.1. This Information was downloaded from the above-mentioned NASA website.

The NASA reported irradiation data were compared against averaged measured data for Bracknell for the period 1981–1983 (three complete years). The statistics within the latter figure shows that there is a close concordance between the satellite-based NASA irradiation and the UK Meteorological Office measured data set (see Figure 9.1).

Table 9.1: Climatic data for Easthampstead (Bracknell) with the NASA reported irradiation data and averaged measured data for the period 1981-1983 (NASA. 2017)

	Unit	Climate data location
Latitude	°N	51.416
Longitude	°E	-0.749
Elevation	m	58
Heating design temperature	°C	-1.74
Cooling design temperature	°C	22.96
Earth temperature amplitude	°C	14.35
Frost days at site	day	37

Month	Air temperature	Relative humidity	Daily solar radiation - horizontal	Atmospheric pressure	Wind speed	Earth temperature	Heating degree-days	Cooling degree-days	Average measured radiation
	°C	%	kWh/m²/d	kPa	m/s	°C	°C-d	°C-d	kWh/m²/d
January	4.2	83.90%	0.77	100.8	6.3	3.1	426	1	0.707
February	4.3	80.20%	1.39	101	5.8	3.6	380	1	1.279
March	6.4	76.80%	2.34	100.9	6	6.2	353	4	2.179
April	8.6	69.80%	3.59	100.7	5.1	9.1	279	21	3.554
May	12.7	64.00%	4.57	100.9	4.7	13.8	168	92	4.111
June	16.1	60.80%	4.84	100.9	4.4	17.7	75	177	4.859
July	18.6	60.20%	4.8	100.9	4.4	20.4	25	261	4.773
August	18.6	61.20%	4.23	100.9	4.3	20.3	26	264	4.229
September	15.5	66.30%	2.86	100.9	5	16.5	83	164	2.847
October	11.7	74.10%	1.73	100.7	5.5	11.5	191	73	1.571
November	7.3	83.20%	0.96	100.7	5.9	6.4	318	11	0.804
December	4.9	85.00%	0.6	100.8	6.1	3.8	404	3	0.602
Annual									
	10.7	72.10%	2.72	100.8	5.3	11	2728	1072	
Measured at (m)					10	0			

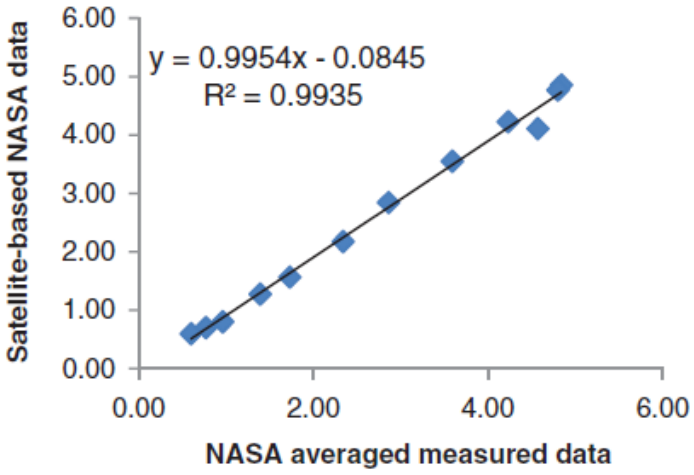

Figure 9.1: Comparison between NASA reported irradiation data and ground-based averaged measured data for Bracknell (own elaboration based on NASA and Climatic data for Easthampstead (Bracknell))

It is therefore possible to construct a three-step computational chain that links with the NASA data that now exists in public domain to obtain all manner of solar energy calculations that require hourly horizontal and slope, global and diffuse irradiation. Figure 9.2 shows the above mentioned computational chain.

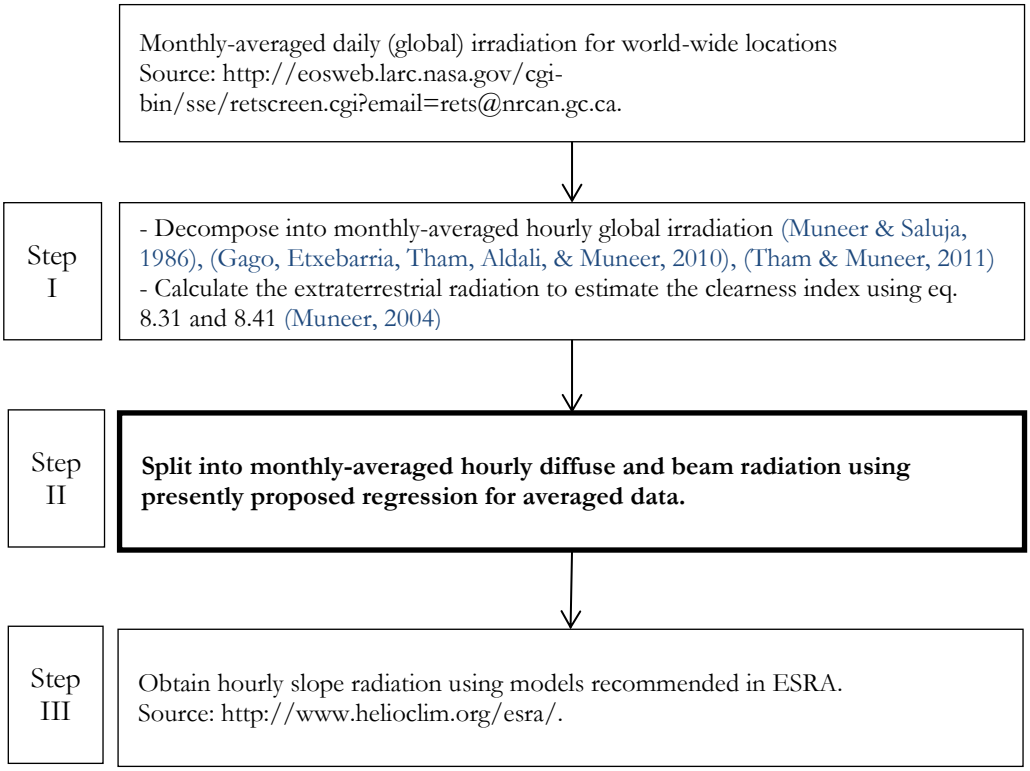

Figure 9.2: Three step computational chain (own elaboration)

9.1 Montly-averaged hourly global irradiation (step 1)

Hourly irradiation data requires a very accurate modelling of solar processes. Therefore, the hourly average irradiation is the nearest approach to the real average radiation which is obtainable form the commonly available solar radiation data (Liu & Jordan, 1960).

Daily solar irradiation records are more accessible since more locations have the technology to measure it. It is logical to consider that there exists a correlation between daily and hourly solar irradiation.

Whillier was pioneer in this field. He plotted experimental ratios between daily to hourly global solar irradiation data derived from widely separated locations against the sunset hour angle (Whillier, 1956).

A mean curve was obtained for each hour, and it was proved that the deviation of any individual point from the mean curve was not higher than +/- 5% for the hours between 9 am and 3 pm sun time.

Meteorological Stations usually publish monthly-averaged values of daily global irradiation. However, when this information is not available, it could be obtained from solar models which use the long-term sunshine data (Muneer, 2004).

Liu and Jordan developed a set of regression curves extending Willier's work (see Figure 9.3), which shows the effect of the day length and the displacement of the hour form solar noon on the ration between the hourly to daily irradiation (Liu & Jordan, 1960).

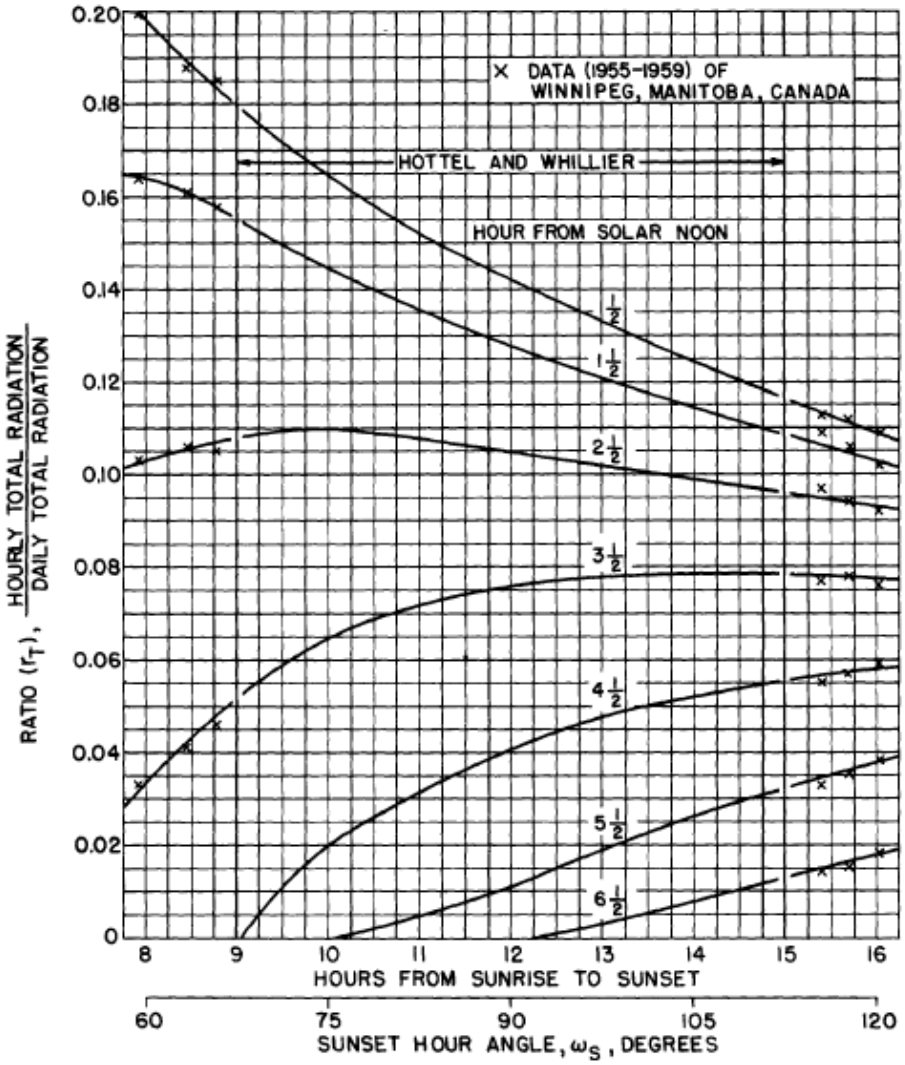

Figure 9.3: Experimental ratio of the hourly to daily total radiaton (Liu & Jordan, 1960)

The correctness of the plots of Liu and Jordan have been tested and reconfirmed by many experts. Collares-Pereira and Rabl (1979) obtained the following equation using a least-squares fit (Collares-Pereira & Rabl, 1979).

$$r_G = \frac{\pi}{24}(a' + b'cos\omega)\frac{cos\omega - cos\omega_s}{sin\omega - \omega_s cos\omega_s} \qquad (9.1)$$

Where:

$$a' = 0.409 + 0.5016\,sin(\omega_s - 1.047) \qquad (9.2)$$

$$b' = 0.6609 - 0.4767 sin(\omega_s - 1.047) \qquad (9.3)$$

Iqbal also verified the applicability of these regression plots usint three Canadian locations (Toronto, Winnipeg and Vancouver) with satisfactory results except for the 4.5 h curve (Iqbal, 1979).

The Figure 9.4 shows the results obtained from the analysis of 20 years of average data for 13 Indian locations by Hawas and Muneer (1984) to test the Liu and Jordan model (Hawas & Muneer, 1984).

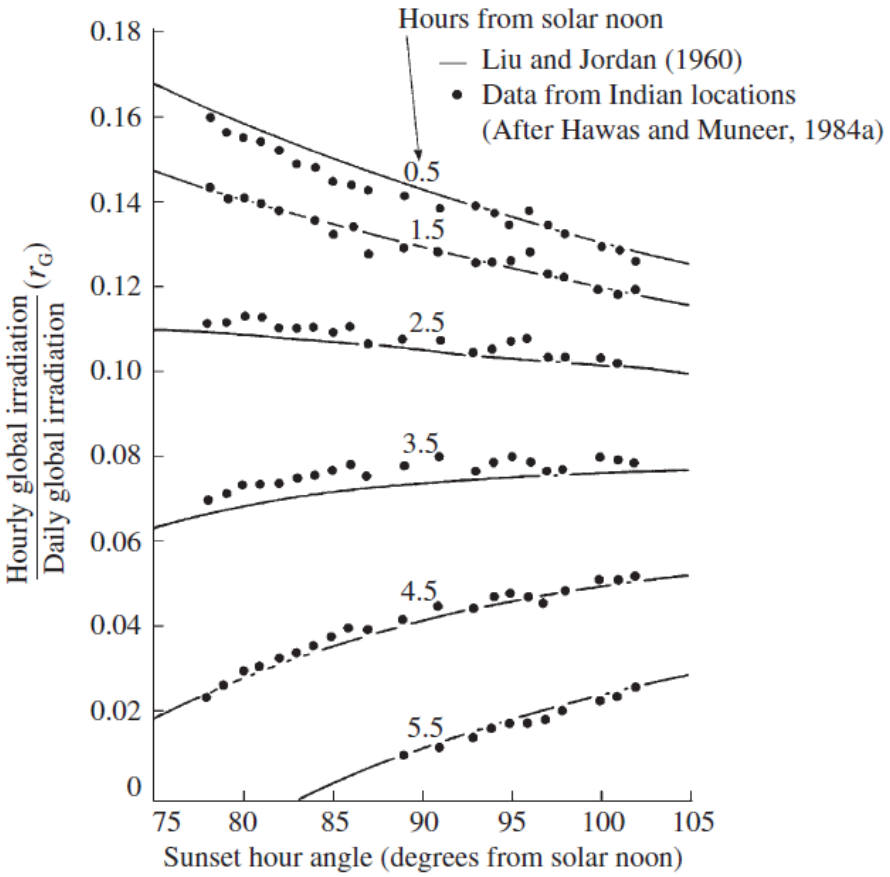

Figure 9.4: Ratio of hourly to daily global irradion and experimental analysis (Muneer, 2004)

These regression curves enable the calculation of the averaged hourly irradiation data when daily irradiation records are available.

9.2 Experimental set-up and data

The aim of this study is to develop models to obtain **monthly-averaged hourly diffuse radiation** data.

For the experimental analysis of this study nineteen worldwide locations were chosen, details of which are shown in Table 9.2. Data consisted of hourly global and diffuse irradiation values for several years, and was obtained from the respective Meteorological Office for each location. The location names have been arranged in increasing order of latitude.

Table 9.2: Nineteen worldwide locations for the study (own elaboration based on data from the respective Meteorological Office for each location)

Country	Location	Latitude	Longitude	Period of observation
India	Chennai	13.08	80.18	1990-1994
	Pune	18.32	73.85	1990-1994
Kingdom of Bahrain	Bahrain	26.03	50.61	2000-2002
State of Kuwait	Kuwait	29.22	47.98	1996-2000
Spain	Almeria	36.83	-2.38	1993-1998
Portugal	Faro	37.02	-7.96	1982-1986
	Lisbon	38.71	-9.15	1982-1990
Spain	Madrid	40.40	-3.55	1999-2001
	Girona	41.97	2.76	1995-2001
United Kingdom	Camborne	50.21	5.30	1981-1995
	Crawley	51.11	0.19	1980-1992
	Bracknell	51.42	0.75	1992-1994
	London WCB	51.52	0.11	1975-1995
	Aberporth	52.13	4.55	1975-1995
	Hemsby	52.70	1.69	1981-1995
	Finningley	53.48	0.98	1982-1995
	Aughton	53.54	2.91	1981-1995
	Aldergrove	54.65	-6.24	1968-1995
	Stornoway	58.22	6.39	1982-1995

Monthly-averaged hourly values were calculated for the global and diffuse radiation considering the data period for each location. A Visual Basic code (see appendix 13.3) was defined for this purpose. For each of them, the monthly average hourly diffuse ratio ($\overline{k}$) and the corresponding clearness index ($\overline{k_t}$) were calculated from sunrise to sunset. The following conditions were used in each case to remove erroneously recorded data.

$$k_t = \frac{H}{H_0} \rightarrow H < H_0 \qquad (9.4)$$

$$k = \frac{H_D}{H} \rightarrow H_D < H \qquad (9.5)$$

The monthly-averaged clearness index was then regressed against the monthly-averaged diffuse ratio for each location. The following figures (Figure 9.5 to Figure 9.23) show the corresponding scatter plot for each location.

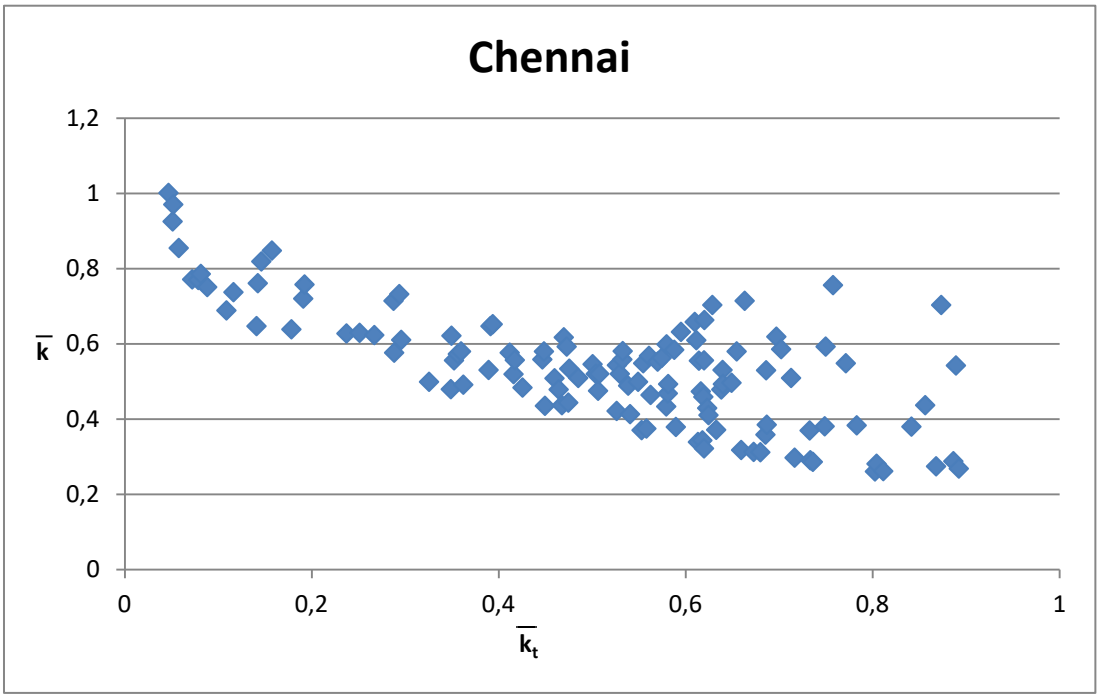

Figure 9.5: Monthly-averaged hourly clearness index vs. diffuse ratio for Chennai (own elaboration)

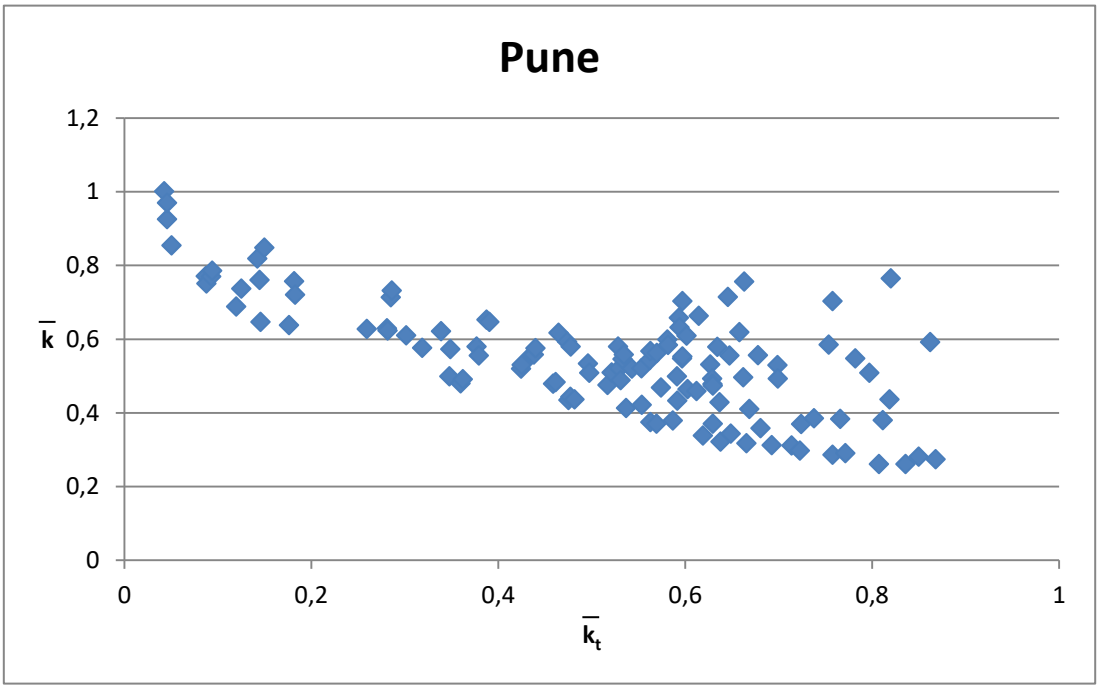

Figure 9.6: Monthly-averaged hourly clearness index vs. diffuse ratio for Pune (own elaboration)

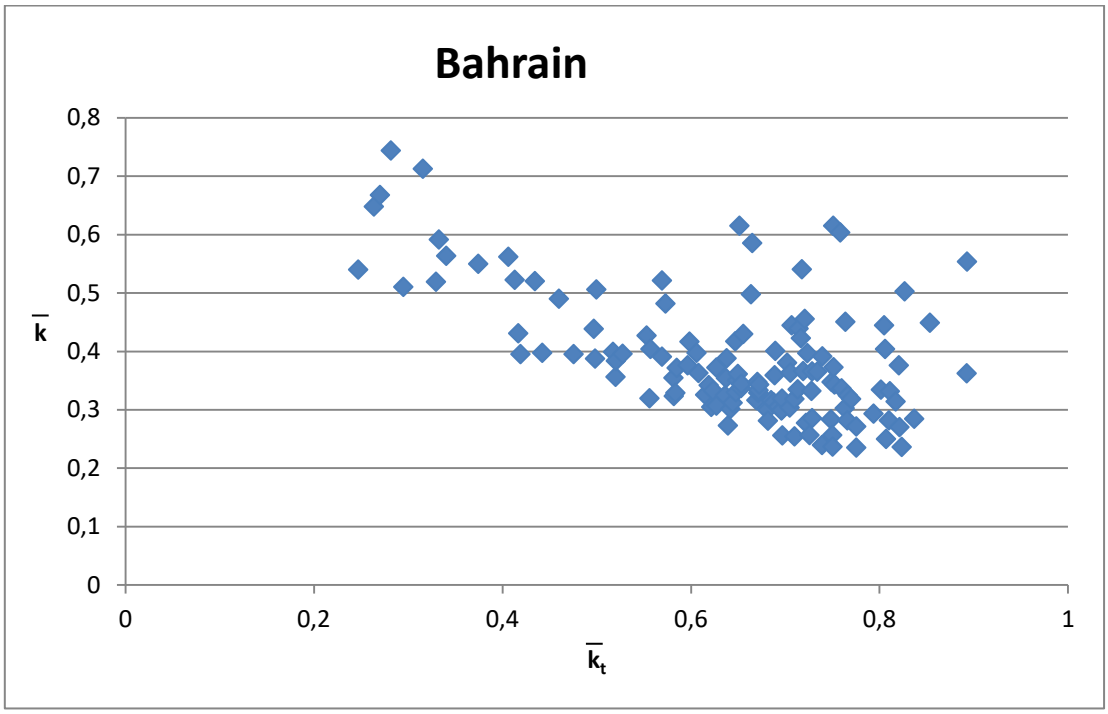

Figure 9.7: Monthly-averaged hourly clearness index vs. diffuse ratio for Bahrain (own elaboration)

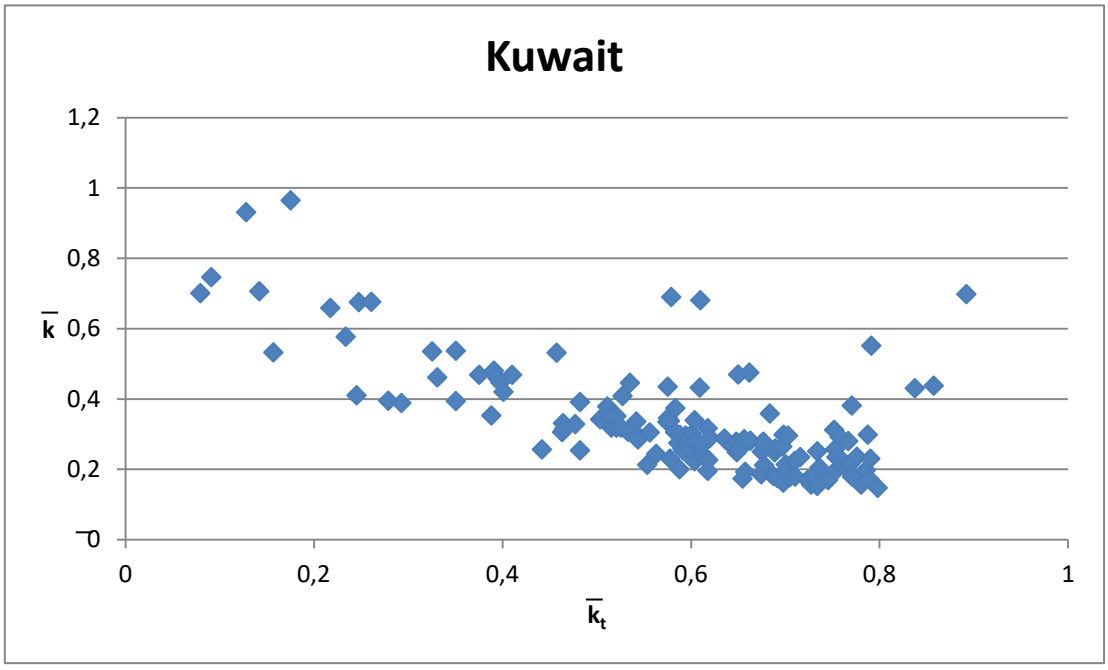

Figure 9.8: Monthly-averaged hourly clearness index vs. diffuse ratio for Kuwait (own elaboration)

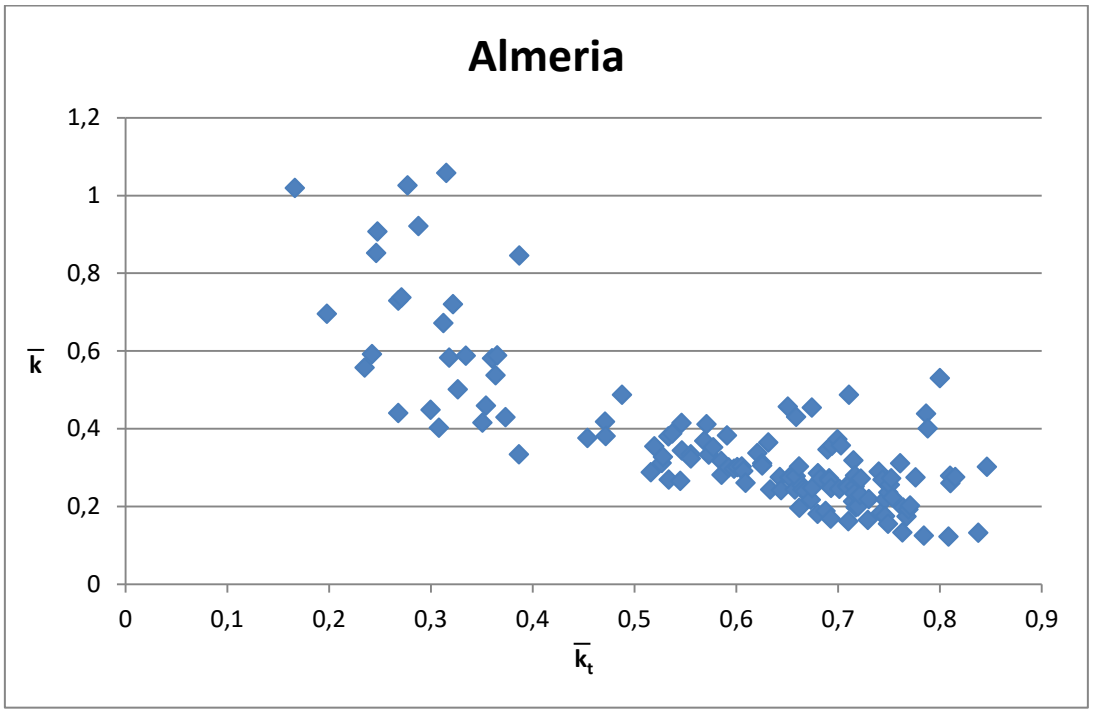

Figure 9.9: Monthly-averaged hourly clearness index vs. diffuse ratio for Almeria (own elaboration)

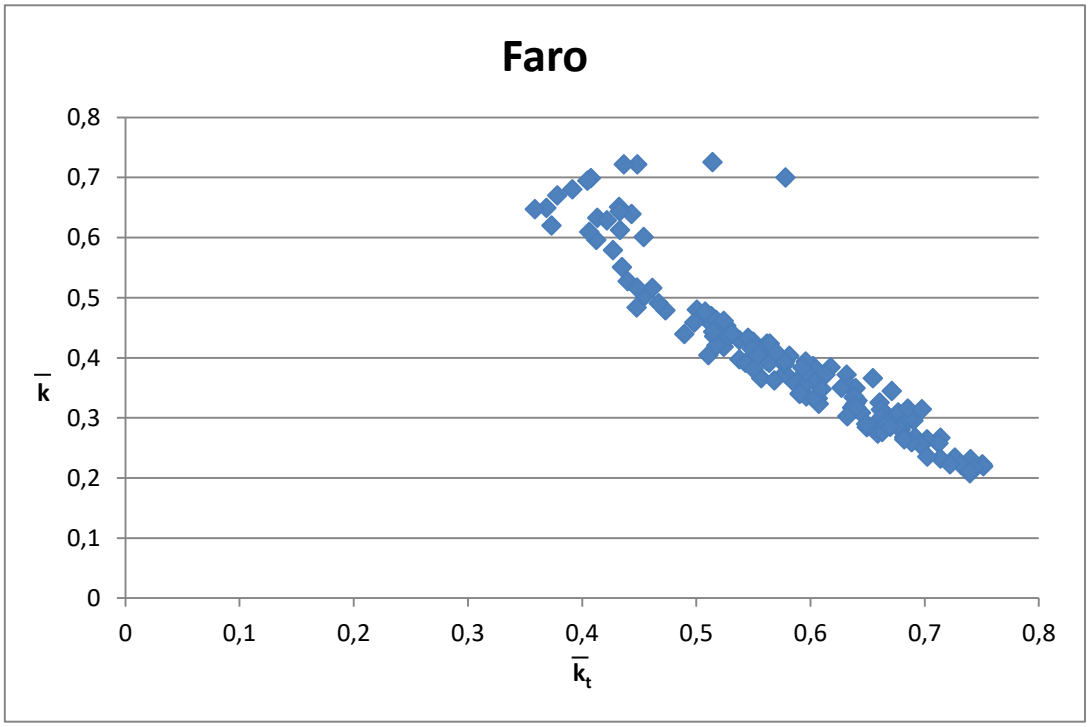

Figure 9.10: Monthly-averaged hourly clearness index vs. diffuse ratio for Faro (own elaboration)

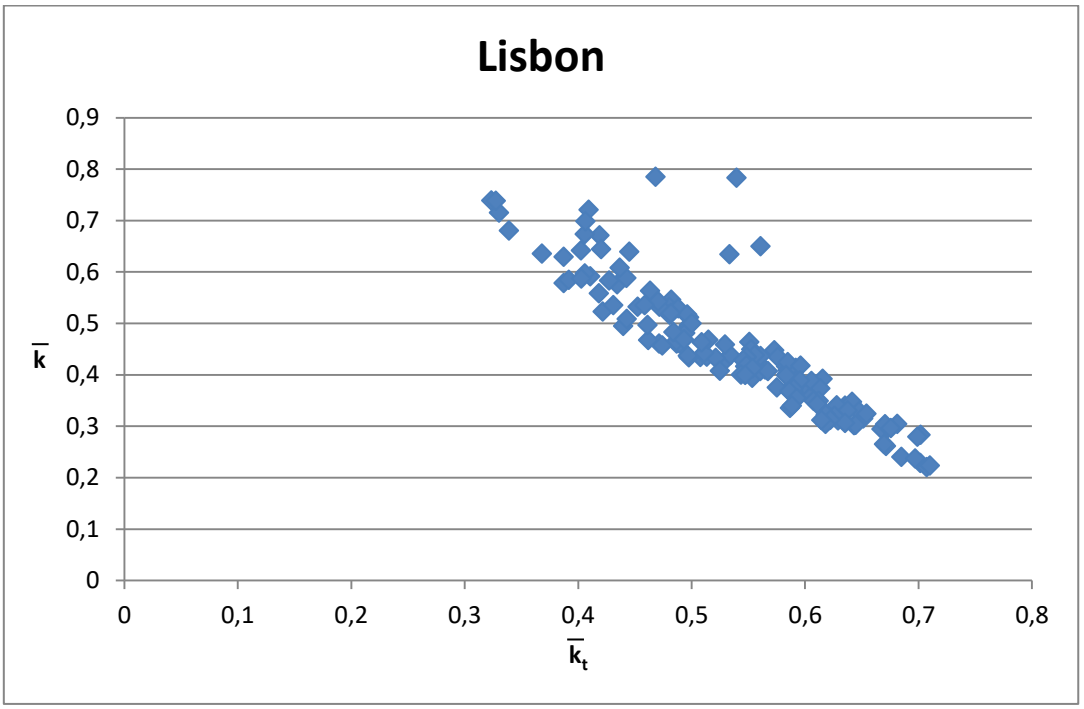

Figure 9.11: Monthly-averaged hourly clearness index vs. diffuse ratio for Lisbon (own elaboration)

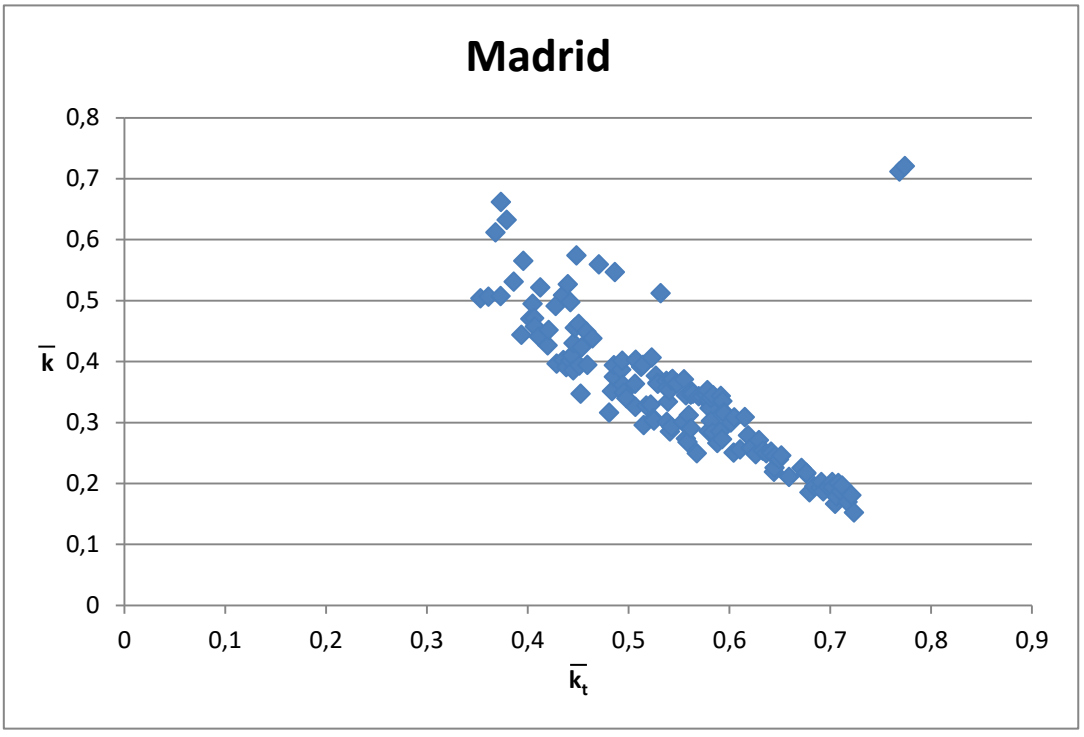

Figure 9.12: Monthly-averaged hourly clearness index vs. diffuse ratio for Madrid (own elaboration)

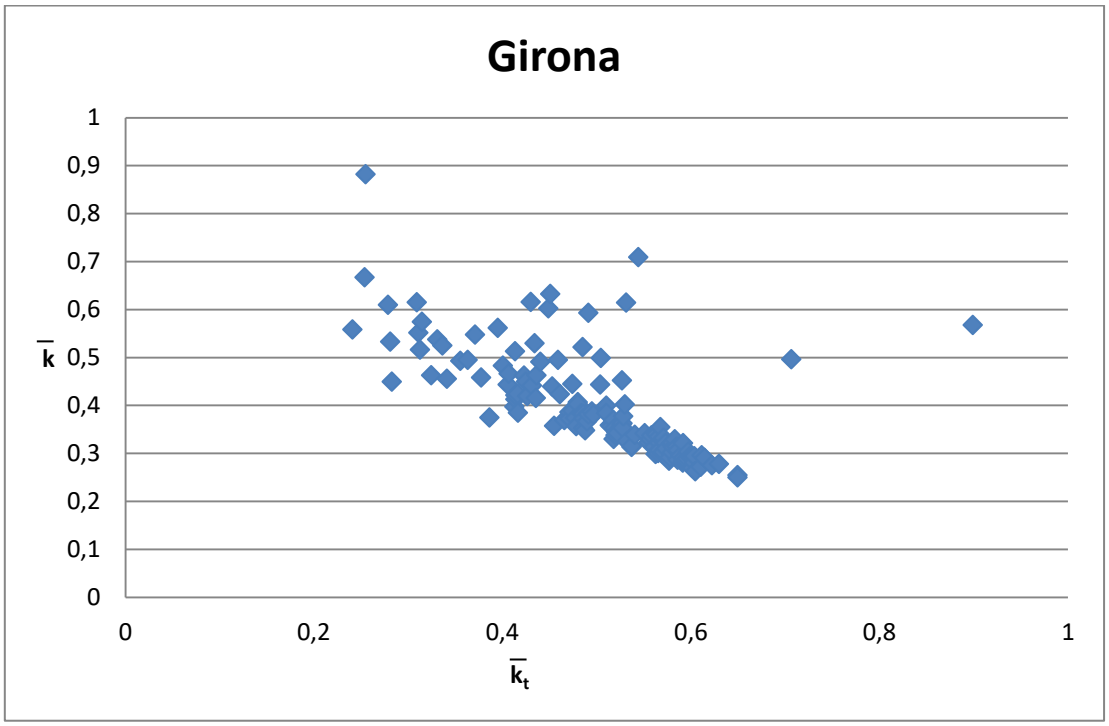

Figure 9.13: Monthly-averaged hourly clearness index vs. diffuse ratio for Girona (own elaboration)

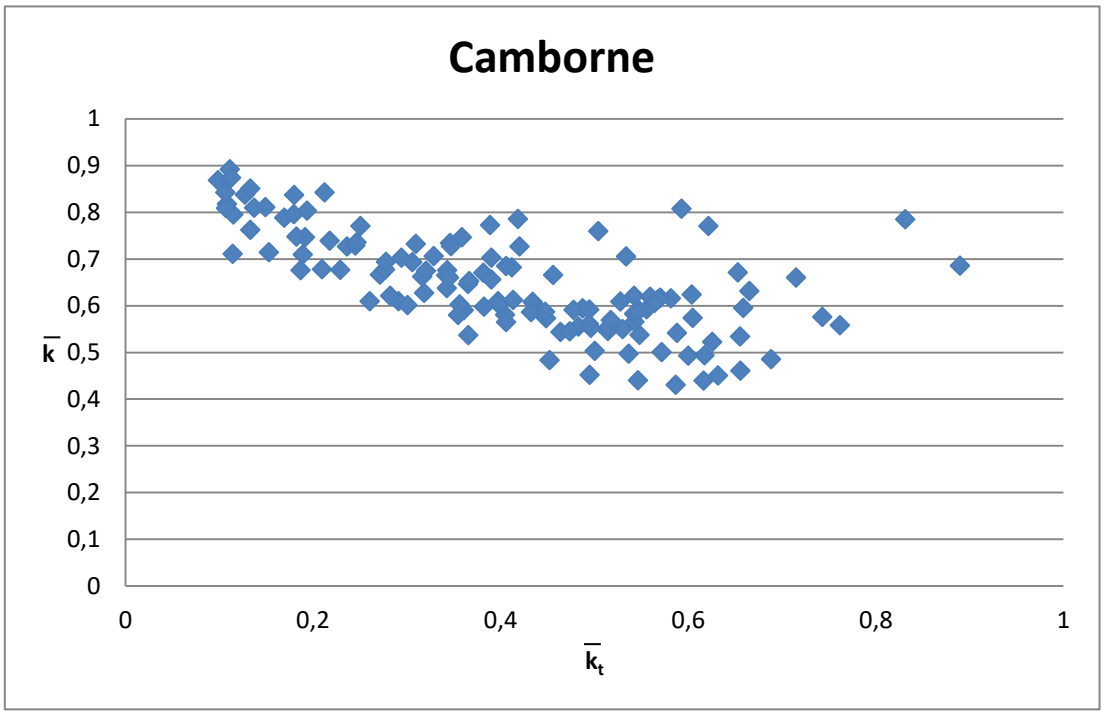

Figure 9.14: Monthly-averaged hourly clearness index vs. diffuse ratio for Camborne (own elaboration)

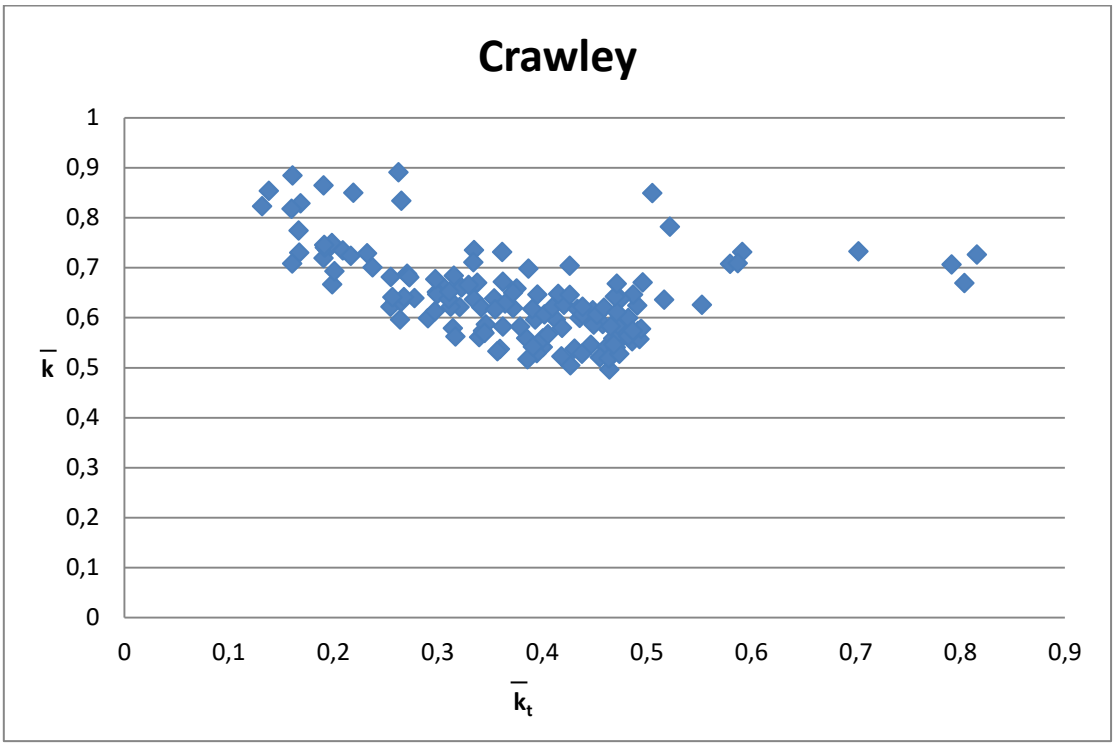

Figure 9.15: Monthly-averaged hourly clearness index vs. diffuse ratio for Crawley (own elaboration)

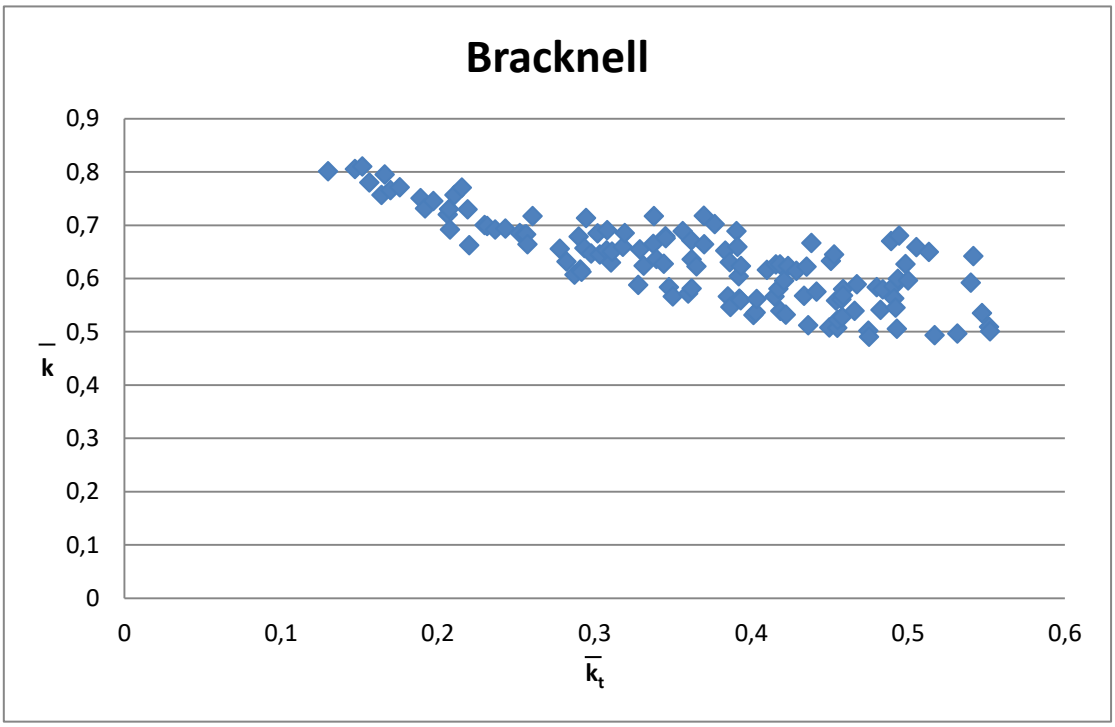

Figure 9.16: Monthly-averaged hourly clearness index vs. diffuse ratio for Bracknell (own elaboration)

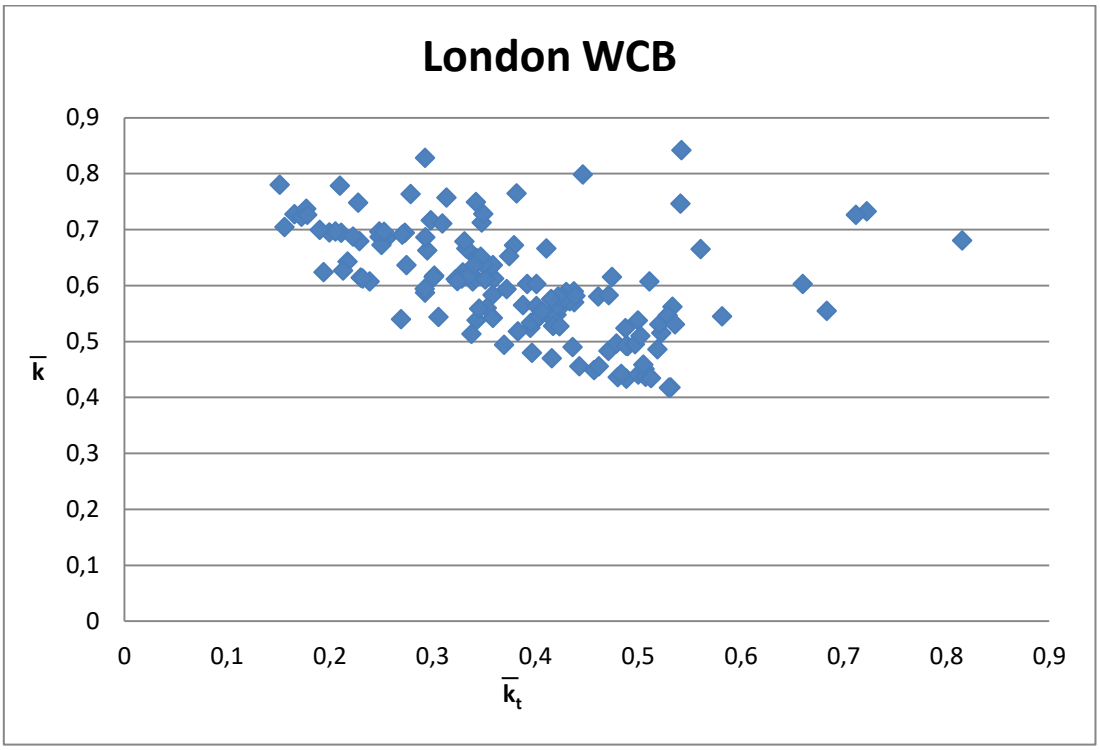

Figure 9.17: Monthly-averaged hourly clearness index vs. diffuse ratio for London WCB (own elaboration)

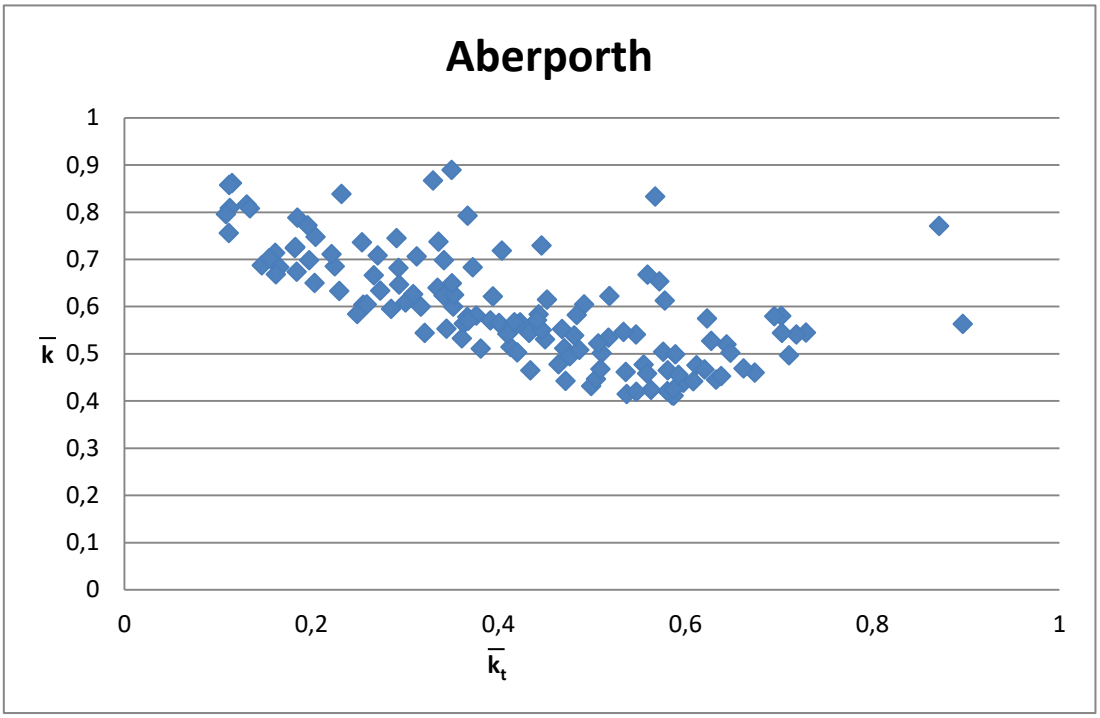

Figure 9.18: Monthly-averaged hourly clearness index vs. diffuse ratio for Alberporth (own elaboration)

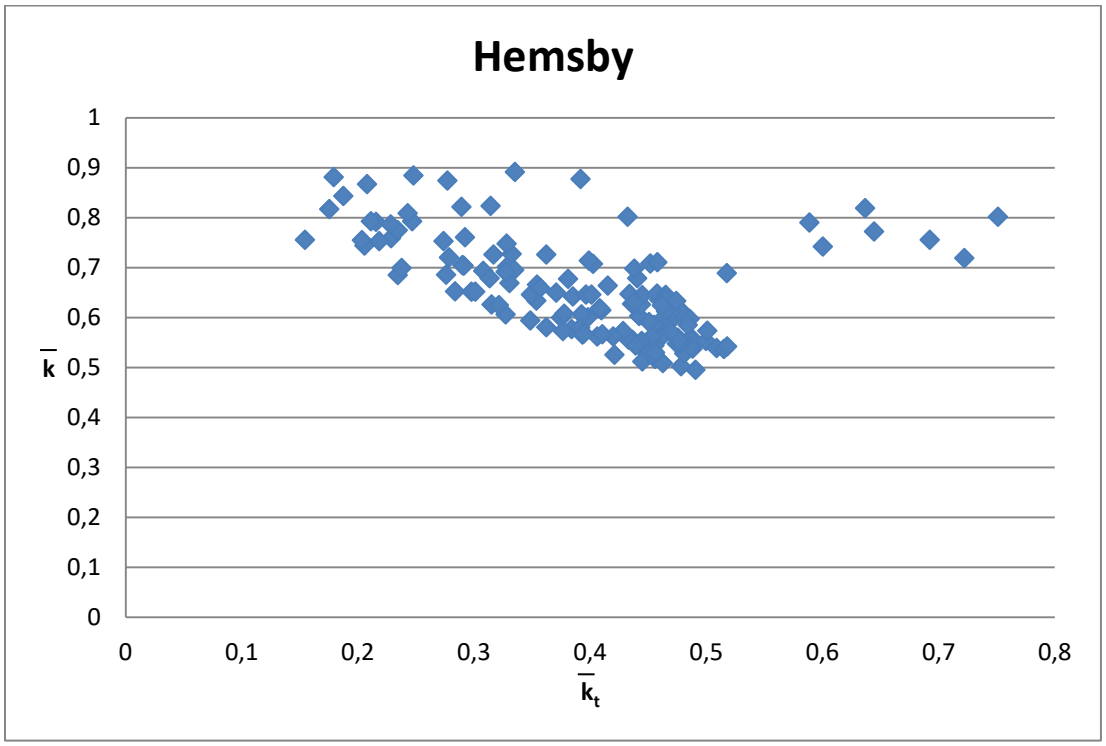

Figure 9.19: Monthly-averaged hourly clearness index vs. diffuse ratio for Hemsby (own elaboration)

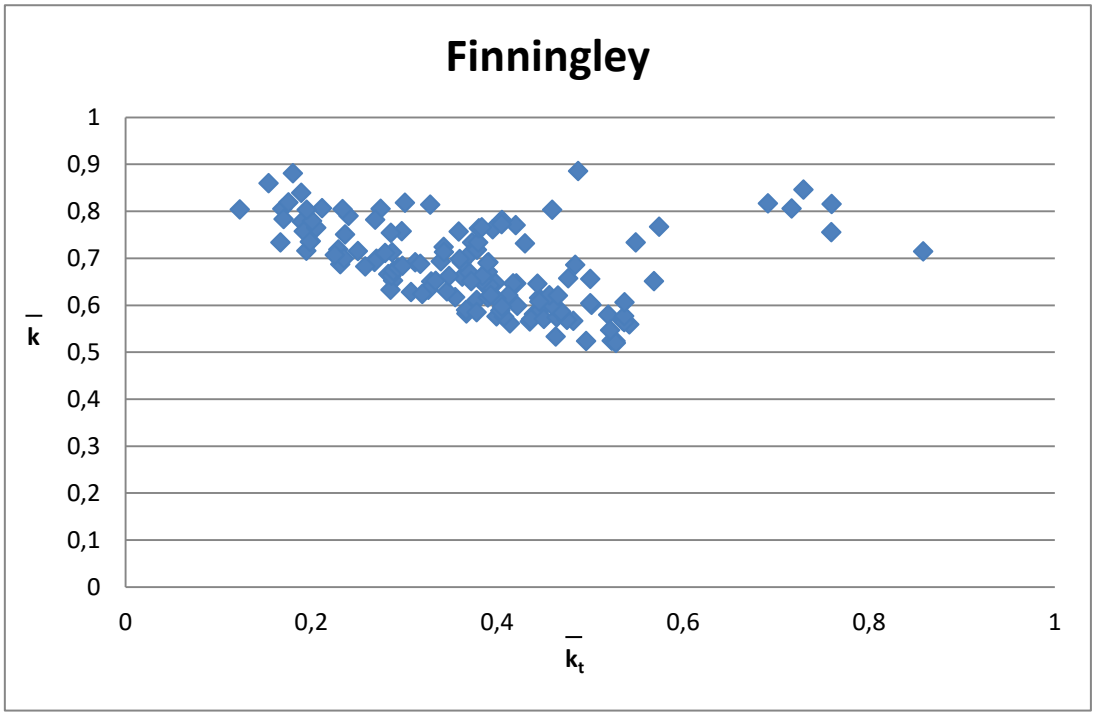

Figure 9.20: Monthly-averaged hourly clearness index vs. diffuse ratio for Finningley (own elaboration)

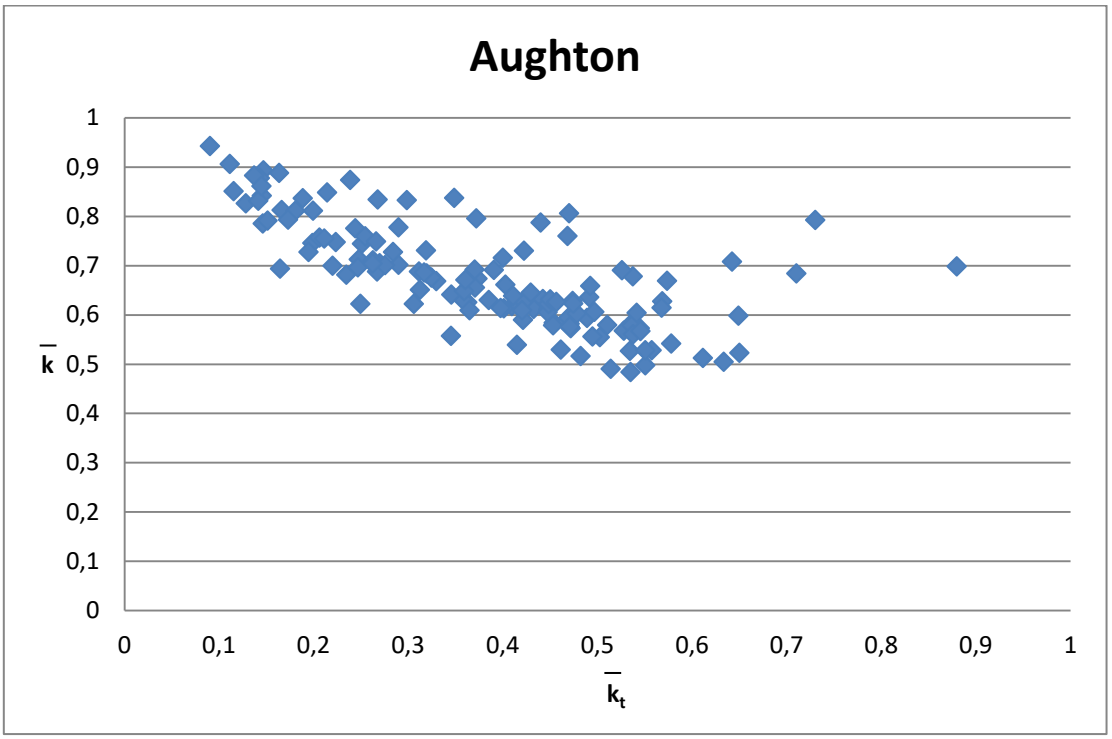

Figure 9.21: Monthly-averaged hourly clearness index vs. diffuse ratio for Aughton (own elaboration)

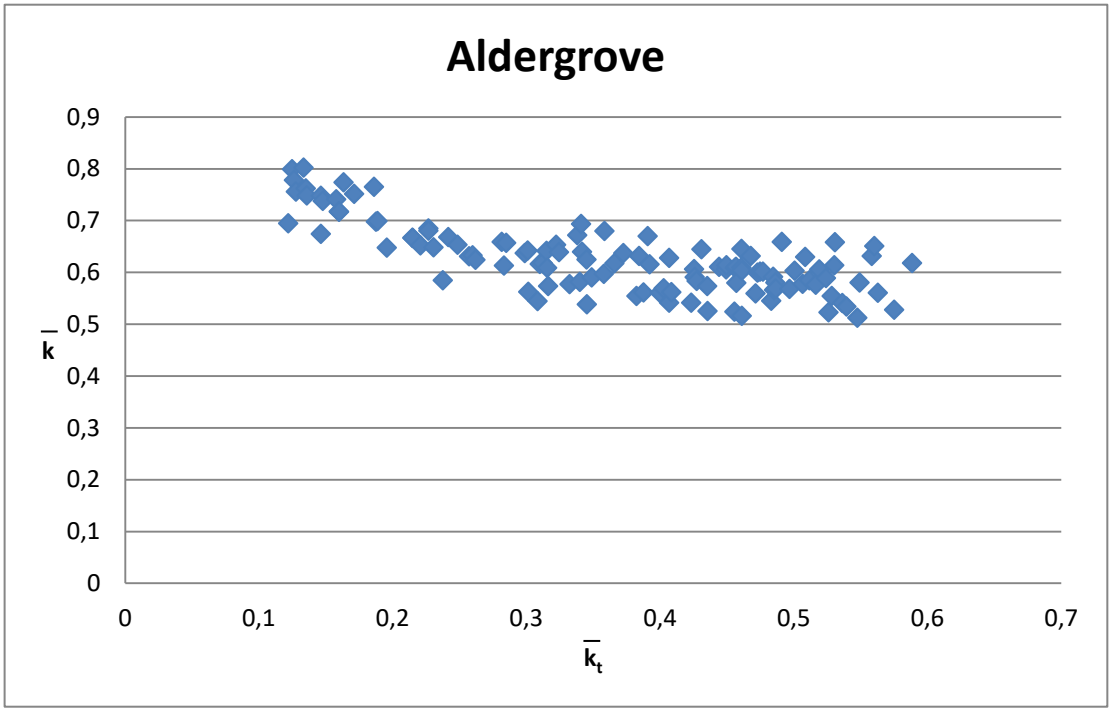

Figure 9.22: Monthly-averaged hourly clearness index vs. diffuse ratio for Aldergrove (own elaboration)

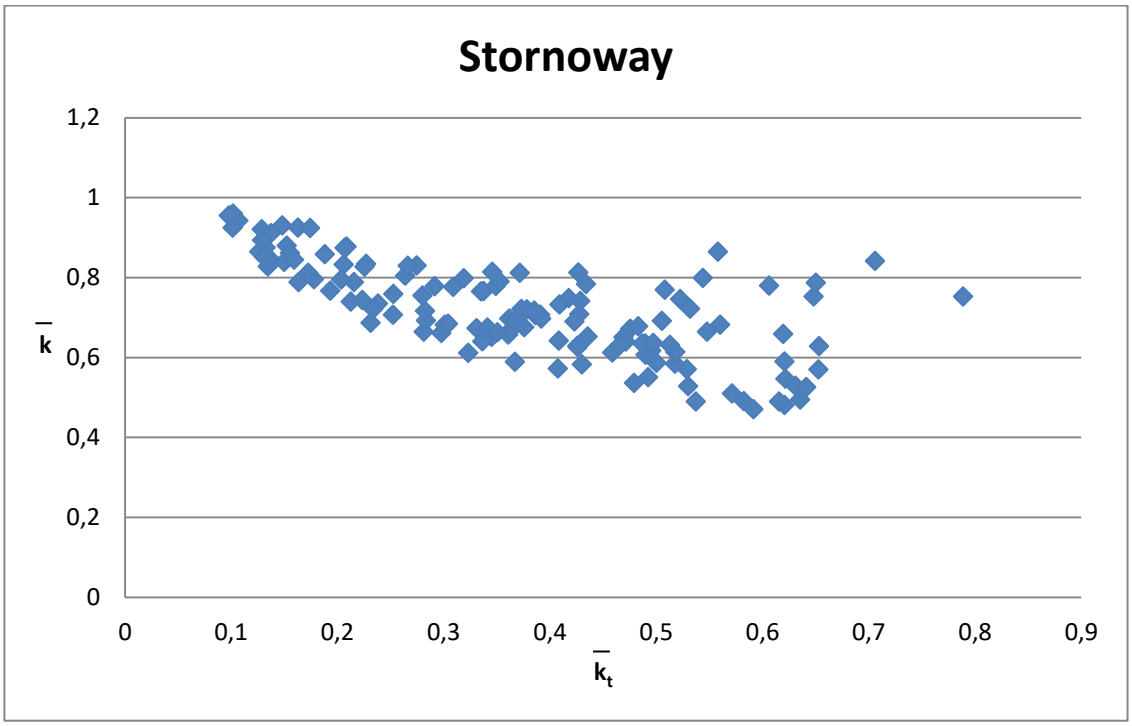

Figure 9.23: Monthly-averaged hourly clearness index vs. diffuse ratio for Stornoway (own elaboration)

Furthermore, for each increment at bandwidth of clearness index of 0.05 widths, the corresponding values of averaged diffuse ratio shown in Table 9.3 were obtained. Another Visual Basic code was used for this purpose (see appendix 13.3). The first and second column of the table of each location presents the average diffuse ratio and the average clearness index respectively. The third column presents the number of points that have been considered to calculate the average value.

Table 9.3: Averaged diffuse ratio values for each increment at bandwidth of clearness index of 0.05 widths (own elaboration)

CHENNAI			PUNE			BARHAIN			KUWAIT			ALMERIA		
0.069	0.832	7	0.083	0.786	5	*0.247*	*0.540*	*1*	*0.085*	*0.723*	*2*	*0.182*	*0.857*	*2*
0.131	0.73	5	0.138	0.749	6	0.278	0.642	4	*0.135*	*0.818*	*2*	0.243	0.727	4
0.180	0.74	4	0.180	0.705	3	0.330	0.596	4	*0.166*	*0.748*	*2*	0.275	0.771	5
0.237	0.627	1	0.279	0.665	5	*0.374*	*0.55*	*1*	0.236	0.58	4	0.317	0.621	8
0.281	0.647	6	0.331	0.575	5	0.422	0.471	6	0.278	0.486	3	0.368	0.524	8
0.342	0.533	3	0.376	0.567	6	0.486	0.443	5	*0.328*	*0.498*	*2*	0.471	0.415	4
0.373	0.575	7	0.433	0.548	5	0.521	0.384	4	0.378	0.448	7	0.533	0.334	10
0.431	0.529	7	0.476	0.51	10	0.576	0.393	12	0.418	0.382	3	0.578	0.336	11

0.472	0.514	8	0.531	0.512	9	0.632	0.342	18	0.471	0.351	7	0.623	0.294	11
0.525	0.507	12	0.579	0.522	18	0.677	0.36	22	0.526	0.343	13	0.674	0.283	25
0.574	0.501	14	0.628	0.488	16	0.722	0.355	23	0.580	0.313	18	0.724	0.244	24
0.625	0.493	18	0.677	0.484	10	0.763	0.349	15	0.620	0.297	19	0.768	0.246	13
0.677	0.458	9	0.725	0.34	4	0.816	0.336	12	0.676	0.264	20	0.818	0.271	7
0.726	0.388	7	0.707	0.471	7				0.722	0.199	15			
0.766	0.569	4	0.824	0.397	6				0.772	0.251	19			
0.815	0.295	4							*0.838*	*0.43*	*1*			

FARO			LISBON			MADRID			GIRONA			CAMBORNE		
0.374	0.653	5	0.330	0.718	4	0.376	0.551	9	*0.241*	*0.558*	*1*	0.121	0.817	12
0.429	0.618	17	0.384	0.607	4	0.429	0.457	21	0.207	0.628	5	0.181	0.757	9
0.471	0.498	7	0.422	0.602	19	0.475	0.405	18	0.323	0.53	8	0.228	0.732	7
0.525	0.451	25	0.481	0.508	27	0.528	0.354	25	0.375	0.488	6	0.276	0.668	8
0.575	0.396	24	0.530	0.462	20	0.575	0.317	29	0.423	0.465	19	0.328	0.676	13
0.628	0.336	23	0.576	0.411	29	0.628	0.259	17	0.477	0.413	25	0.376	0.640	14
0.674	0.295	27	0.623	0.335	23	0.679	0.206	11	0,524	0.393	24	0.424	0.631	12
0.724	0.233	12	0.675	0.285	12	0.711	0.182	10	0.576	0.312	38	0.480	0.557	11
0.751	*0.221*	*2*	0.705	0.239	4	*0.771*	*0.716*	*2*	0.617	0.276	12	0.530	0.574	17
									0.707	*0.496*	*1*	0..574	0.594	10
												0.615	0.545	8
												0.663	0.562	6

CRAWLEY			BRACKNELL			LONDON			ABERPORTH			HEMSBY		
0.180	0.766	13	0.174	0.767	9	0.135	0.750	10	0.122	0.798	8	0.174	0.824	4
0.219	0.738	6	0.221	0.713	11	0.176	0.713	9	0.177	0.714	10	0.226	0.778	14
0.274	0.669	18	0.278	0.661	14	0.226	0.675	13	0.224	0.692	7	0.285	0.732	10
0.328	0.629	20	0.327	0.648	19	0.278	0.675	14	0.275	0.662	10	0.325	0.693	17
0.375	0.607	20	0.378	0.629	19	0.332	0.636	24	0.326	0.654	11	0.380	0.637	20
0.426	0.590	23	0.423	0.579	19	0.375	0.585	19	0.368	0.626	14	0.429	0.605	27

0.474	0.579	30	0.474	0.571	24	0.422	0.566	24	0.424	0.567	17	0.471	0.578	40
0.515	0.755	3	0.525	0.583	8	0.479	0.501	15	0.475	0.523	12	0.512	0.576	5
0.578	0.693	4				0.521	0.525	17	0.525	0.497	11	0.627	0.777	3
						0.571	*0.605*	*2*	0.577	0.509	16			
						0.672	*0.579*	*2*	0.629	0.489	9			
						0.717	*0.729*	*2*	0.677	0.502	3			
						0.815	*0.680*	*1*	0.713	0.541	5			

FINNINGLEY			AUGHTON			ALDERGROVE			STORNOWAY		
0123	*0.804*	*1*	0.136	0.856	10	0.135	0.750	10	*0.098*	*0.955*	*1*
0.183	0.788	13	0.178	0.791	10	0.175	0.723	9	0.126	0.896	12
0.225	0.751	10	0.231	0.742	11	0.229	0.656	9	0.168	0.845	11
0.280	0.704	17	0.272	0.741	13	0.275	0.636	7	0.219	0.788	12
0.328	0.687	14	0.325	0.676	11	0.326	0.612	18	0.275	0.745	11
0.379	0.668	31	0.372	0.661	12	0.377	0.618	9	0.330	0.713	14
0.423	0.634	20	0.424	0.638	17	0.425	0.583	15	0.372	0.701	15
0.470	0.625	15	0.473	0.612	21	0.472	0.588	20	0.423	0.686	13
0.526	0.583	14	0.532	0.574	15	0.525	0.579	15	0.481	0.623	13
0.572	*0.709*	*2*	0.564	0.572	7	0.569	0.597	5	0.523	0.646	13
0.691	*0.817*	*1*	0.634	0.581	4				0.573	0.603	5
0.723	*0.826*	*2*							0.626	0.585	10
0.760	*0.785*	*2*							0.652	0.662	3
									0.706	*0.841*	*1*
									0.789	*0.753*	*1*

The values shown in red correspond to average values calculated only with one or two points. These average values have not been considered in the research since there is not enough information to assure those data are reliable.

The following figures (Figure 9.24 to Figure 9.42) show the averaged diffuse ratio and clearness index plots for each location.

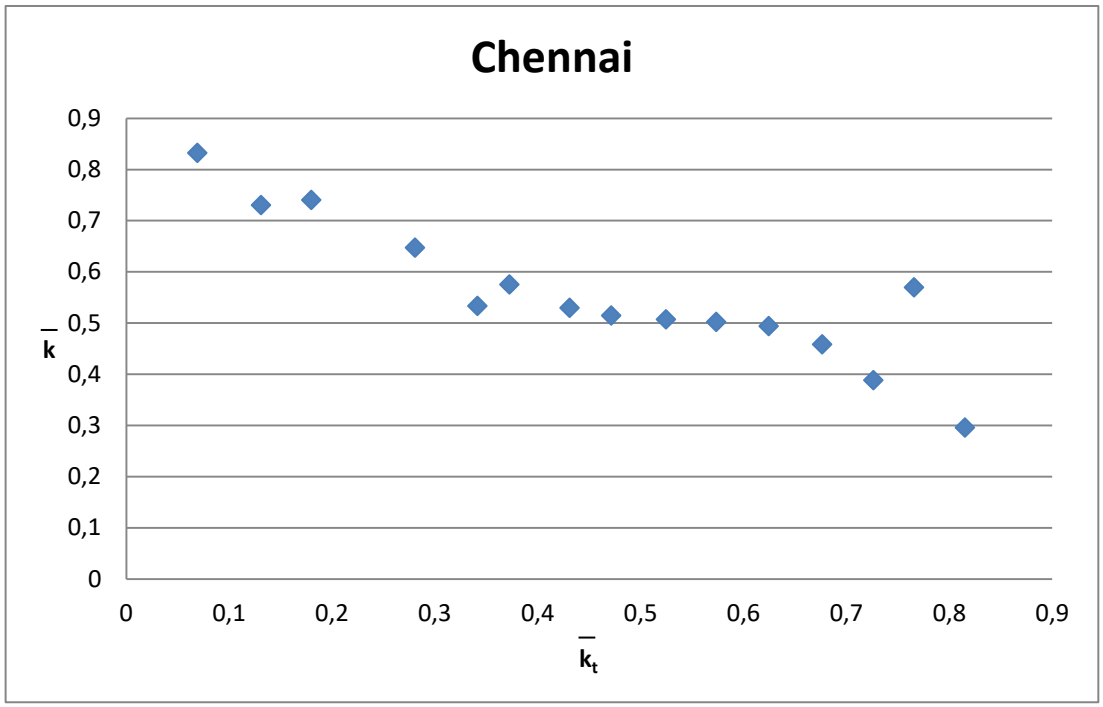

Figure 9.24: Averaged values of diffuse ratio vs. clearness index for Chennai (own elaboration)

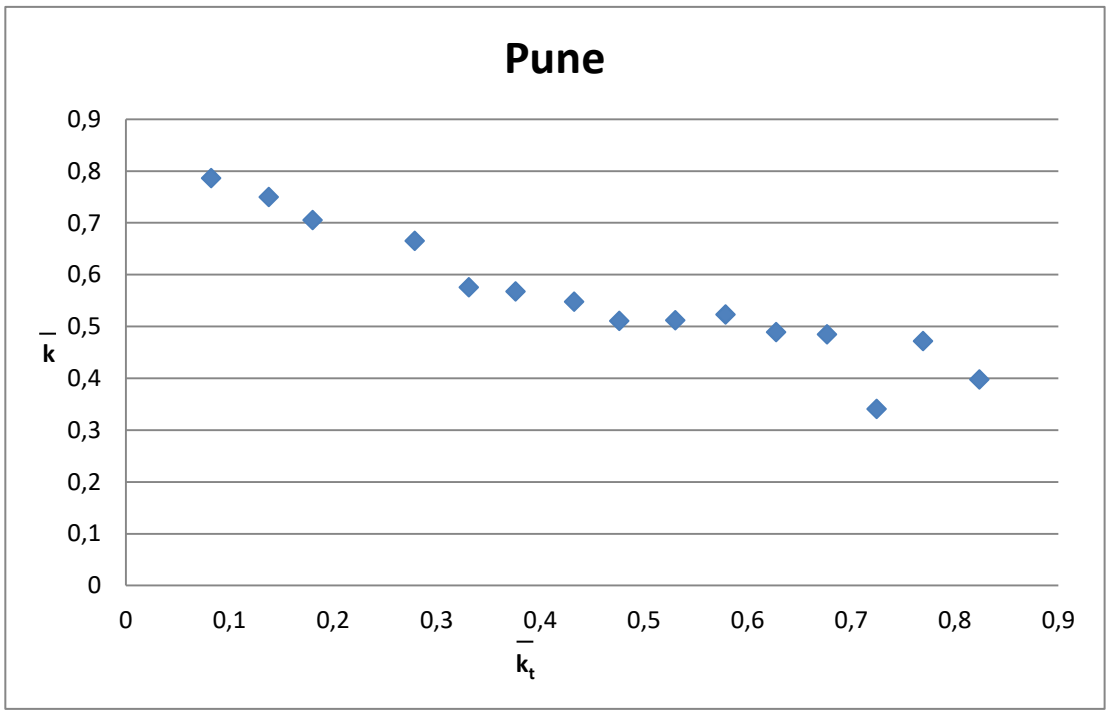

Figure 9.25: Averaged values of diffuse ratio vs. clearness index for Pune (own elaboration)

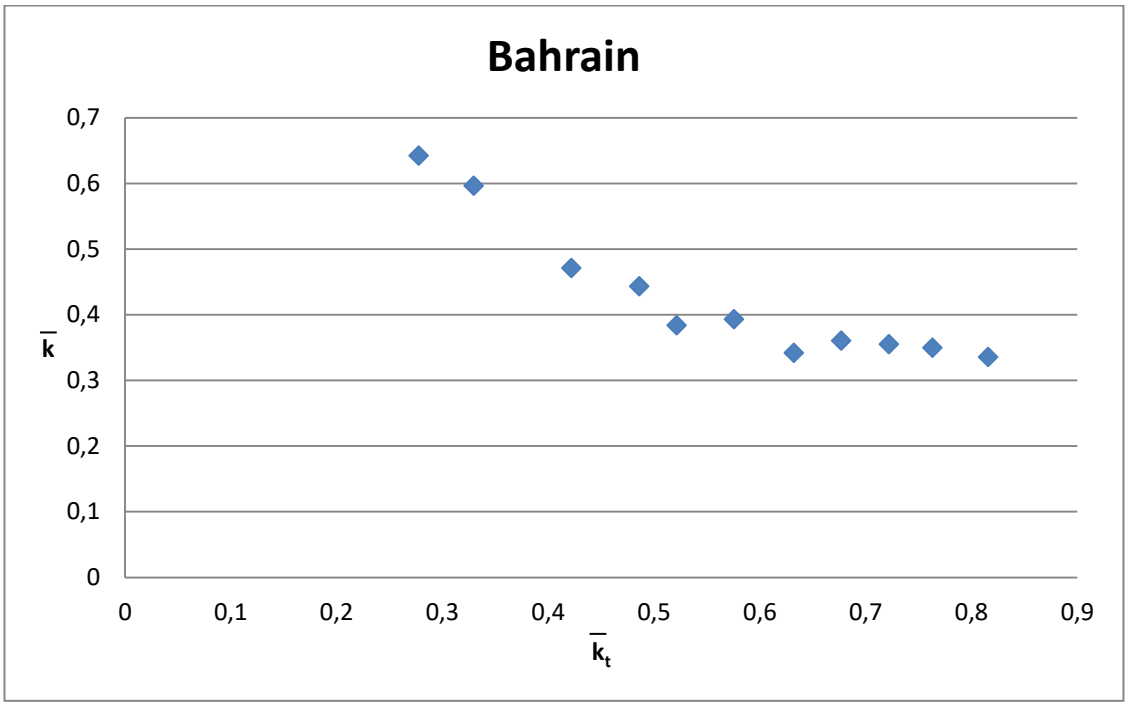

Figure 9.26: Averaged values of diffuse ratio vs. clearness index for Bahrain (own elaboration)

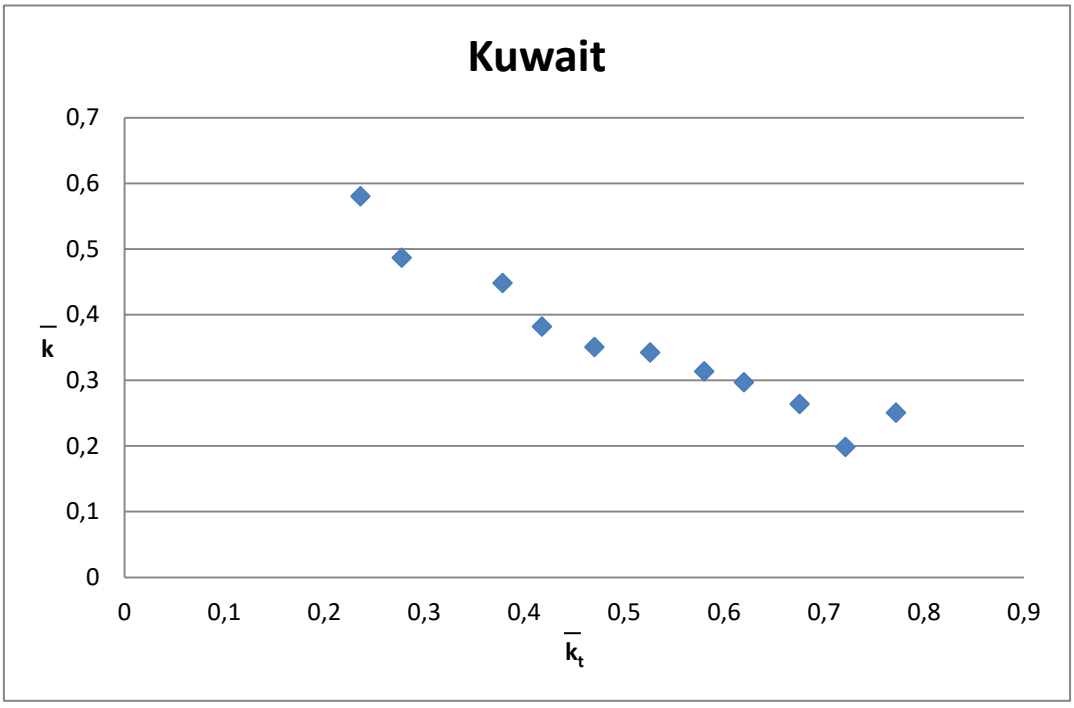

Figure 9.27: Averaged values of diffuse ratio vs. clearness index for Kuwait (own elaboration)

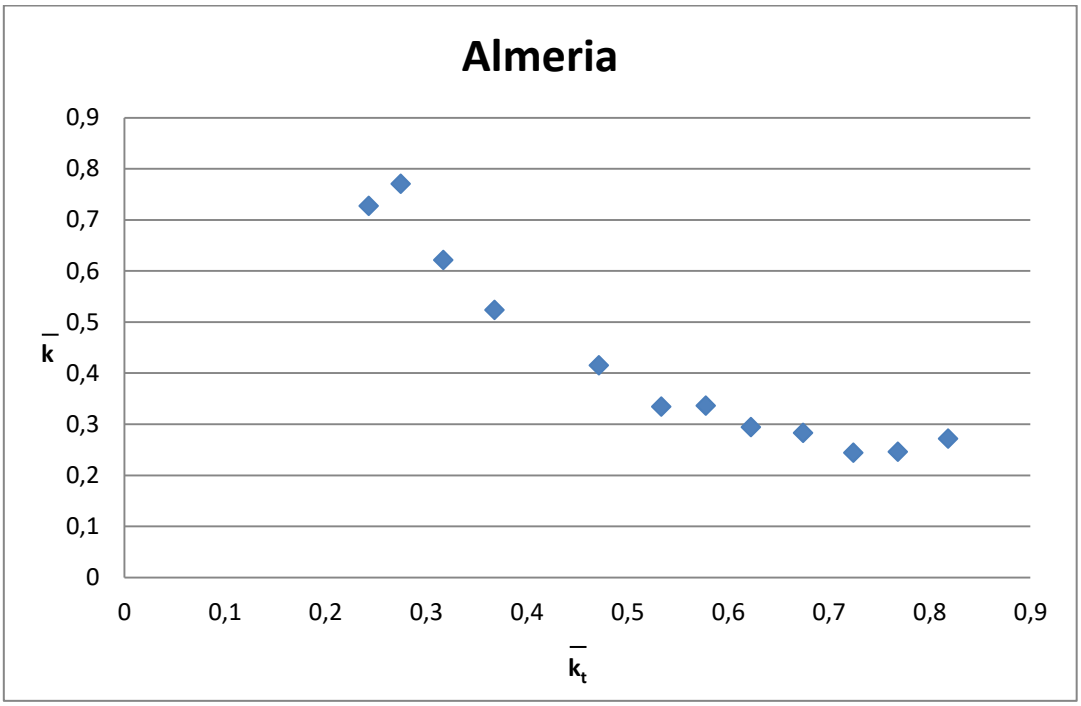

Figure 9.28: Averaged values of diffuse ratio vs. clearness index for Almeria (own elaboration)

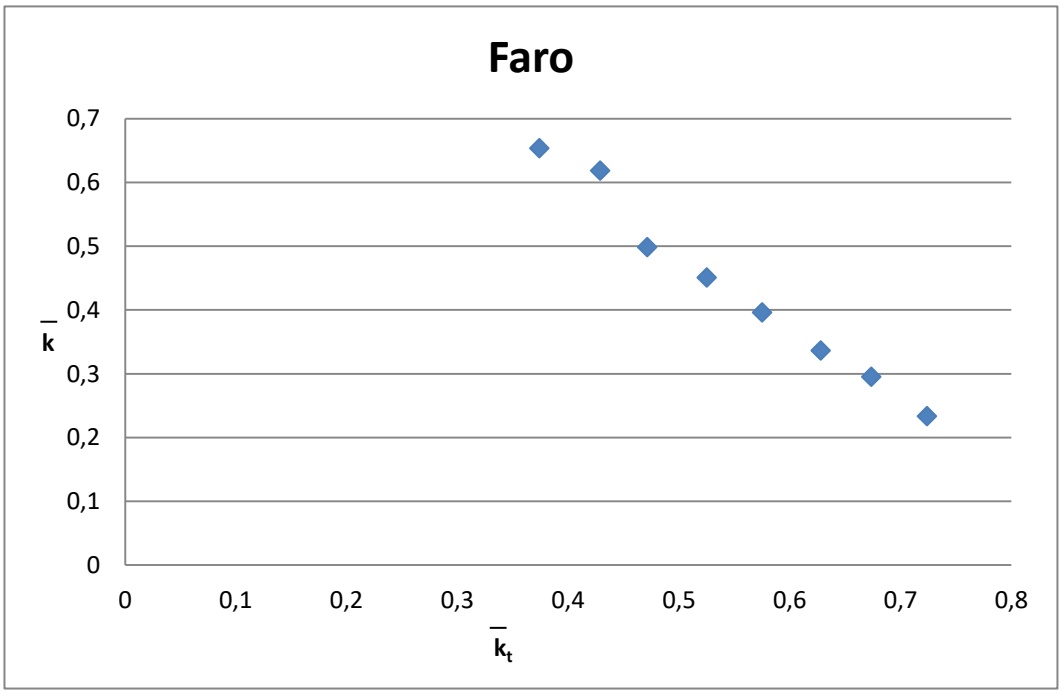

Figure 9.29: Averaged values of diffuse ratio vs. clearness index for Faro (own elaboration)

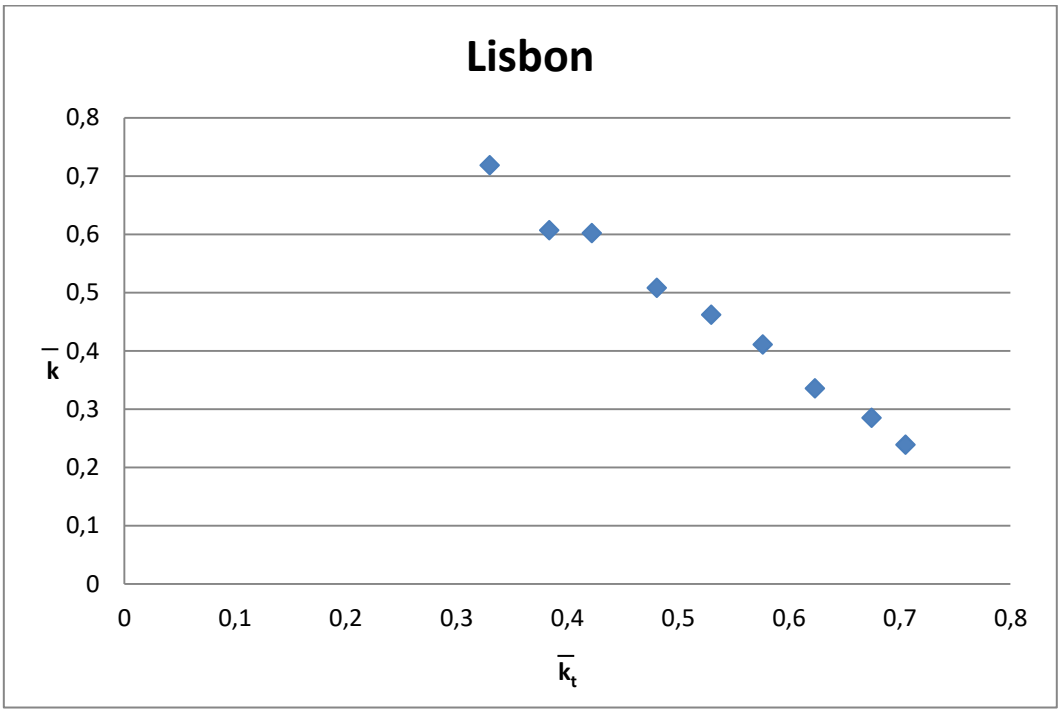

Figure 9.30: Averaged values of diffuse ratio vs. clearness index for Lisbon (own elaboration)

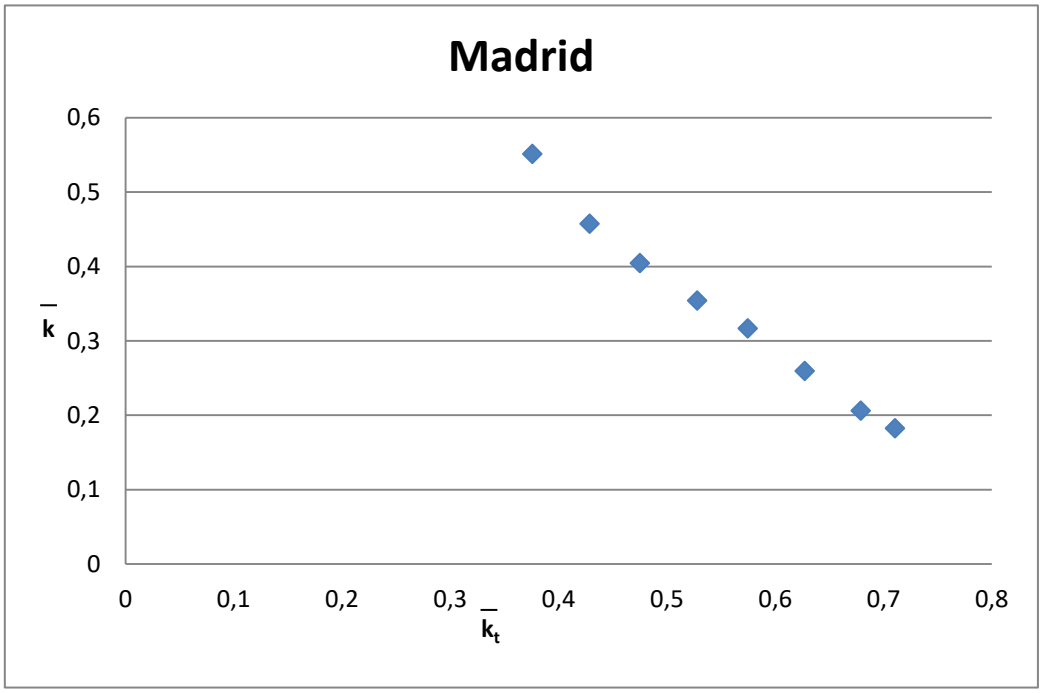

Figure 9.31: Averaged values of diffuse ratio vs. clearness index for Madrid (own elaboration)

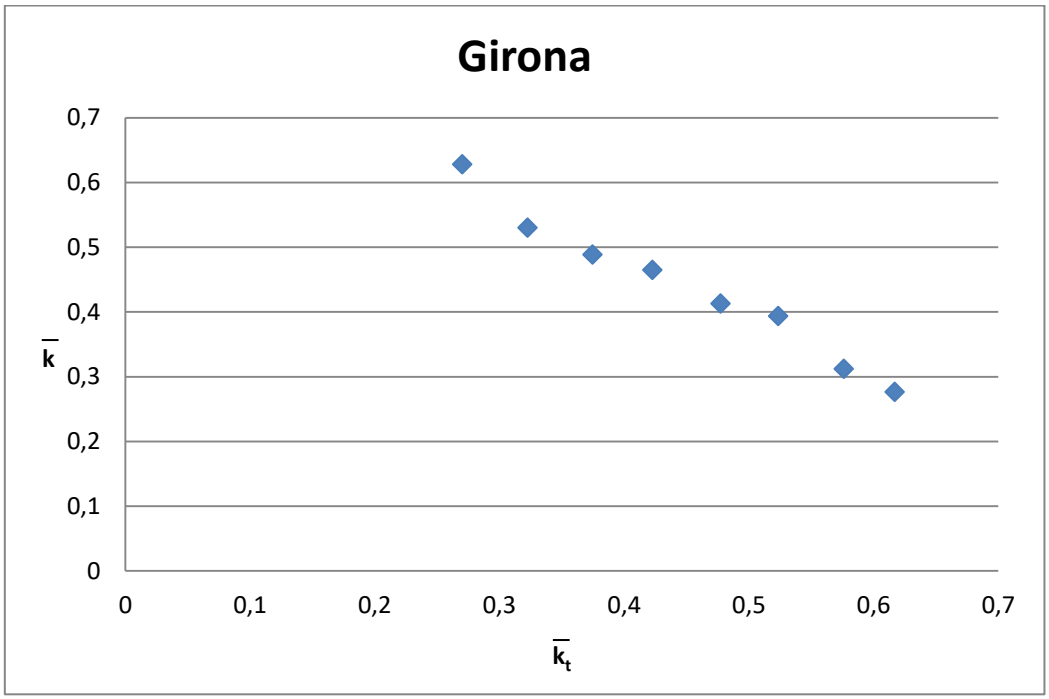

Figure 9.32: Averaged values of diffuse ratio vs. clearness index for Girona (own elaboration)

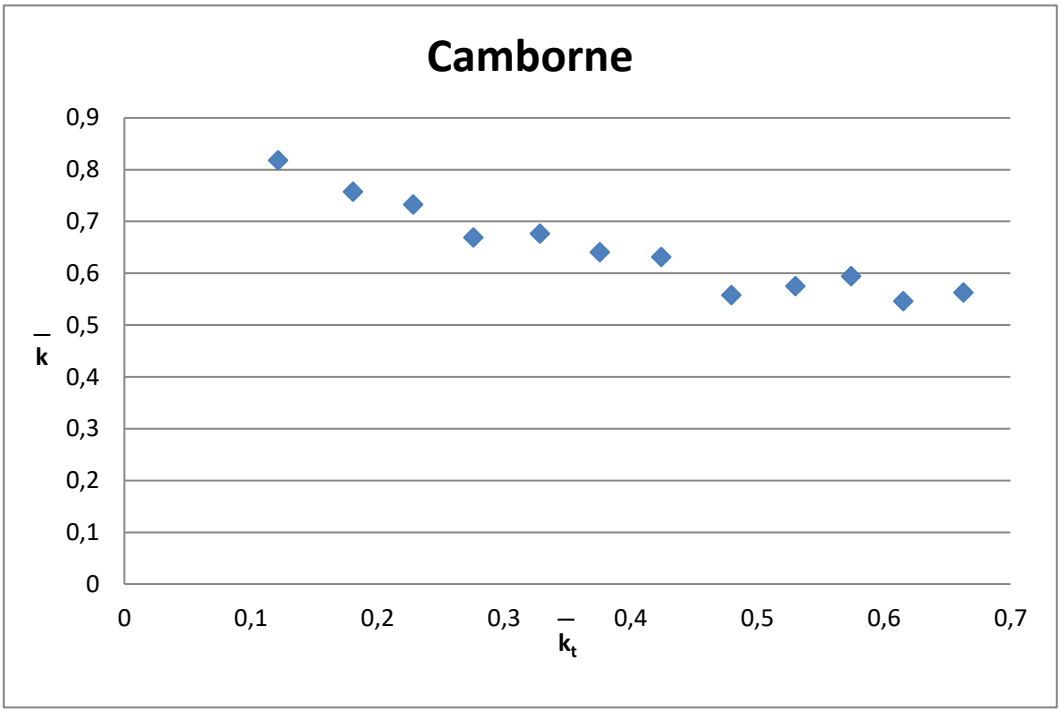

Figure 9.33: Averaged values of diffuse ratio vs. clearness index for Camborne (own elaboration)

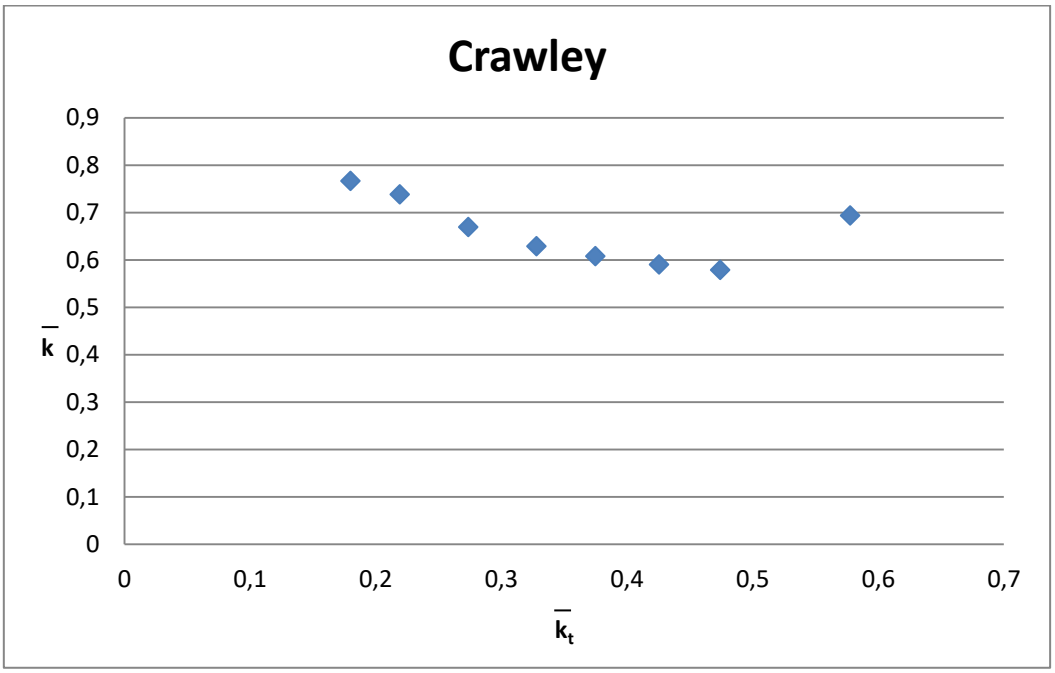

Figure 9.34: Averaged values of diffuse ratio vs. clearness index for Crawley (own elaboration)

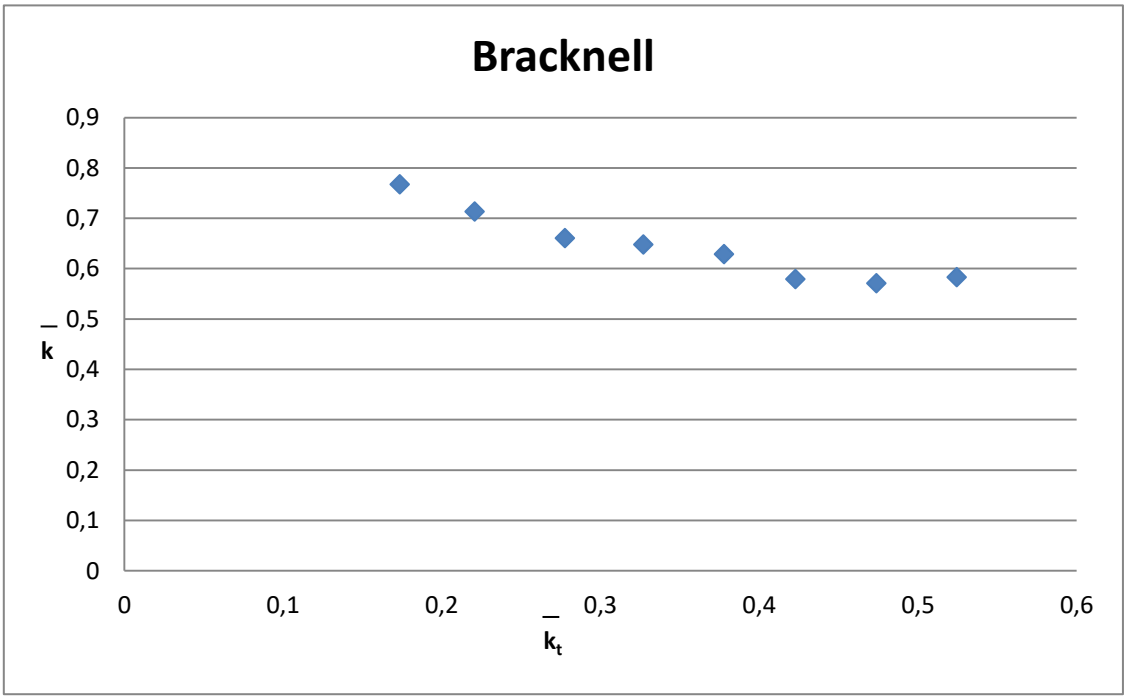

Figure 9.35: Averaged values of diffuse ratio vs. clearness index for Bracknell (own elaboration)

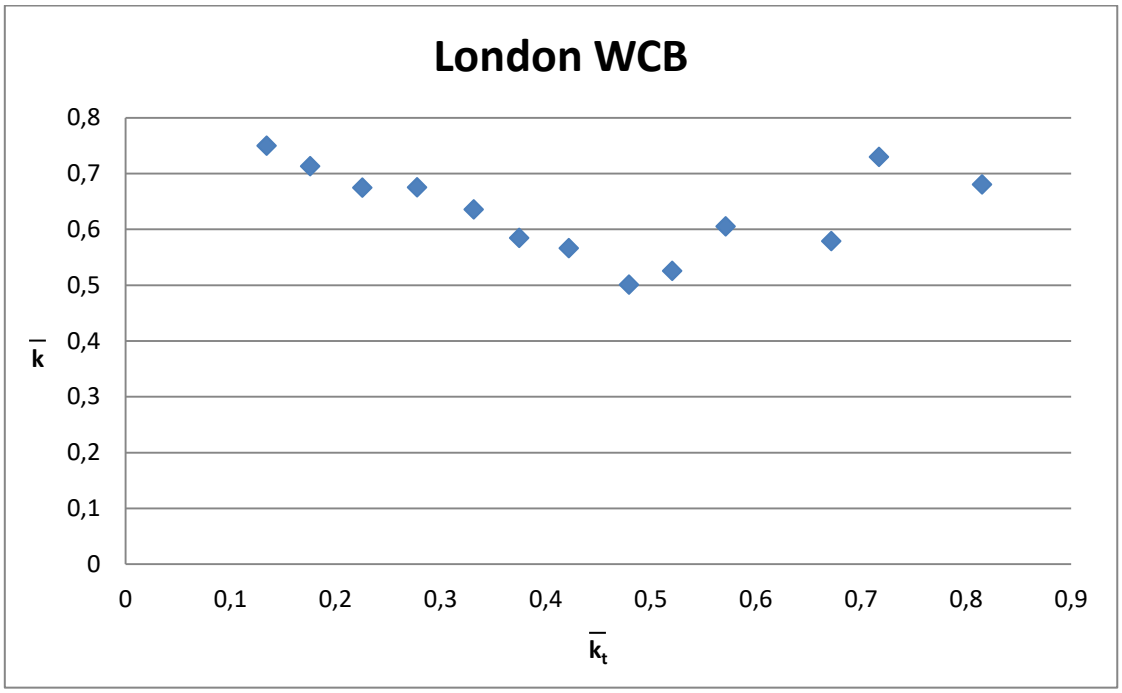

Figure 9.36: Averaged values of diffuse ratio vs. clearness index for London WCB (own elaboration)

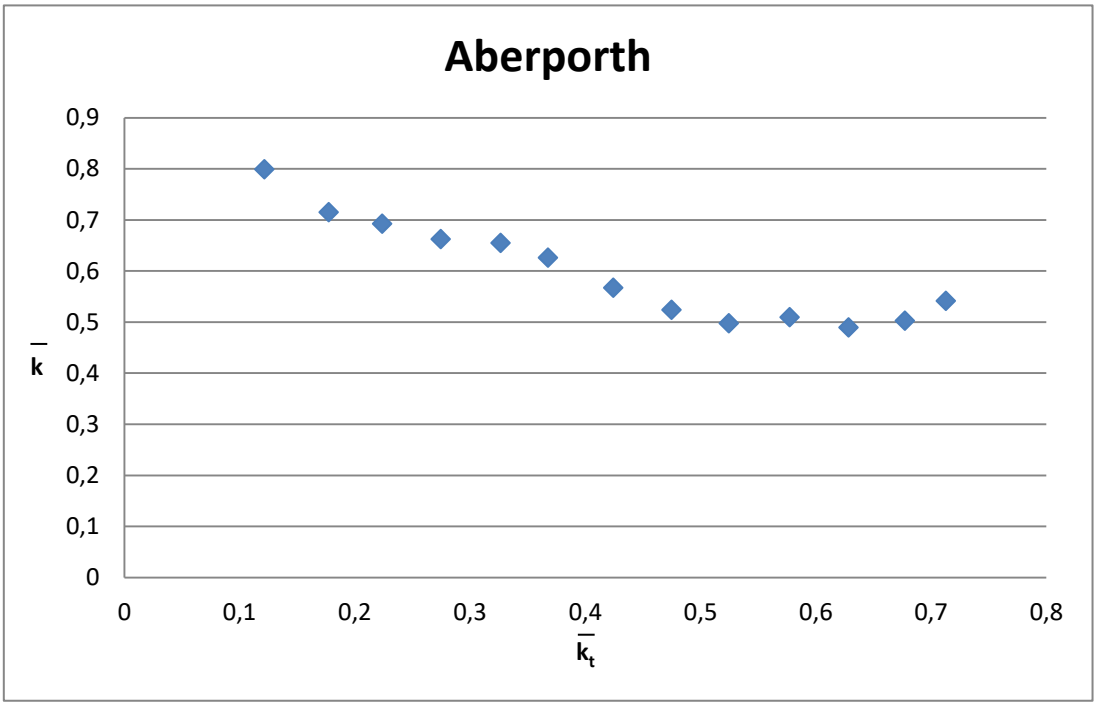

Figure 9.37: Averaged values of diffuse ratio vs. clearness index for Aberporth (own elaboration)

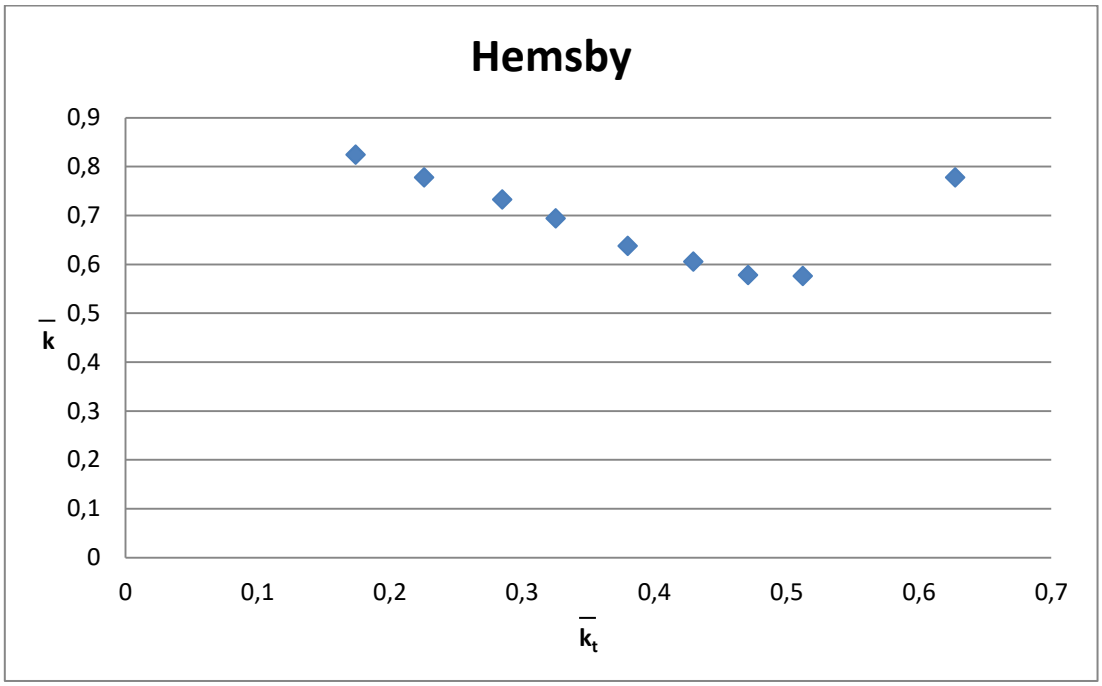

Figure 9.38: Averaged values of diffuse ratio vs. clearness index for Hemsby (own elaboration)

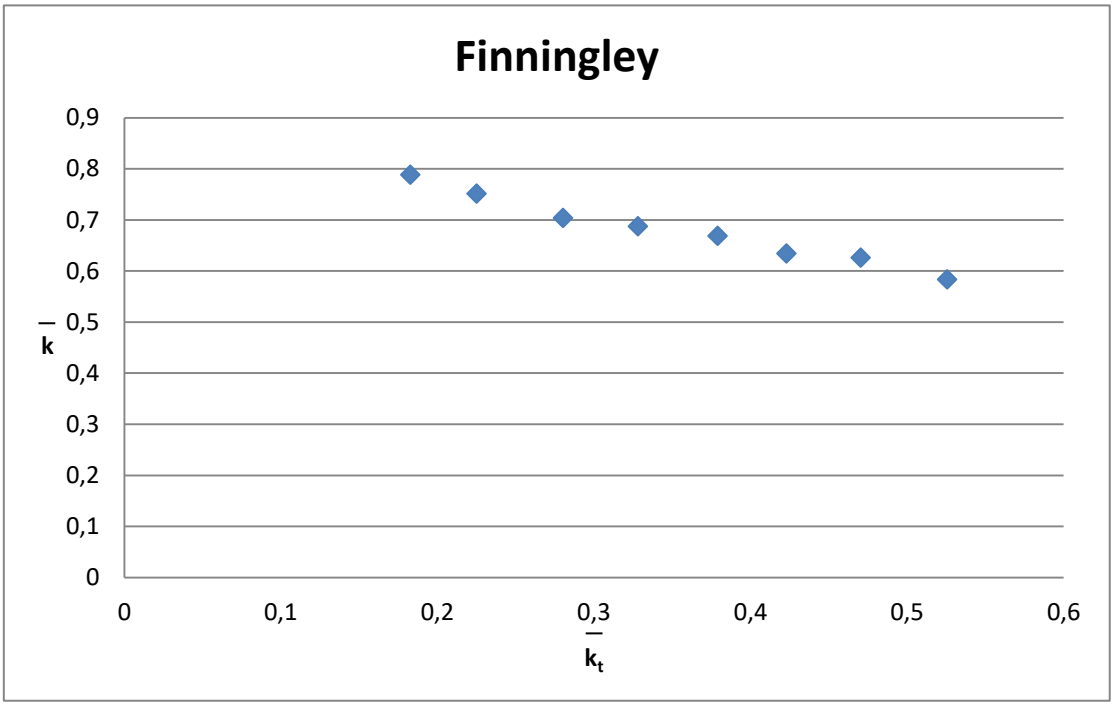

Figure 9.39: Averaged values of diffuse ratio vs. clearness index for Finningley (own elaboration)

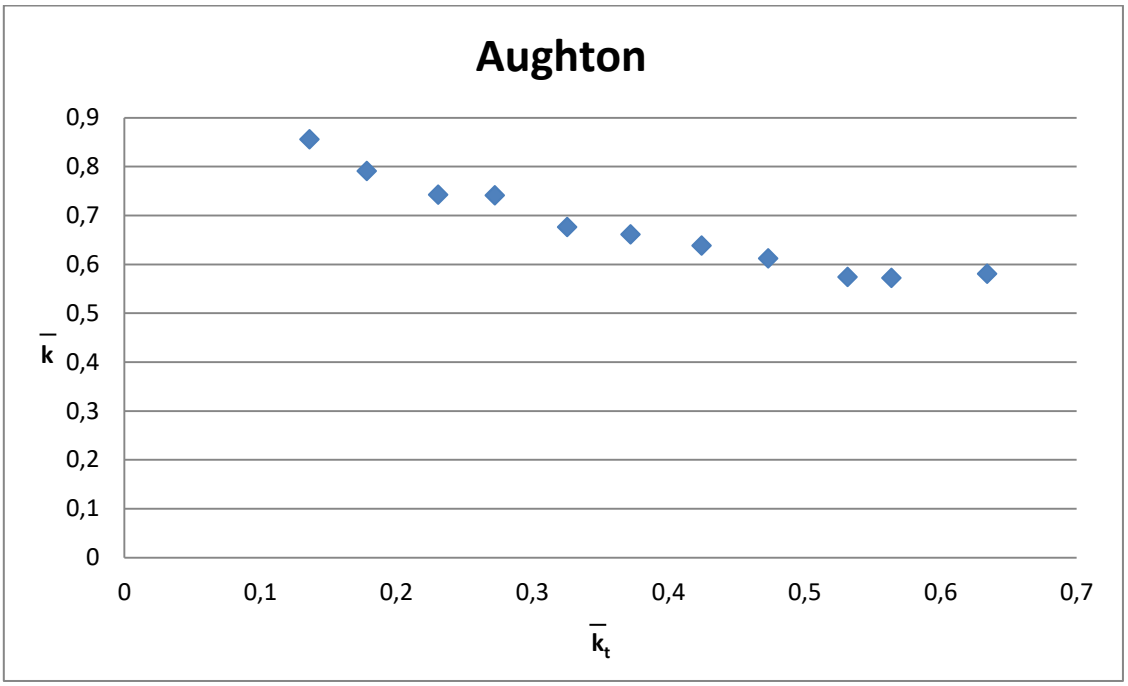

Figure 9.40: Averaged values of diffuse ratio vs. clearness index for Aughton (own elaboration)

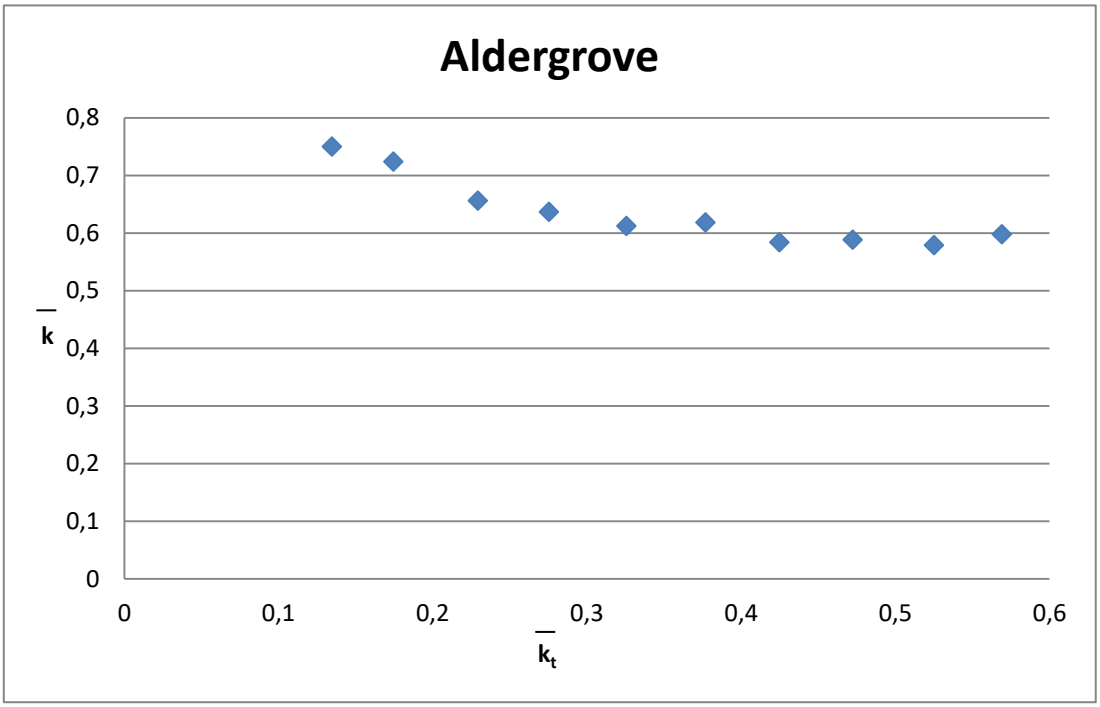

Figure 9.41 Averaged values of diffuse ratio vs. clearness index for Aldergrove (own elaboration)

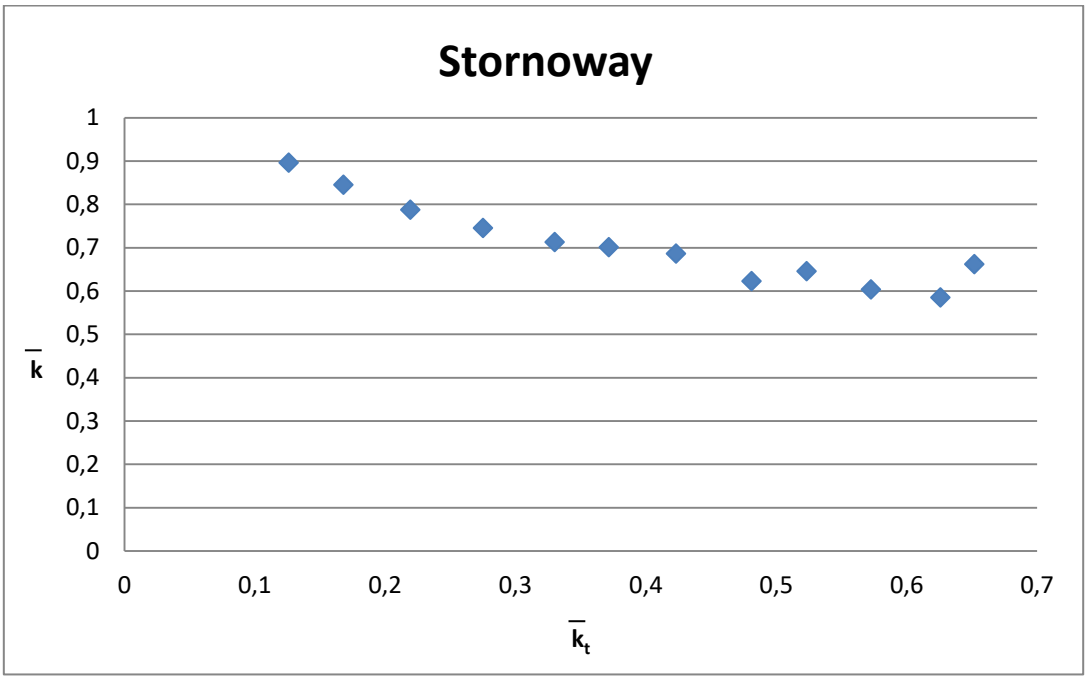

Figure 9.42: Averaged values of diffuse ratio vs. clearness index for Stornoway (own elaboration)

A regression equation has been estimated to each plot. In all the cases a second-degree polynomic equation fit the best in the correlation between the clearness index and diffuse ratio. The table below (see Table 9.4) presents regression equations and coefficient of determination (R^2) obtained for each location.

Table 9.4: Regression equations and coefficient of determination (R^2) for each location (own elaboration)

Country	Location	Regression equations	Eq. n°	R^2
India	Chennai	$k = 0.512k_t^2 - 0.9809k_t + 0.8733$	(9.6)	0.83
		$k = 0.4083k_t^2 - 0.873k_t + 0.853$	(9.7)	0.92
Kingdom of Bahrain	Bahrain	$k = 1.4455k_t^2 - 2.13k_t + 1.1262$	(9.8)	0.98
		$k = 0.7088k_t^2 - 1.3237k_t + 0.8299$	(9.9)	0.96
Spain	Almeria	$k = 1.9414k_t^2 - 2.9329k_t + 1.3637$	(9.10)	0.98
Portugal	Faro	$k = 0.8423k_t^2 - 2.1391k_t + 1.346$	(9.11)	0.99
	Lisbon	$k = 0.0721k_t^2 - 1.3001k_t + 1.1246$	(9.12)	0.99
Spain	Madrid	$k = 0.9087k_t^2 - 2.0465k_t + 1.1808$	(9.13)	0.99

	Girona	$k = 0.1781k_t^2 - 1.0867k_t + 0.887$	(9.14)	0.98
United Kingdom	Camborne	$k = 0.8188k_t^2 - 1.1127k_t + 0.9365$	(9.15)	0.96
	Crawley	$k = 3.3648k_t^2 - 2.8072k_t + 1.1794$	(9.16)	0.96
	Bracknell	$k = 1.4394k_t^2 - 1.5414k_t + 0.9878$	(9.17)	0.97
	London WCB	$k = 0.024k_t^2 - 0.6414k_t + 0.8317$	(9.18)	0.96
	Aberporth	$k = 0.9797k_t^2 - 1.3032k_t + 0.9403$	(9.19)	0.95
	Hemsby	$k = 3.6236k_t^2 - 3.1742k_t + 1.3051$	(9.20)	0.86
	Finningley	$k = 0.451k_t^2 - 0.876k_t + 0.9267$	(9.21)	0.98
	Aughton	$k = 0.9701k_t^2 - 1.2976k_t + 1.0041$	(9.22)	0.98
	Aldergrove	$k = 1.402k_t^2 - 1.34k_t + 0.904$	(9.23)	0.97
	Stornoway	$k = 0.7441k_t^2 - 1.1382k_t + 1.0147$	(9.24)	0.98

9.3 Experimental analysis by latitudes

Figure 9.43 shows the regression of the average values of diffuse ratio and clearness index of the 19 worldwide locations together. Although it is not possible to obtain a unique regression equation for the 19 locations, the graph clearly indicates the existence of different sub-models.

The data for the locations have been arranged in an increasing order of latitude. The mentioned sub-models could be latitude dependant.

Figure 9.44, Figure 9.45 and Figure 9.46 respectively show the regression curves for the locations in a narrower range of latitude. Figure 9.44 shows the regressions for the latitudes 13-20° N, which includes the locations Chennai and Pune in India. The Figure 9.45 shows the regressions for locations in the 20-42° N latitude. In this group, there are Bahrain, Kuwait, Almeria, Faro, Lisbon, Madrid and Girona. And the Figure 9.46 shows the regressions for higher latitude locations, 50-58° N, with ten locations from the UK including Camborne, Crawley, Bracknell, London WCB, Aberporth, Hemsby, Finningley, Aughton, Aldergrove and Stornoway.

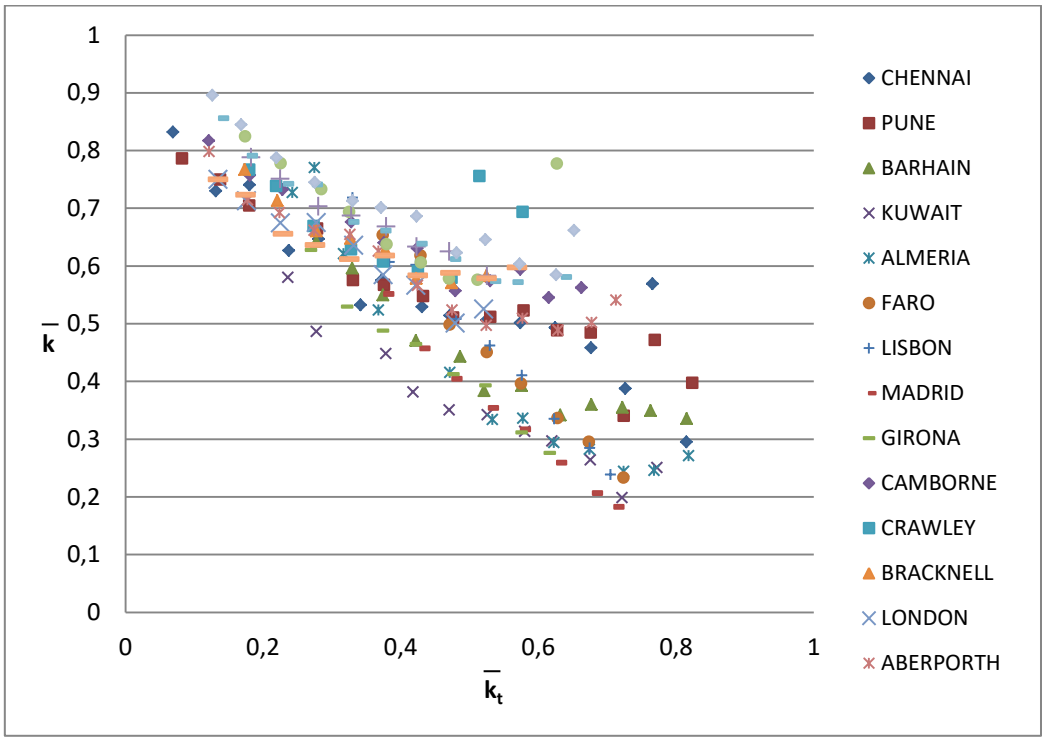

Figure 9.43: Regression of averaged values of clearness index vs. diffuse ratio for the 19 locations (own elaboration)

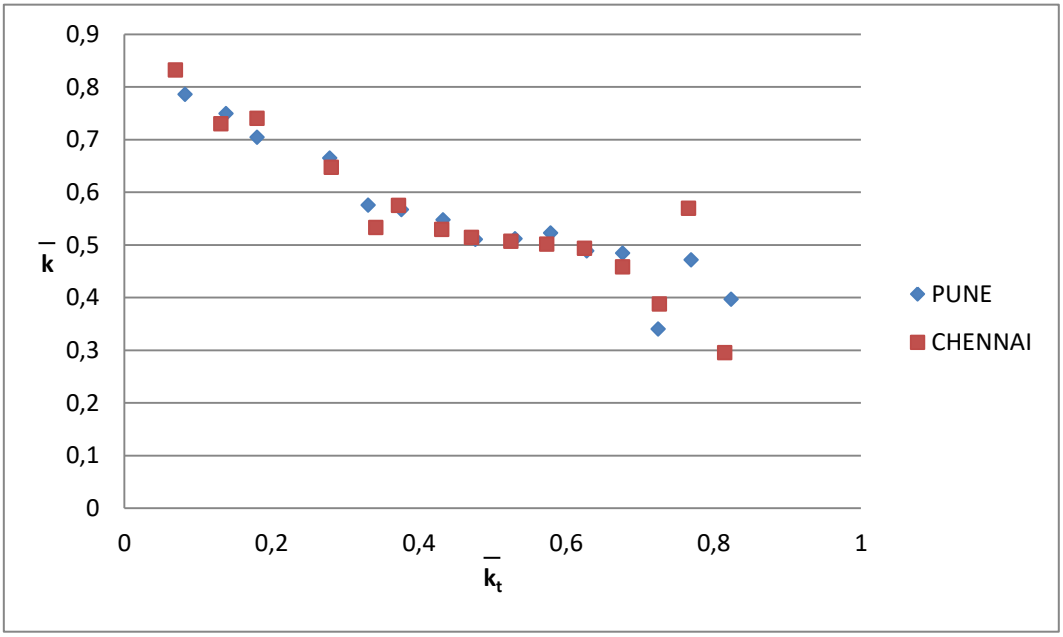

Figure 9.44: Averaged values of diffuse ratio for the locations between latitude 13-20° North (own elaboration)

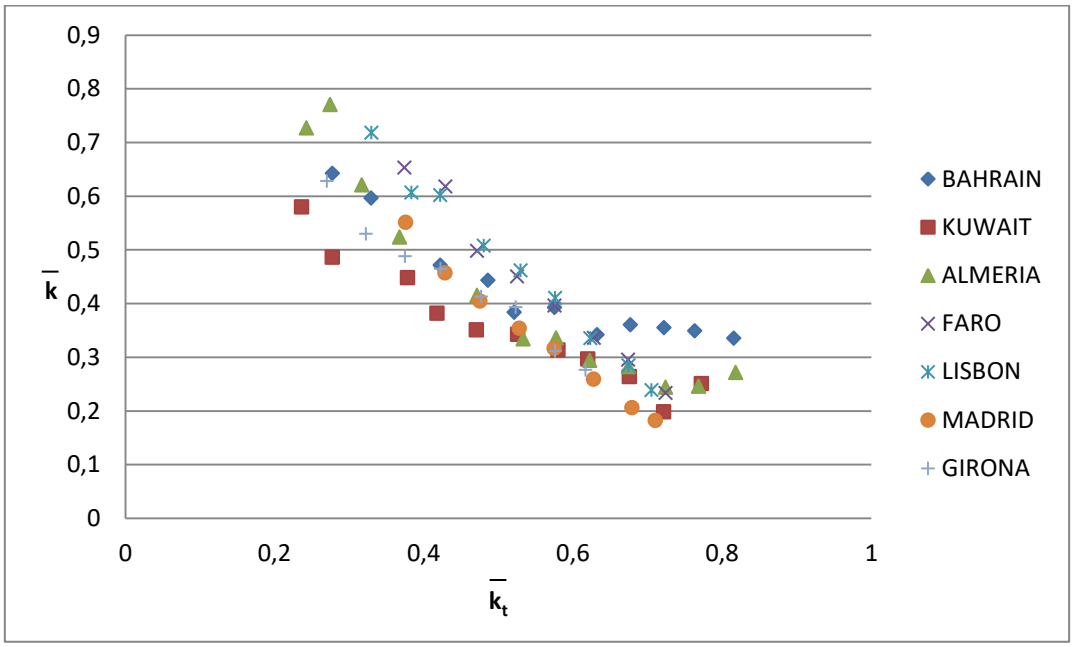

Figure 9.45: Averaged values of diffuse ratio for the locations between latitude 20-42° North (own elaboration)

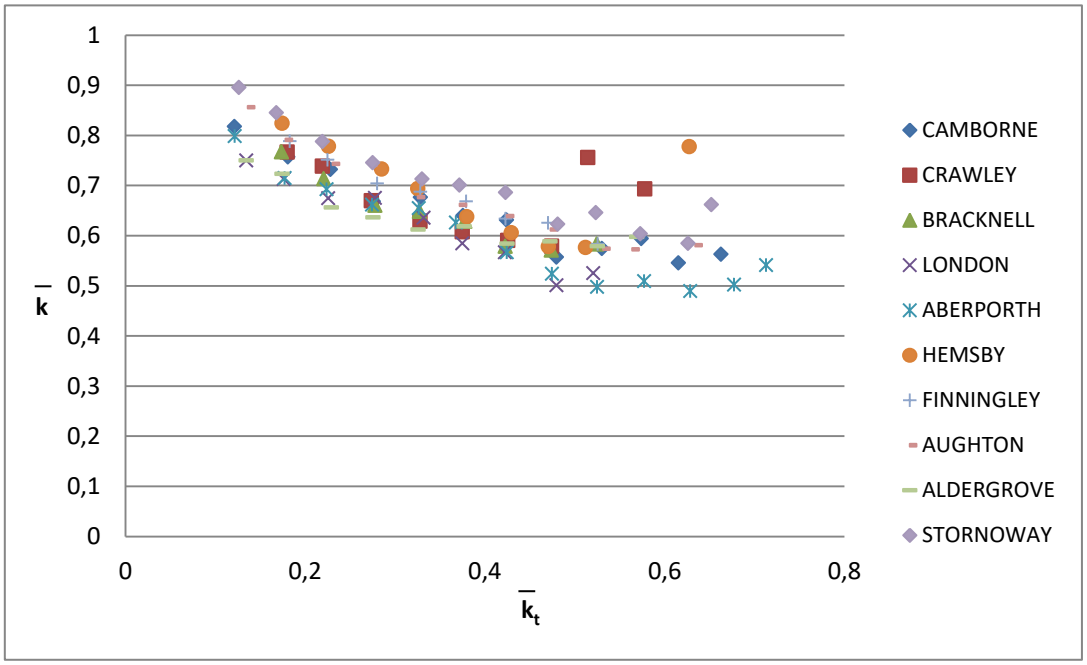

Figure 9.46: Averaged values of diffuse ratio for the locations between latitude 50-58° North (own elaboration)

The three figures (Figure 9.44, Figure 9.45 and Figure 9.46) show the potential for a single regression model for each latitude group.

9.4 Outliers analysis

As mentioned in the section 2, in solar studies it is common to find data that lie unusually far from the bulk of data population. These data are called outliers. In this study, there are data that lie far from the bulk, as it has been pointed in Figure 9.44 and Figure 9.46 among others.

Quartile ranges have been used to evaluate if these unusual data are or are not outliers. The Table 9.5 shows the quartile ranges for each latitude group. As shown in Figure 9.47, Figure 9.48 and Figure 9.49 all the data are between the near upper and lower limits.

Table 9.5: Quartile ranges for each latitude group (own elaboration)

LATITUDE	Q1	Q3	LOWER OUTLIER	UPPER OUTLIER
13-20°N	0.489610549	0.660132978	0.233826905	0.915916621
20-42°N	0.304363410	0.503053209	0.006328710	0.801087909
50-58°N	0.583485121	0.723190315	0.373927330	0.932748106

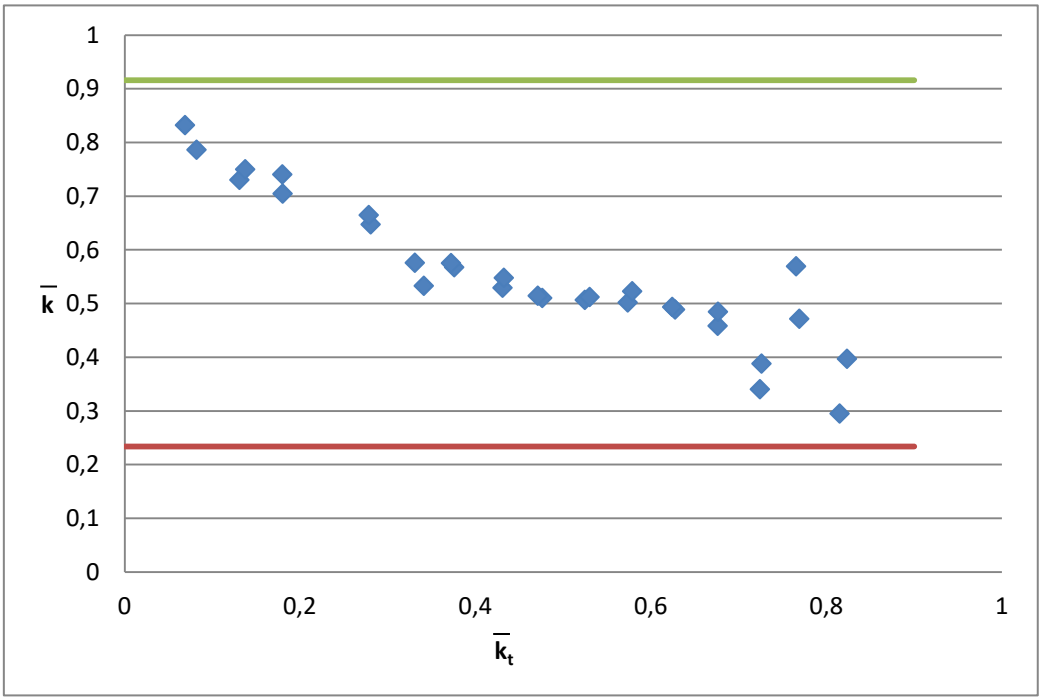

Figure 9.47: Outlier limits in the average values of the diffuse ratio in the latitudes 13-20° North (own elaboration)

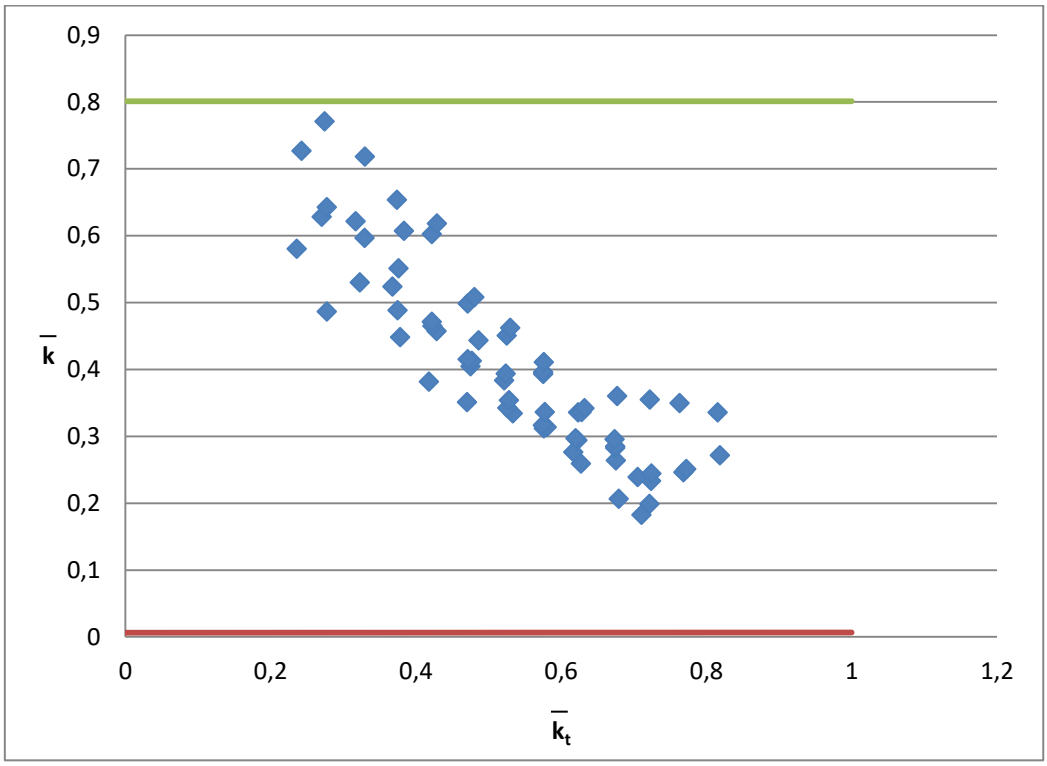

Figure 9.48: Outlier limits in the average values of the diffuse ratio in the latitudes 20-42° North (own elaboration)

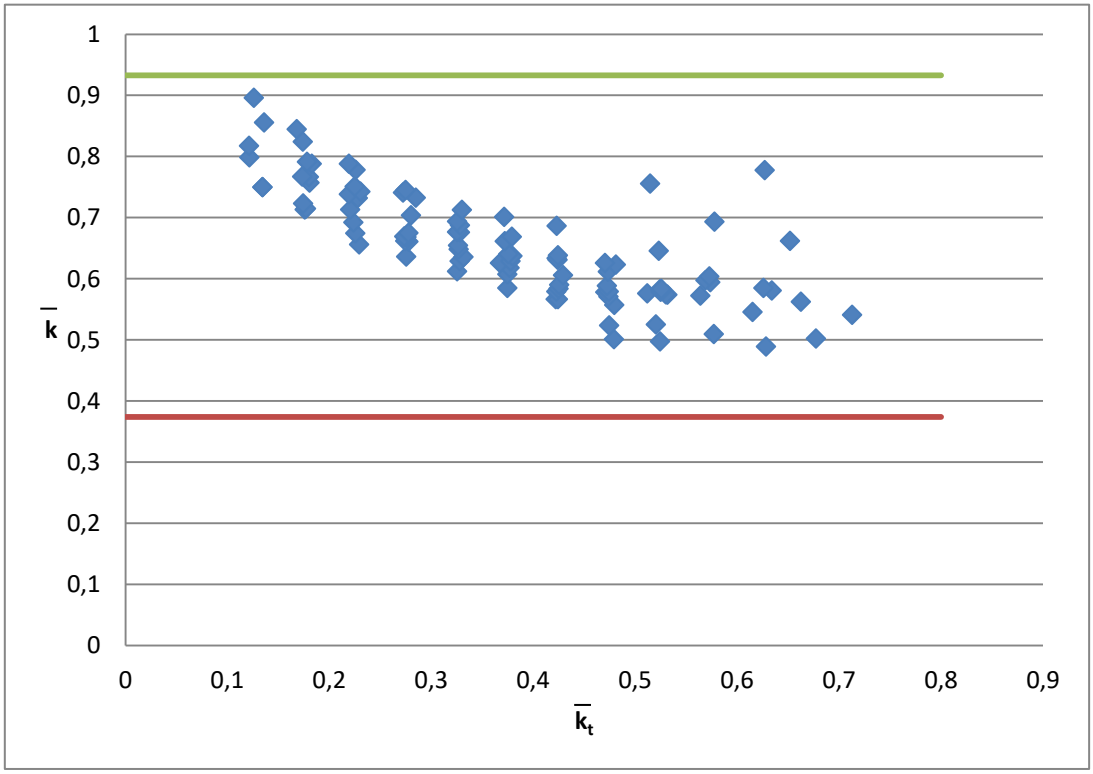

Figure 9.49: Outlier limits in the average values of the diffuse ratio in the latitudes 50-58° North (own elaboration)

A point worth mentioning here is that in almost all cases of the data from the 10 locations of the highest latitude group that are under examination, there is an increasing trend of diffuse ratio for the top end of clearness index. This fact is especially notorious in the high latitude locations, as can be seen in the Figure 9.49. This is a well-known phenomenon that is associated with simultaneous occurrence of two astronomical / weather-related conditions:

- Low solar altitude angle, and
- Sun shining strongly through a broken cloud

The result is that a high clearnes index is obtained from a high beam irradiation augmented with sky-diffuse and cloud-reflected radiation as is also a high value of diffuse ratio. This phenomenon is common in most diffuse solar radiation studies. Orgill and Hollands (1977) attribute this fact to "beam radiation being reflected from clouds and recorded as diffuse radiation during periods when the sun is unobscured by the surrounding clouds" (Orgill & Hollands, 1977). The above phenomenon is depicted in Figure 9.50, and Table 9.6 sheds further light on those points that belong to the class of data under discussion.

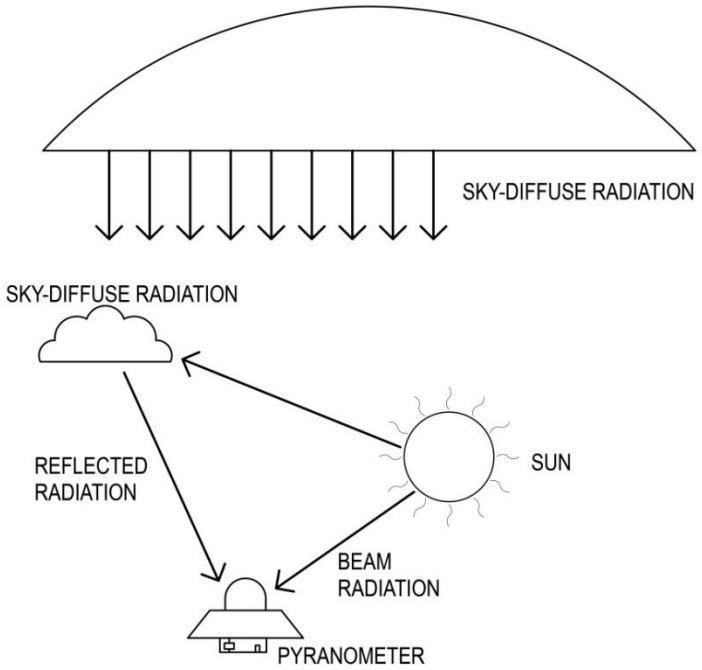

Figure 9.50: Demonstration of atmospheric condition when diffuse irradiation is enhanced under a partly clouded sky with a low solar altitude (own elaboration)

Table 9.6: High clearness index data

	Averaged diffuse ratio *point number	Clearness index	Hourly diffuse ratio	Solar altitude, degree
Stornoway	0.66 (1*)	0.65	0.63	12.3
		0.65	0.57	20.1
		0.65	0.79	4.1
Hemsby	0.78 (2*)	0.60	0.74	3.7
		0.64	0.82	1.7
		0.64	0.77	3.3
Crawley	0.75 (3*)	0.51	0.85	1.5
		0.52	0.64	10.1
		0.52	0.78	2.8
	0.69 (4*)	0.55	0.63	6.9
		0.58	0.71	4.6
		0.59	0.71	5.9
		0.59	0.73	4.9
Chennai	0.57 (5*)	0.75	0.59	16.4
		0.76	0.76	21.2
		0.77	0.55	22.6
		0.78	0.38	39.4

9.5 Practical application of statistical tools

Statistical tools provide further information about the adequacy of a given mathematical model. In this study, the MEB, MAD, RMSE and R^2 (further information about these tools in section 4) statistical tools have been applied to evaluate the application of the models.

Although there are not outliers in this solar radiation study, there are some points that lie apart from the bulk of the population data, due to the simultaneous occurrence of low solar altitude angle and sun shinning strongly through a broken cloud. This fact has an effect in the calculation of the solar models for each latitude group, and to evaluate the adecuacy of the regression curves and to test the effect of the data mentioined in Table 9.6, the statistical tools mentioned in section 2 have been used.

Figure 9.51, Figure 9.53 and Figure 9.54 respectively present regression models that were obtained by pooling all data from locations with a latitude range of 13-20° N, 20-42° N and 50-58° N, and Figure 9.52, Figure 9.55, Figure 9.56, Figure 9.57 and Figure 9.58 show the same figures after taking out the data that lie far from the bulk.

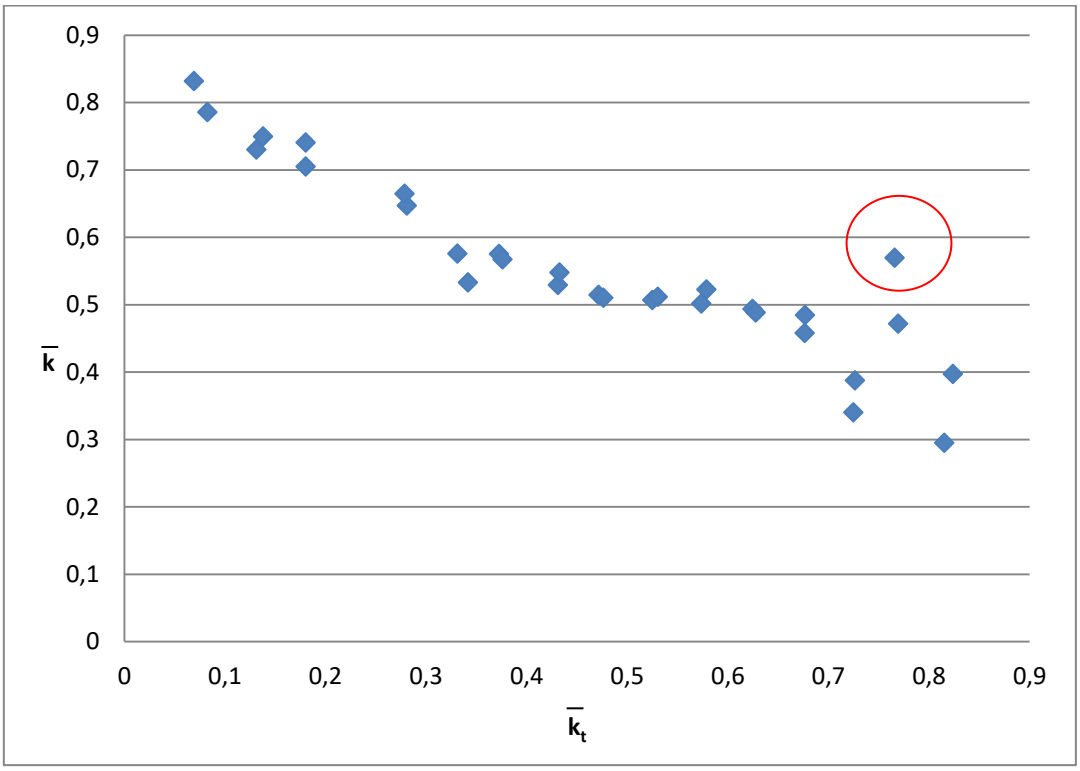

Figure 9.51: Averaged values of diffuse ratio for the locations between latitude 13-20° North (own elaboration)

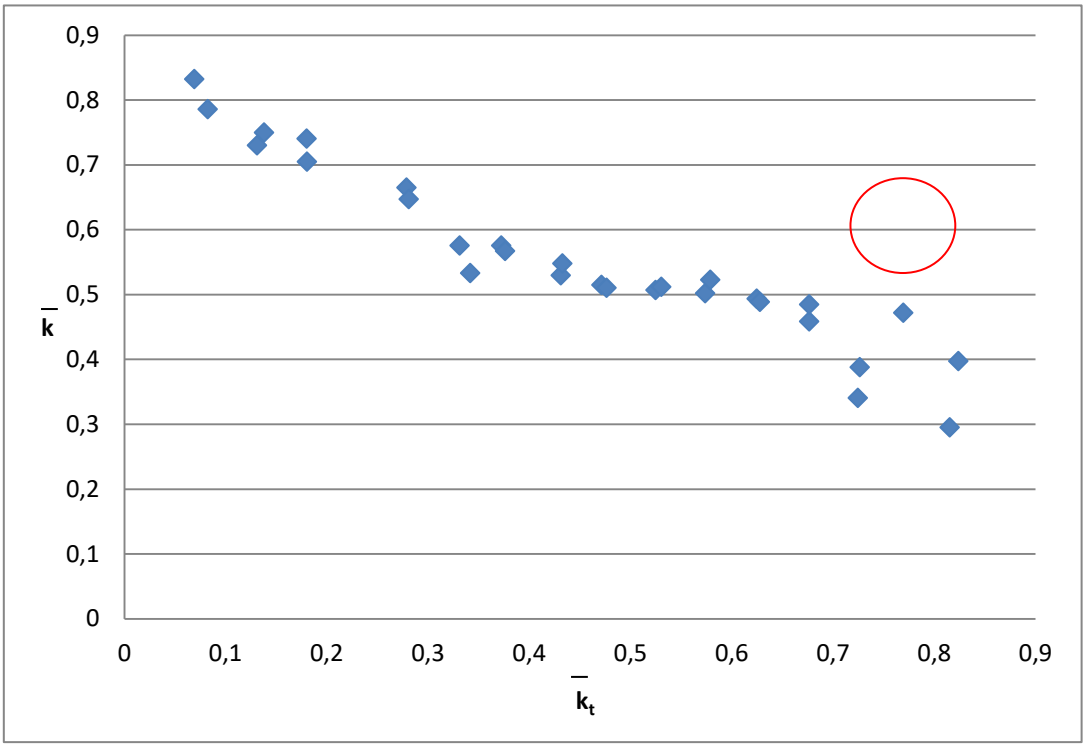

Figure 9.52: Averaged values of diffuse ratio for the locations between latitude 13-20° North without point 5* (own elaboration)

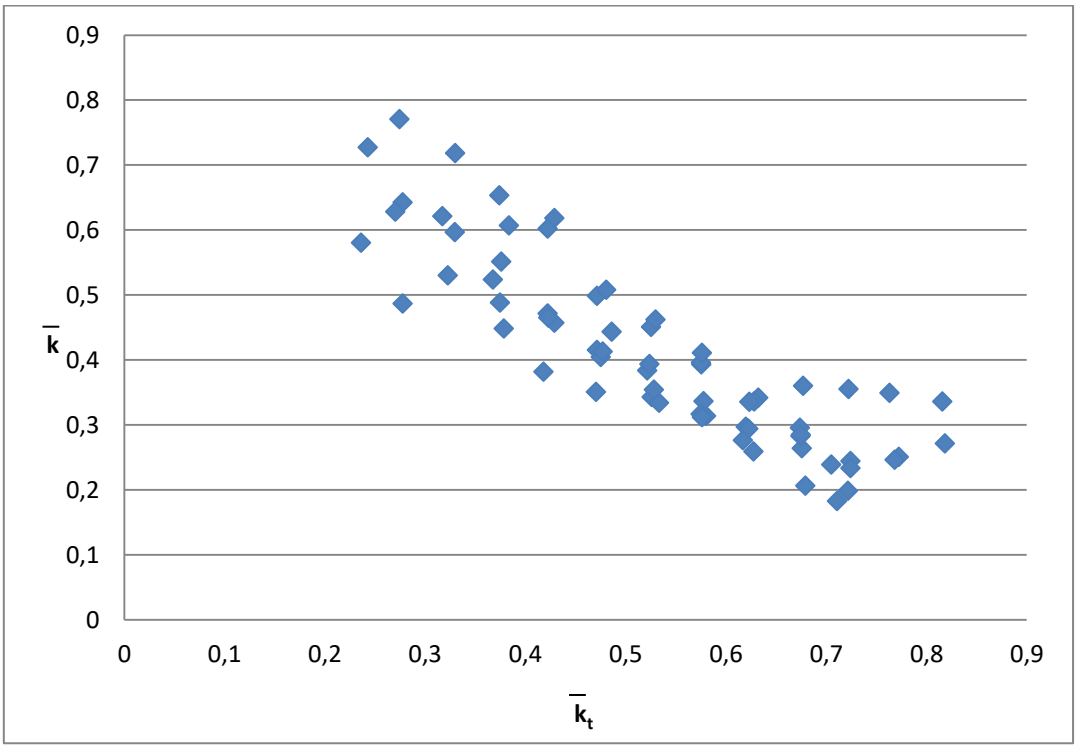

Figure 9.53: Averaged values of diffuse ratio for the locations between latitude 20-42° North (own elaboration)

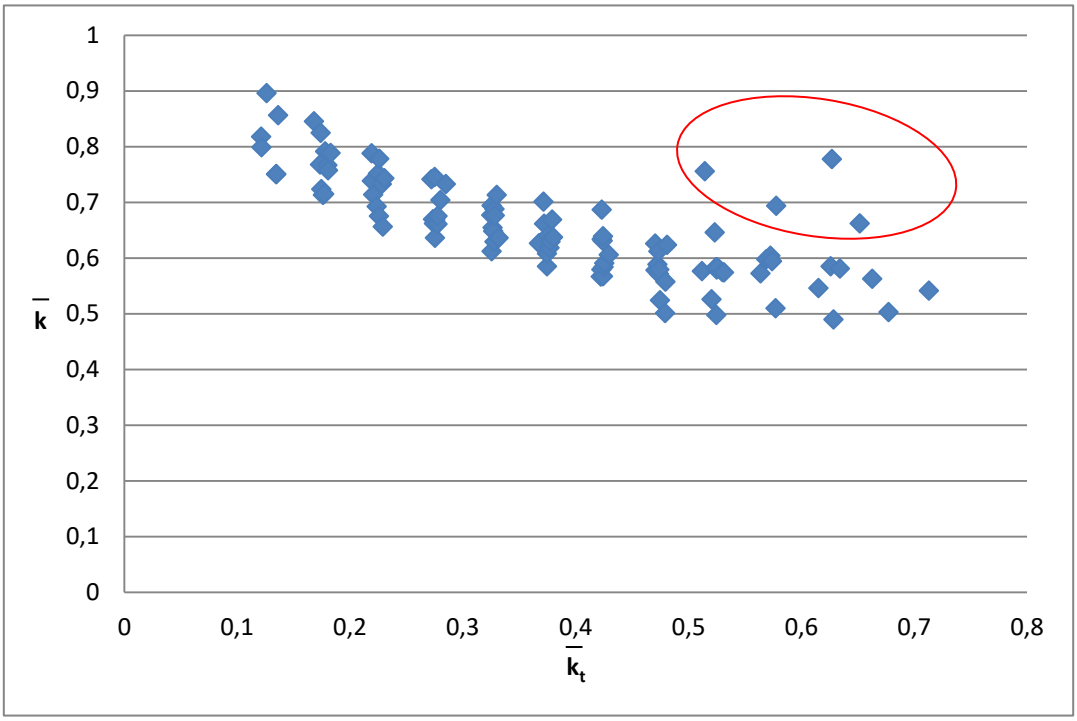

Figure 9.54: Averaged values of diffuse ratio for the locations between latitude 50-58° North (own elaboration)

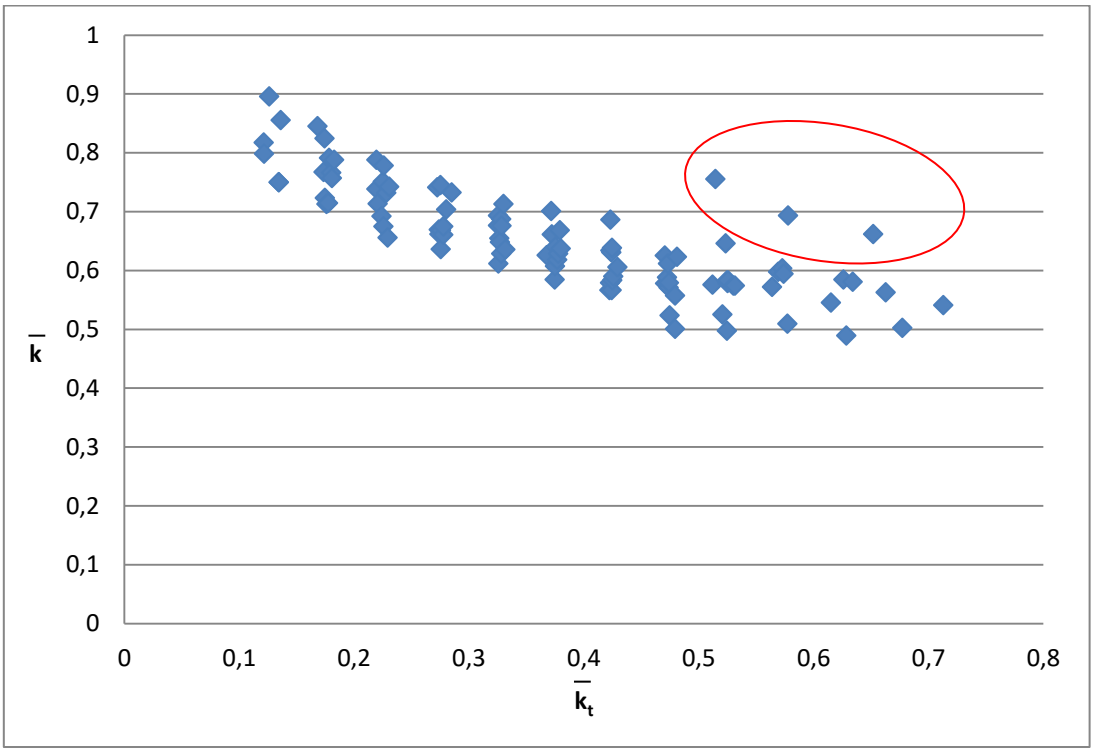

Figure 9.55: Averaged values of diffuse ratio for the locations between latitude 50-58° North without point 2* (own elaboration)

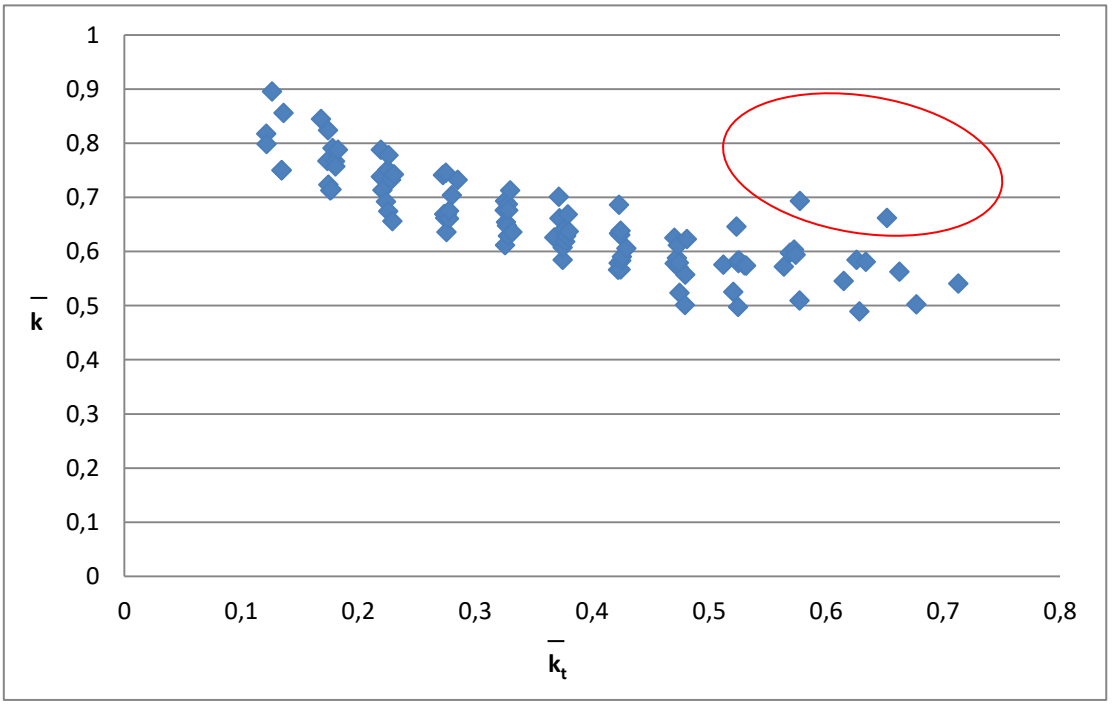

Figure 9.56: Averaged values of diffuse ratio for the locations between latitude 50-58° North without points 2* and 3* (own elaboration)

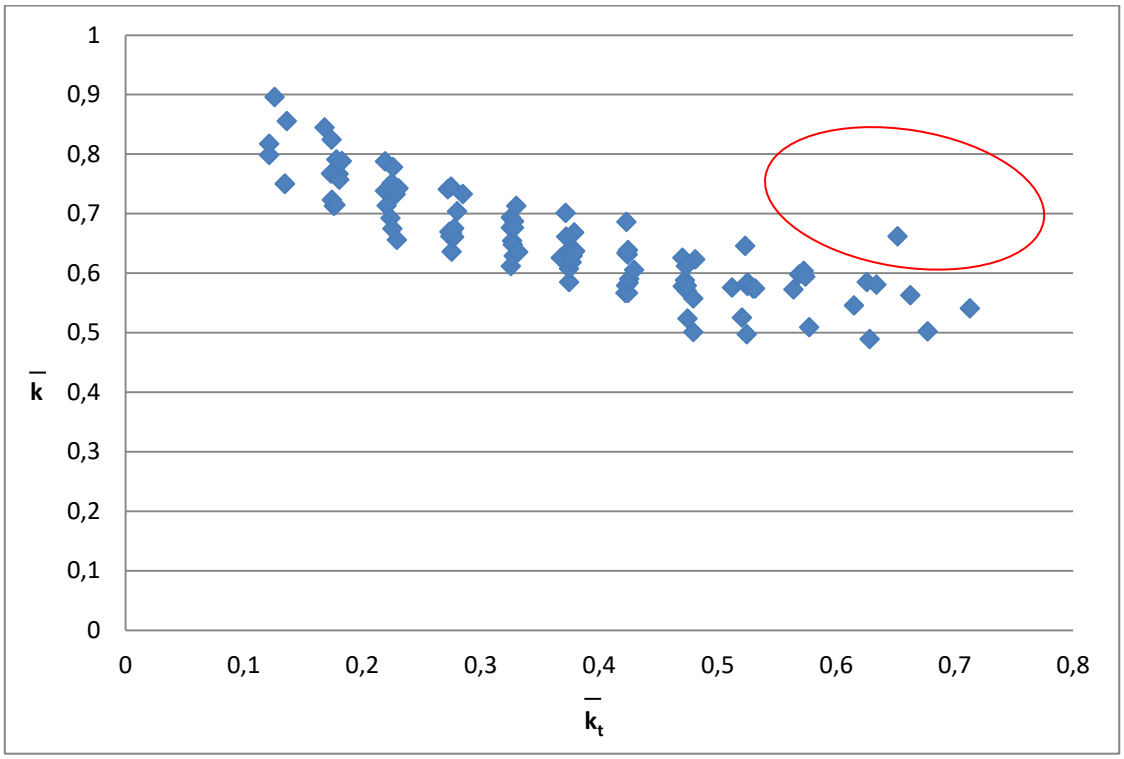

Figure 9.57: Averaged values of diffuse ratio for the locations between latitude 50-58° North without points 2*, 3* and 4* (own elaboration)

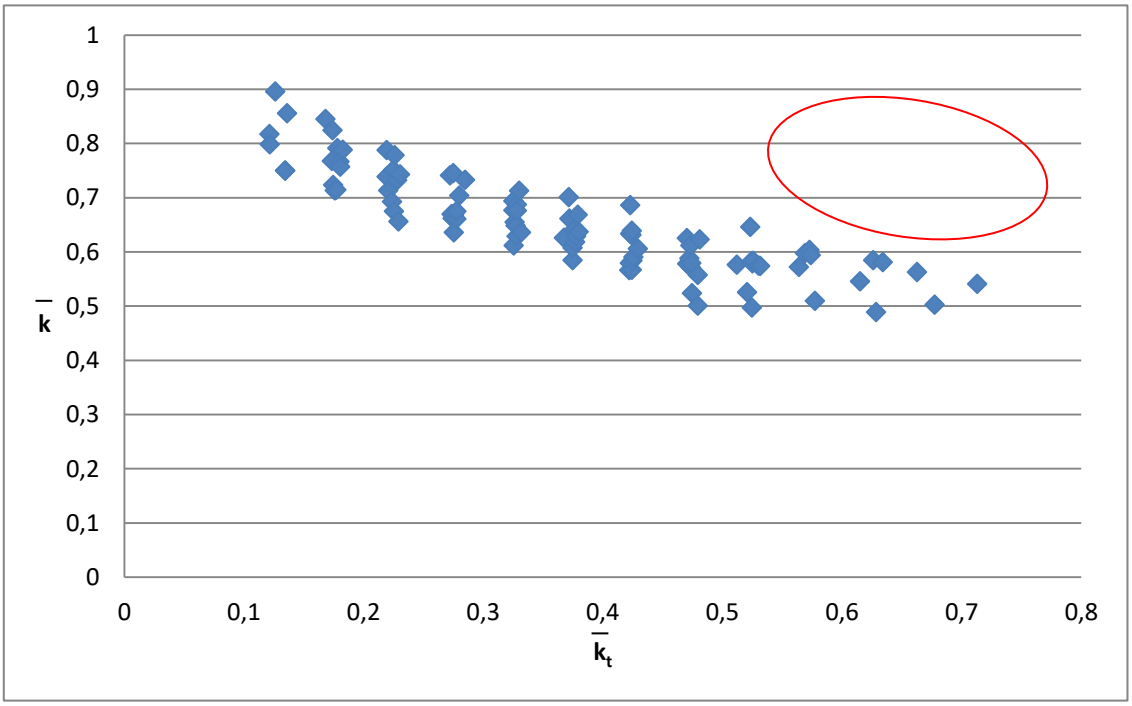

Figure 9.58: Averaged values of diffuse ratio for the locations between latitude 50-58° North without points 2*, 3*, 4* and 1* (own elaboration)

The Table 9.7 shows the corresponding statistical values for each graph.

Table 9.7: Regression equations and corresponding statistical values for each figure (own elaboration)

LATITUDE	FIGURE	EQUATION		R^2	R	MBE	MAD	RMSE
13-20°N	9.51	$k = 0.4623k_t^2 - 0.9291k^t + 0.8636$	(9.25)	0,87	0.93	3.99811E-05	0.03135152	0.04596766
	9.52	$k = 0.3443k_t^2 - 0.8551k^t + 0.853$	(9.26)	0.92	0.96	-0.00499490	0.02739634	0.03808327
20-42°N	9.53	$k = 0.994k_t^2 - 1.8386k^t + 1.0815$	(9.27)	0.80	0.89	6.81776E-06	0.05004819	0.06323689
50-58°N	9.54	$k = 1.0257k_t^2 - 1.2458k^t + 0.9559$	(9.28)	0.69	0.83	6.3881E-05	0.03650876	0.04893337
	9.55	$k = 0.8993k_t^2 - 1.17k^t + 0.9461$	(9.29)	0.74	0.86	-0.00192920	0.03488012	0.04495471
	9.56	$k = 0.9211k_t^2 - 1.1976k^t + 0.951$	(9.30)	0.77	0.88	-0.00365730	0.03352384	0.04186077
	9.57	$k = 0.8896k_t^2 - 1.185k^t + 0.9502$	(9.31)	0.80	0.89	-0.00486524	0.03269530	0.04044640
	9.58	$k = 0.7885k_t^2 - 1.1214k^t + 0.9417$	(9.32)	0.81	0.9	-0.00576259	0.03218517	0.03978889

9.6 Results and discussion

The statistical results shown in Table 9.7 prove the effect of the points under the effect of low solar altitude angle and sun shinning strongly through a broken cloud. The higher the number of points appart from the population bulk, the lower the coefficient of determination (R^2).

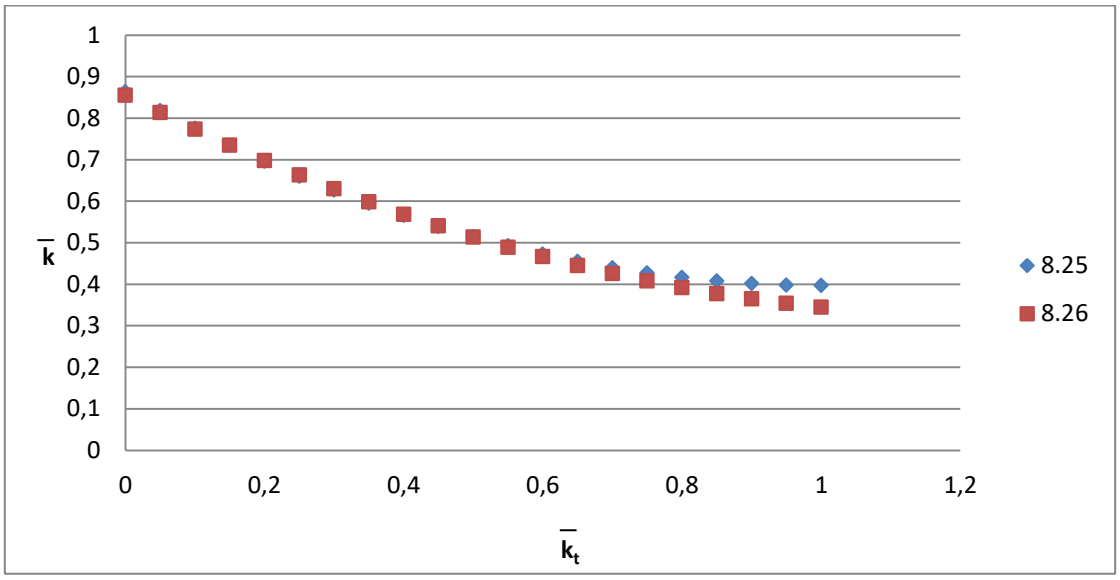

Figure 9.59: Regression curves for locations between latitiude 13-20° North (own elaboration)

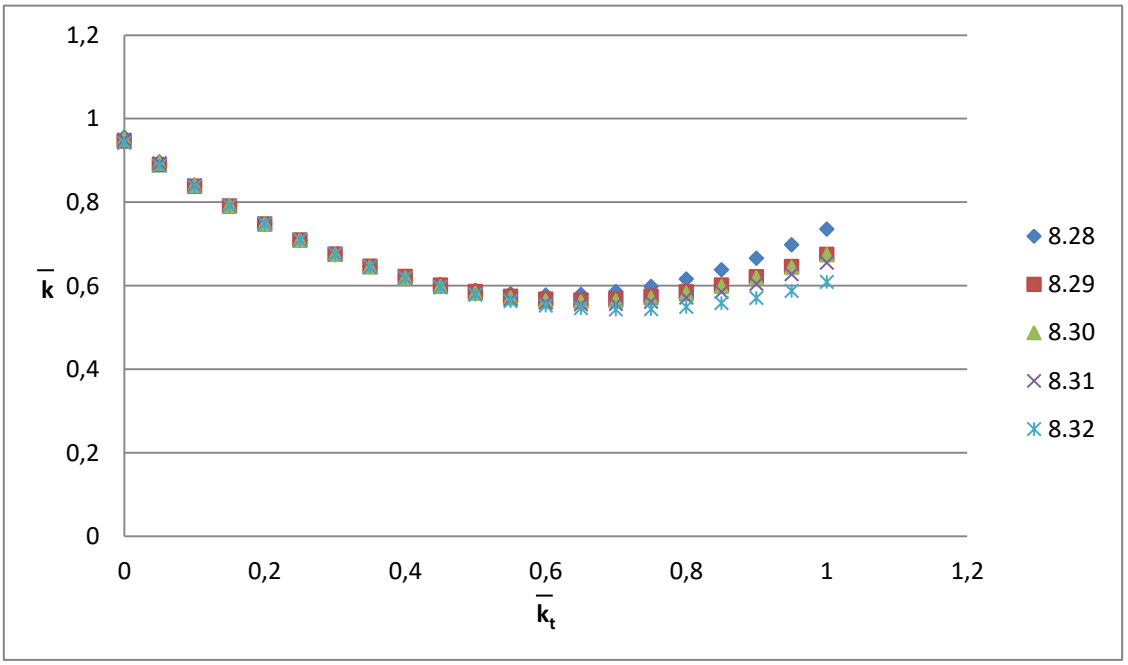

Figure 9.60: Regression curves for locations between latitiude 50-58° North (own elaboration)

However, the effect on the regression equation is almost imperceptible and it is located in the high values of clearness index, as can be seen in the figures above (see Figure 9.59 and Figure 9.60). In the case of the high latitude group, 50-58 N, the coefficient of determination (R^2) lies between 0.69 and 0.81. To avoid the elimination of the all the points that lie far from the bulk, but to maintain proper statistical results, 0.8 has been considered as a minimum value for the definitive regression equation.

There are three main points worth mentioning in this study.

- First, it is not possible to obtain a unique regression equation for the nineteen worldwide locations. This point is reinforced via Figure 9.43.

- However, a strong correlation is observed between the average diffuse ratio and clearness index, with high values of the corresponding coefficient of determination (R^2) and coefficient of correlation (R) for narrower range of latitude (Table 9.7).

- It is also important to note that in each case the shape of the regressed curve is concave, contrary to the convex profile for hour-byhour regressions reported by research teams from around the world. The Figure 9.61 shows the shape of the regression equation for each latitude group. Note that for the locations in the range between 13-20° N and locations in latitudes 50-58° N equations 8.25 and 8.31 have been plotted respectively.

The definitive regression equations to estimate monthly-averaged hourly diffuse radiation values for the latitude ranges developed are shown below:

13-20 $$\boldsymbol{k = 0.4623k_t^2 - 0.9291k_t + 0,8636} \quad (9.33)$$

20-42 $$\boldsymbol{k = 0.994k_t^2 - 1.8386k_t + 1.0815} \quad (9.34)$$

50-58 $$\boldsymbol{k = 0.8896k_t^2 - 1.185k_t + 0.9502} \quad (9.35)$$

The Figure 9.61 shows the definitive regression curves for the three latitude ranges.

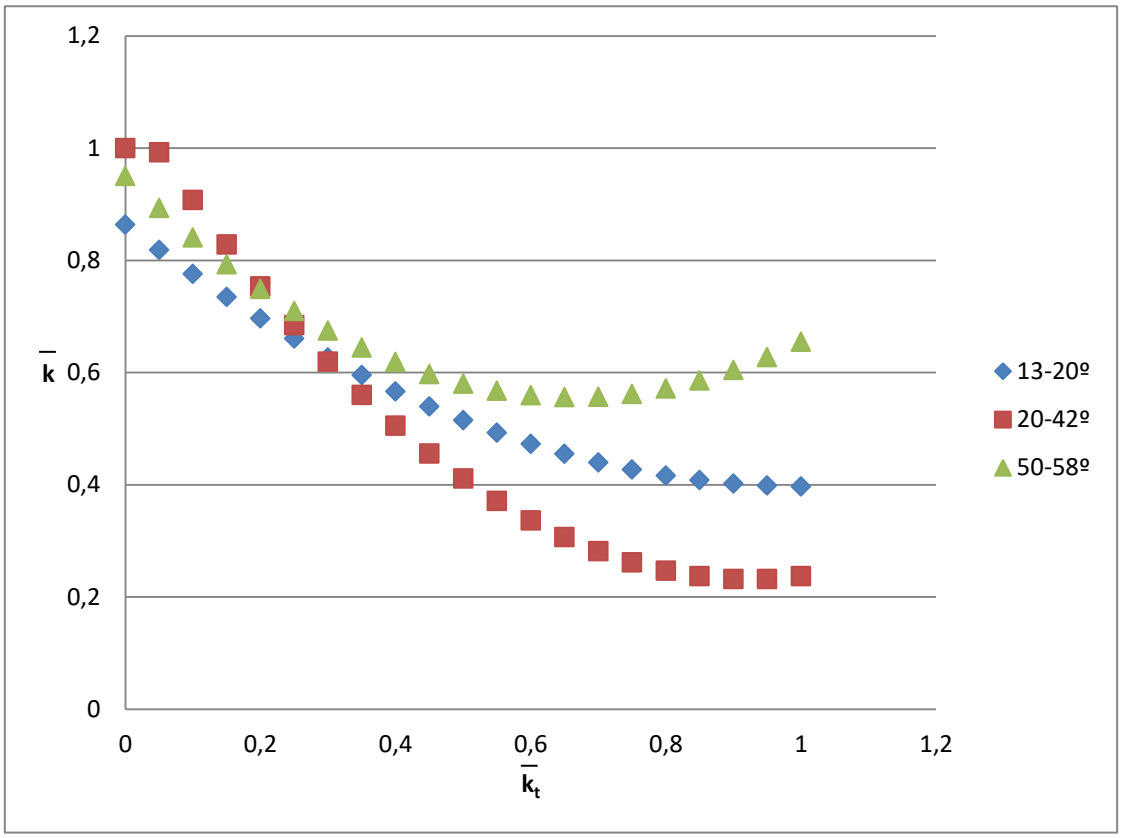

Figure 9.61: Regression curves and equations (own elaboration)

The adequacy of these correlation models has been proven in this study, thus, the equations 9.33, 9.34 and 9.35 can be used to estimate diffuse radiation values in sites located in these latitude ranges.

These equations would fit the step 2 presented in the beginning of section 8 (see Figure 9.2). Using daily radiation data from the NASA website to estimate hourly values as explained in section 8.1, and calculating the extraterrestrial value using the equations presented in Figure 9.2, it is possible to obtain averaged hourly diffuse radiation data.

10. CONCLUSIONS AND FUTURE LINES

The current energy consumption model is not sustainable anymore. The negative effects of fossil fuels in the environment are undeniable, and proof of that is the evident climate change. Besides, the depletion of fossil fuels is obvious and there is no turning back.

Solar energy is abundant, clean and environmentally friendly, and has the capacity to provide energy to fulfil the current and future necessities. Therefore, there is growing need for solar energy. Solar thermal applications for water and space heating are stabilized in the last years. Photovoltaic applications, on the contrary, are growing very fast.

However, accurate solar radiation data are needed for the design and improvement of these devices to increase effectiveness and efficiency and extend their use. The optimum radiation data for this purpose would be the slope solar radiation. Slope radiation is compound by the global and diffuse components. But, there availability of measured records of global and diffuse radiation for hourly and sub-hourly periods is limited or non-existent in most location.

It was presently shown that monthly-averaged hourly data for solar radiation are much more economical to obtain than hour-by-hour records. Furthermore, through NASA website it is possible to freely obtain monthly-average daily global irradiation data for any terrestrial location.

Using established models such as those presented by Liu and Jordan (1960), Collares-Pereira and Rabl (1979), Mani and Rangarajan (1983), Muneer and Saluja (1996) and Lloyd (1982) it is then possible to decompose the daily–to averaged hourly global irradiation. The missing link so far has been hourly averaged diffuse irradiation.

Primarily, the present work has explored a correlation between averaged-hourly diffuse and global irradiation using the diffuse ratio–clearness index envelope and reports regression models to complete the above missing link for 19 world locations. Present results show that a strong correlation is thus obtainable, even though it is not possible to produce a single regressed curve for worldwide locations. The regression curves are distinctly different from previously available hour-by-hour regressions, in each case the shape of the regressed curve is concave, contrary to the convex profile for hour-by-hour regressions reported by research teams from around the world.

There is no reason to doubt the existence of such a relationship for other data sets that are available for other world locations. The present work has the potential for other similar researches to extend the application to locations in latitudes not included in this study and to add more locations to each latitude group in order to gain accuracy in the results.

11. CONCLUSIONES Y LINEAS FUTURAS

El actual modelo de consumo de energía no es sostenible. Los efectos negativos de los combustibles fósiles en el medio ambiente son innegables, y prueba de ello es el evidente cambio climático. Además, el agotamiento de los combustibles fósiles es un hecho y no hay vuelta atrás.

La energía solar es abundante, limpia y respetuosa con el medio ambiente, y tiene la capacidad de proporcionar energía para satisfacer las necesidades actuales y futuras. Por lo tanto, hay una creciente necesidad de energía solar. Las aplicaciones térmicas solares para el calentamiento de agua y la calefacción de espacios se han estabilizado en los últimos años. Por el contrario, las aplicaciones fotovoltaicas están creciendo muy rápido.

Para aumentar la eficacia y eficiencia, así como para incrementar el uso de los dispositivos que aprovechan la energía solar, es necesario disponer de datos precisos de radiación solar. Los datos óptimos de radiación para este propósito son la radiación solar sobre una superficie inclinada. Esta radiación se descompone a su vez en radiación global y difusa. Sin embargo, la disponibilidad de registros medidos de radiación global y difusa para períodos horarios y sub-horarios es limitada o inexistente en la mayoría de los lugares.

En este estudio se ha demostrado que los datos medios por hora de la radiación solar son mucho más económicos que los registros de hora por hora. Además, a través de la página Web oficial de la NASA es posible obtener gratuitamente datos medios de irradiación global para cualquier ubicación terrestre.

Utilizando modelos ya establecidos como los obtenidos por Liu y Jordan (1960), Collares-Pereira y Rabl (1979), Mani y Rangarajan (1983), Muneer y Saluja (1996) y Lloyd (1982), es posible descomponer los datos diarios para promediar la irradiación global por hora. El eslabón perdido hasta el momento ha sido el cálculo de datos medios por hora de la radiación difusa.

Primeramente, en el presente trabajo se ha analizado la correlación existente entre la irradiación difusa y la radiación global por hora utilizando la envolvente entre el índice de claridad y el ratio entre la radiación difusa y global, para así completar el eslabón perdido para 19 ciudades del mundo. Los resultados muestran que se puede obtener una fuerte correlación, aunque no es posible producir una única curva regresiva para las ciudades de

todo el mundo. Las curvas de regresión son claramente diferentes de las regresiones hora por hora disponibles hasta el momento, en este caso la forma de la curva regresiva es cóncava, contrariamente al perfil convexo para las regresiones hora por hora reportadas por investigadores de todo el mundo.

No hay razón para dudar de la existencia de tal relación para otros conjuntos de datos que están disponibles para otros lugares del mundo. El presente trabajo tiene el potencial para extender la aplicación a ubicaciones en latitudes no incluidas en este estudio y para agregar más ubicaciones a cada grupo de latitud con el fin de obtener precisión en los resultados.

12.REFERENCES

Agencia estatal de meteorologia. (2017). Retrieved from http://www.aemet.es/documentos/es/eltiempo/observacion/radiacion/Radiacion_Solar.pdf

Aguiar, R., Collares-Pereira, M., & Conde, J. (1988). Simple procedure for generating sequences of daily radiation values using a library of markov transition matrices. *Solar Energy, 40*(3), 269-279.

Aguiar, R., & Collares-Pereira, M. (1992). *TAG: A time-dependent, autoregressive, gaussian model for generating synthetic hourly radiation* doi:http://dx.doi.org/10.1016/0038-092X(92)90068-L

Akinoğlu, B., & Ecevit, A. (1990). A further comparison and discussion of sunshine-based models to estimate global solar radiation. *Energy, 15*(10), 865-872.

Akpabio, L. E., & Etuk, S. E. (2003). Relationship between global solar radiation and sunshine duration for onne, nigeria. *Turkish Journal of Physics, 27*(2), 161-167.

Aksoy, B. (1997). Estimated monthly average global radiation for turkey and its comparison with observations. *Renewable Energy, 10*(4), 625-633.

Almorox, J., & Hontoria, C. (2004). Global solar radiation estimation using sunshine duration in spain. *Energy Conversion and Management, 45*(9), 1529-1535.

Alsaad, M. (1990). Characteristic distribution of global solar radiation for amman, jordan. *Solar & Wind Technology, 7*(2-3), 261-266.

Amrouche, B., & Le Pivert, X. (2014). Artificial neural network based daily local forecasting for global solar radiation. *Applied Energy, 130*, 333-341. doi:http://doi.org/10.1016/j.apenergy.2014.05.055

Angstrom, A. (1924). Solar and terrestrial radiation. report to the international commission for solar research on actinometric investigations of solar and atmospheric radiation. *Quarterly Journal of the Royal Meteorological Society, 50*(210), 121-126.

Antonanzas-Torres, F., Cañizares, F., & Perpiñán, O. (2013). Comparative assessment of global irradiation from a satellite estimate model (CM SAF) and on-ground measurements (SIAR): A spanish case study. *Renewable and Sustainable Energy Reviews, 21*, 248-261. doi:http://doi.org/10.1016/j.rser.2012.12.033

Aras, H., Balli, O., & Hepbasli, A. (2006). Estimating the horizontal diffuse solar radiation over the central anatolia region of turkey. *Energy Conversion and Management, 47*(15–16), 2240-2249. doi:http://dx.doi.org/10.1016/j.enconman.2005.11.024

Asif, M., & Muneer, T. (2007). Energy supply, its demand and security issues for developed and emerging economies. *Renewable and Sustainable Energy Reviews, 11*(7), 1388-1413. doi:http://dx.doi.org/10.1016/j.rser.2005.12.004

Badescu, V. (2008). *Modeling solar radiation at the earth surface* Springer-Verlag Berlin Heidelberg.

Bahel, V., Bakhsh, H., & Srinivasan, R. (1987). A correlation for estimation of global solar radiation. *Energy, 12*(2), 131-135.

Bahel, V., Srinivasan, R., & Bakhsh, H. (1986). Solar radiation for dhahran, saudi arabia. *Energy, 11*(10), 985-989.

Bakirci, K. (2009). Models of solar radiation with hours of bright sunshine: A review. *Renewable and Sustainable Energy Reviews, 13*(9), 2580-2588. doi:http://dx.doi.org/10.1016/j.rser.2009.07.011

Barbaro, S., Cannata, G., Coppolino, S., Leone, C., & Sinagra, E. (1981). Diffuse solar radiation statistics for italy. *Solar Energy, 26*(5), 429-435.

Bartoli, B., Cuomo, V., Amato, U., Barone, G., & Mattarelli, P. (1982). Diffuse and beam components of daily global radiation in genova and macerata. *Solar Energy, 28*(4), 307-311.

Basalla, G. (1980). 4 - energy and civilization. In C. Starr, , & P. C. Ritterbush (Eds.), *Science, technology and the human prospect* (pp. 39-52) Pergamon. doi:http://doi.org/10.1016/B978-0-08-024650-5.50009-4

Benson, R., Paris, M., Sherry, J., & Justus, C. (1984). Estimation of daily and monthly direct, diffuse and global solar radiation from sunshine duration measurements. *Solar Energy, 32*(4), 523-535.

Boland, J., Scott, L., & Luther, M. (2001). Modelling the diffuse fraction of global solar radiation on a horizontal surface. *Environmetrics, 12*(2), 103-116.

Boland, J., Huang, J., & Ridley, B. (2013). Decomposing global solar radiation into its direct and diffuse components. *Renewable and Sustainable Energy Reviews, 28*, 749-756. doi:http://dx.doi.org/10.1016/j.rser.2013.08.023

Bortolini, M., Gamberi, M., Graziani, A., Manzini, R., & Mora, C. (2013). Multi-location model for the estimation of the horizontal daily diffuse fraction of solar radiation in europe. *Energy Conversion and Management, 67*, 208-216. doi:http://dx.doi.org/10.1016/j.enconman.2012.11.008

BP statistical review of world energy. (2016). Retrieved from https://www.bp.com/content/dam/bp/pdf/energy-economics/statistical-review-2016/bp-statistical-review-of-world-energy-2016-full-report.pdf

Cano, D., Monget, J. M., Albuisson, M., Guillard, H., Regas, N., & Wald, L. (1986). *A method for the determination of the global solar radiation from meteorological satellite data* doi:http://dx.doi.org/10.1016/0038-092X(86)90104-0

Chandrasekaran, J., & Kumar, S. (1994). Hourly diffuse fraction correlation at a tropical location. *Solar Energy, 53*(6), 505-510.

Chegaar, M., & Chibani, A. (2001). Global solar radiation estimation in algeria. *Energy Conversion and Management, 42*(8), 967-973.

Choudhury, N. (1963). Solar radiation at new delhi. *Solar Energy, 7*(2), 44-52.

Climate change and global warming introduction. (2015). Retrieved from http://www.globalissues.org/article/233/climate-change-and-global-warming-introduction

Climate change: How do we know. (2017). Retrieved from https://climate.nasa.gov/evidence/

CO2 emissions from fuel combustion highlights 2016. (2016). Retrieved from http://www.iea.org/publications/freepublications/publication/co2-emissions-from-fuel-combustion-highlights-2016.html

Collares-Pereira, M., & Rabl, A. (1979). The average distribution of solar radiation-correlations between diffuse and hemispherical and between daily and hourly insolation values. *Solar Energy, 22*(2), 155-164.

de Miguel, A., Bilbao, J., Aguiar, R., Kambezidis, H., & Negro, E. (2001). Diffuse solar irradiation model evaluation in the north mediterranean belt area. *Solar Energy, 70*(2), 143-153. doi:http://dx.doi.org/10.1016/S0038-092X(00)00135-3

Despotovic, M., Nedic, V., Despotovic, D., & Cvetanovic, S. (2016). Evaluation of empirical models for predicting monthly mean horizontal diffuse solar radiation. *Renewable and Sustainable Energy Reviews, 56*, 246-260. doi:http://dx.doi.org/10.1016/j.rser.2015.11.058

Dincer, I. (2000). Renewable energy and sustainable development: A crucial review. *Renewable and Sustainable Energy Reviews, 4*(2), 157-175. doi:http://dx.doi.org/10.1016/S1364-0321(99)00011-8

Dincer, I., & Zamfirescu, C. (2014). Chapter 2 - energy, environment, and sustainable development. In I. Dincer, & C. Zamfirescu (Eds.), *Advanced power generation systems* (pp. 55-93). Boston: Elsevier. doi:http://dx.doi.org/10.1016/B978-0-12-383860-5.00002-X

Drummond, A. (1956). On the measurement of sky radiation. *Archiv Für Meteorologie, Geophysik Und Bioklimatologie, Serie B, 7*(3-4), 413-436.

Duffie, J., & Beckman, W. (1991). Solar engineering of solar processes.

Earth observatory. (2014). Retrieved from https://earthobservatory.nasa.gov/Features/WorldOfChange/decadaltemp.php

Ediger, V. Ş, Akar, S., & Uğurlu, B. (2006). Forecasting production of fossil fuel sources in turkey using a comparative regression and ARIMA model. *Energy Policy, 34*(18), 3836-3846.

Elhadidy, M., & Abdel-Nabi, D. (1991). Diffuse fraction of daily global radiation at dhahran, saudi arabia. *Solar Energy, 46*(2), 89-95.

El-Sebaii, A. A., Al-Hazmi, F. S., Al-Ghamdi, A. A., & Yaghmour, S. J. (2010). Global, direct and diffuse solar radiation on horizontal and tilted surfaces in jeddah, saudi arabia. *Applied Energy, 87*(2), 568-576. doi:http://dx.doi.org/10.1016/j.apenergy.2009.06.032

El-Sebaii, A. A., & Trabea, A. A. (2003). Estimation of horizontal diffuse solar radiation in egypt. *Energy Conversion and Management, 44*(15), 2471-2482. doi:http://dx.doi.org/10.1016/S0196-8904(03)00004-9

Energy, climate change & environment. (2016). Retrieved from http://www.iea.org/publications/freepublications/publication/ECCE2016.pdf

Erbs, D., Klein, S., & Duffie, J. (1982). Estimation of the diffuse radiation fraction for hourly, daily and monthly-average global radiation. *Solar Energy, 28*(4), 293-302.

Furlan, C., de Oliveira, A. P., Soares, J., Codato, G., & Escobedo, J. F. (2012). The role of clouds in improving the regression model for hourly values of diffuse solar radiation. *Applied Energy, 92*, 240-254. doi:http://dx.doi.org/10.1016/j.apenergy.2011.10.032

Gopinathan, K. (1988). Empirical correlations for diffuse solar irradiation. *Solar Energy, 40*(4), 369-370.

Gopinathan, K., & Soler, A. (1992). A sunshine dependent global insolation model for latitudes between 60 N and 70 N. *Renewable Energy, 2*(4-5), 401-404.

Gueymard, C. A., & Myers, D. R. (2008). Solar radiation measurement: Progress in radiometry for improved modeling. *Modeling solar radiation at the earth's surface* (pp. 1-27) Springer.

Hawas, M., & Muneer, T. (1984). Study of diffuse and global radiation characteristics in india. *Energy Conversion and Management, 24*(2), 143-149.

Hawlader, M. (1984). Diffuse, global and extra-terrestrial solar radiation for singapore. *International Journal of Ambient Energy, 5*(1), 31-38.

Hay, J. E. (1993). *Satellite based estimates of solar irradiance at the earth's surface—I. modelling approaches* doi:http://dx.doi.org/10.1016/0960-1481(93)90105-P

Hondo, H. (2005). Life cycle GHG emission analysis of power generation systems: Japanese case. *Energy, 30*(11–12), 2042-2056. doi:http://doi.org/10.1016/j.energy.2004.07.020

Ibrahim, S. M. (1985). Diffuse solar radiation in cairo, egypt. *Energy Conversion and Management, 25*(1), 69-72.

International energy outlook 2016. (2016). Retrieved from https://www.eia.gov/outlooks/ieo/

Iqbal, M. (1979). A study of canadian diffuse and total solar radiation data—I monthly average daily horizontal radiation. *Solar Energy, 22*(1), 81-86.

Iqbal, M. (2012). *An introduction to solar radiation* Elsevier.

Jäger-Waldau, A. (2007). Photovoltaics and renewable energies in europe. *Renewable and Sustainable Energy Reviews, 11*(7), 1414-1437. doi:http://dx.doi.org/10.1016/j.rser.2005.11.001

Jain, P. (1986). Global irradiation estimation for italian locations. *Solar & Wind Technology, 3*(4), 323-328.

Jain, P. (1990). A model for diffuse and global irradiation on horizontal surfaces. *Solar Energy, 45*(5), 301-308.

Jain, S., & Jain, P. (1988). A comparison of the angstrom-type correlations and the estimation of monthly average daily global irradiation. *Solar Energy, 40*(2), 93-98.

Johansson, T. B., McCormick, K., Nei, L., & Turkenburg, W. (2004). The potentials of renewable energy. International Conference for Renewable Energies, Bonn.

Karatasou, S., Santamouris, M., & Geros, V. (2003). Analysis of experimental data on diffuse solar radiation in athens, greece, for building applications. *International Journal of Sustainable Energy, 23*(1-2), 1-11.

Kaygusuz, K., & Ayhan, T. (1999). Analysis of solar radiation data for trabzon, turkey. *Energy Conversion and Management, 40*(5), 545-556.

Khadse, A., Qayyumi, M., Mahajani, S., & Aghalayam, P. (2007). Underground coal gasification: A new clean coal utilization technique for india. *Energy, 32*(11), 2061-2071.

Khogali, A., Ramadan, M., Ali, Z., & Fattah, Y. (1983). Global and diffuse solar irradiance in yemen (YAR). *Solar Energy, 31*(1), 55-62.

Khorasanizadeh, H., Mohammadi, K., & Goudarzi, N. (2016). Prediction of horizontal diffuse solar radiation using clearness index based empirical models; A case study. *International*

Journal of Hydrogen Energy, *41*(47), 21888-21898. doi:http://dx.doi.org/10.1016/j.ijhydene.2016.09.198

Klein, S. (1977). Calculation of monthly average insolation on tilted surfaces. *Solar Energy*, *19*(4), 325-329.

Linares-Rodríguez, A., Ruiz-Arias, J. A., Pozo-Vázquez, D., & Tovar-Pescador, J. (2011). Generation of synthetic daily global solar radiation data based on ERA-interim reanalysis and artificial neural networks. *Energy*, *36*(8), 5356-5365. doi:http://doi.org/10.1016/j.energy.2011.06.044

Liu, B. Y. H., & Jordan, R. C. (1960). The interrelationship and characteristic distribution of direct, diffuse and total solar radiation doi:http://dx.doi.org/10.1016/0038-092X(60)90062-1

Lloyd PB (1982) A Study of Some Empirical Relations Described by Liu and Jordan. Report no. 333, *Solar Energy Unit*, University College, Cardiff

Louche, A., Notton, G., Poggi, P., & Simonnot, G. (1991). Correlations for direct normal and global horizontal irradiation on a french mediterranean site. *Solar Energy*, *46*(4), 261-266.

Luhanga, P., & Andringa, J. (1990). Characteristics of solar radiation at sebele, gaborone, botswana. *Solar Energy*, *44*(2), 77-81.

Lund, H. (2007). Renewable energy strategies for sustainable development. *Energy*, *32*(6), 912-919. doi:http://dx.doi.org/10.1016/j.energy.2006.10.017

Mani, A., & Chacko, O. (1973). Solar radiation climate of india. *Solar Energy*, *14*(2), 139-156.

Mani A, Rangarajan S (1983) Techniques for the precise estimation of hourly values of global, diffuse and direct solar radiation. Solar Energy 31:577

Midilli, A., Dincer, I., & Ay, M. (2006). Green energy strategies for sustainable development. *Energy Policy*, *34*(18), 3623-3633. doi:http://dx.doi.org/10.1016/j.enpol.2005.08.003

Muneer, T., & Hawas, M. (1984). Correlation between daily diffuse and global radiation for india. *Energy Conversion and Management*, *24*(2), 151-154.

Muneer, T., & Saluja, G. (1985). A brief review of models for computing solar radiation on inclined surfaces. *Energy Conversion and Management*, *25*(4), 443-458.

Muneer, T., & Saluja, G. (1986). Correlation between hourly diffuse and global solar irradiation for the UK. *Building Services Engineering Research and Technology, 7*(1), 37-43.

Muneer T, Saluja GS (1996) Correlation between hourly diffuse and global solar irradiation for the UK. Building Services Engineering Research &Technology 7, 1

Muneer, T. (2004). *Solar radiation and daylight models* 1997, 2004, Elsevier Ltd.

Muneer, T. (2010). Sustainable energy for world economies. *F. Barbir and S. Ulgiati (Eds.), Energy Options Impact on Regional Security, Springer Science + Business Media B. V.,* , 123. doi:10.1007/978-90-481-9565-7_6

Muneer, T., & Tham, Y. W. (2013). In Myer Kutz (Ed.), *Handbook of measurement in science and engineering* (1st ed.) 2013 JohnWiley & Sons.

Muneer, T., Younes, S., & Munawwar, S. (2007). Discourses on solar radiation modeling. *Renewable and Sustainable Energy Reviews, 11*(4), 551-602. doi:http://dx.doi.org/10.1016/j.rser.2005.05.006

Muneer, T., Asif, M., & Munawwar, S. (2005). Sustainable production of solar electricity with particular reference to the indian economy. *Renewable and Sustainable Energy Reviews, 9*(5), 444-473. doi:http://dx.doi.org/10.1016/j.rser.2004.03.004

National renewable energy laboratory. (2016). Retrieved from http://rredc.nrel.gov/solar/pubs/shining/chap5.html

NASA (2017). Retrieved from http://eosweb.larc.nasa.gov/cgi-bin/sse/retscreen.cgi?

email¼rets@nrcan.gc.ca.

Newland, F. (1989). A study of solar radiation models for the coastal region of south china. *Solar Energy, 43*(4), 227-235.

Olatomiwa, L., Mekhilef, S., Shamshirband, S., Mohammadi, K., Petković, D., & Sudheer, C. (2015). A support vector machine–firefly algorithm-based model for global solar radiation prediction. *Solar Energy, 115*, 632-644. doi:http://doi.org/10.1016/j.solener.2015.03.015

Olatomiwa, L., Mekhilef, S., Shamshirband, S., & Petković, D. (2015). Adaptive neuro-fuzzy approach for solar radiation prediction in nigeria. *Renewable and Sustainable Energy Reviews, 51*, 1784-1791. doi:http://doi.org/10.1016/j.rser.2015.05.068

Oliveira, A. P., Escobedo, J. F., Machado, A. J., & Soares, J. (2002). Correlation models of diffuse solar-radiation applied to the city of sao paulo, brazil. *Applied Energy, 71*(1), 59-73.

Omni instruments. (2015). Retrieved from http://www.omniinstruments.co.uk/cm121-shadow-ring.html

Orgill, J. F., & Hollands, K. G. T. (1977). *Correlation equation for hourly diffuse radiation on a horizontal surface* doi:http://dx.doi.org/10.1016/0038-092X(77)90006-8

Page, J. (1961). The estimation of monthly mean values of daily total short-wave radiation on vertical surfaces from sunshine records for latitude 40 N-40 S. Paper presented at the *UK Conf. on New Sources of Energy, Paper no. S/98,*

Page, J. (1967). The estimation of monthly mean values of daily total short wave radiation on vertical and inclined surfaces from sunshine records 40S-40N. Paper presented at the *Proc. of UN New Sources of Energy (Conference Paper) Rome, , 4* 378-390.

Park, J., Das, A., & Park, J. (2015). A new approach to estimate the spatial distribution of solar radiation using topographic factor and sunshine duration in south korea. *Energy Conversion and Management, 101*, 30-39. doi:http://doi.org/10.1016/j.enconman.2015.04.021

Paulescu, E., & Blaga, R. (2016). Regression models for hourly diffuse solar radiation. *Solar Energy, 125*, 111-124. doi:http://dx.doi.org/10.1016/j.solener.2015.11.044

Population growth by country. (2016). Retrieved from http://www.worldatlas.com/articles/the-20-countries-with-the-highest-population-growth.html

Rao, C. N., Bradley, W. A., & Lee, T. Y. (1984). The diffuse component of the daily global solar irradiation at corvallis, oregon (USA). *Solar Energy, 32*(5), 637-641.

Rapacious consumerism and climate change. (2016). Retrieved from http://www.counterpunch.org/2016/12/20/rapacious-consumerism-and-climate-change/

Reindl, D. T., Beckman, W. A., & Duffie, J. A. (1990). *Diffuse fraction correlations* doi:http://dx.doi.org/10.1016/0038-092X(90)90060-P

Renewables 2016 global status report. (2016). Retrieved from http://www.ren21.net/wp-content/uploads/2016/10/REN21_GSR2016_FullReport_en_11.pdf

Ruth, D., & Chant, R. (1976). The relationship of diffuse radiation to total radiation in canada. *Solar Energy, 18*(2), 153-154.

Sackett, J. I. (2001). The future of nuclear energy. *Fuel Processing Technology, 71*(1), 197-204.

Salameh, M. G. (2003). Can renewable and unconventional energy sources bridge the global energy gap in the 21st century? *Applied Energy, 75*(1), 33-42.

Saluja, G., Muneer, T., & Smith, M. (1988). Methods for estimating solar irradiation on a horizontal surface. *International Journal of Ambient Energy, 9*(2), 59-74.

Samuel, T. (1991). Estimation of global radiation for sri lanka. *Solar Energy, 47*(5), 333-337.

Schleicher-Tappeser, R. (2012). How renewables will change electricity markets in the next five years. *Energy Policy, 48*, 64-75. doi:http://dx.doi.org/10.1016/j.enpol.2012.04.042

Shafiee, S., & Topal, E. (2009). When will fossil fuel reserves be diminished? *Energy Policy, 37*(1), 181-189. doi:http://dx.doi.org/10.1016/j.enpol.2008.08.016

Smil, V. (1994). Energy in world history.

Soares, J., Oliveira, A. P., Božnar, M. Z., Mlakar, P., Escobedo, J. F., & Machado, A. J. (2004). Modeling hourly diffuse solar-radiation in the city of são paulo using a neural-network technique. *Applied Energy, 79*(2), 201-214.

Solar radiation: Sunlight and more. (2016). Retrieved from http://www.solarradiation.net/

Soler, A. (1990). Monthly specific rietveld's correlations. *Solar & Wind Technology, 7*(2-3), 305-308.

Spencer, J. (1982). A comparison of methods for estimating hourly diffuse solar radiation from global solar radiation. *Solar Energy, 29*(1), 19-32.

Stanhill, G. (1966). Diffuse sky and cloud radiation in israel. *Solar Energy, 10*(2), 96-101.

Tarhan, S., & Sarı, A. (2005). Model selection for global and diffuse radiation over the central black sea (CBS) region of turkey. *Energy Conversion and Management, 46*(4), 605-613.

Taşdemiroğlu, E., & Sever, R. (1991). Estimation of monthly average, daily, horizontal diffuse radiation in turkey. *Energy, 16*(4), 787-790.

Taşdemiroğlu, E., & Sever, R. (1991). An improved correlation for estimating solar radiation from bright sunshine data for turkey. *Energy Conversion and Management, 31*(6), 599-600.

The world bank. (2016). Retrieved from http://data.worldbank.org/indicator/EG.USE.PCAP.KG.OE

The world factbook. (2016). Retrieved from https://www.cia.gov/library/publications/resources/the-world-factbook/geos/ag.html

The relationship between consumerism and global warming. (2016). Retrieved from http://www.postconsumers.com/education/consumerism-global-warming/

Thielemann, T., Schmidt, S., & Gerling, J. P. (2007). Lignite and hard coal: Energy suppliers for world needs until the year 2100—An outlook. *International Journal of Coal Geology, 72*(1), 1-14.

Tiris, M., Tiris, Ç, & Türe, İ E. (1996). Correlations of monthly-average daily global, diffuse and beam radiations with hours of bright sunshine in gebze, turkey. *Energy Conversion and Management, 37*(9), 1417-1421. doi:http://dx.doi.org/10.1016/0196-8904(95)00227-8

Total energy. (2016). Retrieved from https://www.eia.gov/totalenergy/data/monthly/#renewable

Trabea, A. (1999). Technical note a multiple linear correlation for diffuse radiation from global solar radiation and sunshine data over egypt. *Renewable Energy, 17*(3), 411-420.

Tuller, S. E. (1976). The relationship between diffuse, total and extra terrestrial solar radiation. *Solar Energy, 18*(3), 259-263.

Ulgen, K., & Ozbalta, N. (2000). Measured and estimated global radiation on horizontal surface for bornova, izmir. Paper presented at the *Proceedings of the XIIth National Thermal Science and Technical Congress. Izmit, Turkey,* 113-118.

Ulgen, K., & Hepbasli, A. (2004). Solar radiation models. part 2: Comparison and developing new models. *Energy Sources, 26*(5), 521-530.

Ulgen, K., & Hepbasli, A. (2009). Diffuse solar radiation estimation models for turkey's big cities. *Energy Conversion and Management, 50*(1), 149-156. doi:http://dx.doi.org/10.1016/j.enconman.2008.08.013

Veeran, P., & Kumar, S. (1993). Analysis of monthly average daily global radiation and monthly average sunshine duration at two tropical locations. *Renewable Energy, 3*(8), 935-939.

Wang, L., Kisi, O., Zounemat-Kermani, M., Salazar, G. A., Zhu, Z., & Gong, W. (2016). Solar radiation prediction using different techniques: Model evaluation and comparison. *Renewable and Sustainable Energy Reviews, 61*, 384-397. doi:http://dx.doi.org/10.1016/j.rser.2016.04.024

When will fossil fuels run out. (2017). Retrieved from http://www.carboncounted.co.uk/when-will-fossil-fuels-run-out.html

Whillier, A. (1956). The determination of hourly values of total solar radiation from daily summations. *Theoretical and Applied Climatology, 7*(2), 197-204.

World population prospect. (2015). Retrieved from https://esa.un.org/unpd/wpp/DataQuery/

Yildiz, M., & Oz, S. (1994). Evaluation of the solar energy potential of turkey. Paper presented at the *Proceedings of the 6th National Energy Congress*, 250-260.

Youinou, G. J. (2016). Powering sustainable low-carbon economies: Some facts and figures. *Renewable and Sustainable Energy Reviews, 53*, 1626-1633. doi:http://dx.doi.org/10.1016/j.rser.2015.08.067

Zhang, J., Zhao, L., Deng, S., Xu, W., & Zhang, Y. (2017). A critical review of the models used to estimate solar radiation. *Renewable and Sustainable Energy Reviews, 70*, 314-329. doi:http://dx.doi.org/10.1016/j.rser.2016.11.124

13. APPENDICES

13.1 ARTICLE 1: Monthly averaged-hourly solar diffuse radiation model for the UK

13.2 ARTICLE 2: Monthly-averaged hourly solar diffuse radiation models for world-wide locations

13.3 VBA CODES

Article

BUILDING SERVICES ENGINEERING RESEARCH & TECHNOLOGY

Building Serv. Eng. Res. Technol.
0(0) 1–12

DOI: 10.1177/0143624414522639
bse.sagepub.com

SAGE

Monthly averaged-hourly solar diffuse radiation model for the UK

T Muneer[1], S Etxebarria[2] and EJ Gago[2]

Abstract

Monthly-averaged daily global irradiation data are now easily available from NASA website. Using established models it is then possible to decompose the daily to averaged-hourly global irradiation. The missing link so far has been hourly averaged diffuse irradiation. In this article data was pooled from 10 UK locations to obtain a regression model to complete the above missing link. It was presently shown that the averaged-data regressions are distinctly different from previously available hour-by-hour regressions. ***Practical application***: The present work has explored a correlation between averaged-hourly diffuse and global irradiation using the diffuse ratio–clearness index envelope. Results show that a strong regression relationship is thus obtainable. The present work has therefore the potential for other similar research that may be followed up in a likewise manner.

Keywords

Solar radiation, averaged-hourly diffuse fraction, clearness index, solar diffuse radiation model

Introduction

Solar radiation data are essential for the design of building services. These data are needed for obtaining solar energy transmission through glazing and also through opaque fabric such as walls and roof.

In response to the above demand posed by industry, CIBSE provides, and is in the process of extending the work related to production of computed data sets of:

a. Hourly time series of global and diffuse illuminance with the view to obtain frequency of any given level of illuminance
b. Sol–air temperature tables for horizontal and vertical surfaces. These are produced for days that belong to 97.5th percentile when daily irradiation totals are arranged in an ascending order.
c. Monthly-average irradiation for horizontal, vertical and sloped surfaces.

In the preparation of successive editions of CIBSE Guides A,[1–6] Guide J[7] and weather data sets a long-term series of hourly global and diffuse irradiation were required.

[1]School of Engineering and Built Environment, Edinburgh Napier University, Edinburgh, UK
[2]School of Civil Engineering, University of Granada, Spain

Corresponding author:
EJ Gago, School of Civil Engineering, University of Granada, Avenida Severo Ochoa, s/n. Granada, 18071, Spain.
Email: ejadraque@ugr.es

Measurements of diffuse radiation are not always available for all locations especially within countries which cannot afford the measurement equipment and techniques involved.

Furthermore, as of year 2000, the UK Meteorological Office has stopped recording diffuse irradiation at all but two locations – Camborne (50.21 N) and Lerwick (60.15 N). Therefore, for all of the other major and minor conurbations in the UK the latter component has to be estimated from models that are based on historical records.

The new CIBSE Guide A, to be published in the year 2014, will contain solar radiation tables for 14 UK locations. The above tables will contain information on global and diffuse illuminance, irradiation totals for surfaces of various aspects and slopes, and sol–air temperatures for walls and roof. To produce these tables it is necessary to obtain horizontal-diffuse irradiation, provided global energy data are available. For the above-mentioned 14 locations within the UK it is not always possible to acquire measured diffuse irradiation data as these are seldom available. Hence, it is necessary to develop a mathematical model, built from measured data that is available for some of the above locations.

Another constraint in the present CIBSE Guide A production was that in view of costs, only averaged-hourly data were provided by the UK Meteorological Office. The models that were previously developed[8] were not for averaged-data. Rather, they were for use for hour-by-hour records. Hence the previous work[8] was found to be redundant for the present production of CIBSE Guide A.

This article detailed the prior work that has been undertaken in this respect and then progresses to report newer, averaged-hourly diffuse irradiation models. The use and justification of such models is also presented.

The need for diffuse irradiation models

In addition to their use in other disciplines such as agriculture, there are a large number of engineering applications where, beam and diffuse irradiation hourly or sub-hourly are required. The two components are used to estimate, among other things, slope radiation. A brief list of those applications may be drawn thus:

- Solar transmission through building fenestration
- Daylight transmission through building fenestration
- Sol–air temperature estimation for opaque building fabric
- Solar water heating design and product assessment
- Solar PV design and product assessment

For above-mentioned items (a) and (b), in 'Introduction' section, an hour-by-hour diffuse irradiation model is required and previous research has made such work available for the UK.[9,10]

In the following section some of the above work is reviewed.

For generation of tables related to item (c) in 'Introduction' section, new work had to be undertaken to develop monthly-averaged hourly regressions and that is the main subject of this article.

A typical scatter plot for diffuse ratio (ratio of hourly diffuse to global irradiation) – clearness index (ratio of global to extraterrestrial irradiation) relationship is shown in Figure 1. The diffuse ratio is represented by k and the clearness index by k_t.

This plot, obtained from hour-by-hour data provided by the UK Meteorological Office for the period 1981–1983 displays a convex shape. The regressed curve reported by Muneer and Saluja[8] is

$$\frac{I_D}{I_G} = k = a_0 + a_1 k_t + a_2 k_t^2 + a_3 k_t^3; k_t > 0.2 \quad (1)$$

Values of a coefficients are different for each location (Easthampstead, Aberporth, Aldergrove, Eskdalemuir, Lerwick, United Kingdom).

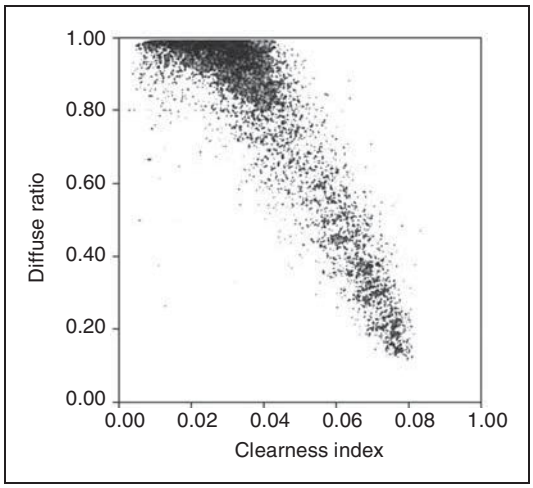

Figure 1. Hourly diffuse ratio versus clearness index for the UK.

Figure 2(a) and (b) respectively show the regressed curves for locations in UK and other countries. Three points are worth mentioning:

(i) For all locations the k-k_t relationship displays a convex profile, and
(ii) For the UK as a whole, it is possible to build a single curvilinear relationship between k and k_t; however,
(iii) A single curve cannot be constructed to include world-wide locations.

In section 'Monthly-averaged, $\bar{k}-\overline{k_t}$ relationship' a $\bar{k}-\overline{k_t}$ relationship will be developed based on monthly-averaged hourly data. A justification shall also be stated for such work.

Previous work

As mentioned in the 'Introduction' section, this work attempts to present a new model that relates averaged-diffuse irradiation to its global counterpart. All previous work has been related to regressions that involve hour-by-hour energy quantities. In the following paragraphs a brief review of the older work is carried out as the basic mathematical formulation is unchanged, i.e. diffuse ratio is regressed against clearness index.

Liu and Jordan[11] were pioneers in correlating the relationship between diffuse and global radiation on a horizontal surface; however, the original correlation of Liu and Jordan was developed for daily-not hourly values.

Many research teams have since developed hourly regressions that primarily relate k, the diffuse ratio (diffuse to global irradiation) to k_t, the clearness index (global to extra-terrestrial irradiation ratio) (see Table 1).

Orgill and Hollands,[12] from information gathered in Toronto, Canada, proposed the linear model for the diffuse ratio (k) according to the hourly clearness index (k_t). This study was based upon 4 years of data for Toronto in Canada. The diffuse radiation was measured with a shadow-band pyranometer.

Erbs et al.[13] followed the procedure of Orgill and Hollands to develop a correlation for the US locations (Fort Hood, TX; Maynard, MA; Raleigh, NC; Livermore, CA) with a latitude range of 31–42°N. Pyroheliometric data was used by them in which diffuse radiation was obtained via subtraction of direct radiation from global, measured with a pyranometer.

Reindl et al.[14] using data respectively from five European and North American locations analysed the influence of commonly measured climatic variables on the diffuse fraction and correlating the significant variables to reduce the standard error of Liu and Jordan[11] type models. The new correlation reduced the composite residual sum of squares by 14.4% when compared to k_t, correlation derived from the same data set. The reduced form of the correlation reduced the composite residual sum squares by 9.2%. When an independent data set is used, the new correlation reduced the residual sum of squares by 26% compared to the Erbs' correlation.

Hawlader[15] using data from a tropical site in Singapore derived the second-order polynomial correlation. Equations were developed to estimate diffuse fraction of the hourly, daily and monthly global insolation on a

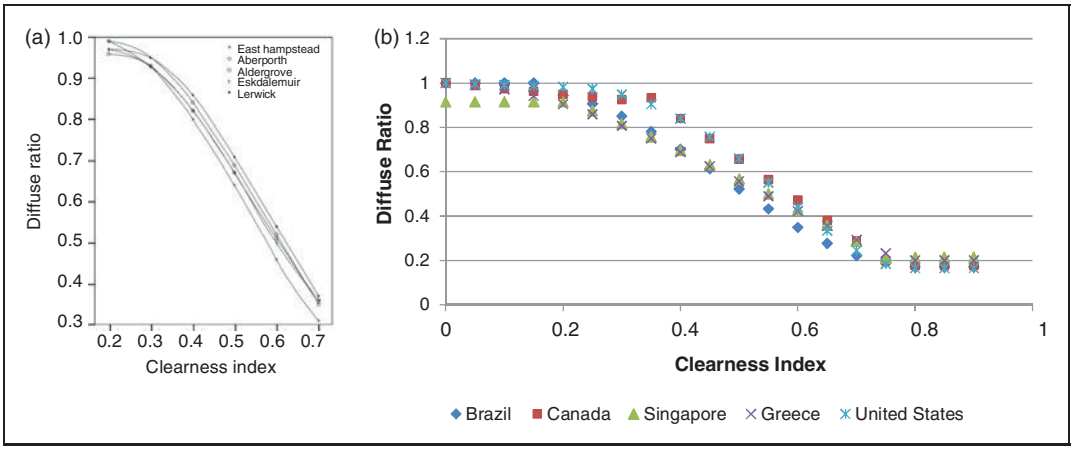

Figure 2. (a) Average hourly diffuse ratio versus clearness index for five locations in the UK; (b) average hourly diffuse ratio (*y*-axis) versus clearness index (*x*-axis) for five world locations.

horizontal surface. The hourly correlation equations showed a fairly similar trend to that of Orgill and Hollands[12] and Spencer,[16] supporting their views on latitude dependence.

Chandrasekaran and Kumar[17] using data from a tropical environment in Madras, India, derived a fourth-order polynomial correlation. These correlations were compared to those developed by Orgill and Hollands,[12] Erbs et al.[13] and Reindl et al.,[14] which were obtained from data of temperate locations. The comparison was performed in terms of standard deviation and relative standard deviation. The results indicated that the proposed correlations are better. The best fits were obtained when the seasonal effects were taken into account. It is also showed that the hourly diffuse fraction is higher in the tropics than in temperate regions, with a substantially significant diffuse fraction during the rainy season when the hourly clearness index is high.

Boland et al.[18] developed a model with data from a station in Victoria, Australia. Another model was also developed for 15-minute data values in order to ascertain if the smoothing generated by using hourly data makes a significant difference to overall results. A relevant finding was that the same model can be used for both 15-minute and hourly data.

Miguel et al.[19] used an assembled data set from several countries in the North Mediterranean Belt area, and yielded a third-order polynomial for hourly diffuse fraction correlations. The performed data analysis showed that under overcast-sky conditions (low values of k) a large portion of the incoming radiation is scattered by the clouds in the atmosphere resulting in a large diffuse fraction. The significance of low solar altitudes in the diffuse solar fraction increases under clear sky (high values of k). The Liu and Jordan[11] model was recommended to calculate hourly diffuse from daily diffuse values since it reproduces the observed data series extremely well.

Oliveira et al.[20] using data from a tropical Sao Paolo site, Brazil, proposed a fourth-order polynomial correlation. It was deduced that the overall characteristics of the diffuse-fraction correlation curves and their seasonal variations are similar to other places with equivalent latitude for hourly, daily and monthly values.[13]

Karatasou et al.[21] based on data from Athens, Greece, proposed a third-order polynomial correlation. The goal of this study was to reduce the standard error of the current Liu and Jordan[11] type correlations, when used for Athens location.

Table 1. Correlations for k (ratio of hourly diffuse to global irradiation) and k_t (ratio of global to extraterrestrial irradiation).

Investigators	Correlation equation	Number of locations	Amount of data used (year)
Orgill and Hollands[12]	$k = 1.0 - 0.249k_t$ for $k_t < 0.35$ $k = 1.157 - 1.84k_t$ for $0.35 \leq k_t \leq 0.75$ $k = 0.177$ for $k_t < 0.75$	1	4
Erbs et al.[13]	$k = 1.0 - 0.099k_t$ for $k_t < 0.22$ $k = 0.9511 - 0.160k_t + 4.388k_t^2 - 16.638k_t^3 + 12.336k_t^4$ for $0.22 < k_t \leq 0.80$ $k = 0.165$ for $k_t > 0.80$	4	2
Reindl et al.[14]	$k = 1.02 - 0.249k_t$ for $k_t < 0.3$ $k = 1.45 - 1.67k_t$ for $0.3 < k_t < 0.78$ $k = 0.147k_t$ for $k_t \geq 0.78$	5	2.5
Hawlader[15]	$k = 1.135 - 0.9422k_t - 0.3878k_t^2$ for $0.225 < k_t < 0.775$ $k = 0.915$ for $k_t \leq 0.225$ $k = 0.215$ for $k_t \geq 0.775$	1	6
Spencer[16]	$k = a_3 - b_3k_t$ for $0.35 \leq k_t \leq 0.75$	12	3
Chandrasekaran and Kumar[17]	$k = 0.9686 - 0.1325k_t - 1.4183k_t^2 + 10.1862k_t^3 + 8.3733k_t^4$ for $0.24 < k_t \leq 0.80$ $k = 1.0086 - 0.178k_t$ for $k_t \leq 0.24$ $k = 0.197$ for $k_t > 0.80$	1	5
Boland et al.[18]	$k = 1/[1 + \exp(-5.0033 + 8.6025k_t)]$	4	67 days
Miguel et al.[19]	$k = 0.724 + 2.738k_t - 8.32k_t^2 + 4.967k_t^3$ for $0.21 < k_t \leq 0.76$ $k = 0.995 - 0.081k_t$ for $k_t \leq 0.21$ $k = 0.18$ for $k_t > 0.76$	11	22
Oliveira et al.[20]	$k = 0.97 + 0.8k_t - 3.0k_t^2 - 3.1k_t^3 + 5.2k_t^4$ for $0.17 < k_t < 0.75$ $k = 1.0$ for $k_t \leq 0.17$ $k = 0.17$ for $k_t > 0.75$	1	5
Karatasou et al.[21]	$k = 0.9995 - 0.05k_t - 2.4156k_t^2 + 1.4926k_t^3$ for $0 < k_t \leq 0.78$ $k = 0.20$ for $k_t > 0.78$	1	2
Soares et al.[22]	$k = 0.90 + 1.1k_t - 4.5k_t^2 + 0.01k_t^3 + 3.14k_t^4$ for $0.17 < k_t < 0.75$ $k = 1.0$ for $k_t \leq 0.17$ $k = 0.17$ for $k_t > 0.75$	1	3

Soares et al.[22] using the same data set as Oliveira et al.,[20] established a synthetic fourth-order polynomial correlation by means of a neural network technique. It was found that the inclusion of the atmospheric long-wave radiation as input improves the neural-network performance. On the other hand traditional meteorological parameters, like air temperature and atmospheric pressure, are not as important as long-wave radiation which acts as a surrogate for cloud-cover information on the regional scale. An objective evaluation showed that the diffuse solar radiation is better reproduced by neural network synthetic series than by a correlation model.

Monthly-averaged, $\bar{k} - \overline{k_t}$ relationship

The previous section reviewed the $k - k_t$ relationship that was based on hour-by-hour data. It was also shown that during the past 40 years

Table 2. Climatic data for Easthampstead (Bracknell) with the NASA reported irradiation data and averaged measured data for the period 1981–1983.

	Unit	Climate data location							
Latitude	°N	51.42							
Longitude	°E	−0.75							
Elevation	m	58.00							
Heating design temperature	°C	−1.74							
Cooling design temperature	°C	22.96							
Earth temperature amplitude	°C	14.35							
Frost days at site	day	37.00							
Month	Air temperature	Relative humidity	Daily solar radiation - horizontal	Atmospheric pressure	Wind speed	Earth temperature	Heating degree-days	Cooling degree-days	Average measured radiation
	°C	%	kWh/m^2/day	kPa	m/s	°C	°C-d	°C-d	kWh/m^2/day
January	4.2	83.90	0.77	100.8	6.3	3.1	426	1	0.71
February	4.3	80.20	1.39	101.0	5.8	3.6	380	1	1.28
March	6.4	76.80	2.34	100.9	6.0	6.2	353	4	2.18
April	8.6	69.80	3.59	100.7	5.1	9.1	279	21	3.55
May	12.7	64.00	4.57	100.9	4.7	13.8	168	92	4.11
June	16.1	60.80	4.84	100.9	4.4	17.7	75	177	4.86
July	18.6	60.20	4.80	100.9	4.4	20.4	25	261	4.77
August	18.6	61.20	4.23	100.9	4.3	20.3	26	264	4.23
September	15.5	66.30	2.86	100.9	5.0	16.5	83	164	2.85
October	11.7	74.10	1.73	100.7	5.5	11.5	191	73	1.57
November	7.3	83.20	0.96	100.7	5.9	6.4	318	11	0.80
December	4.9	85.00	0.60	100.8	6.1	3.8	404	3	0.60
Annual	10.7	72.10	2.72	100.8	5.3	11.0	2728	1072	
Measured at (m)					10.0	0.0			

such regressions have been presented for very many regions of the world. It is, however, interesting to note that there is a dearth of such knowledge for diffuse ratio–clearness index regressions that are based on averaged data.

The need to produce $\bar{k} - \overline{k_t}$ relationship presently stemmed from three factors:

(i) In the production of the latest version of CIBSE Guide A (2014), in view of the prohibitive cost of measured data only monthly-averaged hourly records were obtained by the CIBSE Solar Data Task Group. These data, obtained for 14 UK locations, are of very high quality as shall be demonstrated in the following section.

(ii) As mentioned earlier that, as of year 2000, all Meteorological Office stations, with the exception of Camborne and Lerwick, have ceased to record diffuse component.

(iii) Through the work of NASA[23] it is now possible to obtain daily-averaged irradiation data for virtually any location in the world. A sample table of climatic data for Easthampstead (Bracknell) is provided in Table 2. This information was downloaded

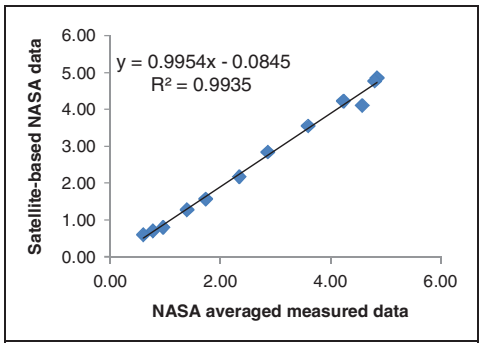

Figure 3. Comparison between NASA reported irradiation data and ground-based averaged measured data for Bracknell.

Table 3. The 10 locations that were presently investigated.

	Latitude	Longitude	Period of observation
Camborne	50.21	5.30	1981–1995
Crawley	51.11	0.19	1980–1992
Bracknell	51.42	0.75	1992–1994
London WCB	51.52	0.11	1975–1995
Aberporth	52.13	4.55	1975–1995
Hemsby	52.70	1.69	1981–1995
Finningley	53.48	0.98	1982–1995
Aughton	53.54	2.91	1981–1995
Aldergrove	54.65	−6.24	1968–1995
Stornoway	58.22	6.39	1982–1995

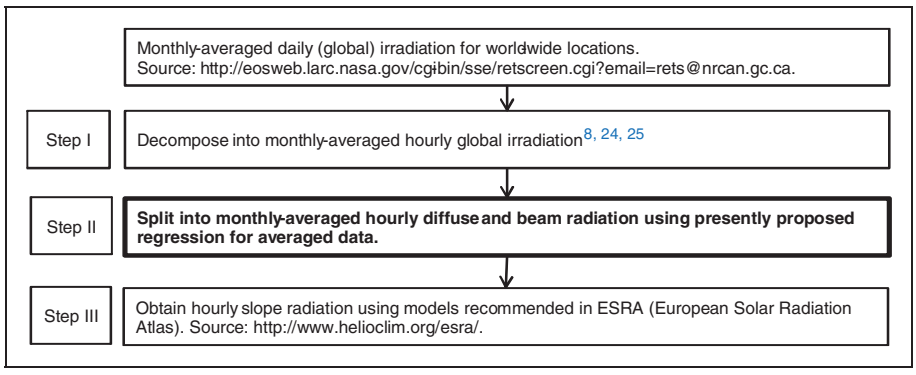

Figure 4. Computational chain.

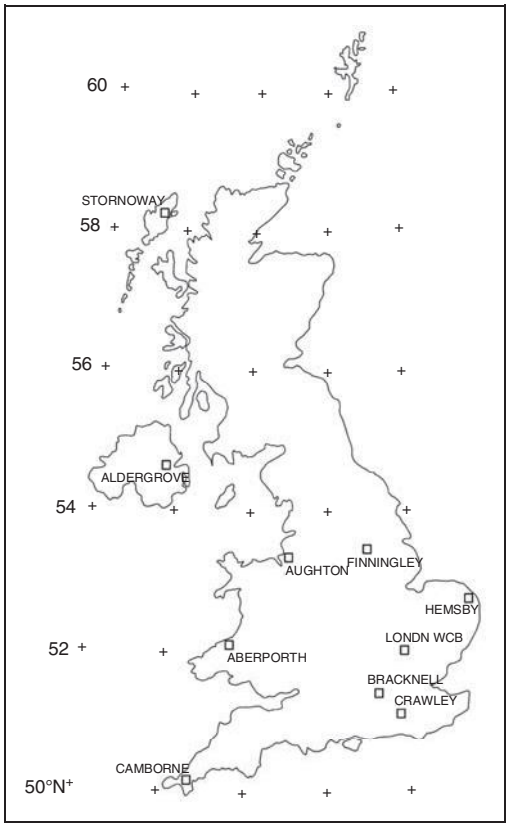

Figure 5. UK map showing the 10 locations that are the basis of present work.

from the above-mentioned NASA website. Note that the NASA reported irradiation data were compared against averaged measured data for the period 1981–1983 (three complete years) (see Figure 3). The statistics within the latter figure shows that there is a close concordance between the satellite-based NASA irradiation and the UK Meteorological Office measured data set.

It is therefore possible to construct a three-step computational chain that links with the NASA data that now exists in public domain to obtain all manner of solar energy calculations that require hourly horizontal and slope, global and diffuse irradiation. Figure 4 shows the above mentioned computational chain.

Analysis and discussion

The data used for this study were obtained from UK Meteorological Office. Ten locations were chosen which are detailed in Table 3 and Figure 5. Data consisted of hourly global and

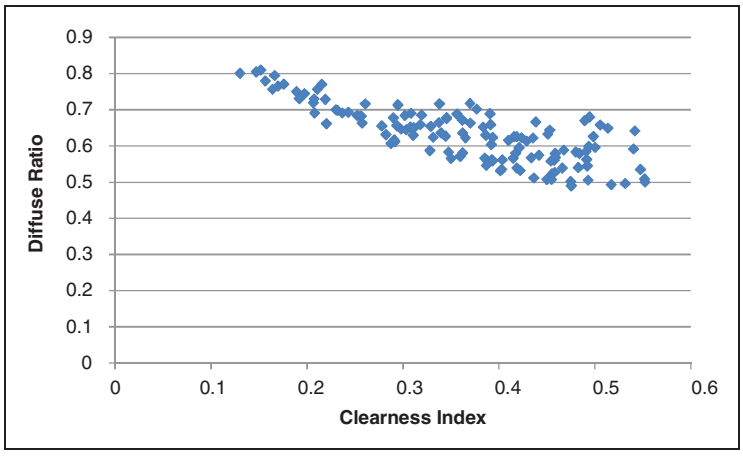

Figure 6. Monthly-averaged hourly diffuse ratio (*y*-axis) versus clearness index (*x*-axis) for Bracknell.

diffuse irradiation values for several years for each location, covering the most of the range of latitude for the country. The location names have been arranged in increasing order of latitude.

Monthly-averaged hourly values were calculated for the global and diffuse radiation considering the data period for each location.

For each of them, the diffuse ratio (k) and the clearness index (k_t) for every hour in each month

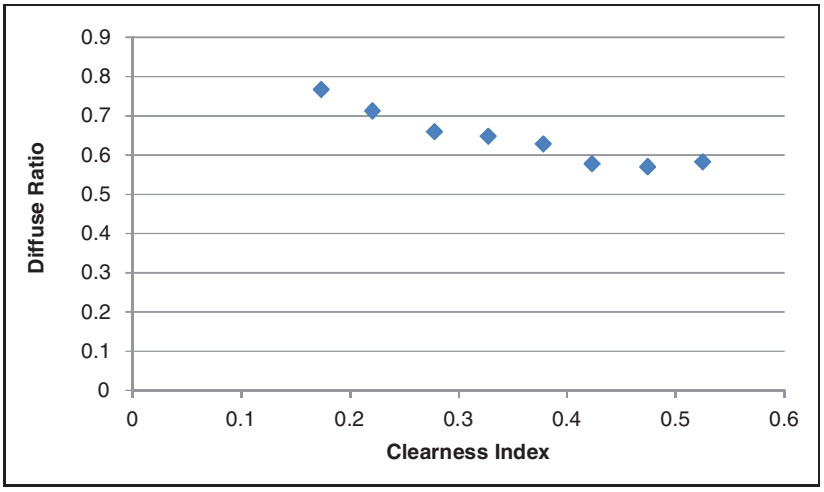

Figure 7. Averaged values of diffuse ratio (*y*-axis) versus clearness index (*x*-axis) for Bracknell.

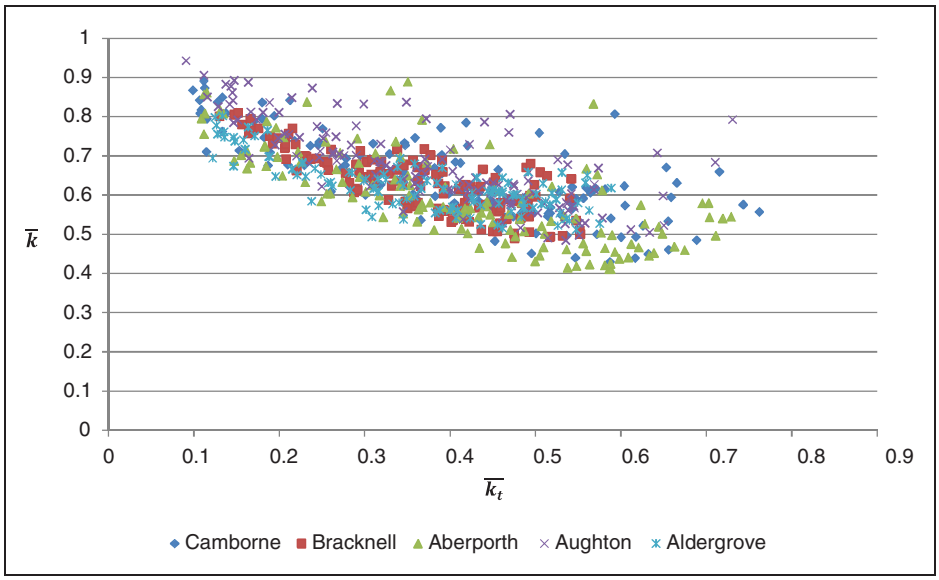

Figure 8. Monthly-averaged hourly $\overline{k}$-$\overline{k_t}$ plot for the UK (locations arranged in an increasing order of latitude). Note: $\overline{k}$ (*y*-axis), $\overline{k_t}$ (*x*-axis).

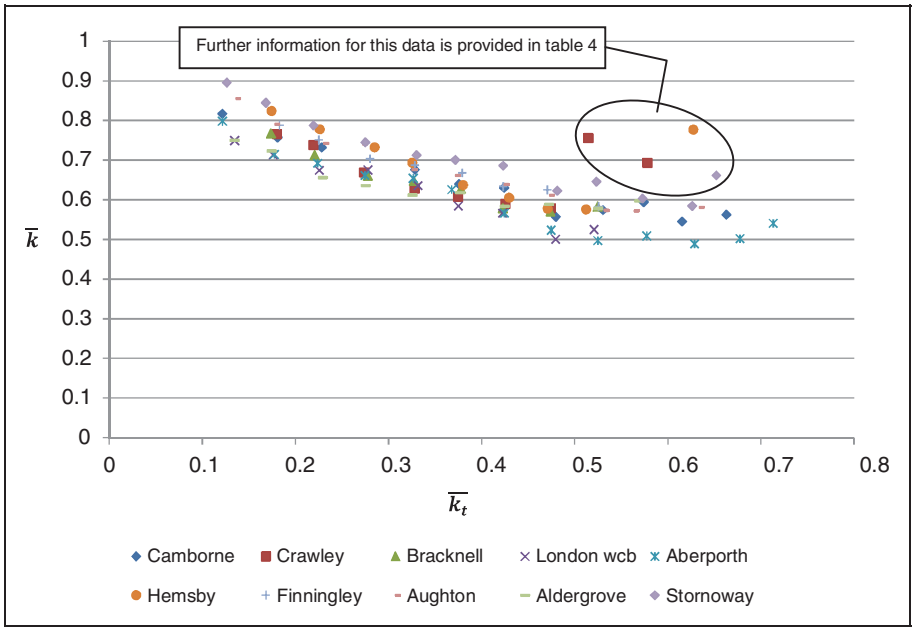

Figure 9. Averaged values of diffuse ratio for the UK (locations arranged in an increasing order of latitude). Note: $\overline{k}$ (y-axis), $\overline{k_t}$ (x-axis).

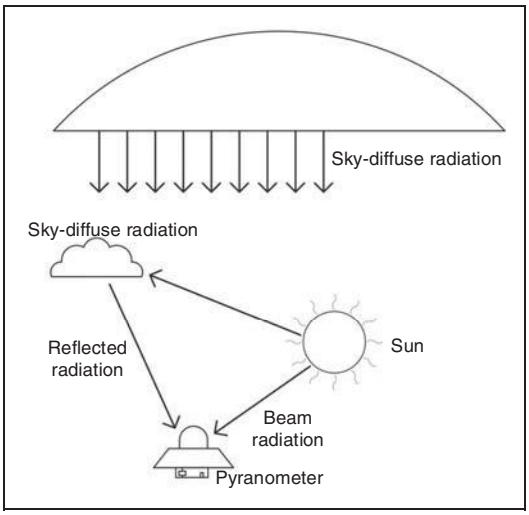

Figure 10. Demonstration of atmospheric condition when diffuse irradiation is enhanced under a partly clouded sky with a low solar altitude.

were calculated. The following conditions were used in each case to remove erroneous recorded data.

$$k_T = \frac{I_G}{I_E} \rightarrow I_G < I_E \tag{2}$$

$$k = \frac{I_D}{I_G} \rightarrow I_D \leq I_G \tag{3}$$

The monthly-averaged clearness index was then regressed against the monthly-averaged diffuse ratio for each location. Figure 6 shows one such scatter plot for Bracknell. Furthermore, for each increment at bandwidth of clearness index of 0.05 width, the corresponding values of diffuse ratio shown in Figure 7 were again averaged.

The data from all ten locations were found to have a similar degree of scatter as depicted by

Table 4. High clearness index data.

	Averaged diffuse ratio	Clearness index	Hourly diffuse ratio	Solar altitude, degree
Stornoway	0.66	0.65	0.63	12.3
		0.65	0.57	20.1
		0.65	0.79	4.1
Hemsby	0.78	0.60	0.74	3.7
		0.64	0.82	1.7
		0.64	0.77	3.3
Crawley	0.75	0.51	0.85	1.5
		0.52	0.64	10.1
		0.52	0.78	2.8
	0.69	0.55	0.63	6.9
		0.58	0.71	4.6
		0.59	0.71	5.9
		0.59	0.73	4.9

Figure 9. Figures 8 and 9 respectively display the all-location scatter plot and bin-wise averaged plot. In these latter figures the data for the locations have been arranged in an increasing order of latitude. No particular trend is, however, identifiable as far as latitude is concerned. In view of this a single regression was presently obtained (equation (4)).

In solar radiation studies, it is common to encounter data that lie unusually far from the bulk of the data population. These data are called outliers and in literature there are standard statistical tests to ascertain if those data are indeed outliers.[26]

In this study though, none of the data were found to be outliers.

A point worth mentioning here is that in almost all cases of the data from 10 locations that is under examination, there is an increasing trend of diffuse ratio for the top end of clearness index. This is a well-known phenomenon that is associated with simultaneous occurrence of two astronomical/weather-related conditions:

- Low solar altitude angle, and
- Sun shining strongly through a broken cloud

The result is that a high clearness index is obtained from a high beam irradiation augmented with sky-diffuse and cloud-reflected radiation as is also a high value of diffuse ratio. The above phenomenon is depicted in Figure 10.

Table 4 sheds further light on those points that belong to the class of data under discussion.

A single regression curve for UK was obtained by pooling all data include in Figure 9. That regression model is given in the following equation

$$\bar{k} = 0.89\overline{k_t^2} - 1.185\overline{k_t} + 0.95 \qquad (4)$$

Conclusions

It was presently shown that monthly-averaged hourly data for solar radiation are much more economical to obtain than hour-by-hour records. Furthermore, through NASA website one may freely obtain daily solar data, which may easily be decomposed into hourly global irradiation time-series. The missing link so far has been averaged-hourly diffuse irradiation.

This work fills that gap. A single regression equation has presently been obtained for the UK as a whole.

Application of this equation has enabled production of Vertical Surface irradiation data for 24 key UK locations that form an important part of CIBSE Guide A (2014).[6]

Primarily, the present work has explored a correlation between averaged-hourly diffuse and global irradiation using the diffuse ratio–clearness index envelope. Present results show that a strong regression relationship is thus obtainable. There is no reason to doubt the existence of such a relationship for other data sets that are available for other world locations. It is hoped that the present work has therefore the potential for other similar research that may be followed up in a likewise manner.

Acknowledgments

The authors would like to thank the referees whose detailed critique has enabled us to significantly improve the quality of this article.

Funding

This research work was carried out as part of development of CIBSE Guide A. As co-ordinator of CIBSE Solar Data Task Group, T Muneer would like to acknowledge the help extended by J Fullwood of UK Meteorological Office and CIBSE staff A Mylona and K Butcher.

References

1. CIBSE/Met. *Office hourly weather data*. October 2005. WCD03-SET (issue 2). Design Summer Year/Test Reference Year.
2. CIBSE/Met. *Office hourly weather data*. 2002.
3. *CIBSE future weather years*. July 2009.
4. *CIBSE Guide A*. London: Chartered Institution of Building Services Engineers, 1999.
5. *CIBSE Guide A*. London: Chartered Institution of Building Services Engineers, 2006.
6. *CIBSE Guide A*. London: Chartered Institution of Building Services Engineers, 2014.
7. *CIBSE Guide J*. London: Chartered Institution of Building Services Engineers, 2000.
8. Muneer T and Saluja GS. Correlation between hourly diffuse and global solar irradiation for the UK. *Building Serv Eng Res Technol* 1986; 7(1): 37–43.
9. Page JK. The estimation of monthly mean values of daily total shortwave radiation on vertical and inclined surfaces from sunshine records for latitudes 40''N-40''s. In: *Proceedings of the UN conference on new sources of energy*, Rome, Italy, 21–31 August 1961. United Nations, paper no. 3515198.
10. http://www.helioclim.org/esra/.
11. Liu YH and Jordan RC. The interrelationship and characteristic distribution of direct, diffuse and total solar radiation. *Sol Energy* 1960; 4: 1–19.
12. Orgill JF and Hollands KGT. Correlation equation for hourly diffuse radiation on a horizontal surface. *Sol Energy* 1977; 19: 357–359.
13. Erbs DG, Klein SA and Duffie JA. Estimation of the diffuse radiation fraction for hourly, daily and monthly average global radiation. *Sol Energy* 1982; 28: 293–302.
14. Reindl DT, Beckman WA and Duffie JA. Diffuse fraction correlations. *Sol Energy* 1990; 45: 1–7.
15. Hawlader MNA. Diffuse, global and extraterrestrial solar radiation for Singapore. *Int J Ambient Energy* 1984; 5: 31–38.
16. Spencer JW. A comparison of methods for estimating hourly diffuse solar-radiation from global solar-radiation. *Sol Energy* 1982; 29(1): 19–32.
17. Chandrasekaran J and Kumar S. Hourly diffuse fraction correlation at a tropical location. *Sol Energy* 1994; 53: 505–510.
18. Boland J, Scott L and Luther M. Modeling the diffuse fraction of global solar radiation on a horizontal surface. *Environmetrics* 2001; 12: 103–116.
19. Miguel A, Bilbao J, Aguiar R, et al. Diffuse solar irradiation model evaluation in the north Mediterranean belt area. *Sol Energy* 2001; 70: 143–153.
20. Oliveira AP, Escobedo JF, Machado AJ, et al. Correlation models of diffuse solar radiation applied to the city of Sao Paulo, Brazil. *Appl Energy* 2002; 71: 59–73.
21. Karatasou S, Santamouris M and Geros V. Analysis of experimental data on diffuse solar radiation in Athens, Greece, for building applications. *Int J Sustain Energy* 2003; 23(1–2): 1–11.
22. Soares J, Oliveira AP, Boznar MZ, et al. Modeling hourly diffuse solar radiation in the city of Sao Paulo using a neural-network technique. *Appl Energy* 2004; 79: 201–201.
23. http://eosweb.larc.nasa.gov/cgi-bin/sse/retscreen.cgi?email=rets@nrcan.gc.ca.
24. Gago EJ, Etxebarria S, Tham Y, et al. Inter-relationship between mean-daily irradiation and temperature, and decomposition models for hourly irradiation and temperature. *Int J Low-Carbon Technol* 2011; 6: 22–37.
25. Tham Y and Muneer T. Sol-air temperature and daylight illuminance profiles for the UKCP09 data sets. *Build Environ* 2011; 46: 1243–1250.
26. Muneer T. *Solar radiation and daylight models*, 2nd ed. New York: Elsevier, 2004.

Muneer et al. Future Cities and Environment (2015) 1:5
DOI 10.1186/s40984-015-0008-5

Future Cities & Environment
a SpringerOpen Journal

TECHNICAL ARTICLE Open Access

Monthly-averaged hourly solar diffuse radiation models for world-wide locations

T. Muneer[1], EJ Gago[2*] and S. Etxebarria[2]

Abstract

Monthly-averaged daily global irradiation data are now easily available from NASA website for any global location. Using established models it is then possible to decompose the daily to averaged-hourly global irradiation. The missing link so far has been hourly averaged diffuse irradiation. In this article data was pooled from 14 world-wide locations to obtain a regression model to complete the above missing link. It was presently shown that the averaged–data regressions are distinctly different from previously available hour-by-hour regressions.

Keywords: Solar radiation; Averaged-hourly solar diffuse fraction; Insolation; Solar diffuse radiation

Introduction

Solar radiation data are essential for the design of very many energy systems. These data are needed for obtaining solar energy resource assessment, its transmission and also to obtain the efficiency of energy delivery. A few examples are solar water heating, and space PV systems, daylighting, building air conditioning load and solar-driven ventilation. The starting point for the above computational chain is almost always global and diffuse horizontal radiation. Usually, the computations are carried out using hourly or sub-hourly data.

Note that not always it is possible to obtain a long-term series of hourly or sub-hourly data for the above parameters.

The most commonly measured solar data are global irradiation and these are available for a limited number of stations within any given country at an hourly, daily or monthly frequency. For example within the UK and Spain a historical records of hourly data are available for 71 and 31 stations, respectively.

Of these stations due to higher operational costs associated with diffuse radiation measurements the respective meteorological offices tend to record the latter variable at much fewer locations. For example, since the year 2002 within the UK the diffuse radiation is recorded at only two locations, at North latitudes of Camborne (50.21°) and Lerwick (60.80°).

On the contrary, through the work of NASA (http://eosweb.larc.nasa.gov/cgi-bin/sse/retscreen.cgi?email=rets@nrcan.gc.ca) it is now possible to obtain daily-averaged irradiation data for virtually any location in the world. A sample table of climatic data for Easthampstead (Bracknell) is provided in Table 1.

This information was downloaded from the above-mentioned NASA website. The NASA reported irradiation data were compared by the present research team against averaged measured data for one UK location for the period 1981–1983 (three complete years) (see Fig. 1). The statistics within the latter figure shows that there is a close concordance between the satellite-based NASA irradiation and the UK Meteorological Office measured data set.

Following the original work of Liu and Jordan (Liu & Jordan 1960) a great many number of research teams from around the world have produced regressions relating diffuse ratio (k) and clearness index (kt) regressions at an hourly, daily, monthly and annual frequency. Each of the above four category of regression is unique and statistically different as shown in the work of Muneer (Muneer 2004) and Saluja et al. (Saluja et al. 1988).

The present article was pooled from 14 world-wide locations to obtain a regression model to complete the above missing link. It was presently shown that the averaged–data based regressions are distinctly different from previously available hour-by-hour regressions.

* Correspondence: ejadraque@ugr.es
[2]University of Granada, Granada, Spain
Full list of author information is available at the end of the article

Table 1 Climatic data for Easthampstead (Bracknell) with the NASA reported irradiation data and averaged measured data for the period 1981-1983

	Unit	Climate data location							
Latitude	°N	51,42							
Longitude	°E	−0,75							
Elevation	m	58,00							
Heating design temperature	°C	−1,74							
Cooling design temperature	°C	22,96							
Earth temperature amplitude	°C	14,35							
Frost days at site	day	37,00							
Month	Air temperature	Relative humidity	Daily solar radiation-horizontal	Atmospheric pressure	Wind speed	Earth temperature	Heating degree-days	Cooling degree-days	Average measured radiation
	°C	%	kWh/m^2/day	kPa	m/s	°C	°C-d	°C-d	kWh/m^2/day
January	4,2	83,90	0,77	100,8	6,3	3,1	426	1	0,71
February	4,3	80,20	1,39	101,0	5,8	3,6	380	1	1,28
March	6,4	76,80	2,34	100,9	6,0	6,2	353	4	2,18
April	8,6	69,80	3,59	100,7	5,1	9,1	279	21	3,55
May	12,7	64,00	4,57	100,9	4,7	13,8	168	92	4,11
June	16,1	60,80	4,84	100,9	4,4	17,7	75	177	4,86
July	18,6	60,20	4,80	100,9	4,4	20,4	25	261	4,77
August	18,6	61,20	4,23	100,9	4,3	20,3	26	264	4,23
September	15,5	66,30	2,86	100,9	5,0	16,5	83	164	2,85
October	11,7	74,10	1,73	100,7	5,5	11,5	191	73	1,57
November	7,3	83,20	0,96	100,7	5,9	6,4	318	11	0,80
December	4,9	85,00	0,60	100,8	6,1	3,8	404	3	0,60
Annual									
	10,7	72,10	2,72	100,8	5,3	11,0	2728	1072	
Measured at (m)					10,0	0,0			

Website: http://eosweb.larc.nasa.gov/cgi-bin/sse/retscreen.cgi?email=rets@nrcan.gc.ca

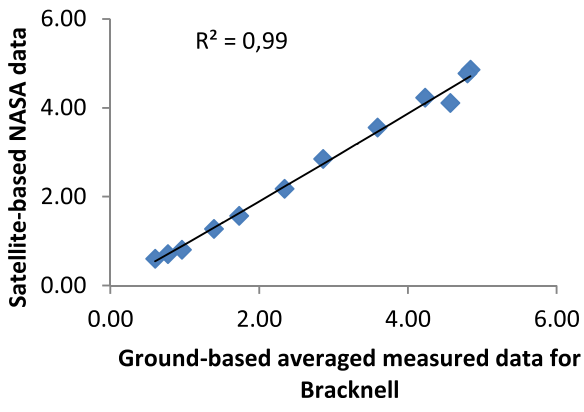

Fig. 1 Comparison between NASA reported irradiation data and ground-based averaged measured data for Bracknell, kWh/m^2-day

The unique nature of solar radiation regressions

Historically speaking, a large number of research teams from around the world have produces k-kt regressions that were based on an hour-by-hour, daily, monthly or annual data. Examples that may be cited here, are Liu and Jordan (daily, and monthly-averaged daily) (Liu & Jordan 1960), Erbs et al. (hourly, daily and monthly-averaged daily) (Erbs et al. 1982), Hawas and Muneer (hour-by-hour, daily, monthly- and annual-averaged daily) (Hawas & Muneer 1984; Muneer & Hawas 1984; Muneer et al. 1984) and Stanhill (monthly- and annual-averaged daily) (Stanhill 1966).

Presently, Figs. 2 and 3 show the unique nature of hour-by-hour (Fig. 2: $k - k_t$ plot) and monthly-averaged hourly regressions (Fig. 3: $\bar{k} - \bar{k}_t$). An important point to note is that while Fig. 2 shows a convex profile, Fig. 3

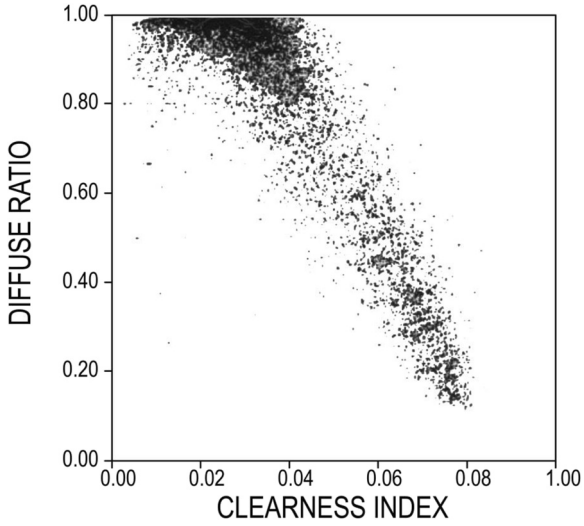

Fig. 2 Hourly diffuse ratio versus clearness index for UK locations

demonstrates a concave behaviour. The latter two figures are based on data from common UK locations.

While there are established models for data of Fig. 2 there are no regressions available in literature for averaged-hourly data such as those shown in Fig. 3. The object of this article is to present the latter type of regressions.

Presently developed monthly-averaged hourly $\bar{k}$–$\bar{k}_t$ regressions

Fourteen worldwide locations were chosen for this study, details of which are shown in Table 2.

Data consisted of hourly global and diffuse irradiation values for several years for each location, covering most of the range of latitude for the country. The location names have been arranged in an increasing order of latitude.

Monthly-averaged hourly values were calculated for the global and diffuse radiation considering the data period for each location. For each of them, the monthly-averaged hourly diffuse ratio $(\bar{k})$ and the corresponding clearness index $(\bar{k}_t)$ were calculated from sunrise to sunset. The following conditions were used in each case to remove erroneously recorded data.

$$k_T = \frac{I_G}{I_E} \rightarrow I_G < I_E \tag{1}$$

$$k = \frac{I_D}{I_G} \rightarrow I_D \leq I_G \tag{2}$$

The monthly-averaged clearness index was then regressed against the monthly-averaged diffuse ratio for each location. Figure 4 shows one such scatter plot for Chennai and Lisbon. Furthermore, for each increment at bandwidth of clearness index of 0.05 width, the corresponding values of averaged diffuse ratio shown in Fig. 5 were obtained, shown here for pooled data from two Indian locations.

Figures 6 and 7 respectively show the regressions for locations in a narrower range of latitudes (20-42° N) and worldwide sites with a more diverse range of latitudes (13-58°N).

Note that Fig. 6 shows the potential for a single regression model. Figure 7 on the other hand indicates the existence of different sub-models and these shall now be explored further.

Figures 8, 9 and 10 respectively present regressions models that were obtained by pooling data from locations with a latitude range of 13-20° N, 20-42° N and 50-58° N.

Table 3 presents regressions equations and coefficient of determination (R^2) for each location.

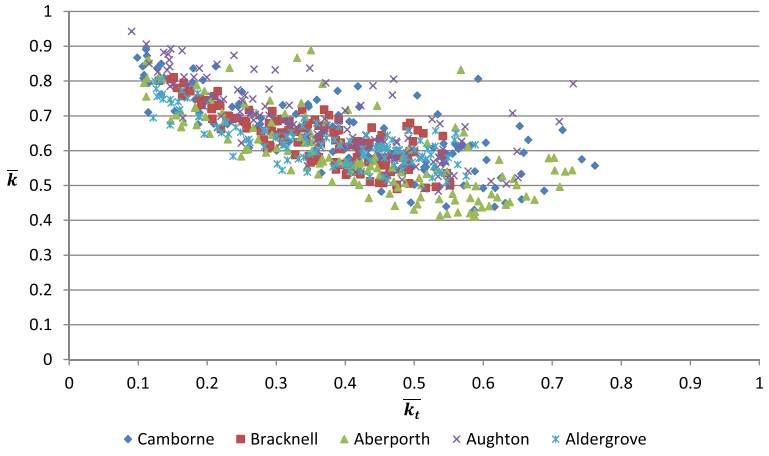

Fig. 3 Monthly-averaged hourly plot for UK locations (arranged in an increasing order of latitude: Camborne 50.21° N, Aldergrove 54.65° N)

Table 2 The 14 worldwide locations that were presently investigated

Country	Location	Latitude	Longitude	Period of observation
India	Chennai	13.08	80.18	1990–1994
	Pune	18.32	73.85	1990–1994
Kingdom of Bahrain	Bahrain	26.03	50.61	2000–2002
State of Kuwait	Kuwait	29.22	47.98	1996–2000
Spain	Almeria	36.83	−2.38	1993–1998
Portugal	Faro	37.02	−7.96	1982–1986
	Lisbon	38.71	−9.15	1982–1990
Spain	Madrid	40.40	−3.55	1999–2001
	Girona	41.97	2.76	1995–2001
United Kingdom	Camborne	50.21	5.30	1981–1995
	Bracknell	51.42	0.75	1992–1994
	Aberporth	52.13	4.55	1975–1995
	Finningley	53.48	0.98	1982–1995
	Stornoway	58.22	6.39	1982–1995

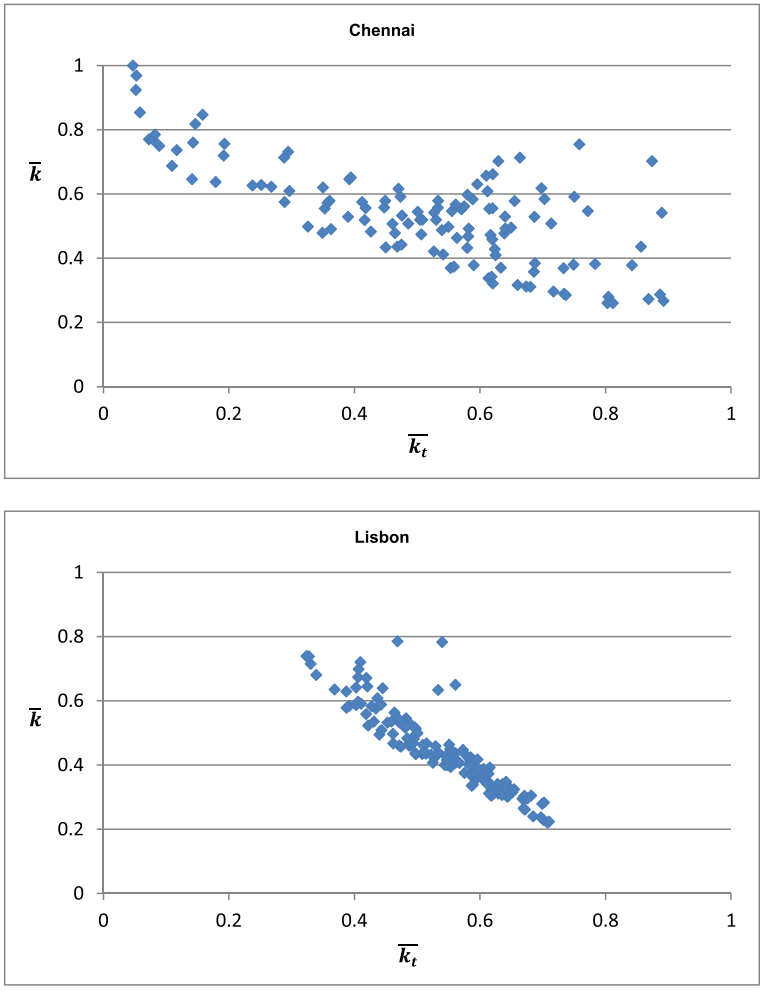

Fig. 4 Monthly-averaged hourly diffuse ratio (y-axis) versus clearness index (x-axis) fot two locations. One Indian and other a South European

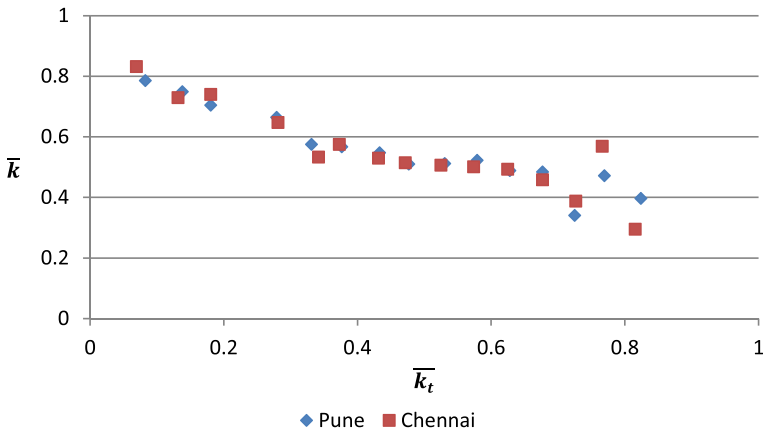

Fig. 5 Averaged values of diffuse ratio for the locations between latitude 13-20° North

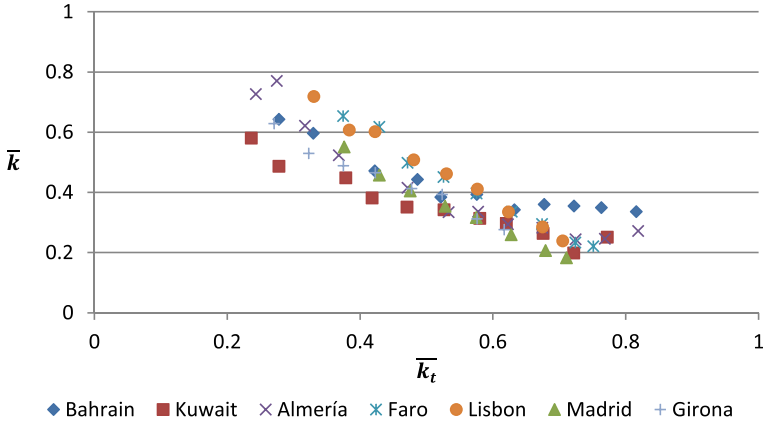

Fig. 6 Averaged values of diffuse ratio for the locations between latitude 20-42° North

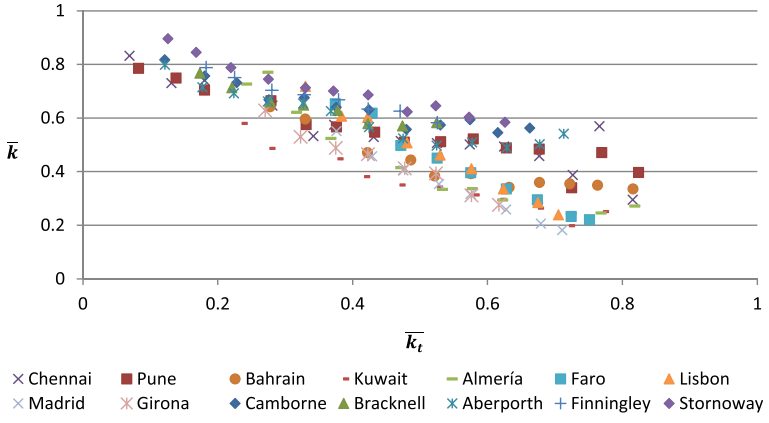

Fig. 7 Averaged values of diffuse ratio for the all locations

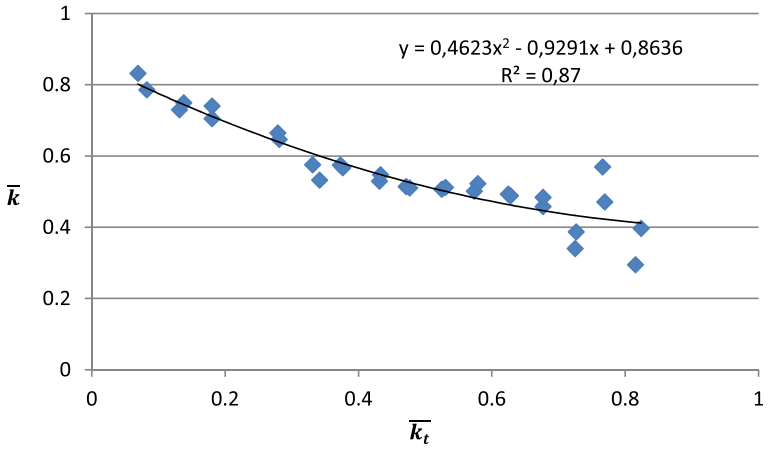

Fig. 8 Averaged values of diffuse ratio for the locations between latitude 13-20° North (Chennai and Pune)

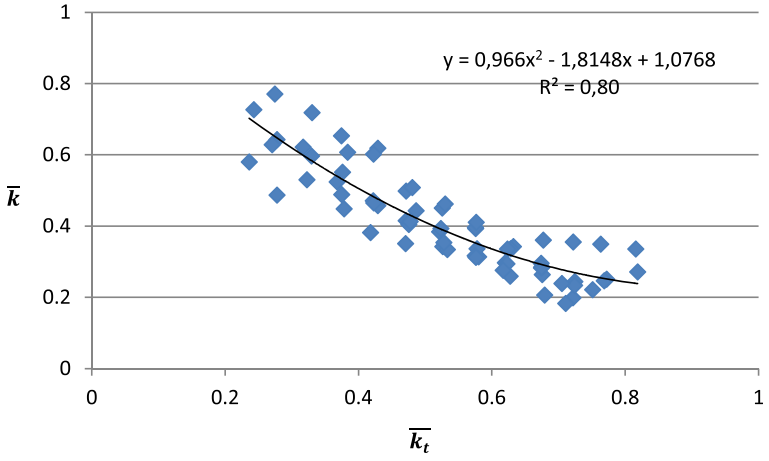

Fig. 9 Averaged values of diffuse ratio for the locations between latitude 20-42° North (Bahrain, Kuwait, Almeria, Faro, Lisbon, Madrid and Girona)

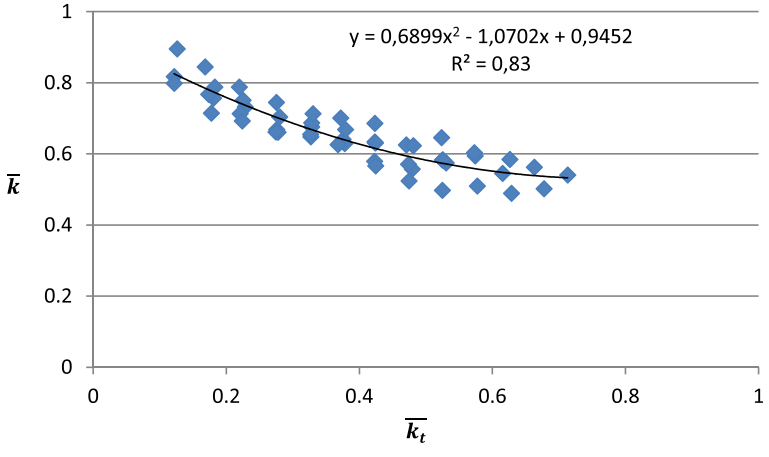

Fig. 10 Averaged values of diffuse ratio for the locations between latitude 50-58° North (Camborne, Bracknell, Aberporth, Finningley and Stornoway)

Table 3 The regressions equations and coefficient of determination (R^2) for each location

Country	Location	Regression equations	R^2
India	Chennai	$y = 0.5124x^2-0.9809x + 0.8733$	0.83
	Pune	$y = 0.4083x^2-0.873x + 0.853$	0.92
Kingdom of Bahrain	Bahrain	$y = 1.4455x^2-2.113x + 1.1262$	0.98
State of Kuwait	Kuwait	$y = 0.7088x^2-1.3237x + 0.8299$	0.96
Spain	Almeria	$y = 1.9414x^2-2.9329x + 1.3637$	0.98
Portugal	Faro	$y = 0.9184x^2-2.2173x + 1.3654$	0.99
	Lisbon	$y = 0.0721x^2-1.3001x + 1.1246$	0.99
Spain	Madrid	$y = 0.9087x^2-2.0465x + 1.1808$	0.99
	Girona	$y = 0.1781x^2-1.0867x + 0.887$	0.98
United Kingdom	Camborne	$y = 0.8188x^2-1.1127x + 0.9365$	0.96
	Bracknell	$y = 1.4394x^2-1.5414x + 0.9878$	0.97
	Aberporth	$y = 0.9797x^2-1.3032x + 0.9403$	0.95
	Finningley	$y = 0.451x^2-0.876x + 0.9267$	0.99
	Stornoway	$y = 7441x^2-1.1382x + 1.0147$	0.98

Three points are worthy of note from Figs. 8, 9 and 10:

i. A strong correlation is observed between $\bar{k}$ and $\bar{k}_t$ with the respective coefficient of determination of 0.87, 0.80 and 0.83 (corresponding values of coefficient of correlation are 0.93, 0.89 and 0.91),
ii. In each case the shape of the regressed curve is concave, contrary to the convex profile for hour-by-hour regressions reported by research teams from around the world, and
iii. it is not possible to produce a single regressed curve for worldwide locations.

The latter point is reinforced via Fig. 11.

Conclusions

Monthly-averaged daily global irradiation data are now easily available from NASA website for any terrestrial location. Using established models such as those presented by Liu and Jordan (Liu & Jordan 1960), Collares-Pereira and Rabl (Collares-Pereira & Rabl 1979), Mani and Rangarajan (Mani & Rangarajan 1983), Muneer and Saluja (Muneer & Saluja 1996) and Lloyd (Lloyd 1982) it is then possible to decompose the daily–to averaged-hourly global irradiation. The missing link so far has been hourly averaged diffuse irradiation. The authors report a regression model to complete the above missing link for 14 world locations and show that the averaged–data regressions are distinctly different from previously available hour-by-hour regressions.

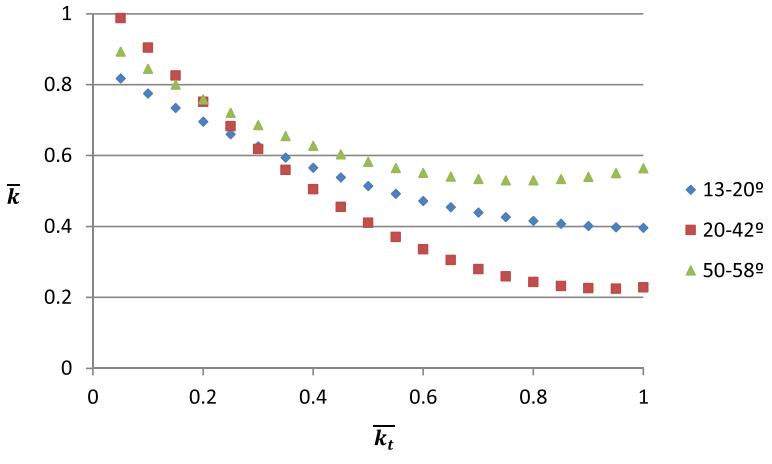

Fig. 11 Monthly-averaged hourly regressions for three ranges of latitudes

Competing interests
The authors declare that they have no competing interests.

Authors' contributions
Authors made substantial contributions to conception and design, and acquisition of data, and analysis and interpretation of data. Authors participated in drafting the article and revising it critically for important intellectual content. Authors give final approval of the version to be submitted and any revised version.

Author details
[1]Edinburgh Napier University, Edinburgh, UK. [2]University of Granada, Granada, Spain.

Received: 15 November 2014 Accepted: 1 May 2015
Published online: 24 August 2015

References

Collares-Pereira M, Rabl A (1979) The average distribution of solar radiation correlations between diffuse and hemispherical and between daily and hourly insolation values. Solar Energy 22:155
Erbs DG, Klein SA, Duffie JA (1982) Estimation of the diffuse fraction of hourly, daily and monthly-averaged global radiation. Solar Energy 28:293
Hawas M, Muneer T (1984) Study of diffuse and global radiation characteristics in India. Energy Convers Manage 24:143
Liu YH, Jordan RC (1960) The interrelationship and characteristic distribution of direct, diffuse and total solar radiation. Sol Energy 4:1–19
Lloyd PB (1982) A Study of Some Empirical Relations Described by Liu and Jordan. Report no. 333, Solar Energy Unit, University College, Cardiff
Mani A, Rangarajan S (1983) Techniques for the precise estimation of hourly values of global, diffuse and direct solar radiation. Solar Energy 31:577
Muneer T (2004) Solar Radiation and Daylight Models, 2nd edn., Elsevier
Muneer T, Hawas M (1984) Correlation between daily diffuse and global radiation for India. En Conv Mgmt 24:151
Muneer T, Saluja GS (1996) Correlation between hourly diffuse and global solar irradiation for the UK. Building Services Engineering Research & Technology 7, 1
Muneer T, Hawas MM, Sahili K (1984) Correlation between hourly diffuse and global radiation for New Delhi. Energy Conv Mgmt 24:265
Saluja GS, Muneer T, Smith ME (1988) Methods for estimating solar radiation on a horizontal surface. Ambient Energy 9:59
Stanhill G (1966) Diffuse sky and cloud radiation in Israel. Solar Energy 10:96

Monthly-averaged hourly calculation

```
Sub avrg1()

givemt = Sheets("Sheet1").Cells(2, 13).Value

'givehr = Sheets("Sheet1").Cells(2, 14).Value


'mistake 1 made by Saioa: wrong units for G & D


For j = 3 To 20

givehr = j + 0.5 'mistake 2 made by Saioa: wrong value of hour

sumnum = 0

sumgrd = 0

sumdrd = 0


For i = 1 To 29216 'mistake 3 made by Saioa: wrong no. of data rows

valmnt = Sheets("Sheet2").Cells(i, 2).Value

valhor = Sheets("Sheet2").Cells(i, 4).Value

grd = Sheets("Sheet2").Cells(i, 5).Value

drd = Sheets("Sheet2").Cells(i, 6).Value


If (valmnt = givemt And valhor = givehr) Then

If (grd > 10 And grd < 999) Then

If (drd > 10 And drd < 999) Then

sumnum = sumnum + 1

sumgrd = sumgrd + grd

sumdrd = sumdrd + drd

End If

End If
```

```
End If

Next i


If (sumnum > 0) Then

Sheets("Sheet1").Cells(j + 4, 16).Value = j + 0.5 'mistake 4 made by Saioa: wrong hour

Sheets("Sheet1").Cells(j + 4, 17).Value = sumgrd / sumnum

Sheets("Sheet1").Cells(j + 4, 18).Value = sumdrd / sumnum

End If

Next j


End Sub
```

Averaged diffuse ratio for each increment at bandwidth of clearness index of 0.05 width

```
Sub avrgkt()

Dim ktlft(16), ktrit(16) As Single

For i = 1 To 16

ktlft(i) = 0.05 * i

ktrit(i) = ktlft(i) + 0.05

nsum = 0

ktsum = 0

drsum = 0

For n = 1 To 200

ktgiven = Sheets("Sheet3").Cells(n, 1).Value

drgiven = Sheets("Sheet3").Cells(n, 2).Value

If (ktgiven >= ktlft(i) And ktgiven < ktrit(i)) Then

nsum = nsum + 1

ktsum = ktsum + ktgiven

drsum = drsum + drgiven

End If

Next n


If (nsum > 0) Then

Sheets("Sheet4").Cells(49 + i, 1).Value = ktsum / nsum

Sheets("Sheet4").Cells(49 + i, 2).Value = drsum / nsum

Sheets("Sheet4").Cells(49 + i, 3).Value = nsum

End If

Next i

End Sub
```

Functions

```
Function eot(xyr, xmo, xdy, YRLNG)
    DTOR = 3.14159 / 180
    XLCT = 12
    UT = XLCT + YRLNG / 15
    If xmo > 2 Then
    IYR1 = xyr
    IMT1 = xmo - 3
    Else
    IYR1 = xyr - 1
    IMT1 = xmo + 9
    End If
    INTT1 = Int(30.6 * IMT1 + 0.5)
    INTT2 = Int(365.25 * (IYR1 - 1976))
    SMLT = ((UT / 24) + xdy + INTT1 + INTT2 - 8707.5) / 36525
    EPSILN = 23.4393 - 0.013 * SMLT
    CAPG = 357.528 + 35999.05 * SMLT
    If CAPG > 360 Then
    G360 = CAPG - Int(CAPG / 360) * 360
    Else
    G360 = CAPG
    End If
    CAPC = 1.915 * Sin(G360 * DTOR) + 0.02 * Sin(2 * G360 * DTOR)
    CAPL = 280.46 + 36000.77 * SMLT + CAPC
    If CAPL > 360 Then
    XL360 = CAPL - Int(CAPL / 360) * 360
    Else
```

```
    XL360 = CAPL
    End If
    ALPHA = XL360 - 2.466 * Sin(2 * XL360 * DTOR) + 0.053 * Sin(4 * XL360 * DTOR)
    eot = (XL360 - CAPC - ALPHA) / 15
End Function

Function dec(xyr, xmo, xdy, YRLNG)
    DTOR = 3.14159 / 180
    XLCT = 12
    UT = XLCT + YRLNG / 15
    If xmo > 2 Then
    IYR1 = xyr
    IMT1 = xmo - 3
    Else
    IYR1 = xyr - 1
    IMT1 = xmo + 9
    End If
    INTT1 = Int(30.6 * IMT1 + 0.5)
    INTT2 = Int(365.25 * (IYR1 - 1976))
    SMLT = ((UT / 24) + xdy + INTT1 + INTT2 - 8707.5) / 36525
    EPSILN = 23.4393 - 0.013 * SMLT
    CAPG = 357.528 + 35999.05 * SMLT
    If CAPG > 360 Then
    G360 = CAPG - Int(CAPG / 360) * 360
    Else
    G360 = CAPG
    End If
```

```
    CAPC = 1.915 * Sin(G360 * DTOR) + 0.02 * Sin(2 * G360 * DTOR)
    CAPL = 280.46 + 36000.77 * SMLT + CAPC
    If CAPL > 360 Then
    XL360 = CAPL - Int(CAPL / 360) * 360
    Else
    XL360 = CAPL
    End If
    ALPHA = XL360 - 2.466 * Sin(2 * XL360 * DTOR) + 0.053 * Sin(4 * XL360 * DTOR)
    GHA = 15 * UT - 180 - CAPC + XL360 - ALPHA
    If GHA > 360 Then
    GHA360 = GHA - Int(GHA / 360) * 360
    Else
    GHA360 = GHA
    End If
    dec = Atn(Tan(EPSILN * DTOR) * Sin(ALPHA * DTOR)) / DTOR
End Function
Function solalt(xlat, xdec, xast, srt, sst)
   DTOR = 3.14159 / 180
   horang = 15 * DTOR * Abs(12 - (xast + 0.5))

   'If ((xast - 1) = Int(srt)) Then
   'horang = 15 * DTOR * Abs(12 - 0.5 * (xast + srt))
   'End If

   'If ((xast - 1) = Int(sst)) Then
   'horang = 15 * DTOR * Abs(12 - 0.5 * (xast - 1 + sst))
   'End If
```

```
    xdum1 = Sin(xlat * DTOR) * Sin(xdec * DTOR) + Cos(xlat * DTOR) * Cos(xdec * DTOR) *
Cos(horang)

   solalt = (Application.Asin(xdum1)) / DTOR

'    solalt = horang / dtor

End Function

Function daynum(IYR, IMT, IDY)

    If (IMT > 2) Then

    IYR1 = IYR

    IMT1 = IMT - 3

    Else

    IYR1 = IYR - 1

    IMT1 = IMT + 9

    End If

    INTT1 = Int(30.6 * IMT1 + 0.5)

    INTT2 = Int(365.25 * (IYR1 - 1976))

    DN1 = (IDY + INTT1 + INTT2)

    IMT9 = 1

    IYR1 = IYR - 1

    IMT1 = IMT9 + 9

    INTT1 = Int(30.6 * IMT1 + 0.5)

    INTT2 = Int(365.25 * (IYR1 - 1976))

    DN2 = (INTT1 + INTT2)

    daynum = DN1 - DN2

End Function

Function ERAD(DN, solalt)

DTOR = 3.14159 / 180

ERAD = 0

If (solalt > 0) Then
```

```
ERAD = 1367 * (1 + 0.033 * Cos(0.0172024 * DN)) * Sin(solalt * DTOR)

End If

End Function
```